Programa de doctorado del Departamento de Microbiología
Facultad de Ciencias
Universidad Autónoma de Madrid

Efecto de la contaminación crónica, factores geoquímicos y bioestimulación en el catabolismo de hidrocarburos en ambientes marinos contaminados: una aproximación multi-ómica

Rafael Mª Bargiela Bargiela
Madrid 2015

Bajo la supervisión de:

1. **Dr. Manuel Ferrer Martínez**

Laboratorio de Biotecnología de Sistemas
Departamento de Biocatálisis Aplicada
Consejo Superior de Investigaciones Científicas
Instituto de Catálisis y Petroleoquímica

Agradecimientos

Aunque esta Tesis lleve mi nombre, nada de lo que aquí se cuenta sería posible sin toda la gente que ha estado detrás de mí todos estos años. Han sido muchas la personas que han participado directa o indirectamente para hacer de este trabajo una realidad. Por ello, a todos ellos quiero agradecerles de corazón su aportación:

En primer lugar, quiero agradecer a todo el personal del Instituto de Catálisis y Petroleoquímica, y a sus directores, Prof. Joaquín Pérez Pariente y Prof. José Carlos Conesa Cegarra, por permitirme realizar aquí mi Tesis Doctoral. Quiero agradecer en especial la ayuda de todas las personas que componen los departamentos de Recursos Humanos, Contabilidad, Compras e Informática.

Gracias a Coral Barbas y David Rojo, del Centro de Metabolómica y Bioanálisis de la Universidad CEU San Pablo, por su trabajo para los estudios de metabolómica que se han realizado en esta Tesis.

Al ministerio de Economía y Competitividad, la Unión Europea, el CSIC y la UAM, que han sido las instituciones que han financiado y hecho posible los estudios que se han llevado a cabo en esta Tesis Doctoral. En especial a los proyectos europeos ULIXES y KILLSPILL, y a toda la gente que ha participado en las investigaciones realizadas bajo el marco de estos proyectos. En especial al Prof. Peter N. Golyshin y al Dr. Christoph Gertler (Universidad de Bangor, Reino Unido).

A la Dra. Catalina Ribas Núñez, por ser mi tutora durante la Tesis y supervisar cada año el trabajo realizado.

A todos los miembros del tribunal de Tesis, por formar parte de él y juzgar mi trabajo.

A mi director de Tesis, el Dr. Manuel Ferrer Martínez. Ha pasado mucho tiempo desde que entre en el laboratorio en 2011, sin embargo, ha sido imposible corregir todas las faltas y carencias que tengo como investigador, en todos los aspectos. A pasar de ello, Manolo ha tenido conmigo infinita paciencia, ha corregido innumerables documentos, figuras, trabajos, etc. Él me ha enseñado todo lo que sé sobre hacer ciencia y me demuestra cada día que es un filón inagotable de conocimiento del que nunca se deja de aprender. Por todo ello, gracias.

A los miembros del laboratorio del Dr. Miguel Alcaide, con los que no comparto nada de trabajo, pero sí muchas risas y alguna que otra caña, que nunca sobran. En especial a Javi, que desde el Máster ha sido mi compañero inseparable y un amigo fiel. Son impagables las veces que me ha recogido en su coche cuando sufría los peores momentos de mi enfermedad (todavía le debo un tiramisú).

No hay espacio suficiente para agradecerles a mis compañeros del laboratorio 207 que hayan hecho de las largas jornadas de trabajo un tiempo mucho más agradable. Muchísimas gracias a María, que entró conmigo y sabe perfectamente todo lo que hemos pasado juntos estos años, y siempre ha estado ahí para aconsejarme y sufrir juntos las penurias que a veces conlleva hacer una Tesis. A Mercedes, que siempre ha estado ahí apoyándonos y dándonos cariño, y me dio apoyo moral en mi primera charla en inglés. A Alvarito, por su tranquilidad y por vivir conmigo las debacles y glorias de nuestro querido Madrid. A Jesús, con el que he compartido risas y complicidad el uno al lado del otro, y al que echo mucho de menos para poder frikear. También a Lucía, que estaba en nuestra laboratorio cuando entré, cuya serenidad y amabilidad no dejan de asombrarme. Pero en especial, a Mónica, con la que he remado estos últimos dos años. Ha sido mi amiga, mi confidente, mi compañera, mi consejera e incluso correctora también de mi Tesis, a pesar de los momentos difíciles que ha pasado. Muchas gracias.

A Iria, sin la que probablemente ahora estaría hundido en un mar de tristeza y desolación. Su amor y su cariño son lo mejor que me ha pasado en los últimos 3 años. Con ella todo recobra el sentido. Ella es la que más ha soportado el lado oscuro de realizar esta Tesis.

Pero si hay alguien al que tengo que agradecer el haber terminado este trabajo es a mis padres. Ellos son la razón por la que he llegado a donde he llegado. Jamás he dejado de sentir su fe ciega en mí, su orgullo inquebrantable, su apoyo constante y su amor y cariño. Yo no hubiera dado ni la mitad por mí mismo. A pesar de las diferencias, a pesar de

los problemas, siempre han tenido un objetivo claro y conciso, y lo han cumplido a la perfección. No puedo estar más orgulloso y feliz de tener los padres que tengo y de tenerlos a mi lado.

A mis dos hermanas,
a las que quiero con locura.
Pase lo que pase,
hacer siempre lo que os gusta.

Tabla de contenidos

Abreviaturas

Muestras analizadas	
ANC	Muestra del puerto de Ancona (Italia)
AQ	Muestra del golfo de Ácaba (Jordania)
BIZ	Muestra del lago Bizerta (Túnez)
ELF	Muestra de la bahía de Elefsina (Grecia)
ELMAX	Muestra de la zona de El Max (Egipto)
HAV	Muestra de la zona del hundimiento de carguero Haven (Italia)
MCh	Muestra del lago de Mar Chica (Marruecos)
MES	Muestra del puerto de Messina (Italia)
PRI	Muestra del puerto de Priolo Gargallo (Italia)

Enzimas	
1,2-CTD	Catecol 1,2-dioxigenasa
2,3-CTD	Catecol 2,3-dioxigenasa
ACSL	Acil-CoA sintetasa
ADH	Alcohol dehidrogenasa
AH	Alcano hidroxilasa
ALDH	Aldehido dehidrogenasa
ASS	Acilsuccinato sintasa
BSCT	Succinil-CoA:bencilsuccinato transferasa
BCRI	Benzoil-CoA reductasa clase I
BCRII	Benzoil-CoA reductasa clase II
EBDH	Etilbenceno dehidrogenasa
FFS	Fenilfosfato sintasa
FFC	Fenilfosfato carboxilasa
GDO	Gentisato dioxigenasa
NDO	Nafataleno dioxigenasa
PH	Fenol hidroxilasa

Bases de datos de rutas metabólicas	
AromaDeg	*Aromatic Hydrocarbon degradation database*
COG	*Clusters of orthologs genes*
KEGG	*Kyoto Encyclopedia of Genes and Genomes*
OxDBase	*Database of biodegradative oxygenases*
Metacyc	*Metabolic pathways database*
Pfam	*Protein families database*
UM-BBD	*University of Minnesota Biocatalysis / Biodegradation database*

Otras abreviaturas	
ADNc	ADN complementario, copia de un ARNm
AlkB	Alcano hidroxilasas
AMM	Microcosmos enriquecido con amonio
ANME	Archaea metanotróficas anaerobias
API	*Application programming interface*
ARNm	ARN mensajero
ARNr 16S	ARN ribosomal de 16S
ATP	Adenosín trifosfato
ATPasa	ATP sintasa
AU	Ácido úrico
BHO	Bacterias hidrocarbonoclásticas obligadas
BLAST	*Basic Local Aligment Search Tool*
rpsBLAST	*Reversed position specific* BLAST
BTEX	Benceno, tolueno, etilbenceno y xileno
CTE	Cadena de transporte electrónico
C-C	Enlace carbono-carbono
CoA	Coenzima A
C-H	Enlace carbono-hidrógeno
C:N:P	Proporción carbono/nitrógeno/fosfato
EXDO	Extradiol dioxigenasa
Fe-no hemo	Enzima dependiente de Hierro sin grupo hemo
FAD	Flavín adenín dinucleótido
FMN	Flavín mononucleótido
INTRA	Intradiol dioxigenasa
NADH/NAD(P)H	Nicotinamida adenina dinucleótido (fosfato)
NCBI	*National Center for Biothecnology Information*
MCP	Hidrolasas de productos de fisión meta
MMO	Metano monooxigenasa
MMOs	MMO soluble
MMOp	MMO adherida a membrana
OAM	Oxidación anaerobia del metano
OTU	Unidad operacional taxonómica
ORF	Marco de lectura abierta
PAH	Hidrocarburos poliaromáticos
ppm	Partes por millón
RHO	Oxigenasas de ruptura de anillo
RISA	Análisis de los espaciadores intergénicos ribosomales
SIP	Prueba de isótopos radioactivos

Índice de tablas y figuras

Capítulo 1: Biorremediación del petróleo en el medio marino. Introducción a la Tesis Doctoral.

Contenido del capítulo

Capítulo 1: Biorremediación del petróleo en el medio marino. Introducción a la Tesis Doctoral.

Introducción

1. El problema del petróleo en el medio marino

El petróleo constituye una de las reservas de energía más importantes dentro de los recursos que encontramos en el planeta, sólo superado por el carbón. El 94% aproximadamente es utilizado como principal fuente de combustible en sectores como la industria, el transporte y el ámbito doméstico (Awal, 2009; Ball & Truskewycz, 2013). La expansión de su utilización ha llevado a la exploración, perforación y extracción masiva de sus yacimientos por todo el mundo, creciendo su demanda año tras año (**Figura 2**). Actualmente, la producción de petróleo supera los 4.000 millones de toneladas al año (más de 90 millones de barriles al día, *http://www.iea.org*) y se estima que su consumo crece un 2,3% cada año, impulsado por el incremento mundial de la población (*Oil in the Sea III*, 2003).

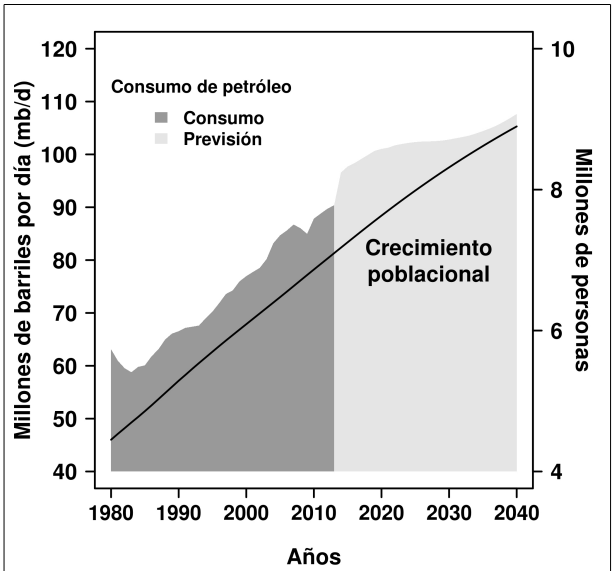

Figura 2: Consumo de petróleo y previsión hasta 2040. El consumo registrado hasta la fecha se muestra en gris oscuro, mientras que en color claro se muestra la previsión para los próximos años. La línea representa el crecimiento poblacional registrado hasta 2014 y su previsión hasta 2040 Fuente: http://www.iea.org.

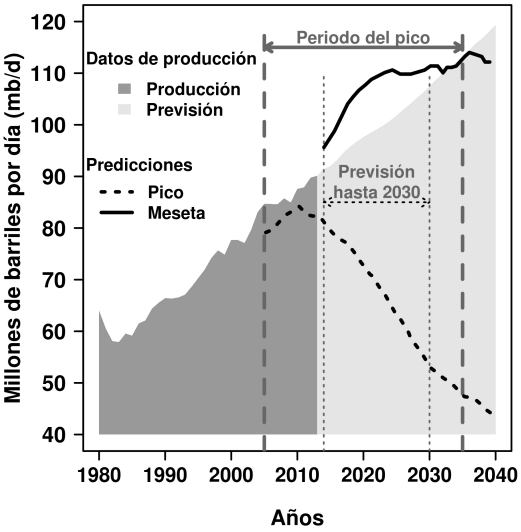

Figura 1: Producción de petróleo y previsión hasta 2040. En gris oscuro se muestra la producción registrada hasta la fecha. En gris claro se muestra la previsión para los próximos años. La línea continua representa la predicción según la teoría de la meseta ondulante, mostrando un estancamiento en la producción. La línea discontinua muestra la predicción según la teoría del pico del petróleo, con un tope a partir del cual la producción se desploma. Las diferentes predicciones fechan la llegada del pico entre la actualidad y el año 2035. Datos obtenidos de http://www.iea.org. Las curvas han sido adaptadas de Jackson & Smith, 2014.

Las predicciones estiman que el petróleo será la principal fuente de combustible al menos hasta 2040. Sin embargo, según los distintos métodos de estimación (**Figura 1**) su producción podría seguir creciendo hasta 2040, o bien podría alcanzarse un pico de producción (estimado entre la actualidad y 2030) sobre el que se estancaría (Jackson & Smith, 2014) o comenzaría a descender (Brandt et al., 2013). En cualquier caso, su condición de recurso fósil hace inevitable que la producción comience a descender en algún momento.

Al margen de la cuestión energética, el suministro y consumo de petróleo conllevan la liberación de residuos en el entorno natural, con dramáticas consecuencias am-

bientales (Ball & Truskewycz, 2013). Gran parte de estos residuos terminan depositados en los mares y océanos, donde la entrada de petróleo se estima por encima de 1,3 millones de toneladas al año. Aunque los vertidos pueden deberse a filtraciones naturales, un gran porcentaje son originados por la actividad humana (**Figura 3**), ya sea de forma accidental o bien intencionada durante las actividades de extracción, transporte, almacenamiento, eliminación de residuos de los cargueros (producidos en la limpieza de los tanques, la eliminación del agua de lastre o en el mantenimiento de los motores) (Kluser et al., 2006), o durante el propio consumo de los productos derivados del petróleo (Awal, 2009; Gong et al., 2014; Kluser et al., 2006; *Oil in the Sea III*, s. f.; C. Wang et al., 2014).

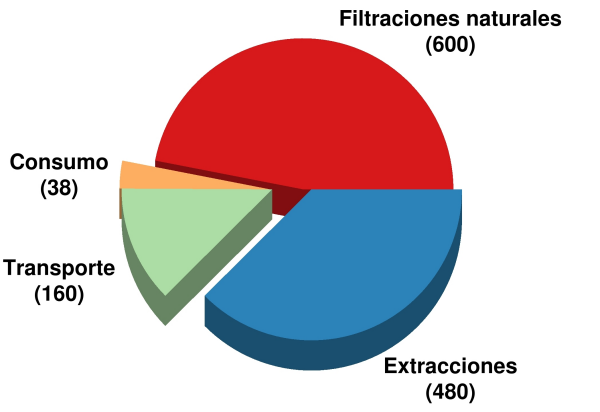

Figura 3: Liberaciones anuales de petróleo en el medio marino. Estimación a partir de datos recogidos entre 1990 y 1999, en miles de toneladas (Awal, 2009).

El petróleo está constituido principalmente de hidrocarburos. Estos compuestos son altamente tóxicos debido a la dificultad que presentan para ser degradados y a su alta hidrofobicidad, que les permite atravesar las bicapas de las membranas celulares que forman las células de los seres vivos (Ball & Truskewycz, 2013; Sikkema et al., 1995). Además, en el caso de los ambientes marinos los residuos se ven sometidos a una serie de procesos físico-químicos que afectan de diferente forma a los distintos tipos de hidrocarburos, haciendo que el comportamiento de los vertidos en el mar sea más difícil de predecir.

1.1. El problema en el Mar Mediterráneo

El Mar Mediterráneo presenta una serie de características que lo convierten en un ecosistema marino muy particular. A pesar de contar con un tamaño (unos 3 millones de Km^2) mayor que otros mares como el Mar Báltico o el Mar del Norte, se encuentra situado en una cuenca semi-cerrada, comunicada con el resto de la superficie marina únicamente a través del estrecho de Gibraltar y el Canal de Suez (Karydis & Kitsiou, 2011), lo que limita el intercambio de agua. La alta temperatura media, entre los 12°C en invierno y los 25°C en verano, promueve una alta tasa metabólica en las diferentes comunidades biológicas que lo habitan (Danovaro, 2003). Además, se encuentra sometido a una alta presión antropogénica, ya que unos 466 millones de personas (en datos de 2010) habitan en los países que lo rodean, de los cuales más de un tercio viven en las zonas de costa (UNEP/MAP, 2012). A esta cantidad hay que añadir los 100 millones de turistas que sólo en verano visitan esas zonas al año (Danovaro, 2003; Karydis & Kitsiou, 2011). La combinación de estas características hacen del Mar Mediterráneo un ecosistema propenso para la contaminación.

Una parte importante del transporte marítimo mundial pasa por sus aguas. Esto se debe por una parte a la gran demanda de los países europeos y por otra a que supone la vía de paso hacia otros mercados como el americano o el Norte de Europa. A pesar de que supone sólo un 1% de la superficie marina del planeta, más de un 20% del tráfico de barcos (**Figura 4**) y buques petroleros se realiza a través de sus aguas (Daffonchio et al., 2013). Se transportan alrededor de 55 millones de toneladas al año sólo de petróleo crudo, y un total de 360 millones teniendo en cuenta los productos refinados (Daffonchio et al., 2013; Kluser et al., 2006). Esto, unido al transporte a través de oleoductos y los desechos procedentes de las refinerías de la costa y las plataformas de extracción mar adentro, contribuye a que sobre el Mar Mediterráneo se viertan alrededor de 300 mil toneladas de hidrocarburos al año (Danovaro, 2003). Si tenemos en cuenta el limitado intercambio de agua, con un tiempo de residencia entre 80 y 100 años (Karydis & Kitsiou, 2011),

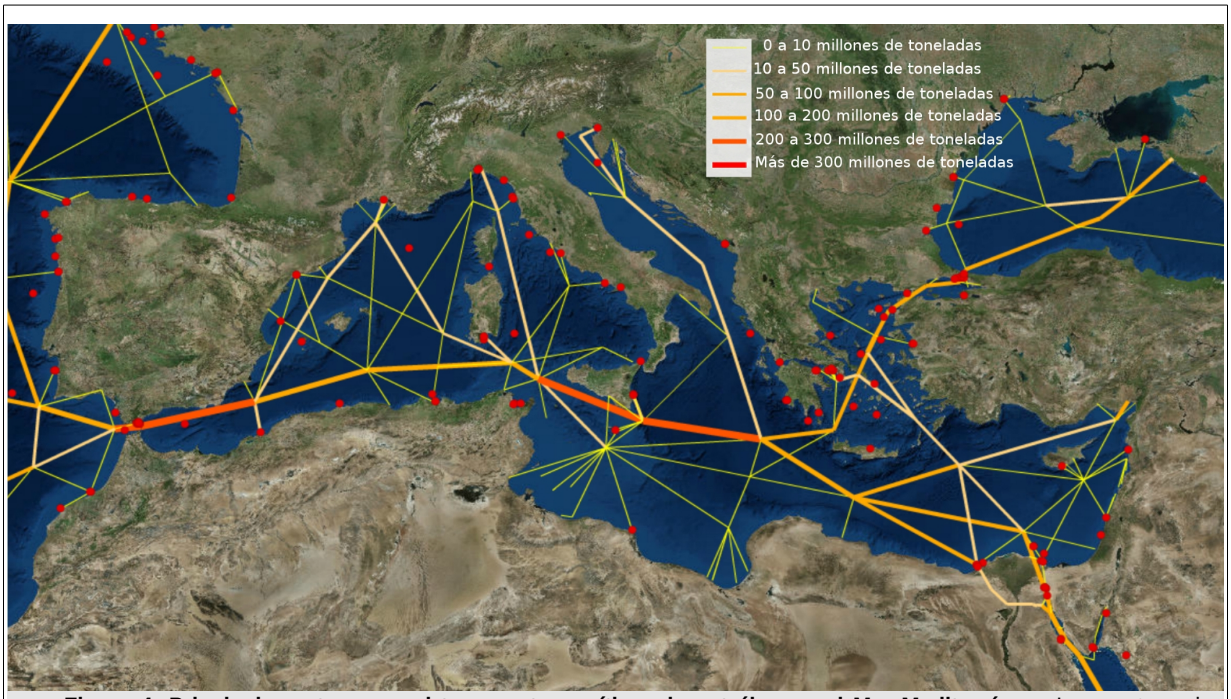

Figura 4: Principales rutas para el transporte marítimo de petróleo en el Mar Mediterráneo. Los puntos rojos indican aquellos lugares donde la ITOPF (siglas en inglés de International Tanker Owners Pollution Federation) ha atendido accidentes de petroleros. Fuente: www.itopf.com.

estos contaminantes permanecen de forma crónica en el Mediterráneo. Además, la presencia de otros contaminantes puede provocar un efecto sinérgico que potencia la toxicidad (Bargiela et al., 2015c; Head, 1998).

El vertido de hidrocarburos es un problema que pone en peligro el medio marino, incluido el Mar Mediterráneo. Éste constituye un ecosistema único, donde se estima que habitan unas 17.000 especies diferentes de eucariotas (Coll et al., 2010) y donde las escasas estimaciones de procariotas muestran una alta diversidad en zonas profundas, entre 1.350 y 35 OTUs (unidad operacional taxonómica) de Bacterias y Arqueas respectivamente (Danovaro et al., 2010). La mejora en las tecnologías de descontaminación como la biorremediación, centrada en aquellos microorganismos capaces de metabolizar los contaminantes, es clave para la conservación de estos ambientes. Sobre este terreno se han realizado estudios en ecosistemas contaminados por hidrocarburos como en el Golfo de México (Bælum et al., 2012; Lu et al., 2011) o la costa Norte de España (Moreno et al., 2013). Sin embargo, a pesar de que existen estudios realizados en el Mediterráneo (Bolognesi et al., 2006), la gran mayoría de ellos se concentran en las zonas situadas al Norte, mientras que las zonas del Sur permanecen muy poco estudiadas (Daffonchio et al., 2013).

1.2. La biorremediación como solución al problema

Existen diferentes métodos para la limpieza y eliminación de los vertidos. Por una parte tenemos los métodos mecánicos como el uso de bombas de agua, separadores y materiales absorbentes que consiguen quitar el material de la superficie (Sheppard et al., 2014). Por otra parte están los métodos químicos como el uso de surfactantes o disolventes, que ayudan a dispersar el petróleo, potencian su degradación o reducen su contacto con otros objetos o la biota (Tamis et al., 2012). Sin embargo, la limpieza mecánica sólo permite la eliminación de una parte del vertido, mientras que los agentes químicos pueden resultar tóxicos para los organismos acuáticos o promover otros fenómenos físicos contraproducentes para la limpieza en caso de no aplicarse de forma adecuada (Tamis et al., 2012). Como alternativa tenemos el uso de

métodos biológicos. Esta tecnología ha recibido especial atención debido a su bajo impacto ambiental, su coste reducido y su gran capacidad para degradar una amplia variedad de compuestos orgánicos (Nikolopoulou et al., 2013).

Los microorganismos autóctonos de los ecosistemas son capaces de degradar de forma natural las sustancias contaminantes, como ocurre con los hidrocarburos (Ron & Rosenberg, 2014). La biorremediación es una rama de la biotecnología que busca potenciar estos procesos de biodegradación para acelerar la eliminación o dispersión de estos compuestos (Sheppard et al., 2014). Dentro de la biorremediación se distinguen dos metodologías diferentes: la bioestimulación y la bioaumentación. La primera consiste en la adición de nutrientes (nitrogenados o fosfatados) para estimular el crecimiento de la microbiota autóctona capaz de degradar los contaminantes. En la bioaumentación se añaden microorganismos especializados en la degradación de un determinado contaminante para multiplicar la tasa de degradación en la zona contaminada (Nikolopoulou et al., 2013; Sheppard et al., 2014).

En la bioestimulación se busca añadir elementos al medio que supongan un factor limitante para el crecimiento microbiano, como es el caso del nitrógeno y el fósforo en los ambientes marinos. Entre los aditivos utilizados encontramos nitratos, fosfatos (Megharaj et al., 2011) o el fosfato amónico (Koren et al., 2003), aunque su alta solubilidad en el agua hacen que se diluyan rápidamente en medios abiertos, por lo que es necesario buscar nuevos fertilizantes más efectivos, económicos y de mayor persistencia en el medio (Ron & Rosenberg, 2014). Algunos compuestos como el ácido úrico parecen ofrecer una posible alternativa (Koren et al., 2003; Nikolopoulou & Kalogerakis, 2008), ya que es un fertilizante natural, producido en la excreción de muchos animales, con poca solubilidad en agua y que puede ser utilizado como fuente de nitrógeno por varias especies microbianas diferentes, metabolizándolo en productos que pueden ser utilizados por las bacterias hidrocarbonoclásticas (degradadoras de hidrocarburos) (Gertler et al., 2015; Ron & Rosenberg, 2014).

La proporción de nitrógeno y fósforo añadido con respecto al carbono (C:N:P) varía de unos estudios a otros dependiendo del tipo de comunidad microbiana, de las condiciones ambientales y el tipo de crudo a degradar. Para la degradación de petróleo de Kuwait se utilizaron 3,2mg de nitrógeno amónico y 0,6mg de fosfato, con una concentración de 70mg de petróleo por litro de agua; mientras que para obtener una degradación máxima de petróleo crudo de Suecia se usaron 1mg de nitrógeno y 0,07mg de fósforo, a una concentración de 8g de petróleo por litro de agua (Atlas, 1981). Este rango afecta de diferente forma a los microorganismos, ya que cada uno de ellos presenta diferentes requerimientos de nutrientes, favoreciendo además actividades catabólicas específicas, en lugar de fomentar todas las actividades catabólicas (Head & Swannell, 1999).

Otra forma de acelerar la biodegradación es aumentando el acceso de los microorganismos a los contaminantes. Usando surfactantes y emulsionantes químicos se incrementa la biodisponibilidad de los hidrocarburos, aumentando el contacto de la microbiota con los compuestos. Algunas bacterias son capaces de sintetizar estas sustancias de forma natural, conocidas como biosurfactantes, y pueden ser utilizados en los procesos de biorremediación sin los problemas ecológicos asociados a los productos de origen químico (Nikolopoulou & Kalogerakis, 2008). Los ramnolípidos, derivados de la L-ramnosa, son actualmente los biosurfactantes más prometedores debido a su carácter biodegradable, baja toxicidad en el agua y la posibilidad de producirlos a partir de recursos renovables. Así, la aplicación de los ramnolípidos en el medio marino ayuda a mejorar la tasa de biodegradación de los hidrocarburos (Chen et al., 2013; Müller et al., 2012). Sin embargo, su alto coste de producción limita su uso generalizado en vertidos marinos reales (Geys et al., 2014; Müller et al., 2012).

Por otra parte, el procedimiento en la bioaumentación se basa en añadir al medio microorganismos con una capacidad probada para degradar los compuestos contaminantes. En ambientes que no han sufrido una exposición previa a la contaminación la respuesta microbiana puede demorarse semanas o meses, por lo que añadir microorganismos ya adaptados a esas condiciones puede acele-

rar el proceso (Megharaj et al., 2011). No obstante, los nuevos miembros de la población se ven afectados por una serie de factores de estrés ambiental, como la fluctuación en la temperatura, el pH, la disponibilidad de nutrientes, los niveles de toxicidad de los contaminantes y la competición por el sustrato. Esto hace que a veces los resultados positivos obtenidos en el laboratorio con un microorganismo o consorcio microbiano no se reproduzcan al aplicar el mismo procedimiento en el medio natural (Tyagi et al., 2011).

Algunas técnicas en desarrollo permiten reducir el estrés ambiental en la bioaumentación. Una de ellas consiste en el uso de materiales de transporte que proporcionan a los inóculos microbianos un nicho que facilita la captación de nutrientes y a su vez ofrece protección frente a los diversos factores físicos. Uno de estos métodos consiste en la encapsulación o inmovilización de las células microbianas usando materiales como alginato, agarosa o poliuretano. La encapsulación ayuda a controlar el flujo de nutrientes, y protege a las células de los factores ambientales y la alta concentración de sustancias tóxicas (Tyagi et al., 2011). Otro material que ha mostrado gran eficiencia en este proceso son las conchas de los moluscos, cuya estructura permite que los microbios se desarrollen en su interior, formando biopelículas, permitiendo así una mayor viabilidad celular que la inducida por otros materiales (Simons et al., 2013). Además esta tecnología supone un método económicamente sostenible, sensible con el medio ambiente y de fácil aplicación (Sheppard et al., 2014; Tyagi et al., 2011).

Como alternativa a la bioaumentación tradicional, donde no se tiene en cuenta el ambiente de origen del inóculo, existe la bioaumentación autóctona (Fantroussi & Agathos, 2005). La gran mayoría de los ecosistemas presentan entre su microbiota especies capaces de degradar los hidrocarburos que forman el petróleo, como los miembros de los géneros *Marinobacter*, *Pseudomonas*, *Alcanivorax* o *Halomonas* (Nikolopoulou et al., 2013a). Así, esta técnica consiste en aislar los microorganismos presentes en el lugar afectado (antes o después de la contaminación) y promover el enriquecimiento de las especies hidrocarbonoclásticas, obteniendo un consorcio de bacterias con potencial para degradar los contaminantes adaptado perfectamente a las condiciones ambientales (Nikolopoulou et al., 2013a; Nikolopoulou et al., 2013b).

La aplicación de bioestimulación o bioaumentación dependerá de las circunstancias dominantes del lugar afectado. Los parámetros físico-químicos (como la temperatura, pH o concentración de O_2) o los biológicos (capacidad de supervivencia, la competencia con la microbiota autóctona o el ambiente de origen de los microorganismos añadidos) determinan la eficacia de cada método (Fodelianakis et al., 2015). La combinación de ambas técnicas supone una estrategia muy prometedora al beneficiar por bioestimulación tanto a microorganismos alóctonos como autóctonos (Fantroussi & Agathos, 2005). Estudios combinando nutrientes, microorganismos y biosurfactantes han mostrado que las mayores tasas de degradación se alcanzan cuando ambas técnicas son utilizadas simultáneamente (Hassanshahian et al., 2014; McKew et al., 2007).

1.3. Perspectivas de futuro en la biorremediación

Hoy por hoy, la remediación basada en la biorremediación está un paso por delante de otros métodos (Tyagi et al., 2011). Sin embargo, todavía se necesita investigar más profundamente para dar con una solución rápida, económica y sostenible que elimine por completo la contaminación asociada a vertidos de hidrocarburos en el mar. Entender como funcionan las comunidades microbianas y sus actividades es uno de los procesos clave para un avance firme en este campo (Kouzuma & Watanabe, 2014). Los avances en las tecnologías de secuenciación han permitido profundizar en dos áreas de investigación diferentes en esta línea: la modificación genética de organismos y las técnicas basadas en la metagenómica.

El acceso a la información genómica permite generar organismos modificados genéticamente para mejorar su rendimiento, los cuales han sido probados en muchas ocasiones para mejorar las tasas de biodegradación de

compuestos especialmente recalcitrantes en sistemas de biorremediación cerrados (Gillespie & Philp, 2013). Mediante técnicas de ingeniería genética se pueden modificar las bacterias para que sean capaces de completar nuevas rutas metabólicas, adquieran resistencia a determinados factores de estrés o para que mejoren su capacidad para captar nutrientes. Esto se consigue mediante la introducción de nuevos genes funcionales, bien a través de su inserción directa en el genoma bacteriano o bien mediante el uso de plásmidos (Dash et al., 2013).

Por otra parte, el análisis de estas comunidades mediante la identificación de marcadores taxonómicos (genes del ARNr 16S), y el desarrollo de técnicas como la metagenómica han superado las limitaciones de los métodos de cultivo. Gracias a esto se han identificado microorganismos y genes implicados en degradación al analizar el material genómico completo presente en una muestra (Gillespie & Philp, 2013; Kouzuma & Watanabe, 2014), permitiendo conocer mejor la composición y el funcionamiento de los microorganismos encargados de la biodegradación en los ambientes contaminados.

En resumen, la biorremediación es una de las tecnologías de limpieza más económica, eficiente y menos agresiva con el medio ambiente de todas las utilizadas. Sin embargo, un mayor entendimiento de las rutas de degradación y las redes metabólicas que llevan a cabo los microorganismos, junto a sus mecanismos de adaptación a las condiciones ambientales, ayudará a mejorar estos métodos de cara a un tratamiento específico para cada tipo de contaminación y ambiente (Tyagi et al., 2011).

2. Composición, transformación y toxicidad del petróleo

Debido al carácter altamente recalcitrante de los hidrocarburos, comprender su composición, su interacción con el medio y las consecuencias que provocan es fundamental para mitigar su efecto en los ecosistemas. Para entender como los microorganismos pueden ayudar en la descontaminación de vertidos marinos, es fundamental conocer las moléculas a las que se enfrentan.

En concreto, cuando hablamos de petróleo asociamos la palabra directamente al petróleo crudo. Sin embargo, este concepto engloba además una gran variedad de sustancias sintéticas originadas tras su procesado. El crudo se origina de forma natural por medio de procesos geoquímicos, y a partir de éste se sintetizan una gran variedad de productos derivados del petróleo. A pesar de que la proporción de diferentes compuestos varía mucho de unos tipos a otros, hablar de cualquier variedad de petróleo es hablar de hidrocarburos, ya que forman casi la totalidad de su composición. Sin embargo, es importante señalar que no todos los hidrocarburos provienen del petróleo, por lo que en esta Tesis Doctoral siempre que mencionamos la palabra hidrocarburos hacemos referencia únicamente a los hidrocarburos alifáticos y aromáticos del petróleo.

2.1. Composición

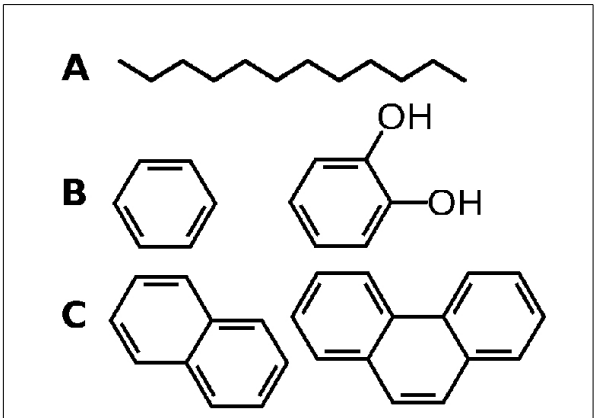

Figura 5: Tipos de Hidrocarburos. a) Hidrocarburo alifático (dodecaeno); b) Hidrocarburos aromáticos (benceno y catecol); c) PAH (naftaleno y fenantreno).

Aunque el petróleo crudo es una mezcla extremadamente compleja de compuestos orgánicos, los hidrocarburos representan aproximadamente el 97% de su composición (*Oil in the Sea III*, 2003). Estos compuestos están formados principalmente por hidrógeno y carbono, y los podemos clasificar en varios grupos (**Figura 5)** según su complejidad: saturados, insaturados, aromáticos y poliaromáticos (PAH), formados a partir de uno o varios anillos de origen bencénico; y también compuestos polares

(con átomos de azufre, nitrógeno u oxígeno), donde se incluyen resinas y asfaltenos (Head et al., 2006; Meghraj et al., 2011; *Oil in the Sea III*,s. f.).

A pesar de esta sencilla clasificación, el petróleo está formado por más de 17.000 compuestos diferentes, con distintas propiedades de densidad, solubilidad y toxicidad. Su concentración en el agua varía dependiendo de si hablamos de un ambiente donde se ha producido un vertido o bien de una zona que se encuentra crónicamente contaminada. En un vertido, como el producido en el golfo de México, la concentración media de los hidrocarburos en los sedimentos marinos es de 18.000 ppm (Romero et al., 2015); en los sedimentos de la bahía de Priolo (Sicilia), afectado por la contaminación crónica debida a la fuerte industrialización y la presencia del puerto marítimo, se observan 4.000 ppm; en comparación con las 15 partes por millón (ppm) del agua limpia (Bargiela, Mapelli, et al., 2015). Además, la proporción de cada tipo de hidrocarburo será distinta dependiendo de la clase de crudo o refinado vertido (**Figura 6**), otorgándoles características físico-químicas diferentes que afectan a su comportamiento y destino final en el ambiente (*Oil in the Sea III*, 2003; Sammarco et al., 2013).

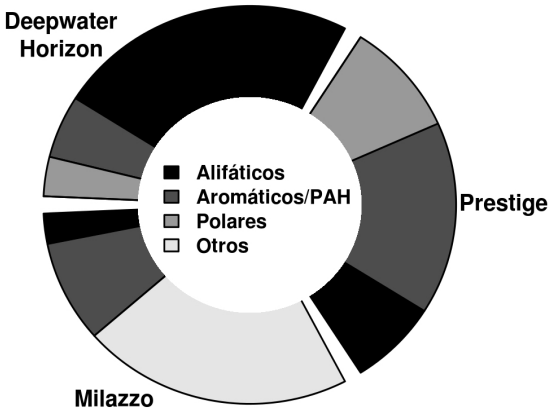

Figura 6: Proporción de cada tipo de hidrocarburo según el tipo de vertido. El vertido del Prestige, en las costas del Noroeste de España, estaba compuesto por crudo de tipo pesado. El vertido en el Golfo de México debido al escape en el Deepwater Horizon estaba compuesto de crudo de tipo ligero. El puerto de Milazzo (Sicilia), al igual que el de Priolo, constituye un ejemplo de zona crónicamente contaminada por la entrada de hidrocarburos. Dentro de la categoría de "Otros" se incluyen: Ácidos grasos, alcoholes y derivados de ambos.

2.2. Destino y transformación de los diferentes componentes del petróleo en el mar

Una vez el petróleo llega al medio marino, éste se ve afectado por múltiples procesos que dependen considerablemente de las condiciones meteorológicas, las condiciones físico-químicas del agua (como su temperatura o la intensidad del oleaje y las corrientes marinas), la diversidad microbiana de la zona y de las propias propiedades del petróleo, incluida la composición. Esto último condiciona la densidad, la solubilidad en el agua y la viscosidad del material. Por una parte, cuanto mayor es el componente en hidrocarburos más complejos, como los aromáticos, la densidad del material es mayor, mientras que será menor si la proporción de alcanos es grande (Rogowska & Namieśnik, 2010). Los petróleos de carácter más denso tenderán a hundirse en la columna de agua, mientras que los de menor densidad permanecerán en la superficie. Por otra parte, la solubilidad de cada compuesto condicionará qué parte del petróleo será disuelta en el agua, la cual es en todo caso siempre pequeña, y no suele superar el 1% del petróleo vertido, normalmente situado entre 1,0 y 100 ppm (*Oil in the Sea III*, 2003; Rogowska & Namieśnik, 2010a; Sammarco et al., 2013). Sin embargo, aunque esta fracción no sea muy grande, los componentes que acaban disueltos en el agua son de gran importancia, ya que presentan un nivel muy elevado de toxicidad. Por último, la tercera propiedad a tener en cuenta es la viscosidad, que determina la resistencia del material a fluir en un líquido, y viene determinada por la proporción entre componentes de alto y bajo peso molecular en el petróleo. Cuanto mayor es el porcentaje en alcanos y compuestos volátiles, como los BTEX, menor es la viscosidad. Sin embargo, será mayor cuanto más alta sea la concentración de PAH, resinas, asfaltenos y alcanos de alto peso molecular (cadenas de más de 30 carbonos) (Martin et al., 2014; *Oil in the Sea III*, 2003). La viscosidad afecta a la forma en la que el petróleo se expande en el medio, formando manchas uniformes en la superficie cuando es poco viscoso o fragmentándose formando pequeñas emulsiones con el agua

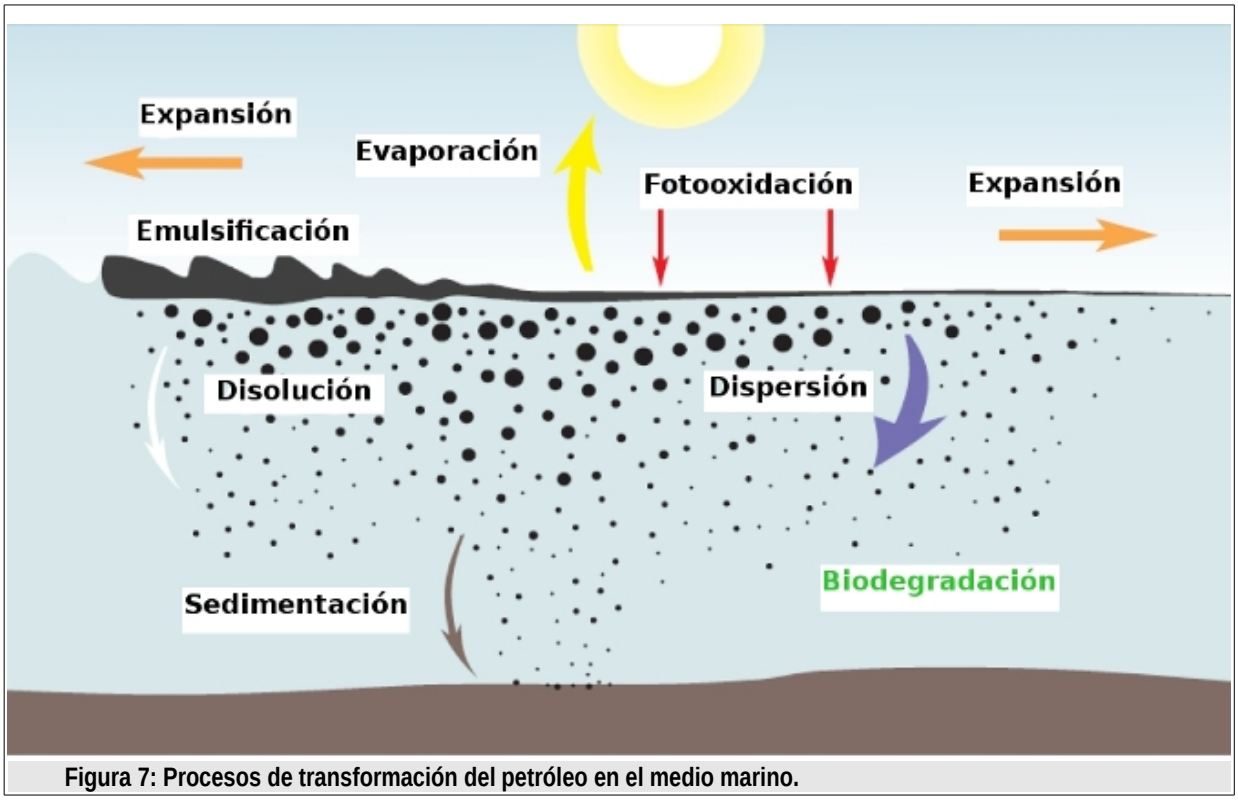

Figura 7: Procesos de transformación del petróleo en el medio marino.

cuando es muy viscoso (Rogowska & Namieśnik, 2010a).

Más allá de sus propiedades intrínsecas, sobre el petróleo ocurren una serie de procesos de desgaste (conocidos como *weathering* en inglés) que provocan cambios físico-químicos que influyen en la transformación, degradación y transporte del material vertido. El conjunto de estos procesos (**Figura 7**) lo componen la evaporación, la fotooxidación, la disolución, la emulsificación, el transporte (debido a la expansión horizontal y la dispersión en sentido vertical) y la biodegradación (Daling et al., 2014; *Oil in the Sea III*, 2003; Rogowska & Namieśnik, 2010a; C. Wang et al., 2014). El efecto conjunto de todos estos fenómenos lleva al desplazamiento y diseminación de los distintos componentes, moviéndolos hasta llegar a las zonas de costa, mezclándolos con la columna de agua o provocando su sedimentación en el fondo, afectando de diferente manera al medio ambiente.

Estos procesos (resumidos en la **Figura 7**) presentan una gran importancia en el destino y modificación de la composición del petróleo; sin embargo, en esta Tesis Doctoral nos centraremos únicamente en el fenómeno de biodegradación.

2.3. Consecuencias ambientales de los vertidos

El vertido de hidrocarburos afecta al sistema marino en diferentes niveles. Por una parte, en el caso de liberarse una cantidad considerable de golpe, como ocurre en los accidentes de barcos petroleros, la mancha forma una capa que cubre la zona superficial, dificultando el intercambio de gases con el aire (Guitart et al., 2008) y limita la penetración de la radiación solar, afectando a la tasa de fotosíntesis (Rogowska & Namieśnik, 2010a), con los consecuentes efectos sobre la flora y los organismos marinos que se sirven de este proceso. Los efectos nocivos debido al contacto, inhalación o ingestión del petróleo sobre peces, aves y mamíferos han sido ampliamente estudiados, provocando su muerte directamente o afectando a su crecimiento y capacidad reproductiva. Además, la acumulación de los contaminantes en los tejidos de los organismos puede provocar su transmisión a través de la cadena alimenticia al ser consumidos por los niveles superiores (Almeda et al., 2013; Ball & Trus-

kewycz, 2013; de Soysa et al., 2012; Gray, 2002; Martin et al., 2014; *Oil in the Sea III*, 2003; Pérez-Cadahía et al., 2004; Rebar et al., 1995; Rogowska & Namieśnik, 2010b).

La toxicidad de los hidrocarburos está muy relacionada con su hidrofobicidad o lipofilia, permitiéndoles interactuar con las membranas lipídicas de las células (Sikkema et al., 1995). Esta propiedad les permite ser transportados a través del flujo sanguíneo por todo el organismo (Ball & Truskewycz, 2013), o producir daños a nivel de membrana, alterando enzimas (ATPasas, oxidorreductasas o enzimas de transducción de señales) alojadas en la bicapa lipídica (Sikkema et al., 1995). Si se introducen en la célula, pueden sufrir modificaciones que dan lugar a metabolitos que interaccionan con el ADN desencadenando diferentes efectos mutagénicos o carcinogénicos, como ocurre con muchos PAH (Ball & Truskewycz, 2013; Xue & Warshawsky, 2005).

3. Biodegradación de los hidrocarburos del petróleo

Dentro de todos los procesos a los que el petróleo se ve sometido al entrar en contacto con el medio marino, el más interesante y complejo desde el punto de vista biotecnológico es la biodegradación, en donde parte de los hidrocarburos son metabolizados y degradados por la microbiota marina, eliminándolos del medio.

Los hidrocarburos son degradados por microorganismos autóctonos cuyo tipo de metabolismo les permite utilizar estos compuestos como fuente de carbono (Cappello et al., 2007a). Cuando el petróleo entra en el medio natural se produce un fuerte descenso de la diversidad microbiana. Yakimov et al. observaron en experimentos con microcosmos que el índice Shannon de diversidad descendía de 2,593 en la comunidad microbiana natural hasta 1,201 en la crecida con naftaleno (Yakimov et al., 2005). Este descenso viene acompañado de una selección en favor de las especies degradadoras de hidrocarburos, que normalmente presentan una baja frecuencia cuando el medio marino no está contaminado (Cappello et al., 2007a; Head, Jones, & Röling, 2006). Muchas de ellas han podido ser caracterizadas, sin embargo, la gran mayoría de las especies microbianas presentes en el medio siguen sin identificarse debido a la imposibilidad de cultivarlas en el laboratorio (Harayama et al., 2004).

El mecanismo de degradación más rápido y completo es el que se realiza bajo condiciones aerobias, en donde la reacción enzimática clave consiste en un primer ataque oxidativo sobre el contaminante y la activación de la molécula mediante la incorporación de oxígeno, catalizada por diferentes tipos de oxigenasas (Das & Chandran, 2010). La biodegradacion de hidrocarburos también es posible bajo condiciones anaerobias, existiendo varias alternativas catabólicas basadas en reacciones de reducción en las que se emplean otro tipo de enzimas diferentes a las oxigenasas (Boll et al., 2014; Díaz et al., 2013).

Una vez que comienza el proceso de biodegradación, tanto la distribución y la abundancia de los grupos microbianos como la cantidad de las diferentes enzimas que estos contienen, varían de acuerdo a una dinámica ambiental que depende fundamentalmente de: 1) la abundancia y disponibilidad de los diferentes tipos de hidrocarburos en el medio (Head et al., 2006); 2) la susceptibilidad de éstos a ser degradados por los microorganismos (Das & Chandran, 2010; Head et al., 2006); y 3) las condiciones físico-químicas del entorno como la temperatura (Gutierrez et al., 2013), la concentración de O_2 (Kimes et al., 2013) o la disponibilidad de nutrientes (Das & Chandran, 2010; McGenity et al., 2012).

3.1. Principales microorganismos degradadores de hidrocarburos

Cada tipo de microorganismo presenta capacidades metabólicas distintas, degradando diferentes tipos de sustratos. Dentro de aquellos que son capaces de metabolizar los hidrocarburos encontramos el grupo de bacterias hidrocarbonoclásticas obligadas (BHO), las cuales utilizan únicamente este tipo de compuesto como fuente de carbono. Las bacterias más representativas dentro de

este grupo se encuentran dentro de la clase *γ-Proteobacteria* del filo *Proteobacteria*, donde destacan los géneros *Alcanivorax*, *Cycloclasticus*, *Oleispira*, *Thalassolituus* y *Oleiphilus* (Harayama et al., 2004; Liu & Liu, 2013). *Alcanivorax* es uno de los géneros mejor estudiados, siendo *A. borkumensis* la primera bacteria hidrocarbonoclástica de que se ha secuenciado su genoma (Golyshin et al., 2003; Yakimov et al., 1998; Yakimov et al., 2007). Los miembros de este género crecen en presencia de n-alcanos y alcanos ramificados, siendo incapaces de utilizar cualquier azúcar o amino ácido como fuente de carbono. Lo mismo ocurre con *Thalassolituus* (Yakimov et al., 2004), *Oleiphilus* (Golyshin et al., 2002) *y Oleispira* (Yakimov et al., 2003), con una alta especificidad por los alcanos alifáticos (Yakimov et al., 2004). Los miembros del género *Cycloclasticus* (Dyksterhouse et al., 1995) crecen en medios con PAHs como el naftaleno, el fenantreno o el antraceno (Harayama et al., 2004; Messina et al., n.d.).

Además de las BHO, otros tipos de bacterias son capaces de metabolizar los hidrocarburos como una de sus posibles fuentes de carbono. Dentro de la misma clase *γ-Proteobacteria* encontramos algunos ejemplos como *Neptunomonas,* cuyas especies son capaces de degradar diferentes tipos de PAHs, como el naftaleno (Harayama et al., 2004; Hedlund et al., 1999). Los géneros *Marinobacter* o *Pseudomonas* son ampliamente conocidos por su versatilidad para degradar tanto alcanos alifáticos como PAHs (Fathepure, 2014; Harayama et al., 2004; Tapilatu et al., 2010). En la clase *α-Proteobacteria* podemos señalar otros ejemplos como los miembros de los siguientes géneros: *Sphingomonas*, capaces de degradar una gran variedad de compuestos recalcitrantes, entre ellos PAHs como naftaleno, fluoreno, antraceno o fenantreno (Luo et al., 2012); *Thalassospira*, relacionados con la degradación de hidrocarburos alifáticos (Jiménez et al., 2011); o *Paracoccus,* involucrados en la degradación de PAHs como el fenantreno (Sauret et al., 2014).

A pesar de que las clases *α-* y *γ-Proteobacteria* suelen dominar las comunidades microbianas en los ecosistemas marinos tras su exposición a los hidrocarburos, otros filos también tienen miembros capaces de degradar estos compuestos, como ocurre con los géneros *Rhodococcus* y *Gordonia*, pertenecientes al filo *Actinobacteria*, capaces de degradar tanto alcanos como PAHs (Gallego et al., 2014; Wang et al., 2014; Yang et al., 2014); o el género *Planococcus*, del filo *Firmicutes*, que presenta miembros capaces de degradar tanto alcanos de diferente longitud, como hidrocarburos monoaromáticos y PAHs (Awadhi et al., 2012; H. Li et al., 2006).

Hasta ahora, todas los géneros bacterianos citados degradan los hidrocarburos en condiciones aerobias, utilizando la capacidad oxidativa del O_2 mediante mono- y dioxigenasas que rompen los diferentes enlaces que forman estos compuestos. Sin embargo, aunque más lenta, la degradación en ausencia de O_2 también es posible. En este caso, las comunidades microbianas marinas que se encuentran en condiciones anóxicas suelen estar dominadas por bacterias de la clase *δ-Proteobacteria* (Acosta-González et al., 2013; Genovese et al., 2014; Kimes et al., 2013), implicadas en la degradación de hidrocarburos alifáticos y aromáticos en anaerobiosis, como los miembros de los órdenes *Desulfovibrio*, *Desulfobacterales* y *Desulfuromonadales* (Kimes et al., 2013).

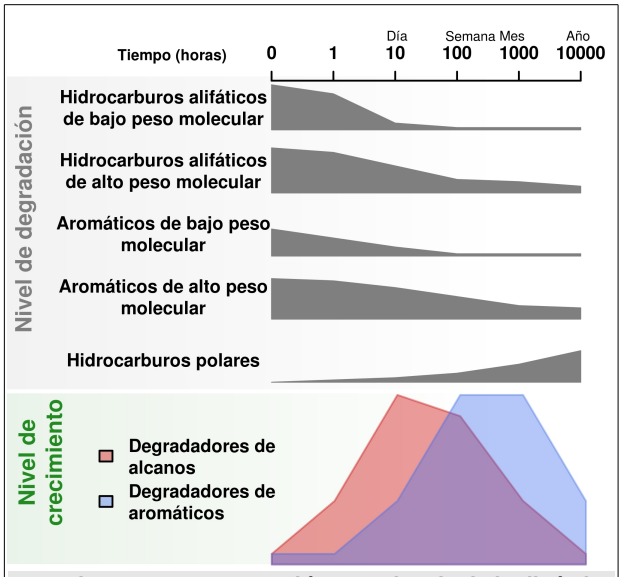

Figura 8: Representación aproximada de la dinámica de degradación de los hidrocarburos. Arriba se muestra como los hidrocarburos alifáticos son degradados más rápidamente que los hidrocarburos más complejos. Abajo se representa cómo los organismos degradadores de hidrocarburos alifáticos proliferan antes que los encargados de degradar los aromáticos y poliaromáticos. Figura adaptada de Head et al., 2006.

En lo que respecta a las arqueas (dominio *Archaea*), su respuesta a los efectos debidos al vertido de hidrocarburos es todavía un tema en controversia. Bajo condiciones aerobias, la capacidad de estos organismos para degradar hidrocarburos sólo ha sido demostrada en ecosistemas hipersalinos, donde se han detectado géneros como *Haloferax*, *Halobacterium* y *Halococcus* creciendo en medios tanto con PAHs como con alcanos de diferente longitud como única fuente de carbono (Fathepure, 2014; Jurelevicius et al., 2014). Sin embargo, en medios marinos aerobios no están muy claros los efectos que la entrada de petróleo produce en las poblaciones de este tipo de microorganismos, ni tampoco han mostrado un papel significativo en la degradación de hidrocarburos (Redmond & Valentine, 2012). No obstante, sí es conocida su actividad bajo condiciones anaerobias, donde las arqueas metanotróficas anaerobias (ANMEs) intervienen en la oxidación anaerobia del metano (OAM) (Hawley et al., 2014).

En un medio contaminado por hidrocarburos, el afloramiento de estos microorganismos dependerá de la complejidad del tipo de compuestos que estén especializados en degradar, ya que cada tipo de hidrocarburo tardará más tiempo o menos en degradarse, como se muestra en la **Figura 8** (Head et al., 2006).

3.2. Rutas catabólicas y enzimas involucradas en la biodegradación de hidrocarburos

Como se ha comentado anteriormente, las dos estrategias principales para la degradación de los hidrocarburos dependen de la disponibilidad de oxígeno (Díaz et al., 2013). Sin embargo, en ambas alternativas el primer paso en la ruta de degradación de los sustratos consiste en un primer ataque (activación) para desestabilizar la molécula (Fuchs et al., 2011).

En presencia de oxígeno el paso principal se realiza a través de reacciones oxidativas llevadas a cabo por oxigenasas/hidroxilasas que catalizan la inserción de oxígeno en un sustrato orgánico (Torres Pazmiño et al., 2010).

Las oxigenasas e hidroxilasas que intervienen en la degradación aerobia son un tipo de enzimas que constituyen un subtipo dentro las oxidoreductasas que se divide a su vez en monooxigenasas, enzimas que catalizan la inserción de un único átomo de oxígeno, y dioxigenasas, que catalizan la inserción de dos átomos de oxígeno (Torres Pazmiño et al., 2010) (**Figura 9**). Estas enzimas activan por oxidación el compuesto a degradar, dando lugar a productos hidroxilados que, en el caso de los compuestos aromáticos, sufren un posterior ataque oxidativo para producir la ruptura del anillo (Fuchs et al., 2011).

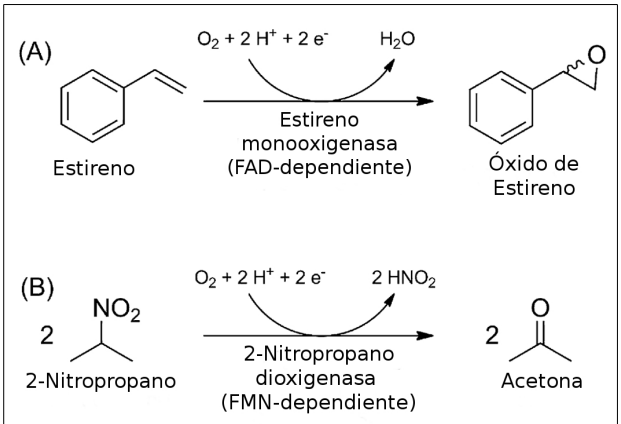

Figura 9: Acción enzimática de las oxigenasas. A), ejemplo modelo de la acción de una monooxigenasa (estireno monooxigenasa), B), ejemplo modelo de la acción de una dioxigenasa (2-nitropropano dioxigenasa). Adaptación de Torres Pazmiño et al., 2010.

En ausencia de oxígeno las oxigenasas ya no pueden actuar, y la degradación se realiza a través de reacciones de reducción. Para ello, primero la molécula necesita ser activada, por lo que se necesita realizar una oxidación del sustrato en ausencia de O_2. Hasta la fecha se conocen tres estrategias diferentes (adición de fumarato, hidroxilación y carboxilación), cuya elección dependerá de la energía de disociación del enlace C-H del átomo de carbono que vaya a ser oxidado (Boll et al., 2014; Fuchs et al., 2011).

En todo caso, una vez iniciada su activación, los sustratos son transformados para dar lugar a unos poco intermediarios centrales que son más fácilmente sometidos a reacciones de reducción (Boll et al., 2002; Fuchs et al., 2011).

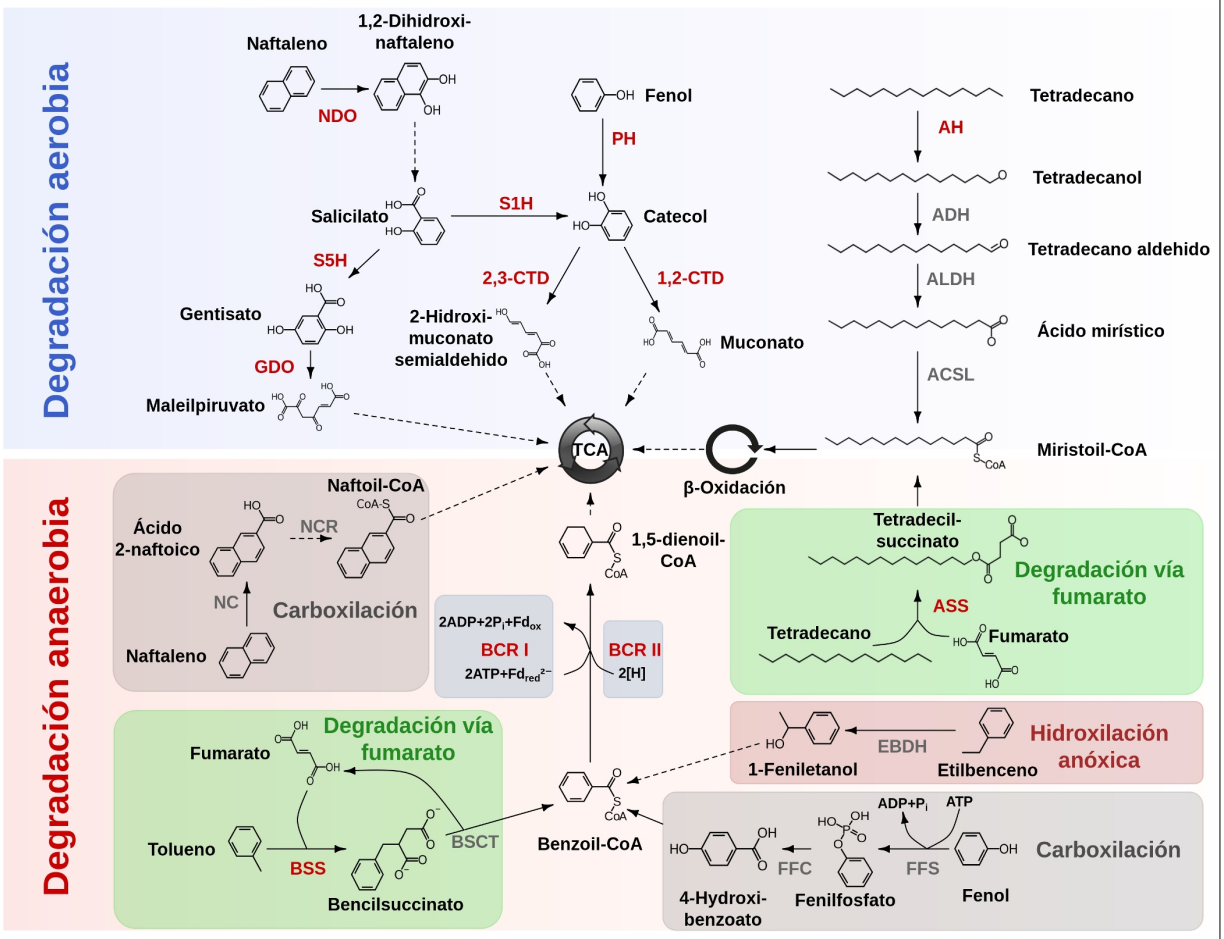

Figura 10: Ejemplos de rutas de biodegradación de hidrocarburos. En la parte superior (sombreada en azul) se muestran ejemplos clásicos de degradación aerobia, destacando en rojo aquellas reacciones catalizadas por monooxigenasas/hidrolasas o dioxigenasas y el resto de enzimas en gris: naftaleno dioxigenasa, NDO; salicilato 1-hidroxilasa, S1H; salicilato 5-hidroxilasa, S5H; Gentisato dioxigenasa, GDO; Fenol hidroxilasa, PH; catecol 2,3-dioxigenasa, 2,3-CTD; catechol 1,2-dioxigenasa, 1,2-CTD; alcano hidroxilasa, AH; alcohol dehidrogenasa, ADH; aldehido dehidrogenasa, ALDH; acil-CoA sintetasa, ACSL. En la zona inferior (sombreada en rojo) se muestran ejemplos de las 3 estrategias conocidas para la degradación anaerobia, destacando en rojo las enzimas más conocidas de este proceso y en gris el resto: bencilsuccinato sintasa; BSS; acilsuccinato sintasa, ASS; benzoil-CoA reductasa clase I, BCR I; bonzoil-CoA reductasa clase II, BCR II; naftaleno carboxilasa, NC; noftoil-CoA reductasa, NCR; succinil-CoA:bencilsuccinato transferasa, BSCT; etilbenceno dehidrogenasa, EBDH; fenilfosfato sintasa, FFS; fenilfosfato carboxilasa, FFC. La degradación del benzoil-CoA a 1,5-dienoil-CoA se lleva a cabo bien por la BCR I, con gasto de ATP, o bien por la BCR II, sin gasto de ATP.

A continuación se detalla de forma general la degradación anaerobia, que aunque no es una parte central de esta Tesis Doctoral, merece la pena describir (**Figura 10**). Posteriormente, se profundizará más concretamente en la degradación aerobia, que constituye el núcleo principal de los estudios realizados en esta Tesis Doctoral.

3.2.1. Degradación anaerobia

La degradación anaerobia de compuestos aromáticos se basa en la desestabilización del núcleo aromático mediante procesos reductivos, en vez de oxidativos. Aquellos compuestos aromáticos con algún grupo hidroxilo en posición *meta* son convertidos a resorcinol, hidroxihidroquinona o floroglucinol (1,3-dihidroxibenceno, 1,2,4-trihidroxibenceno y 1,3,5-trihidroxibenceno, respectivamente), los cuales son desaromatizados directamente por enzimas dehidrogenasas/reductasas sin necesidad de mayor activación (Boll et al., 2014; Fuchs et

al., 2011). El resto de compuestos sufren una oxidación anóxica que da lugar a intermediarios formados por tioésteres de Coenzima A (CoA), que son posteriormente desaromatizados por enzimas de tipo reductasa. Aquí, la ruta más importante es la del benzoil-CoA, por la que se degradan un gran número de sustratos como el fenol, fenilacetato, anilina, alquilbencenos y varios hidrobenzoatos (Philipp & Schink, 2012).

Se conocen tres estrategias diferentes para el ataque inicial de los hidrocarburos en ausencia de O_2. La primera es la adición fumarato, como ocurre en la degradación del tolueno. Aquí, el sustrato es unido a una molécula de fumarato para dar bencilsuccinato, mediante la enzima bencilsuccinato sintasa, que acaba transformándose para dar benzoil-CoA, regenerándose el fumarato en el proceso (**Figura 10**; Boll et al., 2014). Los alcanos también son degradados siguiendo esta estrategia. El fumarato es añadido de forma similar por una alquil-succinato sintasa a las cadenas de alcanos, dando lugar a un alquil-succinato que es conjugado posteriormente con CoA, formando un derivado acil-CoA, que es degradado a través de la β-oxidación. En este caso, el fumarato acaba degradado a CO_2, acetil-CoA y propionil-CoA, siendo más complicada la regeneración del fumarato (Boll et al., 2002; Khelifi et al., 2014; Kniemeyer et al., 2007; Rojo, 2009).

La segunda estrategia consiste en la hidroxilación independiente de O_2. Este es el caso de compuestos como el etilbenceno (**Figura 10**), sobre el que actúa la enzima etilbenceno dehidrogenasa, capaz de hidroxilar el compuesto utilizando una molécula de agua en lugar de O_2 (Heider, 2007; Szaleniec et al., 2014).

La tercera estrategia conocida es la carboxilación. Por este proceso se degradan anaeróbicamente compuestos como el fenol, el cual primero es fosforilado a fenilfosfato por la enzima fenilfosfato sintasa, consumiendo ATP, que luego es carboxilado por una fenilfosfato carboxilasa para dar 4-hidroxibenzoato, que se conjuga finalmente con CoA para dar benzoil-CoA (Fuchs, 2008; Philipp & Schink, 2012). Hasta la fecha, esta vía de activación parece también la más probable para compuestos no sustituidos como el benceno o poliaromáticos como el naftaleno. Estos sufrirían teóricamente una carboxilación directa a benzoato y ácido 2-naftoico respectivamente, que luego darían lugar a sus correspondientes intermediarios en forma de tioésteres de CoA, benzoil-CoA y naftoil-CoA (Boll et al., 2014; Luo et al., 2014; Meckenstock & Mouttaki, 2011).

La desaromatización del benzoil-CoA presenta como paso clave su reducción a 1,5-dienoil-CoA, que puede seguir dos estrategias diferentes: dependiente de ATP, realizada por benzoil-CoA reductasas de clase I, hidrolizando dos moléculas de ATP y usando dos moléculas de ferredoxina como donador de electrones; o independiente de ATP, donde intervienen benzoil-CoA reductasas de clase II, sin gasto de ATP (Boll et al., 2014; Fuchs et al., 2011; Philipp & Schink, 2012). Ambas rutas dan lugar a la formación de 1,5-dienoil-CoA (**Figura 10**) que luego es sometido a procesos de degradación que incluyen reacciones similares a la β-oxidación, hidrólisis del anillo y descarboxilación que acaban formando derivados del ciclo de Krebs (Foght, 2008; Fuchs et al., 2011).

3.2.2. Degradación aerobia

En el caso de los alcanos, la degradación aerobia la llevan a cabo monooxigenasas que oxidan el extremo metil terminal para dar lugar al correspondiente alcohol, que posteriormente es de nuevo oxidado para formar un aldehido que finalmente es convertido a ácido graso. Este ácido graso se conjuga después con Coenzima A (CoA) para ser procesado en la β-oxidación (**Figura 10**) y generar acetil-CoA que entra en el ciclo de los ácidos tricarboxílicos (TCA) (Rojo, 2009).

En el proceso clásico de degradación aerobia de compuestos aromáticos intervienen dioxigenasas que se encargan de la ruptura del anillo bencénico. La mayoría de las rutas típicas de degradación convergen en determinados intermediarios clave como el catecol o el protocatecuato, sobre los que actúan dioxigenasas que provocan la escisión del anillo para dar lugar a productos que son posteriormente convertidos a intermediarios del TCA (Díaz et al., 2013). En el caso de los compuestos poliaromáticos, éstos se degradan por reiteraciones continuas

de las estrategias seguidas para la degradación de los compuestos monoaromáticos (Vaillancourt et al., 2006), actuando primero un tipo de oxigenasas que activan la molécula formando un intermediario dihidroxilado que es después catabolizado por otras dioxigenasas que realizan la escisión del anillo, formando finalmente, tras varios ciclos, intermediarios centrales como los ya mencionados (Peng et al., 2008).

La ruptura del anillo bencénico se produce en posición *ortho,* entre los dos grupos hidroxilo, o *meta,* adyacente a los grupos hidroxilo (**Figura 10**, Fetzner, 2012), lo que divide a las familias de dioxigenasas en intradiol (INTRA) o extradiol (EXDO) dioxigenasas, respectivamente (Fuchs et al., 2011; Omokoko et al., 2008). Existen también rutas de degradación que forman intermediarios no catecólicos (sin grupos hidroxilo en las posiciones *ortho* y *meta*), como son el gentisato o el homogentisato, los cuales son degradados por otra clase de extradiol dioxigenasas (Díaz et al., 2013; Fetzner, 2012).

3.3. Clasificación de las enzimas de biodegradación

Como hemos visto en los apartados anteriores, los procesos de biodegradación requieren de estrategias especiales por parte de los microorganismos. La degradación aerobia de hidrocarburos engloba una enorme cantidad de rutas catabólicas, que requieren de muchos tipos de enzimas diferentes (ver más adelante en la **Figura 13**). A continuación se describen algunos de los tipos más importantes.

3.3.1. Alcano hidroxilasas y citocromos P450

El proceso de biodegradación de alcanos comienza por una hidroxilación en posición terminal, que se lleva a cabo por diferentes familias de monooxigenasas según la longitud de la cadena del alcano (Wang & Shao, 2013): de 1 a 4 carbonos (de metano a butano, oxidados por enzimas del tipo metano monooxigenasa), de 5 a 16 carbonos (de pentano a hexadecano, oxidados por hidroxilasas dependientes de Fe sin grupo hemo (Fe-no hemo) integradas en la membrana (AlkB) o por citocromos P450), o de más de 17 carbonos (alcanos más largos, oxidados por un grupo de enzimas poco estudiado) (van Beilen & Funhoff, 2007).

Se conocen dos tipos de metano monooxigenasa (MMO), una forma adherida a la membrana (pMMO) presente en todos los organismos metanotrofos, y una forma soluble (sMMO) mucho menos abundante. Estructuralmente son muy diferentes una de otra, pero la diferencia principal reside en su centro activo, compuesto en la pMMO por dos átomos de cobre, mientras que la sMMO es una monooxigenasa Fe-no hemo, con dos átomos de Fe en el centro activo (Culpepper & Rosenzweig, 2012). Esta diferencia hace que la expresión de una u otra forma dependa de la presencia de Cu, expresándose la sMMO cuando su concentración es limitada en aquellos microorganismos que presenten las dos formas (Culpepper & Rosenzweig, 2012; Rojo, 2009).

Las enzimas capaces de degradar etano, propano o butano presentan similitudes con la sMMO y la pMMO, como la butano monooxigenasa (BMO) de *Pseudomonas butanovora*, la cual contiene una estructura similar a la sMMO y puede hidroxilar alcanos de 2 a 9 carbonos de longitud (Austin & Groves, 2011; Cooley et al., 2009; Rojo, 2009).

Las alcano hidroxilasas adheridas a la membrana (AlkB) son un tipo de monooxigenasas Fe-no hemo (Torres Pazmiño et al., 2010) constituidas por el correspondiente dominio monooxigenasa, un dominio rubredoxina reductasa que obtiene electrones del NADH, y otro dominio compuesto por una rubredoxina que facilita el transporte de esos electrones entre los componentes reductasa y monooxigenasa, utilizando FAD (dinucleótido de flavina adenina) como cofactor (Rojo, 2009). Su centro activo presenta, como la sMMO, dos átomos de Fe, y oxidan sustratos de longitud de cadena entre 5 y 16 carbonos (Smith et al., 2013; van Beilen & Funhoff, 2007).

Los citocromos P450 son un tipo de proteínas que se encuentran distribuidas en todo tipo de organismos. Las que se encuentran presentes en bacterias capaces de degradar alcanos pertenecen a la familia CYP153 (Austin & Groves, 2011) y están compuestas por tres componentes diferentes, el citocromo, una ferredoxina reductasa que obtiene electrones del NADH y una ferredoxina que

transporta esos electrones al citocromo. En su centro catalítico presenta un grupo hemo, formado por una anillo de porfirina asociado a un átomo de Fe, y oxidan sustratos de longitud de 5 a 11 carbonos (Rojo, 2009; van Beilen & Funhoff, 2007).

Las alcano hidroxilasas encargadas de oxidar sustratos de cadena larga son totalmente diferentes a las AlkB o los citocromos P450. Aunque se sabe poco acerca de estas enzimas se han identificado dos de ellas, AlmA en *Acinetobacter sp.* M-1 y LadA en *Geobacillus thermodentrificans* NG80-2, que oxidan alcanos de mas de 20 carbonos (Austin & Groves, 2011; Bowman & Deming, 2014). AlmA está clasificada putativamente dentro de las flavina monooxigenasas, con una baja similitud de secuencia con LadA (Austin & Groves, 2011; Wang & Shao, 2012). Por su parte, LadA es una flavoproteína relacionada con la familia de las luciferasas, que utiliza flavina mononucleótido (FMN) como flavina. Además, está compuesta de una flavina reductasa dependiente de NAD(P)H y el correspondiente componente monooxigenasa (Boonmak et al., 2014; Li et al., 2008).

3.3.2. Oxigenasas para la activación del anillo aromático

Los compuestos aromáticos y poliaromáticos requieren de un primer ataque oxidativo que permite desestabilizar la molécula para proceder con la posterior escisión del anillo aromático. Dentro de las enzimas que realizan este primer paso de degradación encontramos algunas monooxigenasas dependientes de flavinas (Huijbers et al., 2014) y las oxigenasas de hidroxilación del anillo (RHO), también conocidas como oxigenasas de tipo Rieske debido al dominio [2Fe-2S] que presentan en la subunidad catalítica (Peng et al., 2010; Pérez-Pantoja et al., 2010).

Las monooxigenasas dependientes de flavinas catalizan la incorporación de un átomo de la molécula de O_2 en el sustrato, reduciendo el restante a H_2O (Huijbers et al., 2014). Estas enzimas (**Figura 11**) presentan una subunidad flavina reductasa que utiliza NAD(P)H como donador de electrones (Huijbers et al., 2014; van Berkel et al., 2006) para reducir la flavina (FAD o FMN), que se encuentra unida a la enzima como grupo prostético o bien actúa como coenzima, la cual es finalmente utilizada por el componente monooxigenasa para oxidar el sustrato (Torres Pazmiño et al., 2010).

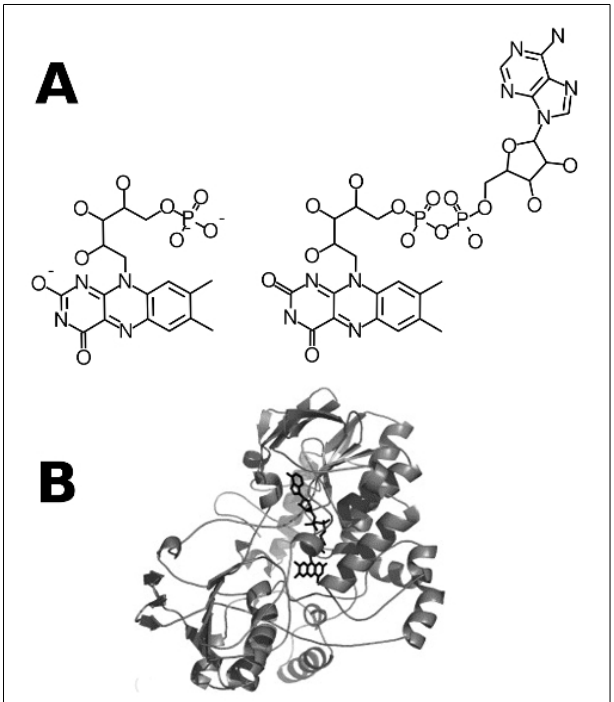

Figura 11: Monooxigenasas dependientes de flavinas. A) Las flavinas FNM (flavín mononucleótido) y FAD (flavín adenín dinucleótido). B) Estructura de la monooxigenasa dependiente de flavina fenilacetona monooxigenasa de *Thermobifida fusca*, con una molécula de FAD en el centro como cofactor (Berkel et al., 2006).

Dentro de este grupo encontramos algunas monooxigenasas que oxidan alcanos de cadena larga (como la LadA del apartado anterior), pero muchas de ellas intervienen en la oxidación de compuestos aromáticos y poliaromáticos, como la salicilato 1-hidroxilasa caracterizada en *Pseudomonas putida (van Berkel et al., 2006),* que cataliza la hidroxilación del salicilato a catecol, o la fenol hidroxilasa de *Rhodococcus erythropolis* UPV-1 (Saa et al., 2009), que cataliza la oxidación del fenol a catecol.

Las RHO son enzimas multicomponente que catalizan la inserción de uno o dos grupos hidroxilo en el sustrato, formadas (**Figura 12**) básicamente por una cadena de transporte electrónico (CTE) y el componente oxige-

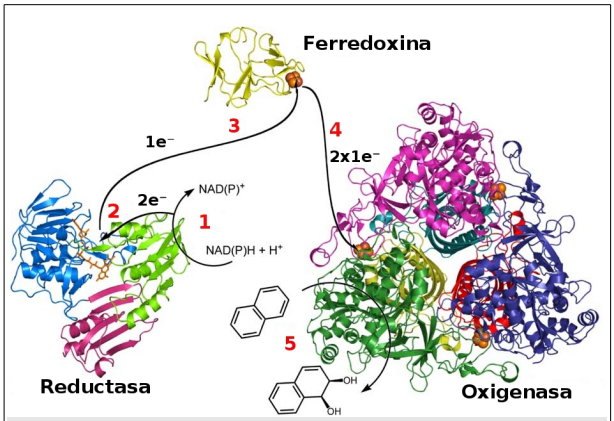

Figura 12: Los tres componentes que forman las oxigenasas de activación del anillo o Rieske no-hemo oxigenasas. (1) La reductasa oxida el NAD(P)H capturando 2 electrones. (2) Los electrones se almacenan en la flavina hasta que la reductasa (3) reduce con uno de ellos la ferredoxina. (4) La ferredoxina lanza el electrón recibido al domino Rieske de la oxigenasa. Este último paso ocurre dos veces por cada producto (5) formado (Ferraro et al., 2005).

nasa (Ferraro et al., 2005). La CTE suele estar compuesta por una flavoproteína reductasa, asociada a FAD o a FMN, y una ferredoxina, que puede estar presente o no dependiendo de la clase a la que pertenezca la enzima dentro de las RHO. Las proteínas de la CTE transfieren electrones desde el NAD(P)H a la oxigenasa, contribuyendo así a la actividad global de la RHO en la oxidación del sustrato (Chakraborty et al., 2012). La oxigenasa a su vez es una proteína multimérica, pudiendo ser un homomultímero de subunidades α (α_n) o un heteromultímero de formado por subunidades α y β ($\alpha_n\beta_n$). La subunidad α contiene un dominio hierro-azufre formado por un centro conservado Rieske [2Fe2S], característico de estas enzimas, y un dominio catalítico con una zona conservada mononuclear de unión a Fe (Chakraborty et al., 2012; Khara et al., 2014), que se cree que es el sitio de activación del oxígeno (Chakraborty et al., 2012). La subunidad β no presenta una interacción directa con el sitio activo, por lo que se piensa que simplemente proporciona estabilidad estructural a la enzima, cuando está presente (Peng et al., 2010).

Algunos ejemplos de RHO son la salicilato 1-hidroxilasa de *Sphingomonas sp.* CHY-1 que, a diferencia de la descrita en *Pseudomonas putida*, presenta una oxigenasa de estructura α3β3, con su respectivos dominios Rieske [2Fe2S], y otros dos componentes reductasa y ferredoxina (Jouanneau et al., 2007). Una estructura similar presenta la naftaleno dioxigenasa de *Pseudomonas putida* o la de *Rhodococcus sp.* (Gakhar et al., 2005; Peng et al., 2010), que cataliza la oxidación de naftaleno a 1,2-dihidroxinaftaleno. Por el contrario, la ftalato dioxigenasa de *Burkholderia cepacia,* encargada de oxidar el ftalato a *cis*-ftalato dihidrodiol, presenta una estructura más simple con sólo dos componentes y una oxigenasa formada únicamente por subunidades de tipo α (Chang & Zylstra, 1998; Peng et al., 2010).

3.3.3. Oxigenasas de escisión del anillo aromático

Las enzimas encargadas de realizar la ruptura del anillo de los compuestos aromáticos se dividen en dos clases diferentes, INTRA y EXDO dioxigenasas (ver apartado 3.2.1), realizando la escisión en posición *ortho* (entre los grupos hidroxilo) y *meta* (adyacente a los grupos hidroxilo) respectivamente, sobre los diferentes intermediarios catecólicos. La escisión en aquellas rutas con intermediarios no catecólicos se lleva a cabo por un grupo de extradiol dioxigenasas diferente (Díaz et al., 2013). Las intradiol dioxigenasas se caracterizan por presentar en su centro activo Fe(III), mientras que las extradiol dioxigenasas presentan en el centro activo un metal divalente, mayoritariamente Fe(II), y en raras ocasiones Mn(II) (Fetzner, 2012; Vaillancourt et al., 2006).

Dentro de las extradiol dioxigenasas se diferencian tres tipos diferentes. Por un lado están las extradiol dioxigenasas de tipo I pertenecientes a la superfamilia *vicinal oxygen chelate,* caracterizada por presentar un dominio con dos copias del de un módulo compuesto por 4 láminas β y una hélice α en el orden βαβββ (Armstrong, 2000; Vaillancourt et al., 2006). Dentro de este grupo encontramos las catecol 2,3-dioxigenasas, que catalizan el paso de de catecol a 2-hidroximuconato semialdehido, las 2,3-dihidroxibifenil 1,2-dioxigenasas, que catalizan la escisión del 2,3-dihidroxibifenil, o las homoprotocatecuato 2,3-dioxigenasas de *Actinobacteria*, que rompen el anillo del homoprotocatecuato (Pérez-Pantoja et al., 2010).

Las extradiol dioxigenasas de tipo II son todas multímeros formadas por uno o dos tipos diferentes de subu-

nidades, localizándose el centro activo en la subunidad β. En este grupo se encuentran por ejemplo las protocatechuate 4,5-dioxigenasas, compuestas por una subunidad α y otra β, las galato dioxigenasas o la homoprotocatecuato 2,3-dioxigenasa encontrada en *Escherichia coli* (a diferencia de las encontradas en *Actinobacteria*) (Barry & Taylor, 2013; Pérez-Pantoja et al., 2010).

El tipo III de extradiol dioxigenasas engloba aquellas enzimas que realizan la escisión del anillo sobre intermediarios no catecólicos. Estas enzimas pertenecen a la superfamilia cupin, donde todos sus miembros presentan una o dos copias del dominio cupin, formado por un barril de láminas β. Dentro de este grupo encontramos las gentisato 1,2-dioxigenasas, que catabolizan el paso de genti-

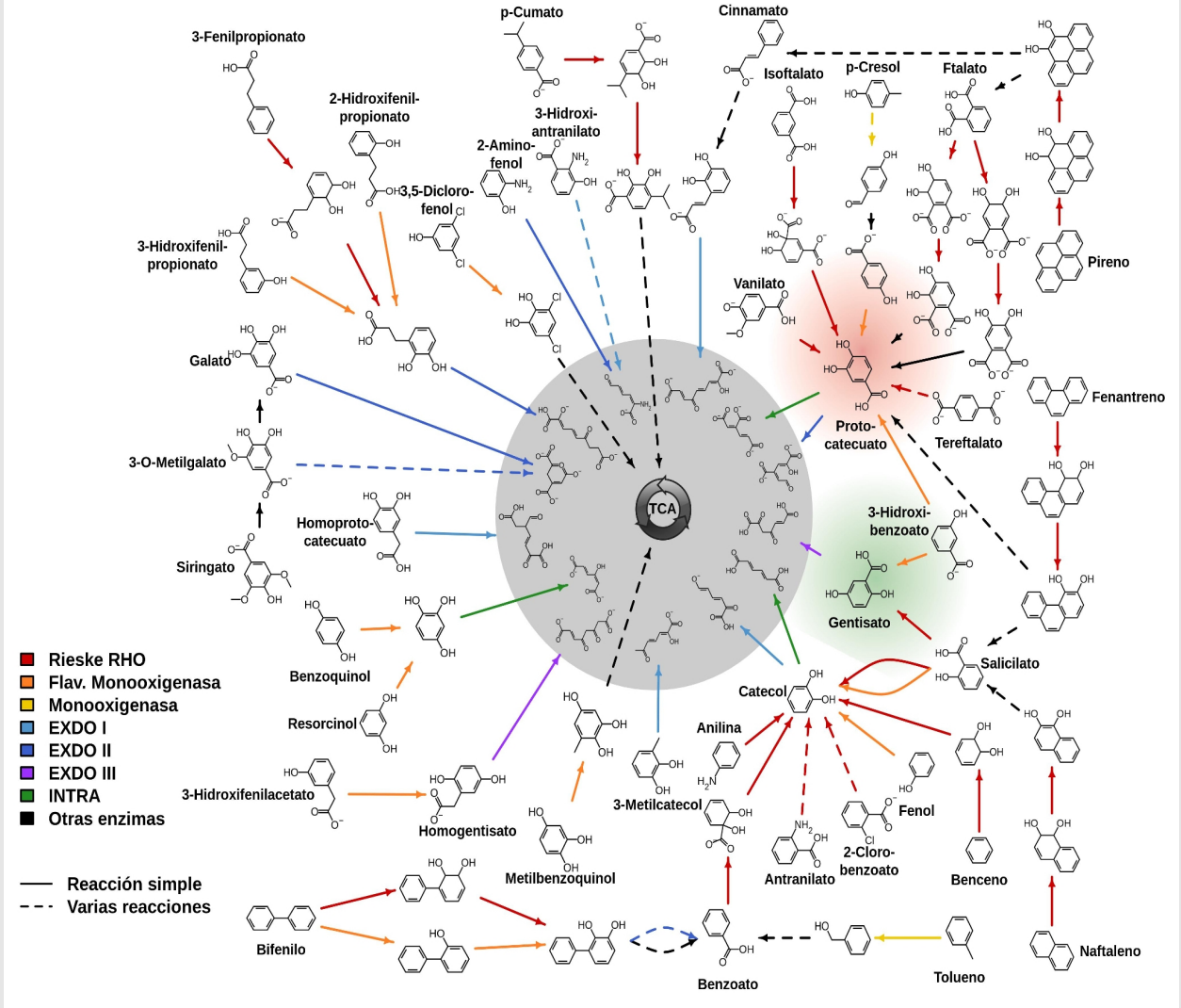

Figura 13: Reconstrucción catabólica de las principales rutas de degradación de compuestos aromáticos y poliaromáticos en las que se muestra la participación de enzimas clave. Las reacciones directas se muestran con líneas continuas, mientras que las discontinuas indican pasos que necesitan de varias reacciones en la ruta. En la leyenda aparecen en orden los tipos de enzimas referidos: Oxigenasas de ruptura de anillo (Rieske RHO); Monooxigenasas dependientes de flavinas (Flav. Monooxigenasas); Monooxigenasas; Extradiol dioxigenasas de tipo I (EXDO I), tipo II (EXDO II) y tipo III (EXDO III); Intradiol dioxigenasas (INTRA); y otras enzimas. Todas las rutas acaban formando intermediarios que terminan siendo degradados a través del los ácidos tricarboxílicos (TCA, resaltado en gris). Algunos de los intermediarios comunes más importantes se resaltan en gradientes de color (catecol, gentisato y protocatecuato).

sato a maleilpiruvato (Fetzner, 2012; Pérez-Pantoja et al., 2010; Vaillancourt et al., 2006).

Entre las intradiol dioxigenasas no encontramos la diversidad estructural que presentan las extradiol dioxigenasas. Esto puede ser un reflejo de la especificidad de sustrato que presentan las intradiol dioxigenasas por derivados catecólicos (Vaillancourt et al., 2006). Entre ellas encontramos la catecol 1,2-dioxigenasa, que transforma el catecol a muconato, o la protocatecuato 3,4-dioxigenasa, que transforma el protocatecuato a 3-carboxi-cis,cis-muconato. Esta última, descrita en *Pseudomonas putida*, presenta una estructura formada por dos subunidades, α y β, con el centro activo situado en la intersección entre ambas (Brown et al., 2004).

En la **Figura 13** se pueden observar algunas de las principales rutas metabólicas de biodegradación en las que intervienen los diferentes tipos de oxigenasas mencionados anteriormente.

3.3.4. Hidrolasas de productos de fisión *meta*

Los productos generados tras la ruptura del anillo siguen rutas diferentes según la ruptura se haya producido en posición *ortho* o *meta*. Las intradiol (*ortho*) dioxigenasas dan lugar a compuestos derivados del cis-cis muconato que son transformados por cicloisomerasas (también llamadas *muconate lactonizing enzymes*, MLE) para dar lugar a mucolactonas, que son posteriormente hidrolizadas a compuestos de las rutas centrales (Contzen & Stolz, 2000; Dobslaw & Engesser, 2015; Somboon et al., 2011). Sin embargo, las extradiol (*meta*) dioxigenasas (EXDO) dan lugar a productos que son hidrolizados directamente por enzimas conocidas como hidrolasas de productos de fisión *meta* (*meta-cleavage product*, MCP) o MCP hidrolasas (Alcaide et al., 2013).

Las MCP hidrolasas pertenecen a la familia de las α/β hidrolasas, catalizando la hidrólisis de enlaces C-C en derivados de 1,5-dicetonas. Estas enzimas presentan una estricta especificidad de sustrato por diversos productos de fisión de aromáticos, pudiendo clasificarlas en tres grupos diferentes según las bases de su especificidad: Los grupos I y II hidrolizan preferentemente productos de fisión de compuestos bicíclicos y monocíclicos, respectivamente; mientras que el grupo III hidroliza heteroaromáticos (Alcaide et al., 2013).

4. Dinámica de las comunidades microbianas tras la contaminación con petróleo

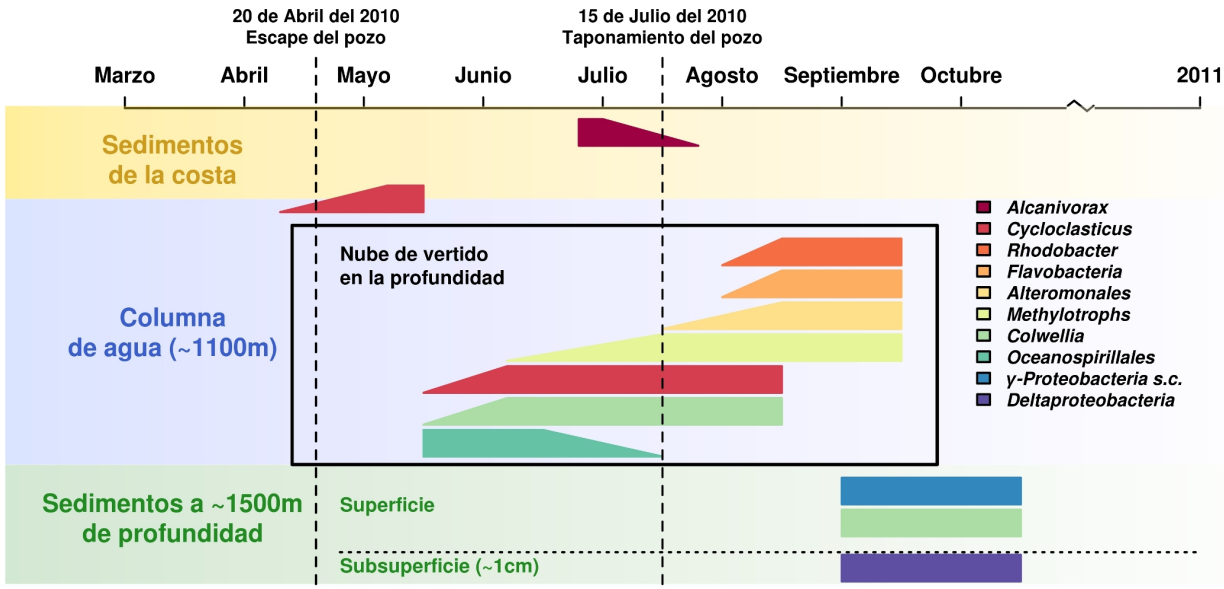

Figura 14: Visión general de la respuesta microbiana al vertido del Deepwater Horizon en el Golfo de México. El esquema se basa en los datos obtenidos a partir de los diferentes trabajos realizados después del vertido. Adaptación de Kimes et al., 2014.

La entrada de hidrocarburos en el ambiente produce una alteración que afecta a las comunidades microbianas presentes en el ecosistema. Estos cambios se producen tanto a nivel taxonómico como funcional.

Las comunidades microbianas responden rápidamente a los cambios ambientales ajustando su composición (Cappello et al., 2007a). La entrada de petróleo en el medio da lugar a una serie de cambios drásticos en estas comunidades, disminuyendo su diversidad. Mason et al. analizaron muestras recogidas tras las primeras semanas del vertido del Golfo de México, procedentes de la zona profunda (~1100m) donde quedó aislada una gran nube de petróleo y gas. Aproximadamente un 90% de las secuencias de ARNr 16S procedentes de estas muestras pertenecían a especies sin cultivar de *y-Proteobacteria* del orden *Oceanospirillales* (**Figura 14**). Estas bacterias están relacionadas con la degradación de hidrocarburos (Kimes et al., 2014; Mason et al., 2012), evidenciando un cambio en la composición de la microbiota. Esto se debe, por una parte, a una selección en favor de microorganismos degradadores de estos compuestos (Harayama et al., 2004), y por otra al efecto tóxico sobre el crecimiento de otros microorganismos (Païssé et al., 2010). Además, los diferentes grupos taxonómicos no varían siempre de la misma manera y su respuesta frente a la entrada de hidrocarburos es distinta según el tiempo y la localización (King et al., 2015). Las condiciones del medio como la temperatura o la concentración de O_2 también son importantes, ya que favorecerán a aquellos taxones mejor adaptados a ellas (Kimes et al., 2014; Redmond & Valentine, 2012). En otras muestras de la zona profunda del Golfo de México no se detectaron secuencias de ARNr 16S asociadas al género *Alcanivorax*, uno de los más comunes en ambientes contaminados por petróleo, y sí un gran número asignadas a *Colwellia*. Sin embargo, sí se encontraron secuencias asociadas a *Alcanivorax* en muestras de sedimentos de la costa del Golfo de México (**Figura 14**). Esta diferencia puede deberse precisamente a la diferencia de temperatura entre los sedimentos de la costa y las aguas de la zona profunda, siendo éstas últimas más frías (4ºC), donde los miembros de *Colwellia* podrían haberse adaptado mejor debido a su carácter psicrófilo (Kimes et al., 2014; Kostka et al., 2011; Redmond & Valentine, 2012). Las condiciones, además, pueden variar en el ecosistema según la temporada estacional (observándose, por ejemplo, diferencias en la temperatura del agua) provocando que los grupos taxonómicos que mejor podrían responder a una entrada de hidrocarburos sean diferentes según la época de año (Lanfranconi et al., 2010).

Estos cambios debidos a la entrada en el medio de los hidrocarburos no son estáticos, sino que el ecosistema sigue cambiando a medida que la concentración y disponibilidad de los diferentes tipos de hidrocarburos varía por efecto de los diferentes factores físico-químicos y la biodegradación. Los hidrocarburos alifáticos son degradados más rápidamente (Reis et al., 2013), mientras que los aromáticos y los poliaromáticos se degradan más lentamente y son más persistentes en el medio (Harayama et al., 2004; Head et al., 2006), dando lugar a una sucesión en los grupos dominantes de la comunidad microbiana. Los microorganismos especialistas en la degradación de alcanos (e.j. *Alcanivorax*) son los primeros en aumentar su frecuencia (Gertler et al., 2009; Jiménez et al., 2011), mientras que los especializados en compuestos aromáticos y poliaromáticos (e.j. *Cycloclasticus*) lo hacen más tarde (Cappello et al., 2007b; Head et al., 2006; Vila et al., 2010). Los diferentes estudios realizados a diferentes fechas en el Golfo de México, basados en la nube de vertido localizada en la columna de agua, muestran que la mayoría de las secuencias de ARNr 16S analizadas en Mayo de 2010 pertenecían al grupo *Oceanospirillales*, asociados a la degradación de hidrocarburos alifáticos, mientras que las analizadas en Junio se relacionaban principalmente con los géneros *Colwellia*, relacionado con la degradación de alcanos y compuestos aromáticos (Bælum et al., 2012), y *Cycloclasticus*, conocido por su capacidad de degradación de hidrocarburos aromáticos y PAH (**Figura 14**). Posteriormente, en Septiembre, la microbiota vuelve a cambiar, dominada por un mayor grupo de taxones (Bælum et al., 2012; Kimes et al., 2014).

Los cambios en la comunidad microbiana van acompañados de cambios a nivel funcional. La entrada de petróleo provoca un aumento de la presencia de genes relacionados con la degradación de hidrocarburos (Lu et al., 2011; Mason et al., 2014) y, al igual que la microbiota, la frecuencia de un tipo de genes u otro dependerá de las condiciones del medio (como la concentración de O_2) y el tipo y concentración de los hidrocarburos a degradar en cada momento (Acosta-González et al., 2013; Kimes et al., 2013). Así, Lu et al. (2011), compararon la expresión génica entre muestras de la columna de agua del Golfo de México que se encontraban dentro y fuera de la nube vertido (contaminadas y no contaminadas). De esta forma comprobaron que las muestras contaminadas, dentro de la nube, presentaban un enriquecimiento en la expresión de genes relacionados con la degradación de alcanos, cicloalcanos, BTEX (benceno, tolueno, etilbenceno y xileno), aromáticos, aromáticos heterocíclicos y poliaromáticos. Ejemplos concretos lo constituyen el gene *alk*B, que codifica la alcano 1-monooxigenasa, genes para degradación aerobia de hidrocarburos, o incluso el gen *bbs*, que codifica la benzilsuccinato sintasa, responsable de la degradación anaerobia del tolueno. Además, pudieron observar también una mayor abundancia en la expresión de genes relacionados con el ciclo del carbono, el azufre o la reducción del hierro, en donde se pueden encontrar muchos procesos metabólicos íntimamente relacionados con la degradación de hidrocarburos (Lu et al., 2011).

Los genes para la degradación de hidrocarburos alifáticos se expresan antes que aquellos para la degradación de hidrocarburos más complejos (Mason et al., 2012; Paissé et al., 2012; Vila et al., 2010). En sedimentos recogidos en la playa de Pensacola (Florida, EE.UU.), afectada por el vertido del *Deepwater Horizon* en el Golfo de México, Rodríguez-R et al., observaron una alta frecuencia del gen *alk*B en las muestras recogidas en Julio de 2010, descendiendo en las recogidas en Octubre, donde, por el contrario, se observa un aumento de la frecuencia de genes asociados con la degradación de aromáticos con respecto a las muestras de Julio (Rodriguez-R et al., 2015).

Por último, cabe destacar que la previa exposición de un ambiente a la contaminación puede influir en su capacidad de respuesta a nuevas entradas de contaminantes (Sauret et al., 2012). Aquellos que permanecen contaminados de forma crónica o que han sufrido previamente alguna alteración o vertido tienden a presentar un mayor número de microorganismos degradadores de hidrocarburos que los ambientes sin contaminar, presentando un menor tiempo de respuesta y una mayor eficiencia en la degradación de los hidrocarburos (Sauret et al., 2012).

5. Aplicación de la biología de sistemas a los estudios de biorremediación

A pesar de los estudios en laboratorio y de los experimentos realizados en microcosmos y otras simulaciones del ecosistema, todavía se desconoce en profundidad el comportamiento de la distribución de las comunidades microbianas y sus capacidades catabólicas en un marco global (Vilchez-Vargas et al., 2010). Para que el uso de la biorremediación tenga éxito es necesario entender como ocurren de forma natural los procesos catabólicos microbianos que transforman los contaminantes del entorno. La biología de sistemas es una disciplina centrada en el estudio de sistemas biológicos, investigando las interacciones y redes que se producen a nivel molecular, celular, de comunidad y de ecosistema combinando diferentes herramientas '-ómicas' que proporcionan una información única sobre la supervivencia, la interacción y el metabolismo de los microorganismos que forman los medios naturales (Chakraborty, Wu, & Hazen, 2012).

Antiguamente, el procedimiento experimental sólo permitía el análisis basado en una cantidad limitada de bacterias cultivables. El desarrollo de nuevas tecnologías de alto rendimiento ha permitido que los estudios no se centren únicamente en lo que ocurre en una pequeña parte del sistema, sino que puedan analizar todas las partes que lo componen, como interaccionan entre sí y como influyen unas sobre las otras (Trigo et al., 2009). De esta forma han aparecido herramientas (**Tabla 1**) como la metagenómica, la metatranscriptómica o la me-

	MATERIAL	RESULTADO	VENTAJAS	LIMITACIONES	APLICACIONES	COMPONENTES CLAVE A IDENTIFICAR
Fenotipado	Amplicones de ARN 16S procedentes de ADN o del ARN/ADNc	Composición de la microbiota o microbiota activa	Secuenciación barata y rápida	Dificultad en la asignación de los taxones más específicos Los grupos mayoritarios pueden enmascarar a los menos abundantes Para hacer comparaciones se necesita amplificar la misma región	Identificación de la microbiota encargada de la degradación de hidrocarburos	*Alcanivorax, Cycloclasticus, Oleispira, Thalassolituus, Oleiphilus, Marinobacter, Psedoalteromonas, Psychrobacter, Alteromonas, Desulfococcus, Desulfosarcina, Pseudomonas, Colwelia, Rhodobacter (Bargiela et al., 2015b; Redmond & Valentine, 2012)*
Metagenómica	ADN	Perfil del contenido genómico y análisis de su presunta función	Sin errores de amplificación Descubre la diversidad microbiana Se encuentran nuevos genes Amplia cobertura y profundidad de secuenciación de los genes totales	Requiere una amplia profundidad de cobertura El ensamblaje es complicado debido a la baja cobertura y la alta cantidad de similitudes No se aporta información sobre los genes activos Los genes desconocidos necesitan análisis bioinformático Las funciones putativas necesitan de validación experimental	Identificación de genes que codifican enzimas relacionadas con biodegradación de hidrocarburos o procesos biogeoquímicos relacionados (GeoChip)	Genes relacionados la degradación aerobia de alcanos y compuestos aromáticos (Bargiela et al., 2015b; Guazzaroni et a., 2012; Kimes et al., 2013; Mason et al., 2014) Genes involucrados en el ciclo del carbono, azufre, nitrógeno, fósforo y reducción de hierro (Lu et al., 2012; Mason et al., 2014)
Metatranscriptómica	ARNm/ADNc	Perfil de la expresión génica	Revela la expresión génica de la microbiota activa	Inestabilidad del ARNm Muchos pasos de purificación No existe un único protocolo Falta de bases de datos de referencia	Identificación de la microbiota activa en zonas afectadas por vertidos de petróleo Identifcación de la expression de genes relacionados con procesos de biodegradación (Mason et al, 2012)	Identificación de grupos taxonómicos activos: *Colwelia, Oceanospirillales, Methylocollales, Methylophaga, Methylosinus, Methylocystis, Methylocella; Alteromonadales, Oceanospirillales, Rhodobacterales* (Lamendella et al., 2014; Mason et al, 2012') Detección de la expresión de genes para la degradación de alcanos, aromáticos, ácidos grasos, aldehidos y alcoholes (Mason et al, 2012)
Metaproteómica	Proteínas	Perfil de expresión proteico	Revela la expresión de las proteínas que están siendo sintetizadas y expresadas por la microbiota activa	Requiere de tecnología especial No hay un único protocolo El análisis bioinformático de las masas de proteínas o secuencias es complejo y requiere tiempo Se necesitan las secuencias metagenómicas Muchas de las proteínas identificadas son desconocidas	Identificación de las proteínas expresas en ambientes contaminados por hidrocarburos Determinación de la contribución relativa de la biodegradación respecto al metabolismo global	Identficación de enzimas relacionadas con el metabolismo de compuestos C1, azufre, conservación energética y detoxificación (Bargiela et al., 2015a) Detección de proteínas relacionadas con la degradación aerobia de naftaleno, gentisato y catecol; protinas relacionadas con el metabolismos del nitrato y el óxido nítico/nitroso, el metabolismo energético, transporte y detoxificación y estrés oxidativo (Guazzaroni et al., 2012)
Metabolómica	Metabolitos	Perfil metabolómico	Supone un paso más allá en la representación del perfil metabólico de la microbiota activa	Falta de bases de datos de referencia No hay un protocolo único En las bases de datos existen muchos metabolitos desconocidos La identificación precisa de los compuestos es laboriosa	Identificación de los diferentes metabolitos, intermediarios o productos finales de biodegradación, en ambientes contaminados con hidrocarburos	Detección de alkilsuccinatos (Kimes et al., 2013) Detección de masas de metabolitos que evidencian la degradación de: naftaleno, Chlorobenzoato, 2-oxo-1,2-dihidroquinolina, 2,4,5-trihidroxitolueno, 3-nitrobenzoato, galato, 4-hidroxifenilacetato, 3-fenixobenzoato, 4-hidroxibenzoato, tetradecano, biffenil, 2,3-dihidroxibifenil, benozato, carbazol, antraceno, fenol, isoftalato, tereftalato, 2,3-dihidroxifenilpropionato, ftalato,salicilato, catecol, fluorobenzoato y geraniol (Bargiela et al., 2015b, Tobalina et al., 2015)

Tabla 1: Resumen de las principales características de principales técnicas "meta-ómicas" mencionadas en la Tesis Doctoral.

taproteómica, capaces de superar las restricciones de otras técnicas y obtener una mayor perspectiva del ecosistema muestreado (Vila et al., 2015). Mediante la metagenómica se estudia simultáneamente todo el material genético de todos los microorganismos contenidos en una muestra, evitando así los procesos de cultivo. La metatranscriptómica permite obtener una visión funcional de la actividad de las comunidades microbianas de una muestra ambiental analizando su perfil de ARNm transcripcional. Por último, la metaproteómica determina el perfil de expresión de proteínas de la comunidad microbiana de la muestra ambiental, reflejando su actividad funcional en el ecosistema (Desai et al., 2010).

Otras técnicas como los microarrays proporcionan información sobre la detección de miles de genes con un simple test. Uno de los array de genes más conocidos es el GeoChip (He et al., 2007; Vila et al., 2015), que comprende una gran variedad de genes involucrados en procesos biogeoquímicos. Recientemente también se ha desarrollado un array compuesto por familias de genes catabólicos de compuestos aromáticos y alcanos, permitiendo el análisis de la diversidad genética (ADN) y expresión (ADNc procedente de la retrotranscripción de ARNm) de las comunidad microbianas degradadoras de hidrocarburos (Vila et al., 2015; Vilchez-Vargas et al., 2013).

Un paso más allá es la opción de la metabolómica, que analiza los diferentes metabolitos primarios y secundarios que las células microbianas hayan podido liberar frente a un cambio ambiental o procesos de estrés (Desai et al., 2010).

La biología de sistemas busca entender el comportamiento de las comunidades microbianas a múltiples niveles, por lo que es necesaria la combinación de las diferentes técnicas "-ómicas" descritas anteriormente para obtener una interpretación global de todo lo que ocurre en un ecosistema. Por esto, es necesario el uso de herramientas bioinformáticas para procesar la gran cantidad de datos producida por los diferentes tipos de análisis e integrar posteriormente los resultados mediante técnicas de estadística y visualización que ofrezcan una percepción holística de lo que ocurre en la comunidad microbiana analizada.

5.1. La bioinformática aplicada a la biorremediación

El enfoque multidimensional de la biología de sistemas requiere del uso de diferentes técnicas de análisis que generan una gran cantidad de información sobre la comunidad microbiana a estudiar. Hoy en día, gracias a la bioinformática, existen diferentes programas, procedimientos, recursos *online* y algoritmos que permiten el análisis *in silico* de todos estos datos "-ómicos" (Desai et al., 2010). Hoy en día, la bioinformática se encuentra integrada como parte fundamental del protocolo de uso de muchas técnicas "-ómicas", interviniendo en el ensamblaje de lecturas en los procesos de secuenciación, la anotación taxonómica o funcional de secuencias, alineamientos múltiples, análisis filogenéticos, o el procesamiento de datos masivos entre muchas otras aplicaciones. La literatura nos ofrece un buen número de revisiones que resumen sus diferentes usos dentro de estas técnicas (Arora & Bae, 2014; Mayer, 2011; Muth et al., 2013; Seifert et al., 2013; Stobbe et al., 2012; Zhou, 2013).

Sin embargo, donde esta multiherramienta es verdaderamente importante dentro de la biología de sistemas es en la integración de todos los datos generados por los diferentes tipos de análisis, formando una visión global de lo que ocurre a todos los niveles dentro de una comunidad microbiana. Esto adquiere una importancia todavía mayor dentro del campo de la biorremediación, principalmente en el análisis de las rutas catabólicas por las que se degradan contaminantes como los hidrocarburos. Estas rutas están constituidas por un complicado entramado de reacciones que implican la expresión de genes, la acción de enzimas y la transformación de metabolitos. Mediante los análisis basados en redes podemos crear una reconstrucción de este tipo de metabolismo que permita la visualización de todos el conjunto de datos, donde cada nodo de la red presenta un elemento de los datos (metabolito, sustrato, etc), mientras que los enlaces que los unen representan las relaciones entre estos elementos (reacciones enzimáticas), conformando lo que se

conoce como redes metabólicas (Trigo et al., 2009). Gracias a la información contenida en las bases de datos como KEGG podemos reconstruir las redes metabólicas y visualizar los resultados de los diferentes estudios en ellas (Tobalina et al., 2015; Trigo et al., 2009). Sin embargo, es necesario un mantenimiento y refinado de estas bases de datos debido a la alta tasa de error que pueden presentar en las anotaciones (Heinemann & Sauer, 2010), y la falta de información en determinadas áreas metabólicas como la biodegradación de compuestos xenobióticos (Duarte et al., 2014).

5.1.1. Bases de datos de utilidad en biodegradación

Para los estudios de biorremediación existen bases de datos específicas que ofrecen una información más precisa sobre la biodegradación microbiana. La UM-BBD (*University of Minnesota Biocatalysis/Biodegradation Database*, http://umbbd.msi.umm.edu/, Gao et al., 2010), presenta actualmente información exhaustiva de 219 rutas y 1503 reacciones, 1396 compuestos, 993 enzimas, 543 entradas de microorganismos, 249 normas de biotransformación, 50 grupos funcionales orgánicos, 76 reacciones de la naftaleno 1,2-dioxigenasa y 109 reacciones para la tolueno dioxigenasa (Desai et al., 2010; Trigo et al., 2009). OxDBase (www.imtech.res.in/raghava/oxdbase/) alberga información sobre oxigenasas relacionadas con biodegradación, basada en artículos publicados y bases de datos (Arora et al., 2009). Bionemo presenta información refinada manualmente sobre genes y proteínas relacionadas con la biodegradación mediante la asociación de las secuencias de la base de datos con información extraída de artículos publicados (Carbajosa et al., 2009), complementándola con el contenido de UM-BBD, más focalizada en los aspectos bioquímicos de la biodegradación. Metacyc (http://metacyc.org, Caspi et al., 2014) es una base de datos de rutas metabólicas formada a partir de literatura científica experimental, con más de 2097 rutas metabólicas determinadas experimentalmente de más de 2460 organismos diferentes procedentes de todos los dominios de la vida (Pankaj et al., 2014).

Todos estos recursos ofrecen una amplia información sobre rutas de biodegradación. Sin embargo, carecen de un sistema de anotación refinado a la hora de anotar un grupo de secuencias (genes o proteínas) del que desconocemos su función. Generalmente las secuencias se compararan con las contenidas en las bases de datos por emparejamiento de secuencia y en caso de ser estadísticamente significativo se infiere la función a partir de su secuencia homóloga (Sjolander, 2004), como normalmente se hace a través de BLAST (Altschul et al., 1990). De esta forma se consigue una predicción rápida de la función, pero este sistema basado únicamente en homología tiende a acumular errores sistemáticamente debido a i) la mezcla de los dominios de las proteínas y ii) no tener en cuenta los procesos de evolución de las proteínas (Sjolander, 2004). Por una parte, los alineamientos no tienen en cuenta la estructura de los dominios, alineando las secuencias globalmente y no localmente (respetando los diferentes dominios). Por otra parte, los fenómenos de duplicación genética contribuyen a la generación de la mayoría de la diversidad de familias y superfamilias de enzimas. Esto hace que se genere una copia del gen que mantiene la función original, evolucionando por especiación, generando diferentes homólogos con función similar, conocidos como ortólogos. La otra copia podrá evolucionar hacia funciones divergentes, dando lugar a genes homólogos por duplicación, conocidos como parálogos (Descorps-Declère et al., 2008; Sjolander, 2004). Además, es importante destacar que pequeños cambios puntuales en determinados aminoácidos pueden provocar cambios notables en el reconocimiento y transformación de los diferentes contaminantes por porte de enzimas similares (Alcaide et al., 2013). Por esta razón se necesita añadir al análisis de las secuencias la construcción de un árbol filogenético que permita diferenciar este tipo de relaciones.

En base a lo mencionado anteriormente encontramos la base de datos Aromadeg, centrada en enzimas clave para el catabolismo de compuestos aromáticos, formada por 3605 secuencias de proteínas revisadas manualmente (Duarte et al., 2014; Guazzaroni et al., 2013). La diferencia que presenta Aromadeg en relación a otras bases

de datos consiste en que permite el análisis filogenómico de las secuencias, consistente en i) la identificación de homólogos dentro de la base de datos para las secuencias de interés, ii) realizar un alineamiento múltiple con el grupo de homólogos identificados y iii) construir un árbol filogenético cuya topología permita señalar los diferentes eventos de especiación o duplicación. Este método, junto a la escrupulosa revisión manual de todas las secuencias de la base de datos, permite una asignación funcional más fiable dentro del catabolismo de compuestos aromáticos (Duarte et al., 2014; Sjolander, 2004).

5.1.2. Reconstrucción catabólica

Las redes metabólicas capturan la inter-conversión de los metabolitos a través de transformaciones químicas catalizadas por enzimas (Saha et al., 2014). La red constituida por el metabolismo de biodegradación presenta una topología en donde diferentes rutas catabólicas convergen en intermediarios comunes, situados más próximos a las rutas centrales del metabolismo general. Los compuestos más grandes e hidrofóbicos tienden a acumularse en la zona periférica de la red, y a medida que nos acercamos al centro, pasando por los intermediarios comunes, el peso molecular y la hidrofobicidad descienden progresivamente hasta llegar al centro, donde se sitúan las rutas centrales (Trigo et al., 2009). Al volcar los datos experimentales obtenidos sobre estas redes podemos reconstruir la huella metabólica y/o catabólica observada en la comunidad microbiana que se halla analizado, utilizando finalmente métodos de proyección gráfica para su presentación visual.

Existen diferentes tipos de herramientas que se pueden combinar para la visualización de estas redes. KEGG permite la extracción de todo tipo de información a través de su interfaz de programación (KEGG API, *application programming interface*). Los programas de visualización como Cytoscape (http://www.cytoscape.org/) admiten la información extraída de KEGG, permitiendo la reconstrucción de la red (Gerasch et al., 2014; Zhou, 2013). Sin embargo, fuera de las aplicaciones y programas ya desarrollados, podemos recurrir a lenguajes de programación y paquetes complementearios que ofrecen una manera totalmente libre para desarrollar un método de visualización a la carta. R es un potente leguaje de programación (R Development Core Team, 2008) ampliamente usado como herramienta de análisis y visualización de datos. Sus capacidades básicas pueden extenderse a través de diferentes paquetes adicionales (van Helden et al., 2012). La programación a través de R, en combinación con paquetes como Igraph (Csardi and Nepusz, 2006), brinda la posibilidad de crear métodos de visualización eficaces y de calidad, que además sean dinámicos y permitan exponer datos procedentes de análisis diferentes. En el caso de redes de biodegradación, nos podemos valer de bases de datos como Pubchem (Bolton et al., 2008) para obtener la información química de los diversos compuestos y manejarlos gráficamente a través del paquete ChemmineR (Cao et al., 2008) para R, o bien utilizando el módulo OASA del programa BKChem (Anonymous Contributors, 2010) para el lenguaje de programación Python (van Rossum & Drake, 2001).

5.2. Ejemplos de la aplicación de las herramientas de la biología de sistemas

En el campo de la biorremediación de hidrocarburos del petróleo, la biología de sistemas se ha aplicado en diferentes casos, como en el vertido del golfo de México. Mason et al., utilizaron técnicas de metagenómica y metatranscriptómica para estudiar la comunidad microbiana procedente de la nube de vertido en la columna de agua, analizando su diversidad taxonómica (ARN 16S) y funcional (ADN), así como su expresión génica (metratranscriptómica), ayudándose de las secuencias contenidas en el GeoChip para el análisis de las rutas de degradación de hidrocarburos. Con ello, observaron un descenso de la diversidad microbiana en comparación con muestras no contaminadas de la columna de agua, con un enriquecimiento del grupo *Oceanospirillales*, el cual era además el más activo en las muestras, en las que aprecian una alta abundancia de genes relacionados con la degradación de alcanos (Mason et al., 2012). Kimes et al. (2013) combinaron metagenómica y metabolómica para el análisis de los sedimentos de la profundidad, obteniendo un perfil de los metabolitos presentes en cada muestra centrado en la búsqueda de derivados del alquil-

succinato, asociados con la biodegradación anaerobia por adición de fumarato. De esta forma intentaron apoyar las evidencias genéticas de degradación anaerobia en la profundidad con la detección de metabolitos relacionados con este metabolismo, sin éxito en este caso (Kimes et al., 2013).

La metaproteómica se ha aplicado en estudios de ambientes marinos para la caracterización de la expresión proteica de comunidades microbianas marinas *in situ*, estudiar el ciclo biogeoquímico de la materia orgánica en el océano o analizar la microbiota de hábitats especiales como ambientes simbióticos, afloramientos de fitoplancton o filtraciones frías en el lecho marino (Wang et al., 2014). En estudios de biorremediación, Herbst et al. (2013), combinaron metaproteómica con técnicas de marcaje radioactivo (SIP) para llevar a cabo un estudio funcional sobre la comunidad microbiana de un acuífero contaminado con hidrocarburos poliaromáticos. Consiguieron observar que la mayoría de las proteínas identificadas pertenecían al orden *Burkohlderiales*, encargados de mineralizar la mayor parte del naftaleno marcado con isótopos radioactivos (Herbst et al., 2013). Guazzaroni et al. (2012) combinaron metagenómica y metaproteómica para el estudio de muestras de suelo contaminado con PAH, mostrando las diferencias entre

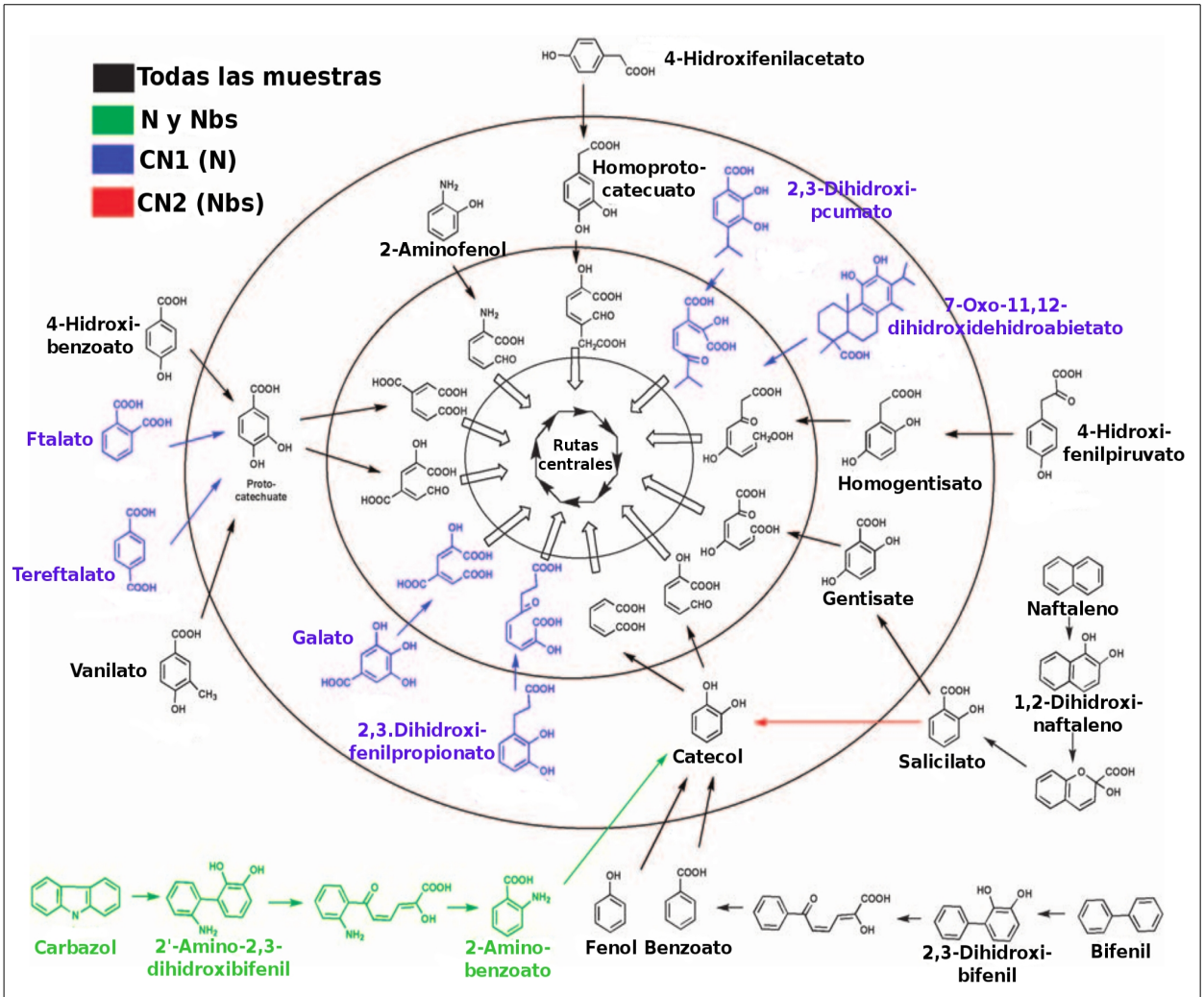

Figura 15: Red metabólica para la degradación aerobia de compuestos aromáticos en muestras de suelo contaminado con hidrocarburos poliaromáticos. El estudio presenta 4 pruebas distintas a partir de las muestras de suelo: control sin aditivos, N; control bioestimulado con NH_4NO_3 y KH_2PO_4, Nbs; enriquecimiento en microcosmos con naftaleno derivado de la muestra N, CN1; enriquecimiento en microcosmos con naftaleno derivado de la muestra Nbs, CN2 (Guazzaroni et al., 2012).

las muestras control, sin aditivos (N) y bioestimulada (Nbs) con una mezcla de NH_4NO_3 y KH_2PO_4, y sus respectivos enriquecimientos con naftaleno (CN1, derivada de N, y CN2, derivada de Nbs). A nivel taxonómico observaron que las muestras sin enriquecer (N y Nbs) con naftaleno presentaban una mayor diversidad que las muestras enriquecidas (CN1 y CN2), mostrando además diferencias entre los grupos dominantes de *α*, *β* y *γ-Proteobacterias*. Utilizando una base de datos interna con secuencias de proteínas relacionadas con procesos de degradación (generada durante esta Tesis Doctoral), realizaron una reconstrucción metabólica (**Figura 15**) de la huella genética de las 4 muestras para el catabolismo aerobio de compuestos aromáticos. Combinando los resultados de la reconstrucción metabólica con los obtenidos de metaproteómica para CN1 CN2 pudieron apreciar que la muestra bioestimulada mostraba una mayor habilidad a la hora de degradar el naftaleno, mientras que la no bioestimulada (CN1) presentaba una mayor plasticidad a la hora de degradar un mayor número de compuestos aromáticos diferentes (Guazzaroni et al., 2013; Tobalina et al., 2015). Con este estudio consiguen un exhaustivo análisis comparativo a múltiples niveles (genético y proteico) sobre los efectos de la bioestimulación y el enriquecimiento en suelos contaminados por hidrocarburos.

Como se ha resumido anteriormente, existen ejemplos en la literatura donde se ha analizado el efecto de la contaminación en hábitats singulares (como en el caso del *Deepwater Horizon* o el *Prestige*). Sin embargo, hasta la fecha no encontramos en la literatura estudios comparativos en el campo de la biorremediación en los que se apliquen de forma conjunta múltiples técnicas "-ómicas" sobre ambientes marinos contaminados con hidrocarburos a escala global.

En base a todo lo expuesto anteriormente, la presente Tesis Doctoral se centra principalmente en el estudio de comunidades microbianas marinas del Mar Mediterráneo, principalmente, y el Mar Rojo, ambas zonas muy afectadas por la contaminación crónica debida al transporte marítimo de petróleo, la industrialización y las actividades antropogénicas. Las zonas marinas del Golfo de México (Deepwater Horizon) o la costa Noroeste de España (Prestige) han sido ampliamente estudiadas, a diferentes niveles "-ómicos", debido a la gran repercusión que han tenido los vertidos petrolíferos ocurridos en ellas. Sin embargo, el Mar Mediterráneo ha sido generalmente ignorado para su estudio por parte de la comunidad internacional, sobre todo la zona Sur de la cuenca (Daffonchio et al., 2013). Además, entre los trabajos que se pueden encontrar localizados en el Mediterráneo, en su mayoría se limitan a estudios de diversidad, por lo que hay una clara falta de investigaciones focalizadas en entender el comportamiento relacionado con las capacidades de biodegradación de las comunidades microbianas en ambientes contaminados de esas zonas (Daffonchio et al., 2013).

Por ello, uno de los motivos que impulsan esta Tesis Doctoral es establecer una primera visión general del comportamiento de las comunidades microbianas presentes en diferentes zonas repartidas por la cuenca del Mediterráneo, tomando también el Mar Rojo como referente futuro del Mediterráneo de acuerdo a la tendencia del calentamiento global (Daffonchio et al., 2013).

Por otra parte, existe la necesidad de profundizar en los estudios de biorremediación, con el objetivo de ampliar nuestro conocimiento sobre: a) la capacidad de las comunidades microbianas marinas para degradar los diferentes compuestos que forman el petróleo y sus derivados, en el marco de los diferentes factores ambientales; y b) el efecto que métodos como la bioestimulación tienen sobre la microbiota, para poder mejorar y perfeccionar estos procedimientos. Para ello, en esta Tesis Doctoral se hace uso de múltiples técnicas "-ómicas" que analizan estas comunidades microbianas a múltiples niveles, integrando todos los datos generados a través de herramientas bioinformáticas que permiten una mejor visualización de lo que ocurren en estos sistemas biológicos. Se pretende, además, indagar en la contribución de los procesos catabólicos (biodegradación) en el marco del metabolismo global de comunidades microbianas que habitan en ambientes crónicamente contaminados.

Objetivos de la Tesis Doctoral

La meta principal de esta Tesis Doctoral es la aplicación de **herramientas bioinformáticas** en combinación con diferentes técnicas **"-ómicas"** para profundizar en el comportamiento de las comunidades microbianas marinas que habitan en diversas zonas afectadas por **la contaminación crónica de hidrocarburos en el Mar Mediterráneo y el Mar Rojo**. Para ello, en el trabajo se persiguen los siguientes objetivos:

- Estudiar como la contaminación afecta a las comunidades microbianas en **ambientes marinos crónicamente afectados por la presencia de contaminantes**, atendiendo a como se ven afectadas por los diferentes **factores ambientales** como la temperatura, la concentración de O_2 o la concentración de hidrocarburos.

- Aplicar técnicas de estudio como la **metagenómica, la metaproteómica o la metabolómica** para obtener datos a múltiples niveles de la microbiota de las muestras estudiadas, valiéndonos de herramientas bioinformáticas para la **integración y visualización de los datos generados** con el fin de obtener una mejor interpretación de la comunidad microbiana como **sistema biológico**.

- Obtener, mediante el uso de herramientas bioinformáticas, **reconstrucciones metabólicas de los procesos de bidegradación**, utilizando para ello datos de diferente origen "-ómico" sobre los **genes, enzimas o compuestos** relacionados con las rutas catabólicas de hidrocarburos utilizadas por las comunidades microbianas. Se hará especial hincapié en el diseño de un método gráfico que permita reconstruir redes catabólicas a partir de datos metagenómicos, y en la validación experimental del mismo.

- Estudiar como la **bioestimulación** con diferentes nutrientes afecta a las comunidades microbianas **fomentando unas rutas catabólicas u otras** dependiendo del compuesto utilizado.

Capítulo 2: Poblaciones bacterianas en ambientes crónicamente contaminados con petróleo

Resumen

El Mar Mediterráneo y el Mar Rojo son dos de las zonas marinas del mundo más contaminadas por vertidos de petróleo crudo o sus derivados. Ambos son por tanto ambientes contaminados de forma crónica. Este alto y persistente grado de contaminación junto al hecho de que estén sometidos a factores geoquímicos muy diferentes al de otros ambientes marinos, pueden desencadenar una serie de efectos sobre la diversidad y estructura de las comunidades microbianas que los habitan y las capacidades catabólicas que éstas contienen, que todavía hoy no se conocen completamente. Con este trabajo se ha pretendido establecer una primera visión global de cómo las variables ambientales y geográficas y la actividad antropogénica (grado de contaminación) influyen en las comunidades microbianas que habitan 8 zonas costeras a lo largo del Mar Mediterráneo y el Mar Rojo. Cada una de ellas presenta parámetros físico-químicos diferentes. La muestra del Mar Rojo se ha estudiado ya que éste representa un posible futuro del Mar Mediterráneo según las tendencias del calentamiento global.

El procedimiento seguido para el análisis de las muestras comprende las siguientes partes: a) recolección de muestras de sedimentos marinos de las zonas estudiadas, b) medida de los parámetros ambientales y geoquímicos y extracción y secuenciación de los ácidos nucleicos, c) análisis de secuencias parciales del gen de 16S ribosomal (ARNr 16S), d) secuenciación del ADN y predicción de genes, e) reconstrucción *in silico* de las redes de biodegradación tras la identificación en los metagenomas de genes que codifican enzimas catabólicas, f) validación experimental de las capacidades biodegradativas mediante el uso de metabolómica dirigida y cultivos enriquecidos, y f) correlación entre las variables ambientales (incluida la composición química obtenida por metabolómica no dirigida) y las capacidades biodegradativas. Un paso clave en la Tesis Doctoral ha sido el centrado en el diseño y aplicación de una herramienta bioinformática que permita el análisis de la abundancia relativa de genes que codifican enzimas involucradas en la biodegradación de hidrocarburos alifáticos y aromáticos, a partir de la cual se pueden generar reconstrucciones de redes de biodegradación.

Tras la generación y el análisis de secuencias correspondientes a 18,435 especies a nivel de unidades taxonómicas operacionales al 97% (OTU_{97}), 238.449 marcos de lectura abierta (ORF) obtenidos por secuenciación masiva, y 610.227 ORF de genomas secuenciados similares filogenéticamente a los de las especies identificadas, se han predicho un total de 15.451 genes involucrados en la degradación de al menos 45 hidrocarburos alifáticos y aromáticos. El análisis comparativo muestra que la composición de las comunidades microbianas y sus capacidades de biodegradación están fuertemente influenciadas por la temperatura y la composición química. Así, aquellas zonas caracterizadas por una menor temperatura presentan una mayor diversidad microbiana pero menor número de genes catabólicos y viceversa. Respecto a la composición química, zonas que presentan un perfil de metabolitos similar muestran capacidades de biodegradación similares. El análisis comparativo con los metagenomas de muestras contaminadas en aguas profundas que se formaron alrededor del masivo vertido de petróleo ocurrido en el *Golfo de México* en 2010, ha revelado que las zonas sometidas a una contaminación crónica, a diferencia de aquellas donde ocurren vertidos ocasionales, presentan comunidades microbianas catabólicamente más diversas.

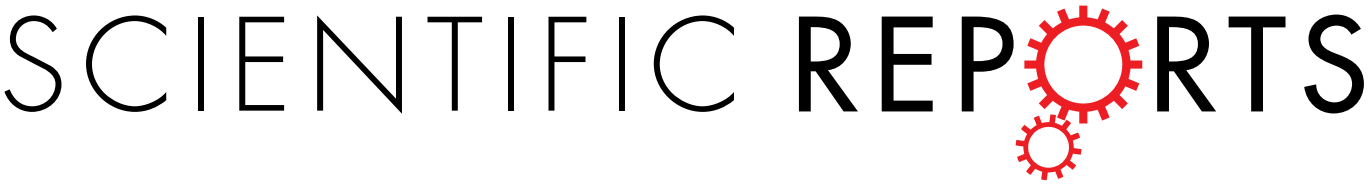

OPEN

Received: 02 November 2014
Accepted: 29 May 2015
Published: 29 June 2015

Bacterial population and biodegradation potential in chronically crude oil-contaminated marine sediments are strongly linked to temperature

Rafael Bargiela[1,*], Francesca Mapelli[2,*], David Rojo[3], Bessem Chouaia[2], Jesús Tornés[1,*], Sara Borin[2], Michael Richter[4], Mercedes V. Del Pozo[1], Simone Cappello[5], Christoph Gertler[6,†], María Genovese[5], Renata Denaro[5], Mónica Martínez-Martínez[1], Stilianos Fodelianakis[7], Ranya A. Amer[8], David Bigazzi[9], Xifang Han[10], Jianwei Chen[10], Tatyana N. Chernikova[6], Olga V. Golyshina[6], Mouna Mahjoubi[11], Atef Jaouanil[12], Fatima Benzha[13], Mirko Magagnini[9], Emad Hussein[14], Fuad Al-Horani[15], Ameur Cherif[12], Mohamed Blaghen[13], Yasser R. Abdel-Fattah[16], Nicolas Kalogerakis[7], Coral Barbas[3], Hanan I. Malkawi[17], Peter N. Golyshin[6,*], Michail M. Yakimov[5,*], Daniele Daffonchio[2,18,*] & Manuel Ferrer[1,*]

Two of the largest crude oil-polluted areas in the world are the semi-enclosed Mediterranean and Red Seas, but the effect of chronic pollution remains incompletely understood on a large scale. We compared the influence of environmental and geographical constraints and anthropogenic forces (hydrocarbon input) on bacterial communities in eight geographically separated oil-polluted sites along the coastlines of the Mediterranean and Red Seas. The differences in community compositions

[1]Institute of Catalysis, Consejo Superior de Investigaciones Científicas, Madrid, Spain. [2]Department of Food, Environmental and Nutritional Sciences (DeFENS), University of Milan, Milan, Italy. [3]Centro de Metabolómica y Bioanálisis (CEMBIO), Facultad de Farmacia, Universidad CEU San Pablo, Campus Montepríncipe, Madrid, Spain. [4]Ribocon GmbH, Bremen, Germany. [5]Institute for Coastal Marine Environment, Consiglio Nazionale delle Ricerche, Messina, Italy. [6]School of Biological Sciences, Bangor University, Bangor, UK. [7]School of Environmental Engineering, TU-Crete, Chania, Greece. [8]Environmental Biotechnology Department, Genetic Engineering and Biotechnology Research Institute, City for Scientific Research & Technology Applications, Alexandria, Egypt. [9]EcoTechSystems Ltd., Ancona, Italy. [10]BGI Tech Solutions Co., Ltd, Main Building, Beishan Industrial Zone, Yantian District, Shenzhen, China. [11]LR Biotechnology and Bio-Geo Resources Valorization (LR11ES31), Higher Institute for Biotechnology - University of Manouba, Biotechpole of Sidi Thabet, 2020, Sidi Thabet, Ariana, Tunisia. [12]Laboratory of Microorganisms and Active Biomolecules, University of Tunis El Manar, Tunis, Tunisia. [13]Laboratory of Microbiology, Biotechnology and Environment, University Hassan II – Ain Chock, Casablanca, Morocco. [14]Department of Biological Sciences, Yarmouk University, Irbid, Jordan. [15]Faculty of Marine Sciences, The University of Jordan-Aqaba, Jordan. [16]Bioprocess Development Department, Genetic Engineering and Biotechnology Research Institute, City for Scientific Research & Technology Applications, Alexandria, Egypt. [17]Hamdan Bin Mohammad Smart University, Academic City, Dubai, United Arab Emirates. [18]King Abdullah University of Science and Technology, BESE Division, Thuwal, 23955-6900, Kingdom of Saudi Arabia. [†]Current address: Friedrich Loeffler Institute - Federal Research Institute for Animal Health, Institute of Novel and Emerging Infectious Diseases, 17493 Greifswald, Germany. *These authors contributed equally to this work. Correspondence and requests for materials should be addressed to M.F. (email: mferrer@icp.csic.es)

and their biodegradation potential were primarily associated ($P < 0.05$) with both temperature and chemical diversity. Furthermore, we observed a link between temperature and chemical and biological diversity that was stronger in chronically polluted sites than in pristine ones where accidental oil spills occurred. We propose that low temperature increases bacterial richness while decreasing catabolic diversity and that chronic pollution promotes catabolic diversification. Our results further suggest that the bacterial populations in chronically polluted sites may respond more promptly in degrading petroleum after accidental oil spills.

The chemical diversity of crude oil components and environmental constraints such as depth, O_2 concentration, temperature, and nutrient input strongly influence microbial populations and the biodegradation processes they mediate in response to accidental oil spills in seawater and sediments[1–4]. In particular, the relative abundance of ubiquitous yet specialized hydrocarbonoclastic bacteria (HCB) of genera *Alcanivorax*, *Marinobacter*, *Oleispira*, *Thalassolituus*, *Oleiphilus*, *Cycloclasticus*, and *Neptunomonas*[5,6], as well as the expression of catabolic genes involved in oil component degradation and genes relevant to carbon, nitrogen, phosphorous, sulfur, and iron cycling, are modulated by variations in crude oil input in seawater and marine sediments[1–4,7–12].

Compared to sites of accidental crude oil spills, such as the Gulf of Mexico[13] or the NW coast of Spain[14], the Mediterranean Sea, particularly the southern part of the basin, has been neglected in studies of marine oil pollution, even though this region hosts large numbers of pipeline terminals, oil refineries, offshore platforms and 20% of global crude oil traffic, with consequent bunker accidents[15–18]. Notably, this region represents just 1% of the total marine surface of the planet. Several studies and reports have also demonstrated that numerous areas in the Mediterranean Sea are also polluted with toxic compounds other than crude oil components (UNEP/WHO, 1999), leading to a synergistic increase in overall toxicity[19,20]. Additionally, in contrast to open-sea areas, the Mediterranean Sea is a semi-enclosed basin with a water turnover time of 70–90 years, with a consequent rapid accumulation of toxic chemical species. This chronic crude oil input likely induces variation in bacterial populations; however the effects of parameters such as water temperature, O_2 concentration and crude oil input on the distribution and degradation potential of these populations are unknown.

The release of thousands of tons of petroleum hydrocarbons (PHs) originating from anthropogenic activity affects the marine environment and causes severe ecological and economical damage. Once released at the sea surface, PHs undergo both weathering processes (evaporation of volatile fraction, photo-oxidation) and emulsification[12,15]; as a result, significant amount of PHs become heavier, form tar and settle on sediments[21]. Marine sediments are often fine-grained, and the abundance of clay minerals coupled with high organic loads encourages sorption of the most hydrophobic PHs. Sedimentary accretion can result in the burial of hydrocarbons in zones of low redox potential. As a consequence, hydrocarbons have been found in fine-grained coastal sediments many decades after a spill due to slow anaerobic biodegradation. Indeed, the analysis of organic contamination in superficial sediments performed in this study revealed high concentrations of different classes of hydrocarbon pollutants originating from human activities. For all these reasons, sediment samples were the focus of the present investigation.

This study is the first to report basin-wide trends of marine bacterial diversity, ecology, and biodegradation potential (using a meta-network approach) in seven major chronically oil-polluted and geographically separated sites along a latitude gradient across the Mediterranean Sea. The chosen Mediterranean regions are characterized by heavy industrialization and dense urbanization with large tanker traffic transporting crude and refined oil to and from the refineries located at these sites[15–20]. We hypothesized that temperature can drive major measurable catabolic changes in the resident microbial communities. For this reason, an oil terminal site in the Gulf of Aqaba in the Red Sea, an area subject to intense maritime traffic and chronic pollution and of particular relevance in light of global warming predictions[22], was also included for comparative purposes. It is noteworthy that the Red Sea represents the potential future of the Mediterranean Sea as a result of its high seawater temperature[22]. By implementing an integrative metagenomic and metabolomics approach, our study highlights major changes at the level of bacterial components at colder and warmer sites in the Mediterranean Sea basin and the Red Sea. Thus, a positive impact of lower temperature on the total bacterial population was found, with a marked negative effect on catabolic diversity. A comparative analysis with pollutant-degrading webs established after the Horizon Oil Spill in the Gulf of Mexico provides further evidence suggesting that chronic pollution favors catabolic diversification.

Results

Study sites. The oil-polluted sites were located along the northern and southern sides of the Mediterranean Sea and the northern Red Sea[16] and included, in order of latitude coordinates, the following (the site code is in parentheses): 1) the site of the 1991 Haven tanker shipwreck (HAV) in the northernmost part of the Ligurian Sea, Genoa, Italy; 2) the harbor of Messina (MES), Sicily, Italy; 3) the coast adjacent to an oil refinery unit in the Elefsina Bay (ELF), northwest of Athens, Greece; 4) the harbor of Priolo (PRI) Gargallo, Syracuse, Italy; 5) the Bizerte lagoon (BIZ), located in Northern Tunisia;

6) the lagoon of Mar Chica (MCh), located on the north-west Mediterranean coast of Morocco; 7) the El-Max site (ELMAX), located on the coast west of Alexandria, Egypt; and 8) the Gulf of Aqaba (AQ), along the Jordanian coast at the northern end of the Red Sea. Information on the sites is provided in the Supplementary Methods.

The eight studied sediment sites exhibited the following characteristics (average values) at the time of sampling (Supplementary Table S1): *i*) a temperature ranging from 13.0 (for ELF) to 26.5 °C (for AQ); *ii*) a pH of 6.85 (for PRI) to 8.62 (for MCh); *iii*) an oxygen concentration (measured at the water level immediately above the sediment) ranging from anoxic (for PRI) to micro-aerobic (for MES: 1.0–2.2 mg/L) to aerobic (maximum 22.0 mg/L for MCh); *iv*) a conductivity ranging from 13.1 (for BIZ) to 89.0 (for AQ) ms/cm; *v*) a total concentration of 116 (for BIZ) to 260,000 (for HAV) mg petroleum hydrocarbons/kg sediment; *vi*) a total NH_4^+ concentration of 0.65 (for BIZ) to 61 μmol/L (for MCh); *vii*) a total Ca^{2+} concentration of 35.8 (for BIZ) to 430 mg/L (for MCh); *viii*) a dissolved organic carbon (DOC) from 5.0 (for HAV) to 143 mg/L (for ELF); *ix*) a particulate organic carbon (POC) from 1.20 (for ELF) to 2.29 μM (for AQ); *x*) a total concentration of microelements of 67.3 (for MCh) to 411 nM (for ELMAX); and *xi*) cell counts ranging from $\sim 1.90e^{+09} \pm 1.15e^{+09}$ (for HAV) to $\sim 2.22e^{+08} \pm 1.41e^{+08}$ (for MES) cell/g sediment. The warmest area was located, as expected, in the Gulf of Aqaba.

The rationale behind the sampling strategy was to target sites with aged and chronic contamination and in diverse environmental locations in the Mediterranean basin and in the North Red Sea. Accordingly, the samples investigated were inevitably rather heterogeneous (e.g., distinct O_2, conductivity, and NH_4^+, Ca^{2+}, DOC, POC, microelements and hydrocarbon inputs). Nonetheless, the samples are representative of some of the most prevalent types of chronically polluted sites distributed within the highly diverse Mediterranean Sea and Red Sea[16]. Moreover, they constitute the basis of proof-of-concept for an integrated, multi-omics approach (metagenome- and metabolome-wide scan), contributing to unraveling the core environmental parameters that regulate microbial population and catabolic activities in chronically polluted marine sites.

Bacterial populations can be categorized based on site temperature. The polluted sediments were first investigated in terms of the taxonomic diversity and composition of the resident bacterial communities using bar-coding of PCR-amplified bacterial 16S rRNA gene fragments obtained by 454 pyro-sequencing. The number of final reads and the number of Operational Taxonomic Units at 97% similarity (OTU_{97}) varied among the samples, with good coverage of the bacterial community diversity in all cases (Supplementary Table S2). The sequencing results demonstrated that each of the sediments hosts a distinct bacterial community (Supplementary Fig. S1), with richness shifting from low Shannon index values, as in the case of samples AQ (3.18) and MCh (4.07), to high Shannon index values, such as those recorded for samples ELF (8.10), PRI (7.39), and HAV (7.32) (Supplementary Table S2).

None of the total 18,435 OTU_{97} identified, which were distributed among 72 taxonomic groups across all phyla (Supplementary Table S3), was common to all the communities examined, suggesting a high metabolic heterogeneity among the clusters of samples (see Supplementary Results and Discussion). To explore bacterial community shifts between the different sediments, principal coordinates analysis was applied to depict similarity according to the OTU_{97} composition of the associated bacterial communities. Based on the sediment distribution in MDS1 (Fig. 1), which explains 20.46% of the total variation observed within the bacterial communities, the samples can be divided into two clusters (*t*-test, $P = 0.0017$): sediments collected at sites HAV, PRI, BIZ, and ELF formed Cluster 1, whereas those collected at sites AQ, MES, MCh, and ELMAX formed Cluster 2. The latter set of samples is characterized by a higher seawater temperature (from 20.0 to 26.5 °C) compared to the samples of Cluster 1 (from 13.0 to 19.3 °C). Moreover, two distinct subgroups are visible within Cluster 2: one corresponding to samples with the highest temperatures (MES [23.0 °C] and AQ [26.5 °C]) and another corresponding to samples with the lowest temperatures (MCh [21.3 °C] and ELMAX [20.0 °C]). No other environmental parameters among those examined herein explained these separations at the level of global species distribution. Taxonomic groups associated with the distinct clusters are discussed in Supplementary Results and Discussion. Taken together, we speculate that site temperature (Fig. 1) is a crucial driving factor controlling the overall species distribution in the chronically polluted sites investigated in this study in comparison to other environmental constraints such as geography, O_2 concentration and crude oil inputs. Note, however, that these factors, alone or in combination with temperature, are also important secondary factors that influence the distribution of particular sets of bacterial groups (Supplementary Table S3 and Results and Discussion).

To evaluate whether community shifts might facilitate the establishment of a basin-scale distribution of catabolic capacities, particularly biodegradation capacities, we employed the recently developed PiCRUST analysis[23]. However, this technique, which is proposed to derive functional information from taxonomic data, failed to identify such differences at the investigated sites (Supplementary Table S4). Considering that one crucial goal of this research was to better understand the differential potential of microbial communities to degrade crude oil contaminants in chronically crude oil-contaminated marine sediments, we explored a second approach based on AromaDeg analysis[24]. AromaDeg is a web-based resource with an up-to-date and manually curated database with an associated query system that exploits phylogenomic analysis of the degradation of aromatic compounds. This database addresses systematic errors produced by standard methods of protein function prediction, such as PiCRUST, by improving

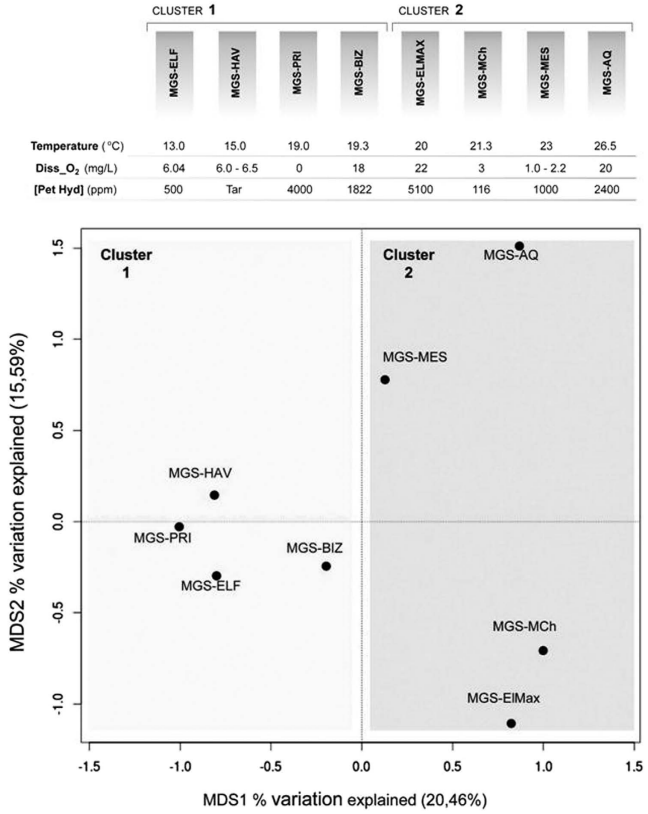

Figure 1. Principal coordinates analysis (PCoA) clustering Mediterranean Sea and Aqaba Gulf (Red Sea) polluted sediments according to the OTU_{97} composition generated from 16S rRNA gene pyrosequencing results. According to the sample distribution along MDS1, two clusters were identified through *t*-tests ($P = 0.0017$). The two clusters are indicated in the figure by light and dark grey boxes.

the accuracy of functional classification of key genes, particularly those encoding proteins of aromatic degradation. In brief, each query sequence from a genome or metagenome that matches a given protein family of AromaDeg is associated with a key catabolic enzyme for an aromatic degradation reaction[24–26]. Individual reactions, and thus the corresponding substrate pollutants and intermediate degradation products (see Supplementary Table S5A), can be manually linked to reconstruct catabolic networks, as has been successfully reported for microbial communities from polluted soils[27]. As the number of samples and degradation reactions examined in this study was high, we decided to design an in-house script that allowed the automatic reconstruction of such networks in a graphical format. The script allowed visualization and comparison of the relative abundance (rel. ab.) of genes encoding catabolic enzymes (to avoid artifacts due to differences in sample size) assigned to distinct degradation reactions and the substrate pollutants or intermediates possibly degraded by each of the communities. The complete workflow, including the scripts and commands used for catabolic network reconstruction, is described in the Supplementary Methods, and the results are presented below.

Reconstruction of catabolic networks: *in silico* prediction and experimental validations. Based on metagenomics data sets (meta-sequences), we identified a total of 238,449 potential protein-coding genes ($\geq$20 amino acids long) (Supplementary Table S6). Among them, 2,011 (or 0.84% of the total) are genes encoding catabolic enzymes with matches in AromaDeg[24,27]. The rel. ab. of catabolic genes assigned to presumptive degradation reactions and the substrate pollutants or intermediates possibly degraded by each of the communities are shown in Supplementary Fig. S2 and Table S5B.

Due to the limited sequence coverage ($\leq$2.9 Gbp of meta-sequences per sample), the reconstructed pathways were incomplete, as has been reported recently[27]. Thus, we refined the search for enzyme-encoding genes to fill the network gaps by examining a set of related genome sequence annotations established on the basis of 16S rRNA phylogenetic affiliations for each sample, as with PiCRUST analysis[23]. Of 610,277 potential protein-coding genes associated with OTU_{97} assignations, 13,440 were selected as matching AromaDeg[24]; these genes are presumptively involved in pollutant catabolism (Supplementary Fig. S3 and Table S5B).

As expected, the number of substrate pollutants or intermediates predicted as being potentially degraded on the basis of DNA and 16S rRNA data sets differed largely for those samples with the lowest DNA sequence coverage, namely HAV (DNA: 14; 16S rRNA: 40) and PRI (DNA: 3; 16S rRNA: 38); only minor differences (from 3 to 6 pollutants) were observed for the other samples for which high coverage was obtained (Supplementary Table S5B).

Experimental validations were conducted to further prove whether the addition of 16S rRNA data could impact interpretation of the results. Briefly, we used a 3-week enrichment protocol to evaluate the degradation of 17 pollutants expected to be degraded based on the DNA and 16S rRNA data sets (Supplementary Table S5B). These pollutants were selected on the availability of standards and the possibility of designing appropriate analytical procedures (see Fig. 2 legend). After 3 weeks of incubation, the rel. ab. of the 17 initial pollutants and of the 9 key degradation intermediates produced during their degradation (see Fig. 2 legend) was quantified by targeted analysis by gas chromatography-mass spectrometry (GC-Q-MS) and liquid chromatography-mass spectrometry (LC-QTOF-MS). Full details for the enrichment and analytical procedures and degradation efficiency can be found in Supplementary Methods and Results and Discussion. The rel. ab. of the mass signatures of all tested pollutants (data available in Supplementary Table S7A) and key degradation intermediates (Supplementary Table S7B) can be further linked to the presence of 21 key genes encoding catabolic enzymes involved either in their degradation (in the case of initial pollutants) or their production (in the case of intermediates). As shown in Fig. 2, a good agreement between the experimental validations and 16S rRNA-based predictions were found for all samples. Such a level of agreement was not found when considering the DNA-based predictions, which is most likely due, as mentioned above, to the fact that catabolic capacities were incomplete due to low sequence coverage. Therefore, biases were not introduced by refining the catabolic network using 16S rRNA data and in fact showed the predictive power of the combined DNA and 16S rRNA approaches. Note that, based on experimental metabolomics evidences, we were able to calculate confidence values, that give an estimation of the possibility that a given chemical is degraded based on a minimum number of catabolic genes (Supplementary Fig. S4) identified in the meta-sequence data sets. Calculated values are given in Supplementary Table S5.

According to the above considerations, a final biodegradation meta-network comprising degradation reactions assigned to genes encoding catabolic enzymes identified as present in the metagenomes (DNA) and those annotated for the most similar organisms in the communities based on 16S rRNA data was created (Fig. 3). The total rel. ab. of catabolic genes assigned to the final presumptive degradation reactions and the total number (45) and identity of substrate pollutants or intermediates possibly degraded, with a confidence of at least 90%, by each of the communities are summarized in Supplementary Table S5B. Such a biodegradation meta-network provides insight into whether each population has selected and evolved different biodegradation capacities on the basis of environmental constraints, which is discussed below.

Temperature is the dominant factor that regulates biodegradation capacities. We found that the members of all communities have the potential to contribute to the cycling of the majority of the 45 chemical species (substrate pollutants or intermediates) found to be presumptively degraded (Fig. 3). This finding suggests that variable combinations of bacterial populations from different phyla (Supplementary Fig. S1) could fulfill overlapping and/or complementary functional roles required to complete the degradation of these pollutants. This result was also confirmed experimentally, as the mass signatures of 26 of 45 (or 58%) pollutants (17 initial substrates and 9 intermediates) were identified in the corresponding enrichment cultures (Fig. 2; Supplementary Table S7).

As a second observation, we noted that the rel. ab. of genes encoding enzymes participating in biodegradation steps (Fig. 3) referred to the total number of genes (to avoid artifacts due to differences in sample size), ranged from 1.8% (for ELF) to 4.21% (for AQ) and was positively correlated with site temperature (Fig. 4). Thus, the highest numbers were obtained at those sites with the highest temperatures ($r^2 \sim 0.8$; $P = 4.5e^{-4}$). Importantly, in contrast to the results for enzyme-coding genes, species richness negatively correlated with temperature (Fig. 4 inset; $r^2 \sim 0.69$; $P = 0.0105$). This suggests that at chronically polluted sites, lower temperature most likely results in an increase in total biodiversity (Fig. 3 inset) while promoting the loss of catabolic (i.e., pollutant degradation) biodiversity, regardless of the geographic location and other environmental constraints.

To explore catabolic capacity shifts between the studied sediments, principal coordinates analysis was applied to depict similarity according to the rel. ab. of genes assigned to particular reactions/pathways. As stated above, the sediments were divided into two distinct clusters (Fig. 5; *t*-test, $P < 0.05$). Sediments collected at sites HAV, PRI and ELF formed Cluster 1, whereas those collected at sites AQ, MES, MCh, ELMAX and BIZ formed Cluster 2; the latter is characterized by a higher seawater temperature (from 19.3 to 26.5 °C) compared to Cluster 1 (from 13.0 to 19.0 °C), thus supporting that temperature is also a driving factor determining the distribution of catabolic genes. Such a distribution is similar to that of the bacterial population-wide scan (Fig. 1), except for BIZ, which had a different result. This finding suggests that a transition in biodegradation capacity may occur around 19–20 °C, though further evidence is required to confirm this assertion.

Major differences were found in the catabolism of at least 20 substrate pollutants. Among them, the effect of temperature is particularly noticeable when examining the rel. ab. of genes encoding enzymes

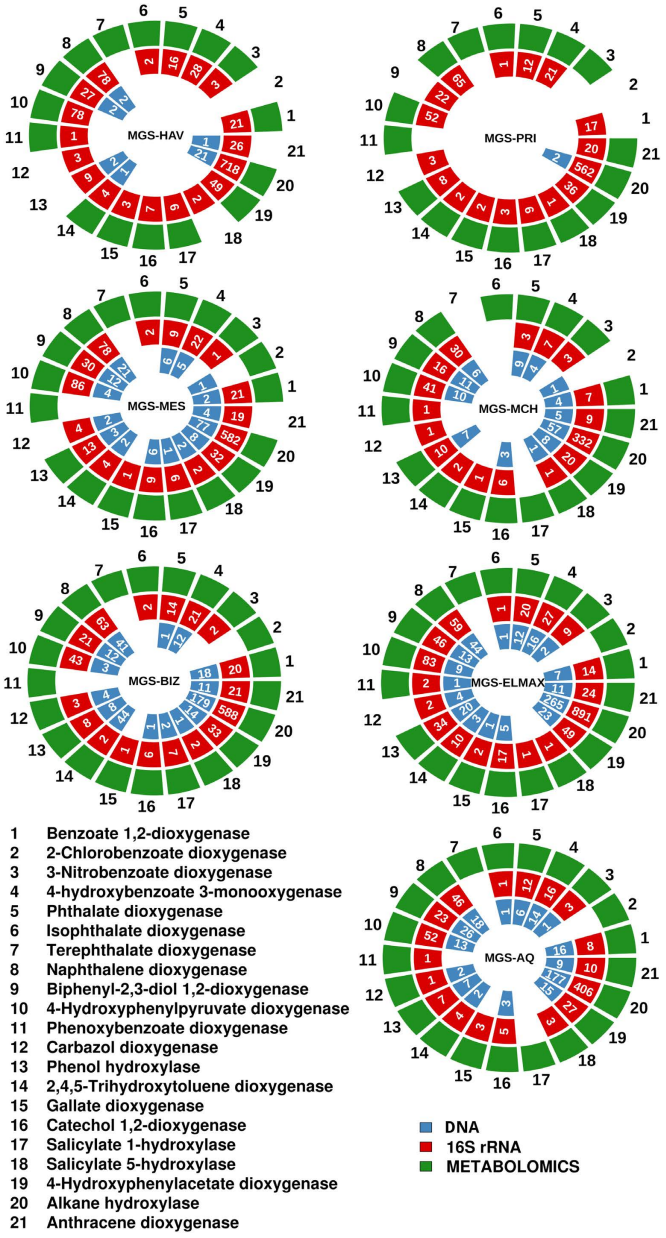

Figure 2. Enrichment and metabolomics-based experimental validation (green color) of degradation capacities mediated by presumptive enzymes encoded by catabolic genes expected on the basis of DNA (blue color) and 16S rRNA (red color) data sets. The number of genes encoding catabolic enzymes per each of the datasets is given inside the colored boxes. Briefly, enrichment cultures in ONR7a medium were performed, as described in Supplementary Methods, for each of the sediment samples in the presence of a pollutant mixture (10 mM total concentration) containing the following pollutants as a unique carbon source: naphthalene, anthracene, 2,3-dihydroxybiphenyl, 3,4-phenoxybenzoate, carbazole, phenol, 2,4,5-trihydroxytoluene, gallate, tetradecane, benzoate, 4-chlorobenzoate, 3-nitrobenzoate, 4-hydroxybenzoate, phthalate, isophthalate, terephthalate, and 4-hydroxyphenylpyruvate. Triplicate cultures for each duplicate sediment samples per site were set up. Two control experiments (in triplicates) were used: i) cultures without the addition of sediments but with chemicals; ii) cultures plus sediments but without the addition of chemicals. After 3 weeks of incubation, the rel. ab. of mass signatures of all the tested pollutants (data available in Supplementary Table S7A) and 9 key degradation intermediates including catechol, chlorocatechol, salicylate, muconate, gentisate, protocatechuate, homogentisate, myristate and homoprotocatechuate (data available in Supplementary Table S7B) was linked to the presence of 21 key genes encoding catabolic enzymes involved either in their degradation (in case of initial pollutants) or their production (in case of intermediates). See Supplementary Methods for descriptions of the links. Quantification was performed by target analysis using GC-Q-MS and LC-QTOF-MS. Colored box indicates DNA-, 16S rRNA- or metabolite-based signatures for a given catabolic gene. Confidence greater than 90% as indicated in Supplementary Table S5. Note: sample ELF was not included for the validation experiment, as no DNA data sets were available.

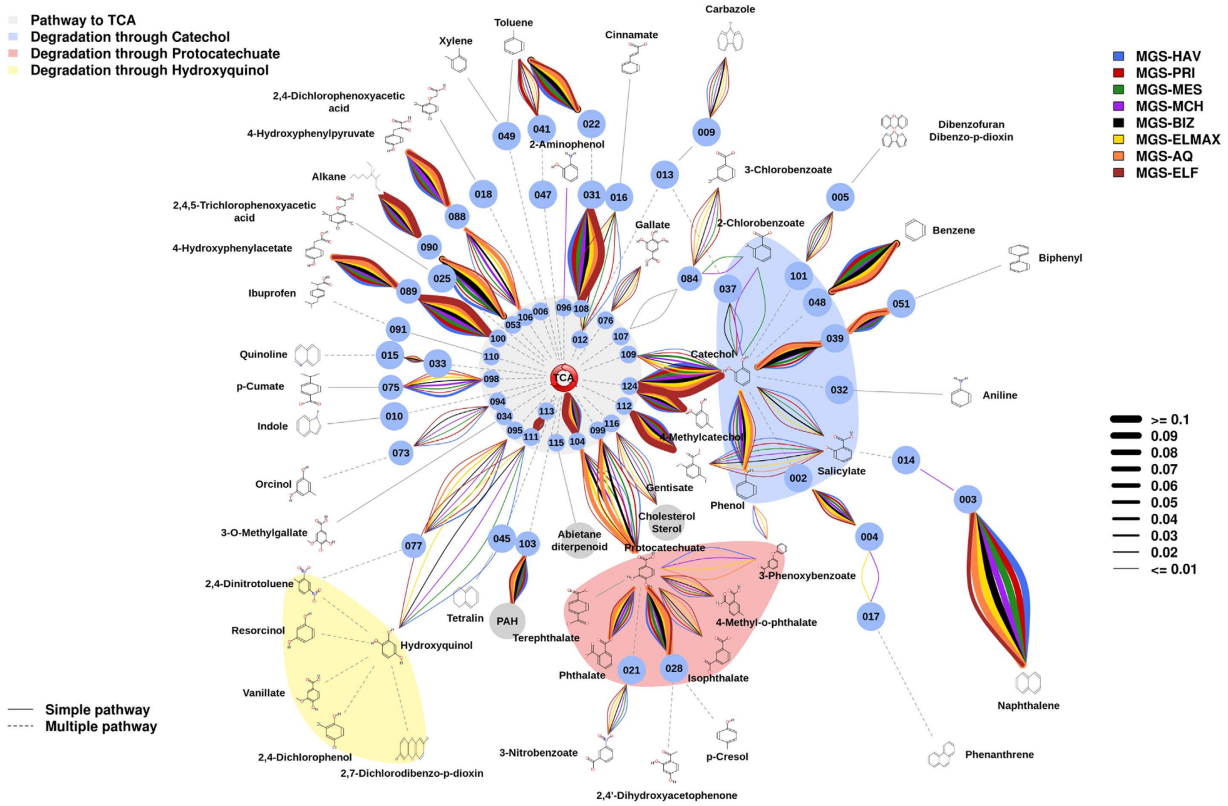

Figure 3. Potential aerobic and/or anaerobic degradation networks of alkanes and aromatics via di- and trihydroxylated intermediates in the investigated communities (see color code) after combining DNA- (Supplementary Fig. S2) and 16S rRNA-based (Supplementary Fig. S3) analyses. The biodegradation network reconstruction was performed as described in Supplementary Methods. Briefly, predicted open reading frames (ORFs) in the DNA or 16S rRNA-derived meta-sequences were filtered by score (>45) and e-value ($<10e^{-3}$) according to their similarity to the sequences of key aromatic catabolic gene families involved in the degradation of aromatic pollutants and alkanes[24,27]. After a manual check, a final list of gene sequences encoding enzymes potentially involved in degradation was prepared. For network reconstruction, each sequence was assigned to a metabolic substrate and a product with an assigned code, and the putative substrates and products processed in the sample were connected, creating a metabolic network using appropriate scripts and commands (for details, see Supplementary Methods). The rel. ab. of each catabolic gene assigned to degradation reactions, as represented by the thickness of the lines in the figure, and the complete list of substrates possibly degraded by the communities are summarized in Supplementary Table S5. Confidence greater than 90% as indicated in Supplementary Table S5. Note that rel. ab. refers to the total number of genes in a given sample to avoid artifacts due to differences in sample size. The codes for the chemical species in each pathway are as described in Supplementary Fig. S2 and Table S5A.

acting on catechol and phthalate (Fig. 6A). Thus, the rel. ab. of CatA catechol 1,2-intradiol (*t*-test; $P = 0.0181$) and XylE catechol 2,3-extradiol (*t*-test; $P = 0.01965$) ring-cleavage dioxygenases as well as OphA phthalate dioxygenases (*t*-test; $P = 0.01301$) positively correlated with the site temperature: the lowest rel. ab. was found at sites with the lowest temperatures (here, ≤19.3 °C) (Fig. 6A). High temperature was also found to be an important driver for the establishment of bacterial species with preferential capacity to degrade naphthalene via gentisate (through NahGH salicylate 5-hydroxylases) rather than via catechol (through salicylate 1-hydroxylases) (Fig. 6B). This was particularly noticeable in the two aerobic sites with the highest seawater temperature, namely, MES (21.3 °C) and AQ (26.5 °C), where only NahGH but not salicylate 1-hydroxylases were found. Note both genes encoding enzymes were found in other sediments, albeit to different extents (Fig. 6B). Temperature was found to also be a relevant factor affecting the presence and abundance of genes encoding catabolic enzymes involved in catechol (by routes others than that from naphthalene) and protocatechuate production, which was most evident in the warmest (26.5 °C) AQ site. Thus, genomic signatures were identified that suggest that all communities exhibited the potential to produce catechol through phenol (via PhO), biphenyl (via Bph and Ben), benzene (via benzene dioxygenase) and polycyclic aromatics (via 1-hydroxy-2-naphthoate dioxygenase,

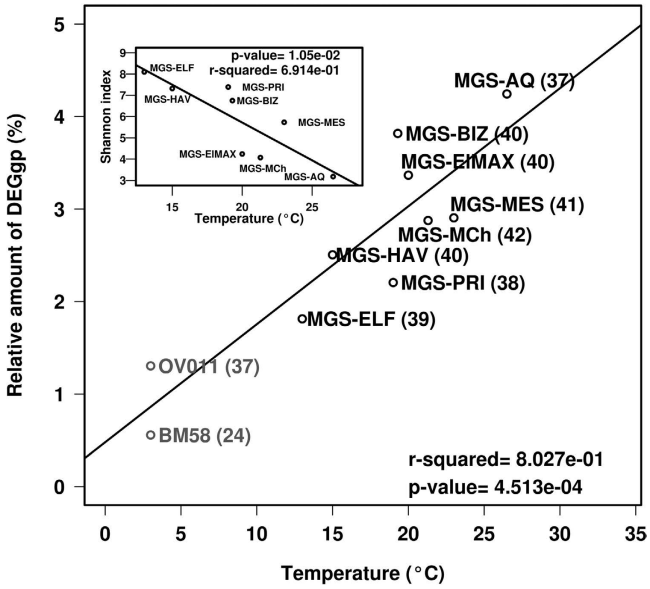

Figure 4. Temperature as an environmental factor driving the size of biodegradation meta-webs at the eight studied sites. A significant positive correlation ($r^2 \sim 0.8$; $P = 4.5e^{-4}$; *t*-test) was found between the relative percentage of genes encoding enzymes participating in biodegradation steps (DEGgp) based on the total number of genes (to avoid artifacts due to differences in sample size) ($\Sigma_{DNA+16SrRNA}$ predictions; see Supplementary Table S5B) and site temperature. The corresponding data for the BM058 and OV011 sites from the Deepwater Horizon oil spill were also included in the correlation analysis. The total number of unique polluting chemicals (initial substrates or intermediates inferred from both DNA and 16S rRNA data) presumptively accepted as substrates for enzymes in each microbial population is shown in brackets. The Shannon index, as a measure of biodiversity, negatively correlates ($r^2 \sim 0.69$; $P = 0.0105$; *t*-test) with site temperature, as shown in the inset graph. Note that a positive correlation ($r^2 \leq 0.78$; $P \leq 3.8e^{-3}$; *t*-test) was also found when considering only gene content based on 16S rRNA or DNA data sets (Supplementary Fig. S5).

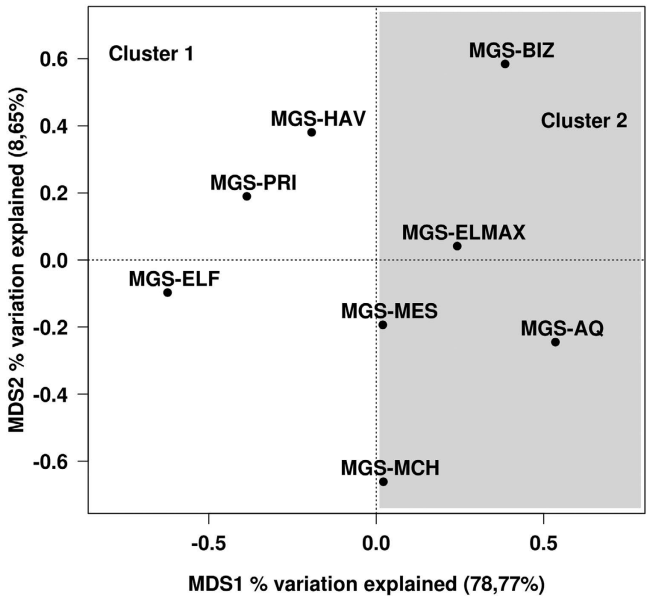

Figure 5. Principal coordinates analysis (PCoA) showing the clustering of catabolic gene distributions (DNA + 16S rRNA) in the Mediterranean Sea and Aqaba Gulf (Red Sea) polluted sediments. According to the sample distribution along MDS1, two clusters were identified, as indicated by light and dark grey boxes.

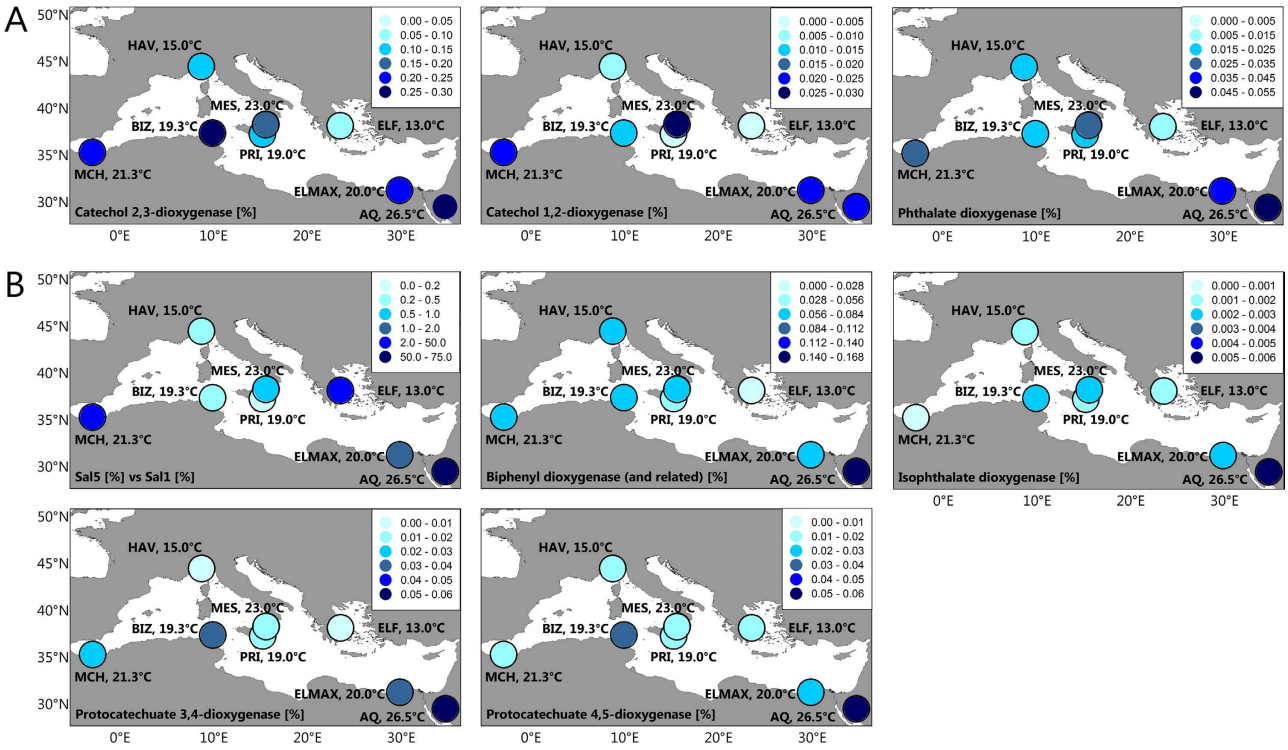

Figure 6. Multi-panel map of the spatial distribution of catabolic genes abundance (DNA + 16S rRNA) in the study area. Panels (A) and (B) represent genes most representative of low- and high-temperature sites, respectively. Site temperatures are indicated in the panels. The values are represented by colored dots. See the legend in each panel as a reference. Spatial distributions of gene percentages in the study area (for details see Supplementary Table S5) were produced using Golden Software Surfer 8.0. The data are plotted as colored dots showing the true values at each sampling station. Note, than in Panel B, the first map illustrates the relative percentage of genes encoding salicylate-5-hydrolyases (Sal5) as compared to salicylate-1-hydroxylases (Sal1). Reactions associated to genes encoding enzymes in panels, as follows: Catechol-2,3-dioxygenase (XylE): catechol ⇒ cis,cis-2-hydroxy-6-oxohexa-2,4-dienoate (code 124, Fig. 3); Catechol-1,2-dioxygenase (CatA): catechol ⇒ cis,cis-muconic acid (code 109, Fig. 3); Phathalate dioxygenase (OphA): phthalate ⇒ Protocatechuate; Salicylate-5-hydrolyase (Sal5 or NahGH): salicylate ⇒ gentisate; Salicylate-1-hydrolyase (Sal1): salicylate ⇒ catechol; Biphenyl dioxygenase (Bph): biphenyl ⇒ biphenyl-2-3-diol (code 51, Fig. 3); Isophathalate dioxygenase: isophthalate ⇒ protocatechuate; Protocatechuate 3,4-dioxygenase: Protocatechuate ⇒ 3-carboxy-cis,cis-muconate (code 104, Fig. 3); Protocatechuate 4,5-dioxygenase: Protocatechuate ⇒ 2-hydroxy-4-carboxymuconate-6-semialdehyde (code 099, Fig. 3).

and Dfd), with the first three substrates being those pollutants that are most likely to result in catechol production (Fig. 3). However, biphenyl to catechol conversion (via Bph) was particularly enriched at the site with the highest seawater temperature (AQ site): up to 6.54-fold compared to the abundance at other sites (Fig. 6B). In addition, all communities also displayed the potential to produce protocatechuate from phthalate (via OphA), iso-phthalate (via isophthalate dioxygenase), methyl-phthalate (via aromatic demethylase), 4-hydroxybenzoate (via 4-hydroxybenzoate 3-monooxygenase) and 3-phenoxybenzoate (via phenoxybenzoate dioxygenase) (Fig. 3). However, the conversion of phthalate (via OphA) and isophthalate (via isophthalate dioxygenase) to protocatechuate was especially enriched at the AQ site (up to 3.23-fold; $P = 5.4e^{-3}$) compared to the relative contribution at other sites (Fig. 6B). Gene signatures for the further degradation of protocatechuate via protocatechuate 4,5-dioxygenase and protocatechuate 3,4-dioxygenase were observed at all sites to a similar degree, though these genes were both most abundant at the AQ site (from 1.85- to 4.94-fold, depending the site; $P = 1.2e^{-5}$) (Fig. 6B).

The spatial distributions of genes encoding enzymes supporting other distinct biodegradation capacities in the study areas are summarized in Supplementary Fig. S6.

Genes encoding enzymes for crude oil degradation are prevalent in chronically polluted sites independently of environmental constraints. A number of major common catabolic features were observed for all sites, independent of the environmental constraints, when analyzing the rel. ab. of catabolic genes (Fig. 3; Supplementary Table S5). First, alkanes were predicted to be the best pollutant

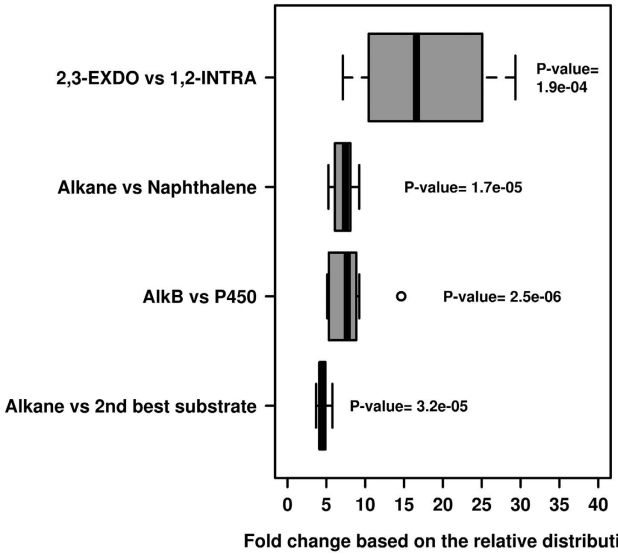

Figure 7. Box plot of the relative contribution of genes involved in degradation steps . Percentages were calculated on the basis of the data obtained from the DNA and 16S rRNA gene content analysis. *P*-values correspond to Student's *t*-test of the average of the relative contribution of the enzyme classes, as based on the Welch approximation.

substrates for all communities, as based on the overabundance of genes encoding alkane-degrading enzymes (AlkB and, possibly, P450) compared to the second most abundant gene class, namely, those encoding gentisate (in HAV, PRI and MES)- and catechol (in the remaining samples)-modifying enzymes (4.53-fold average; $P = 3.2e^{-5}$) (Fig. 7); note that the rel. ab. level of AlkB- and P450-coding genes ranged from 0.68% (for ELF) to 1.36% (for AQ) and that AlkB was, on average, 7.93-fold ($P = 2.5e^{-6}$) more abundant than P450 in all samples (Fig. 7). This suggests that alkanes are more efficiently degraded than recalcitrant polycyclic aromatics in the chronically polluted sites investigated here. A high rel. ab. level of genes encoding fatty acid hydroxylases, ranging from 0.016% (for PRI) to 0.065% (for BIZ), was also observed. These results are in agreement with previous studies that demonstrated that AlkB-coding enzymes and related enzymes (e.g., alkane hydroxylases) are the most prevalently expressed at elevated alkane concentrations[2,9,11]. This finding supports the consideration that chronic pollution, regardless of the crude oil input (from 116 ppm at the BIZ site to 260,000 ppm in HAV; Supplementary Table S1), also results in a preferential enrichment of bacteria possessing genes involved in alkane degradation (Fig. 3 and Fig. 7), regardless of the geographic location and environmental constraints. Accordingly, we speculate that the microbial populations inhabiting chronically polluted sites might be highly adapted, and respond more rapidly, to the degradation of petroleum components after an accidental oil spill than populations at 'clean' seawater, where *alk*B genes constitute minor components[2,9,11]. Second, the rel. ab. level of genes encoding enzymes for the degradation of polyaromatic compounds (such as Ndo, PhdA, Dfd) was, on average, 5.87-fold lower ($P = 3.55e^{-6}$) than that of AlkB (Fig. 7), as was also reported at the Deepwater Horizon oil spill[2]. A third common attribute was an overabundance of genes encoding XylE catechol 2,3-extradiol (EXDO) compared to CatA catechol 1,2-intradiol (INTRA) ring-cleavage dioxygenases (19.78-fold average; $P = 1.9e^{-4}$; Fig. 7), which suggests that EXDO cleavage processes are of greater importance than INTRA cleavage processes at all the studied sites, regardless of geographic location and environmental constraints.

Biodegradation signatures in the Deepwater Horizon oil spill. Accumulated evidence has demonstrated differences in microbial community structures and biodegradation gene contents in different plume sites within the Deepwater Horizon oil spill[2,12]; the differences relate to the amount of time that the respective sites were exposed to hydrocarbons as well as to the crude oil concentration. Two different samples from the Deepwater Horizon oil spill, BM058 (Longitude: −88.4375; Latitude: 28.672222; JGI project ID 403207; taxon IDs 2088090017 and 2081372002) and OV011 (Longitude: −88.4375; Latitude: 28.672222; JGI project ID 403191; taxon ID 2081372001), the metagenomic contents of which have been recently reported[2,12], were further analyzed using the meta-network procedure applied in this study. To this end, meta-sequences corresponding to samples BM058 and OV011 were obtained from the Joint Genome Institute webpage (https://img.jgi.doe.gov/; see accession numbers above) and analyzed in the same way as the meta-sequences generated in this study. A total of 1,174 of 137,924 potential protein-coding genes covering unique proteins were identified. The rel. ab. of sequences presumptively involved in biodegradation compared to the total number of sequences (Supplementary Table S5A) was 2.3-fold higher at the OV011 site (1.30%) compared to BM058 (0.56%), in agreement with the closer

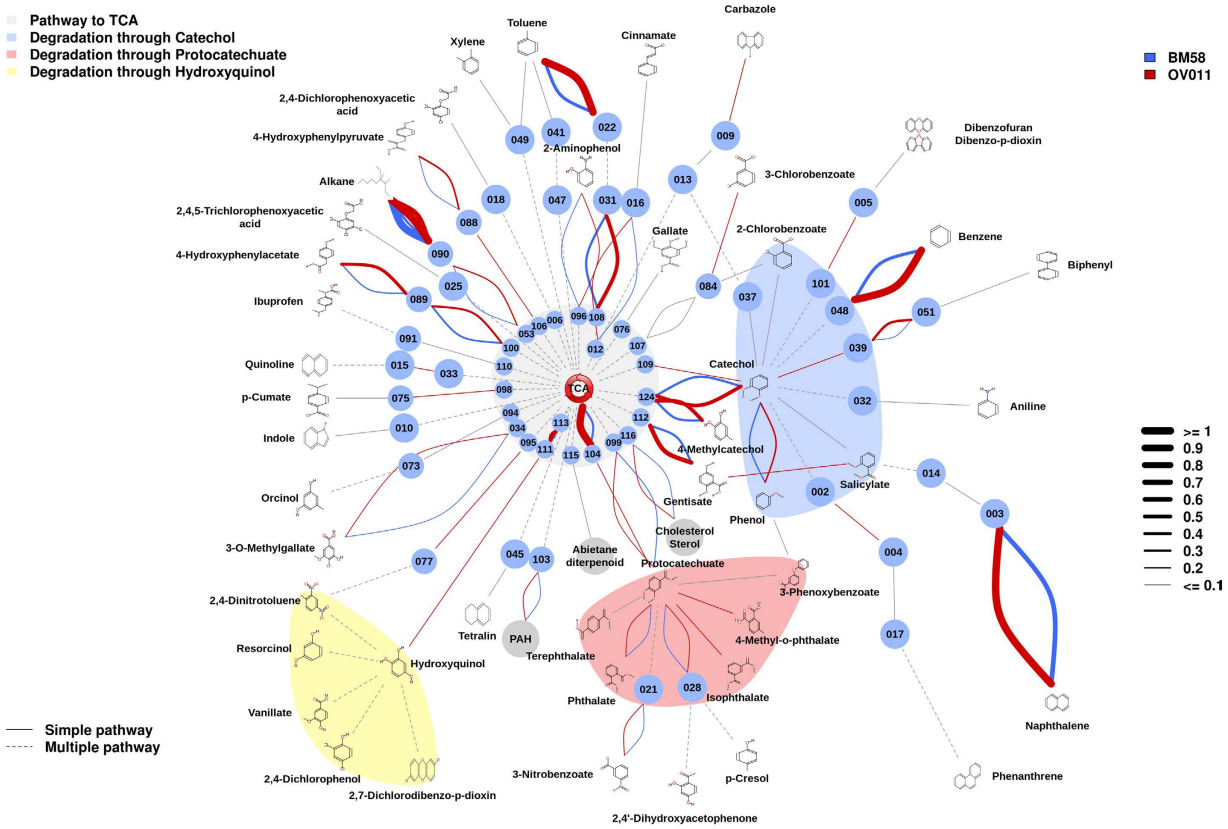

Figure 8. Potential aerobic and/or anaerobic degradation networks of alkanes and aromatics via di- and trihydroxylated intermediates in the investigated communities in the BM058 and OV011 sites within the Deepwater Horizon oil spill. The color code used for the respective pathways is shown. Confidence greater than 90% as indicated in Supplementary Table S5. For details about the graphical representation of the network, the thickness of the lines and the codes for the chemical species, see the legend to Fig. 3.

location of OV011 to the wellhead of the oil spill[6] and with previous observations demonstrating that genes encoding enzymes for biodegradation are prevalent in the plume[2]. Altogether, this result suggests that the meta-network approach applied in the study can be of interest for investigating catabolic diversity in any type of sample. The diversity of genes encoding catabolic enzymes further reveals genomic evidence for the presumptive metabolism of 37 (for OV011) and 24 (for BM058) different substrates and/or their intermediates (Fig. 8; Supplementary Table S5B), indicating that the hydrocarbon input also positively influenced the size of the biodegradation meta-network. A comparison of the OV011 and BM058 meta-webs further revealed the absence of the presumptive genes encoding XylE catechol 2,3-extradiol dioxygenase at BM058, suggesting a positive correlation between the presence of XylE genes and the concentration of crude oil (or the distance to the plume). This agrees with the fact that compared to CatA catechol 1,2-intradiol dioxygenase, XylE genes were most abundant in the chronically contaminated sites investigated herein (Fig. 7).

A direct comparison between the Mediterranean and Red Sea sites and those at the Deepwater Horizon oil spill first highlighted that the number of presumptive substrate pollutants ($\leq$37) is slightly lower than those potentially metabolized in the eight studied sites in the Mediterranean and Red Seas (45 in total, Fig. 3; Supplementary Table S5B). Second, the rel. ab. of total sequences encoding catabolic enzymes in the OV011 (1.30%) and BM058 (0.56%) sites was significantly lower than that in the chronically polluted sites investigated (Fig. 4). This is in agreement with the lower temperature at the Deepwater Horizon oil spill ($<$3 °C)[2,6], compared to those at the sites investigated herein (from 13.0 to 26.5 °C) and the loss of catabolic genes at the lower temperatures demonstrated in this study (Fig. 4). Notably, among catabolic genes, AlkB-, P450- and fatty acid hydroxylase-coding genes, presumptively involved in the initial degradation of crude oil components, accounted for a total of 0.65% (or 50% of the total) and 0.23% (or 41% of the total) at OV011 and BM58, respectively; however, the rel. ab. was higher in the chronically polluted sites: from 0.81% (for PRI) to 1.46% (for AQ). This suggests that chronic pollution may also positively influence the abundance of genes encoding proteins for the initial degradation of major crude oil components such as alkanes.

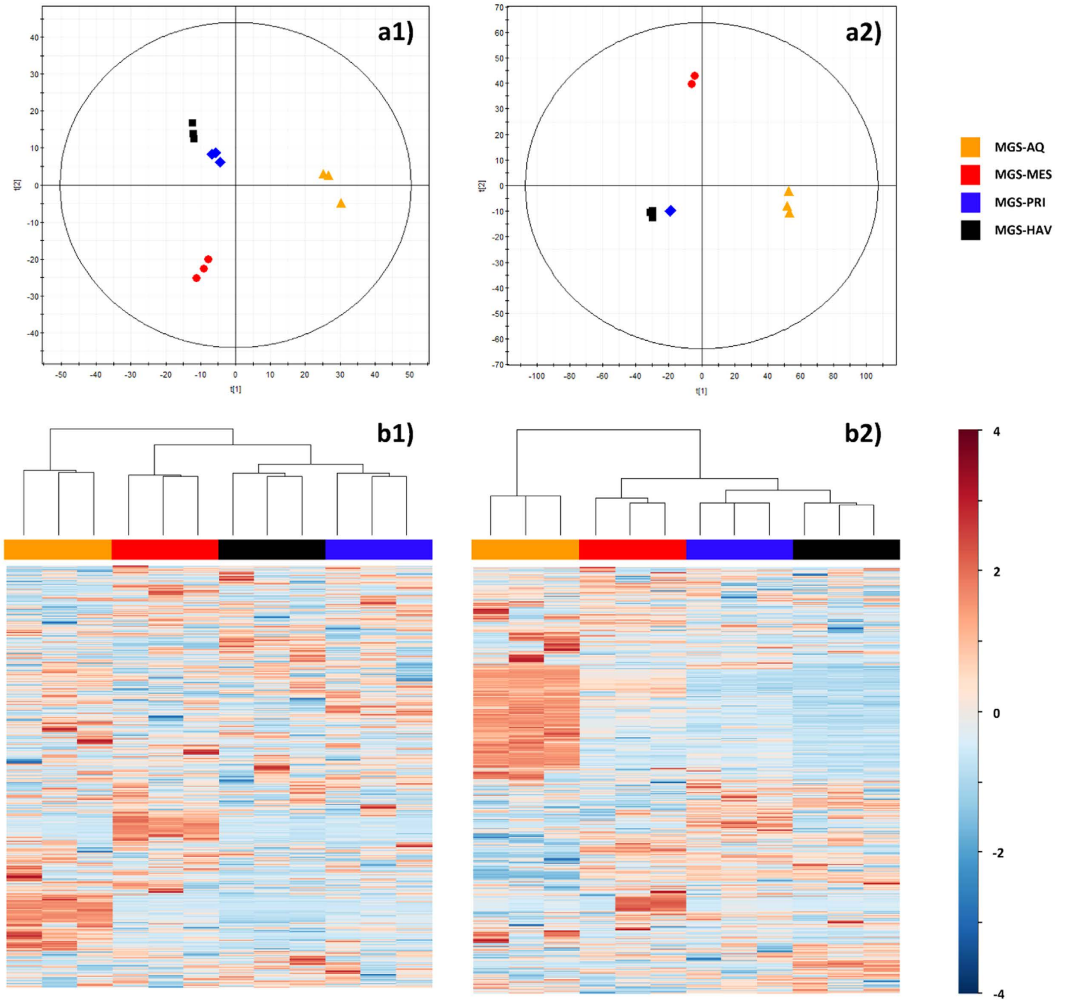

Figure 9. Metabolite profiles in chronically-polluted sites. a) Principal Components Analysis (PCA) plot for models built with the filtered set of metabolome data (metabolites extracted in triplicates). a1) LC-MS (−): 2 components, $R^2 = 0.338$, $Q^2 = 0.013$. a2) LC-MS (+): 2 components, $R^2 = 0.491$, $Q^2 = 0.210$. **b**) Hierarchical clustering analysis performed with the filtered masses, whereby abundances were scaled by mean-centering and dividing by the standard deviation of each variable. b1) LC-MS (−). b2) LC-MS (+).

Metabolome-wide scan revealed strong ecotype-chemical species associations. The data presented above suggest that environmental constraints, particularly temperature, impact biodiversity and pollutant-degrading populations and catabolic web structures. We further examined whether the chemical diversity at the sampling sites, which may be a direct consequence of chronic pollution[16], also had a significant effect on ecosystem diversity and catabolism. Rather than examining the chemical diversity of crude oil components[4], we analyzed a large number of metabolites by a combination of mass spectrometry (MS) with liquid chromatography (LC) separation, which yields rapid and quantitative results in a single analysis in a non-biased manner[28]. Due to sample limitations, only four samples (PRI, HAV, MES and AQ) could be examined. Nonetheless, these samples are representative of the clusters previously identified and are characterized by moderately low (15–19 °C) to moderately high (23–26.5 °C) temperatures, a high level of chronic pollution (≥1,000 ppm total petroleum hydrocarbons) and a wide range of O_2 concentrations (from anoxic to 20.0 mg/L). Metabolites were directly extracted from the sediment samples (see Supplementary Methods) and analyzed. The profiles obtained were complex due to the high number of metabolite signals present in the samples (Supplementary Table S8). During data treatment (*t*-test, $P < 0.05$), the list of significantly different masses obtained in positive mode was reduced from 114,050 after alignment to 3,390 after filtering and from 54,358 to 1,485 in LC-MS negative mode. The filtering criteria were based on the selection of masses that were present in at least 100% of the replicate samples per group. Classification of the samples revealed clusters (Fig. 9) in which PRI and HAV were the most similar with respect to chemical diversity. The robustness of the analytical procedure was demonstrated by the tight clustering of the sample replicates (Fig. 9, panels A1 and A2), confirming that the separation among the groups was due to real biological variability and was not generated randomly.

A direct comparison with the clusters found by examining the bacterial diversity established by the 16S rRNA pyrotag analysis (Fig. 1) and the distribution of genes encoding enzymes involved in biodegradation (Fig. 4) revealed similar trends as for the chemical species (Fig. 9).

Discussion

Polluted environments generally host a finely tuned restricted set of microbes[5,6], with the phylotype richness depending highly on the chemical species released to the environment and the pollution level[1–4]. Moreover, multiple environmental factors have been shown to alter marine microbial communities[7–12]. Nonetheless, it remains to be determined how multiple environmental pressures impact such populations and which of these, if any, is the dominant driving factor determining the final catabolic outcomes. Of particular significance is that information on microbial populations and functional content in marine ecosystems where oil spills have occurred is limited in the specialized literature for the Mediterranean and Red Seas, both of which receive major crude oil inputs[16]. This study went beyond descriptive studies of community composition[16] and utilized taxonomic bar-coding, metagenomic prediction platforms for inferring biodegradation activities, and a metabolome-wide scan to provide deeper insight into the common and distinctive populations and biodegradation biomarkers and deficits associated with seven geographically separated major oil-polluted sites along the coastlines of the Mediterranean Sea and one from the Red Sea. The total concentration of hydrocarbons in the sediments exceeds that of clean seawater (15 ppm) by at least 7.7- to 17,000-fold (Supplementary Table S1), supporting the importance of investigating the degradation processes occurring in polluted sediments, which are influenced by accumulation phenomena.

The results of this study draw attention to the huge undiscovered pool of bacterial species populating the Mediterranean Sea, including the northern and southern parts of the basin, and the Gulf of Aqaba in the Red Sea. These microorganisms might play important roles in the cycling of prevalent and persistent pollutants as well as in total carbon cycling. We demonstrated that the microbial populations in the chronically polluted sites investigated have the presumptive capacity to degrade at least 45 polluting chemicals, and the ability to degrade 26 of these substrates (including initial pollutants and intermediates) was experimentally confirmed in microcosms using targeted metabolomics. This number is slightly higher (up to 1.8-fold) than that observed at the Deepwater Horizon oil spill sites. Our findings further revealed that the sites investigated herein, which are subjected to chronic anthropogenic forces (hydrocarbon input), exhibit selection for bacterial species other than the ubiquitous specialized HCB (see Supplementary Results and Discussion). In addition, although the relative percentage of gene sequences encoding enzymes for biodegradation range from 0.56 to 1.30% in the cold (<3 °C)[2,12] OV011 and BM058 sites at the Deepwater Horizon oil spill, this number, which increased with site temperature, was up to 5.6-fold higher in the moderately warmer sites examined in this study (from 13 to 26.5 °C) (Fig. 4). This finding is of practical importance because it suggests that compared to bacteria inhabiting clean sites where random or accidental oil spills occur, warmer chronically polluted sites might promote the establishment of catabolically adaptable microbial populations, other than HCB, that can respond to an accidental oil spill to a higher degree than previously thought. In relation to this, our results also suggest that approximately half of the genes encoding catabolic enzymes in the Deepwater Horizon oil spill sites, referred to as the total genes, encode enzymes mediating the initial attack of alkanes. Conversely, in the chronically polluted sites of the Mediterranean and Red Seas examined here, such genes accounted for approximately 33–36%, suggesting that the chronic exposure to pollutants may have played a role in catabolic diversification (Fig. 3 and Fig. 7).

We are aware that OV011 and BM058 are highly polluted samples, as they were collected from the Gulf of Mexico approximately one week after the Horizon Oil Spill occurred (cruise date: 27.04.2010–2.06.2010)[2,12]; however, they can also be considered to be characterized by a state of natural chronic pollution from crude oil seepage. Therefore, it is also plausible that the different chemical species accumulated in the naturally influenced deep Gulf of Mexico (yet to be investigated) compared to the more anthropogenically influenced sites examined herein may play a role in the observed differences. The fact that the differences reported here may also be derived from the distinct types of samples that were compared (sediments in this study vs seawater in the OV011 and BM058 samples) cannot be ruled out. Regardless, it should also be highlighted that some of the dominant presumptive bacteria and catabolic genes identified herein may not be the most active degraders in the examined sediment samples, as has been recently demonstrated when comparing untreated and bio-stimulated soils[29], and that the determination of their biodegradation efficiency will require further investigation.

It should also be noted that the sequencing depth ($\leq$2.9 Gbp per sample) presented here may be considered low. However, the main objective of the metagenomic survey was not to access an extensive sequencing depth but rather to obtain sufficient sequence data to allow a determination of whether distinct biodegradation capacities might be linked to environmental constraints and community shifts, which was achieved in the present investigation. This issue was partially resolved by examining genomes established on the basis of phylogenetic affiliations[23] performed at a higher depth. Our study is also the first to highlight the profound shifts in taxonomic and catabolic ecotypes in both basins, which apparently were highly influenced by the seawater temperature, independent of the other environmental constraints (i.e., O_2 and total hydrocarbon concentration). Although temperature has been demonstrated to contribute to marine and soil microbial diversity evolution[30,31], our data show for the first time its

association with the specific loss (low temperature) or gain (high temperature) of catabolic biodiversity as well as with the modulation of the microbial capacity to preferentially degrade certain aromatic pollutants (e.g., naphthalene, gentisate, catechol, phthalate). As an example, the sites with lower temperatures contained the highest bacterial diversity while being characterized by a lower presence of catabolic genes, particularly for catechol and phthalate metabolism. This suggests a positive impact of lower temperature on the total bacterial population while having a marked negative effect on catabolic diversity. In addition, our data suggest that the accumulation of chemical species in the semi-enclosed Mediterranean basin and the Red Sea might contribute to the establishment of such temperature-guided populations and the channeling recalcitrant accumulated pollutant substrates into distinct catabolic pathways. Recently, it has been demonstrated that the abundance of pollutant-degrading bacteria decreased as a consequence of biological treatments such as bio-stimulation and supplementation with pollutants in slurry-phase bioreactors operating for over 3 years at 23 °C[29]. This contrasts with the results of the present study, pointing to the catabolic diversification as a consequence of chronic pollution. It is plausible that the differences in the time frames (decades of contamination in the sites investigated herein vs 3 years) and the chemical diversity (multiple pollutants and chemicals in natural sites vs one (anthracene) in the reported enrichment culture) in the two investigations may be responsible for the observed variation. In addition, the differences could also be due to the fact that Dunlevy and cols[29] investigated phenomena occurring in a bio-reactor-scale system in which enrichment cultures (with their limits) were analyzed, whereas our study reports trends occurring in the environment.

Taken together, for chronically polluted sites, investigating the sediment and water temperature might reveal regular patterns of behavior with predictive value. We believe that these findings, for which no previous evidence exists in the scientific literature, potentially open new research avenues for investigating novel site-tailored bioremediation approaches based on site characteristics as well as for establishing global biodegradation webs based on genomic signatures, pollutant types and geoclimate constraints.

Methods

Experimental settings and data analysis. The full description of the materials and methods used for the: a) environmental measurements, sample collection, and nucleic acid extraction, b) SSU rRNA hypervariable tag analysis, including the workflow scripts and commands, c) DNA sequencing and gene calling, d) biodegradation network reconstruction, including description of scripts and commands for graphics, e) enrichment cultures and target metabolomics for experimental validations of biodegradation capacities, f) metabolomic fingerprint analysis of sediment samples, and g) cell counts is available in the Supplementary Methods.

References

1. Liang, Y. *et al.* Functional gene diversity of soil microbial communities from five oil-contaminated fields in China. *ISME J.* **5,** 403–413 (2011).
2. Mason, O. U. *et al.* Metagenome, metatranscriptome and single-cell sequencing reveal microbial response to Deepwater Horizon oil spill. *ISME J.* **6,** 1715–1727 (2012).
3. Gutierrez, T. *et al.* Hydrocarbon-degrading bacteria enriched by the Deepwater Horizon oil spill identified by cultivation and DNA-SIP. *ISME J.* **7,** 2091–2104 (2013).
4. Kimes, N. E. *et al.* Metagenomic analysis and metabolite profiling of deep-sea sediments from the Gulf of Mexico following the Deepwater Horizon oil spill. *Front. Microbiol.* **4,** 50 (2013).
5. Head, I. M., Jones, D. M. & Röling, W. F. Marine microorganisms make a meal of oil. *Nat. Rev. Microbiol.* **4,** 173–182 (2006).
6. Kube, M. *et al.* Genome sequence and functional genomic analysis of the oil-degrading bacterium *Oleispira antarctica*. *Nat. Commun.* **4,** 2156 (2013).
7. Lu, Z. *et al.* Microbial gene functions enriched in the Deepwater Horizon deep-sea oil plume. *ISME J.* **6,** 451–460 (2012).
8. Kostka, J. E. *et al.* Hydrocarbon-degrading bacteria and the bacterial community response in gulf of Mexico beach sands impacted by the deepwater horizon oil spill. *Appl. Environ. Microbiol.* **77,** 7962–7974 (2011).
9. Beazley, M. J. *et al.* Microbial community analysis of a coastal salt marsh affected by the Deepwater Horizon oil spill. *PLoS One* **7,** e41305 (2012).
10. Ortmann, A. C. *et al.* Dispersed oil disrupts microbial pathways in pelagic food webs. *PLoS One* **7:** e42548 (2012).
11. Rivers, A. R. *et al.* Transcriptional response of bathypelagic marine bacterioplankton to the Deepwater Horizon oil spill. *ISME J.* **7,** 2315–2329 (2013).
12. Mason, O. U. *et al.* Metagenomics reveals sediment microbial community response to Deepwater Horizon oil spill. *ISME J.* **8,** 1464–1475 (2014).
13. Hazen, T. C. *et al.* Deep-sea oil plume enriches indigenous oil-degrading bacteria. *Science* **330,** 204–208 (2010).
14. Acosta-González, A., Rosselló-Móra, R. & Marqués, S. Characterization of the anaerobic microbial community in oil-polluted subtidal sediments: aromatic biodegradation potential after the Prestige oil spill. *Environ. Microbiol.* **15,** 77–92 (2013).
15. Margottini, L. Gulf drilling disaster triggers scrutiny of Mediterranean oil rush. *Science* **333,** 285 (2012).
16. Daffonchio, D. *et al.* Bioremediation of southern Mediterranean oil polluted sites comes of age. *N. Biotechnol.* **30,** 743–748 (2013).
17. Danovaro R. Pollution threats in the Mediterranean Sea: an overview. *Chem. Ecol.* **19,** 15–32 (2003).
18. Ferraro, G. Towards an operational use of space imagery for oil pollution monitoring in the Mediterranean basin: a demonstration in the Adriatic Sea. *Mar. Pollut. Bull.* **54,** 403–422 (2007).
19. Fava, F., Bertin, L., Fedi, S. & Zannoni, D. Methyl-beta-cyclodextrin-enhanced solubilization and aerobic biodegradation of polychlorinated biphenyls in two aged-contaminated soils. *Biotechnol. Bioeng.* **81,** 381–390 (2003).
20. Head, I. M. Bioremediation: towards a credible technology. *Microbiology* **144,** 599–608 (1998).
21. McGenity, T. J. Hydrocarbon biodegradation in intertidal wetland sediments. *Curr. Opin. Biotechnol.* **27,** 46–54 (2014).
22. Lelieveld, J. *et al.* Climate change and impacts in the Eastern Mediterranean and the Middle East. *Climatic Change* **114,** 667–687 (2012).
23. Langille, M. G. *et al.* Predictive functional profiling of microbial communities using 16S rRNA marker gene sequences. *Nat. Biotechnol.* **31,** 814–821 (2013).

24. Duarte, M., Jauregui, R., Vilchez-Vargas, R., Junca, H. & Pieper, D. H. AromaDeg, a novel database for phylogenomics of aerobic bacterial degradation of aromatics. *Database (Oxford)* **2014,** bau118 (2014).
25. Pérez-Pantoja, D., Donoso, R., Junca, H., Gonzalez, B. & Pieper, D. H. Phylogenomics of aerobic bacterial degradation of aromatics. In: Timmis K. N. (ed) *Handbook of Hydrocarbon and Lipid Microbiology*. Springer-Verlag: Berlin, pp. 1356–1397 (2009).
26. Vilchez-Vargas, R. *et al.* Analysis of the microbial gene landscape and transcriptome for aromatic pollutants and alkane degradation using a novel internally calibrated microarray system. *Environ. Microbiol.* **15,** 1016–1039 (2013).
27. Guazzaroni, M. E. *et al.* Metaproteogenomic insights beyond bacterial response to naphthalene exposure and bio-stimulation. *ISME J.* **7,** 122–136 (2013).
28. Villas-Bôas, S. G., Mas, S., Akesson, M., Smedsgaard, J. & Nielsen, J. Mass spectrometry in metabolome analysis. *Mass Spectrom. Rev.* **24,** 613–646 (2005).
29. Dunlevy, S. R., Singleton D. R. & Aitken, M. D. Biostimulation reveals functional redundancy of anthracene-degrading bacteria in polycyclic aromatic hydrocarbon-contaminated soil. *Environ. Eng. Sci.* **30,** 697–705 (2013).
30. Martin, J. E., Amiot, R., Lécuyer, C. & Benton, M. J. Sea surface temperature contributes to marine crocodylomorph evolution. *Nat. Commun.* **5,** 4658 (2014).
31. Garcia-Pichel, F., Loza, V., Marusenko, Y., Mateo, P. & Potrafka, R. M. Temperature drives the continental-scale distribution of key microbes in topsoil communities. *Science* **340,** 1574–1577 (2013).

Acknowledgments

This research was supported by the European Community Projects MAGICPAH (FP7-KBBE-2009-245226), ULIXES (FP7-KBBE-2010-266473) and KILLSPILL (FP7-KBBE-2012-312139). We thank EU Horizon 2020 Program for the support of the Project INMARE H2020-BG-2014-2634486. This work was further funded by grants BIO2011-25012, PCIN-2014-107 and BIO2014-54494-R from the Spanish Ministry of Economy and Competitiveness. The authors gratefully acknowledge the financial support provided by the European Regional Development Fund (ERDF). The present investigation was also funded by the Spanish Ministry of Economy and Competitiveness within the ERA NET IB2, grant number ERA-IB-14-030. F. Mapelli was supported by Università degli Studi di Milano, European Social Fund (FSE) and Regione Lombardia (contract "Dote Ricerca"). CB and DR would like to acknowledge funding from the Spanish Ministry of the Economy and Competitiveness (CTQ2014-55279-R). We thank Dr. C. Méndez-García for her excellent support regarding the partial preparation of Fig. 1 and Lyamlouli Karim for support activities related to the sampling and GS-MS analysis of MCh sediment. MB acknowledges the Marchica agency for their invaluable assistance during the sampling phase of the research project. The authors also greatly acknowledge the support of Lifesequencing SL (Valencia, Spain) for sequencing of MGS-AQ sample.

Author Contributions

The study was conceived by M.F., D.D., M.M.Y. and P.N.G. All authors contributed to the data collection. Data interpretation and manuscript preparation were performed by M.F., F.M., R.B., C.B. and D.R. F.M., B.C. and S.B. provided biodiversity input. R.B., J.T., M.R., X.H. and J.C. contributed to metagenome bioinformatic data analysis. D.B. and M.M. contributed to the multi-panel map for the analysis of the spatial distribution of enzymes. D.R. and C.B. provided analytical and intellectual inputs of the metabolome data. R.B., J.T., M.V.D.P., C.G., M.M.M., T.N.C., O.V.G. and M.F. performed the experiments and contributed to data analysis. S.C., M.G., R.D., S.F., R.A.A., M.M., A.J., F.B., E.H., F.A.H., A.C., M.B., Y.R.A.F., N.K., H.I.M., M.M.Y. provided the marine sediment material and environmental records. All authors have critically reviewed and edited the manuscript and have approved its publication.

Additional Information

Accession numbers. The projects have been registered as an umbrella BioProject at NCBI with the IDs PRJNA222659 [for MGS-HAV], PRJNA222657 [for MGS-MES], PRJNA222658 [for MGS-PRI], PRJNA222660 [for MGS-BIZ], PRJNA222661 [for MGS-MCh], PRJNA222667 [for MGS-AQ], PRJNA222665 [for MGS-BIZ], and PRJNA222666 [for MGS-ELMAX]. The Whole Genome Shotgun projects have been deposited at DDBJ/EMBL/GenBank under the accession numbers AZIB00000000 [for MGS-HAV], AZIC00000000 [for MGS-MES], AZIF00000000 [for MGS-PRI], AZID00000000 and AZII0100000 [for MGS-BIZ], AZIE00000000 [for MGS-MCh], AZIG0100000 [for MGS-AQ], and AZIJ0100000 [for MGS-ELMAX]. All original non-chimeric SSU rRNA hypervariable tag 454 sequences are archived at the EBI European Read Archive under accession number PRJEB5322. Note that code 'MGS' refers to MetaGenome Source (see Supplementary Methods)

Supplementary information accompanies this paper at http://www.nature.com/srep

Competing financial interests: The authors declare no competing financial interests.

How to cite this article: Bargiela, R. *et al.* Bacterial population and biodegradation potential in chronically crude oil-contaminated marine sediments are strongly linked to temperature. *Sci. Rep.* **5**, 11651; doi: 10.1038/srep11651 (2015).

Capítulo 3: Ácido úrico y amonio como agentes bioestimulantes en comunidades microbianas marinas degradadoras de petróleo

Resumen

El nitrógeno y el fósforo son nutrientes esenciales para el crecimiento de microorganismos. Son también claves en el catabolismo de hidrocarburos. Es por ello que la adición artificial de alguno de estos, y otros, nutrientes es clave no sólo para favorecer el crecimiento sino también para potenciar los procesos de biodegradación. Este proceso se conoce como bioestimulación. Este hecho es especialmente crítico en ambientes marinos donde la concentración de nitrógeno es muy baja. Uno de los nutrientes actualmente más prometedores como fuente de nitrógeno es el ácido úrico. Pese a su potencial uso en procesos de bioestimulación se sabe poco de como éste afecta a las comunidades microbianas, como es metabolizado por las mismas y como afecta a la eficacia del procesos de biodegradación. Este estudio trata de analizar cómo el ácido úrico influye en la composición y capacidades de biodegradación de comunidad microbianas que habitan 4 zonas costeras a lo largo de la costa norte (Ancona, Italia) y sur del Mar Mediterráneo (Túnez y Egipto) y el Mar Rojo (Golfo de Aqaba, Jordania).

El procedimiento seguido para el análisis de las muestras comprende las siguientes partes: a) recolección de muestras de sedimentos marinos de cada una de las zonas estudiadas, b) preparación de microcosmos con petróleo crudo ligero y enriquecimientos con ácido úrico (UA) y también con amonio (NP), empleado a modo comparativo, c) seguimiento temporal de variables relacionadas con el metabolismo microbiano, en particular, el consumo amonio y ácido úrico, tasa de respiración, emulsificación y concentración de proteínas, y degradación de hidrocarburos, d) estudio de biodiversidad empleando el análisis de los espaciadores intergénicos ribosomales (RISA) y secuenciación directa del ADN; e) aplicación de métodos de cultivo para identificar bacterias involucradas en el metabolismo de ácido úrico, y f) análisis de secuencias metagenómicas para la identificación de genes que codifican proteínas involucradas en el metabolismo de ácido úrico. Una aportación clave en la investigación realizada en esta Tesis Doctoral ha sido el análisis de las secuencias metagenómicas obtenidas a fin de estudiar la biodiversidad y la presencia de genes involucrados en el metabolismo de ácido úrico en cada uno de los microcosmos generados.

El análisis temporal de los microcosmos en lo que a las curvas de asimilación de NH_4, emulsificación y concentración de proteínas se refiere, revela que la degradación microbiana de hidrocarburos en presencia de ácido úrico se realiza en dos fases: 1) el ácido úrico es convertido a amonio (5 primeros días); 2) los microorganismos utilizan el amonio generado para favorecer la degradación de los hidrocarburos (a partir de los 5-10 días); 3) a los 21 días se producen enriquecimientos con una composición microbiana estable. La asignación taxonómica de las secuencias de ARN 16S muestra que los géneros *Pseudomonas* y *Alcanivorax* son dominantes en todos los microcosmos seleccionados, independientemente del uso de UA o NP. El análisis metagenómico y el cultivo directo revela que bacterias pertenecientes al género *Halomonas* son las principales responsables del metabolismo del ácido úrico a NP, que posteriormente favorece el crecimiento de bacterias degradadoras de hidrocarburos (*Pseudomonas* y *Alcanivorax*). Los resultados no solo demuestran por primera vez el potencial del ácido úrico como agente bioestimulante que favorece la biodegradación de hidrocarburos por bacterias hidrocarbonoclásticas, sino también el papel clave de bacterias del género *Halomonas* en la conversión de ácido úrico a amonio en este proceso.

Microb Ecol
DOI 10.1007/s00248-015-0606-7

ENVIRONMENTAL MICROBIOLOGY

Conversion of Uric Acid into Ammonium in Oil-Degrading Marine Microbial Communities: a Possible Role of Halomonads

Christoph Gertler[1,11] · Rafael Bargiela[2] · Francesca Mapelli[3,10] · Xifang Han[4] · Jianwei Chen[4] · Tran Hai[1] · Ranya A. Amer[5] · Mouna Mahjoubi[6] · Hanan Malkawi[7] · Mirko Magagnini[8] · Ameur Cherif[6] · Yasser R. Abdel-Fattah[5] · Nicolas Kalogerakis[9] · Daniele Daffonchio[3,10] · Manuel Ferrer[2] · Peter N. Golyshin[1]

Received: 5 December 2014 / Accepted: 23 March 2015

Abstract Uric acid is a promising hydrophobic nitrogen source for biostimulation of microbial activities in oil-impacted marine environments. This study investigated metabolic processes and microbial community changes in a series of microcosms using sediment from the Mediterranean and the Red Sea amended with ammonium and uric acid. Respiration, emulsification, ammonium and protein concentration measurements suggested a rapid production of ammonium from uric acid accompanied by the development of microbial communities containing hydrocarbonoclastic bacteria after 3 weeks of incubation. About 80 % of uric acid was converted to ammonium within the first few days of the experiment. Microbial population dynamics were investigated by Ribosomal Intergenic Spacer Analysis and Illumina sequencing as well as by culture-based techniques. Resulting data indicated that strains related to *Halomonas* spp. converted uric acid into ammonium, which stimulated growth of microbial consortia dominated by *Alcanivorax* spp. and *Pseudomonas* spp. Several strains of *Halomonas* spp. were isolated on uric acid as the sole carbon source showed location specificity. These results point towards a possible role of halomonads in the conversion of uric acid to ammonium utilized by hydrocarbonoclastic bacteria.

Keywords Crude oil degradation · Bioremediation · Alcanivorax

Introduction

Microbial hydrocarbon degradation in the sea occurs on a global scale in a large variety of latitudinal zones and at all ocean depths. More than five decades of research have shown that marine oil-degrading microbes are highly specialised with regard to their substrate spectrum and climate zone [21, 52].

Electronic supplementary material The online version of this article (doi:10.1007/s00248-015-0606-7) contains supplementary material, which is available to authorized users.

✉ Christoph Gertler
christoph.gertler@fli.bund.de

[1] School of Biological Sciences, Environment Centre Wales, Bangor University, LL57 2UW Bangor, Gwynedd, UK

[2] Consejo Superior de Investigaciones Científicas (CSIC), Institute of Catalysis, 28049 Madrid, Spain

[3] Department of Food, Environment and Nutritional Sciences (DeFENS), University of Milan, via Celoria 2, 20133 Milan, Italy

[4] BGI Tech Solutions Co., Ltd, Main Building, Beishan Industrial Zone, Yantian District Shenzhen 518083, China

[5] Genetic Engineering and Biotechnology Research Institute, City for Scientific Research & Technology Applications, Alexandria, Egypt

[6] Highe Higher Institute for Biotechnology, Biotechpole of Sidi Thabet, University of Manouba, LR11ES31, 2020 Sidi Thabet, Ariana, Tunisia

[7] Deanship of Research & Doctoral Studies, Hamdan Bin Mohammad Smart University, Dubai, United Arab Emirates

[8] EcoTechSystems Ltd., Ancona, Italy

[9] School of Environmental Engineering, Technical University of Crete, Chania, Greece

[10] BESE Division, King Abdullah University of Science and Technology, Thuwal 23955-6900, Kingdom of Saudi Arabia

[11] Friedrich-Loeffler-Institut - Federal research Institute for Animal Health, Institute of Novel and Emerging Diseases, Südufer 10, 17493 Greifswald, Insel Riems, Germany

Published online: 29 April 2015

Cold-adapted microbes such as *Oleispira* spp. prevail in cold polar zones and in the deep sea whereas oil degrading consortia in temperate zones are dominated by *Alcanivorax* species [29] in the aftermath of major oil spills. Many members of *Oceanospirillales* and *Alteromonadales* (e.g. *Thalassolituus* spp. and *Marinobacter* spp.) become predominant in the early stages of oil-degrading microbial consortia due to their highly adapted metabolism [25, 51]. Late stages of marine hydrocarbonoclastic consortia on the other hand are characterized by bacteria such as *Cycloclasticus* spp. specialized in aromatic and polyaromatic hydrocarbons that are degraded in a slower process [21].

To perform hydrocarbon degradation, microbes depend upon nitrogen and, to a lesser extent, phosphorus sources [4]. Both elements are scarce in seawater in most parts of the oceans and over most of the warmer months due to competition for nutrients by phototrophs that use sunlight and CO_2 as energy and carbon sources. In fact, dissolved organic nitrogen, ammonium and nitrate exist in mere trace amounts after phyoplankton spring blooms from March to June and are recycled in winter months when low temperatures prohibit fast growth of heterotrophic microbes [13]. The artificial addition of nitrogen and phosphorus sources into an oil impacted environment on the other hand leads to a quick growth of hydrocarbonoclastic microbes and substantial microbial hydrocarbon degradation. An example of the successful implementation of this approach was the M/V Exxon Valdez mitigation trial [35]. Studies of marine oil-degrading microbial communities growing in dispersed oil did not show a significant increase of oil-degrading microbes beyond 10^5 cells/mL and no significant biogenic hydrocarbon degradation, either [20].

A variety of different nitrogen sources can be used to support growth of hydrocarbonoclastic bacteria (HCB). Oil spill remediation trials commonly use nitrogen in forms of ammonium, nitrate, urea, uric acid and amino acids [10]. Each nitrogen source has its advantages and disadvantages [42]: ammonium and nitrate are water-soluble and universally accepted by microbes, but they are toxic at high concentrations as well as prone to leaching and losses by denitrification or precipitation in seawater [50]. Urea is water-soluble and widely accepted by microbes but easily leached. Uric acid is less widely accepted by microbes. Its oleophilic nature allows it to attach to oil droplets [28] but it is largely insoluble in water. Lecithin is a complex nitrogen and phosphorus source that has recently been used in aromatic hydrocarbon degradation experiments [10]. While it is readily used and can be supplied in large quantities, the mechanism of lecithin metabolism in PAH-degrading microbial consortia remains unknown. Furthermore, large amounts of lecithin must be applied due to the high C/N ratio of the lecithin molecule. Certain industrial processes can overcome the disadvantages of some nitrogen sources, e.g. sulphur coating of urea [34] or using vegetable oil-coated ammonium/nitrate in slow release fertilizers [14, 15]. This reduces the cost efficiency of such nitrogen sources in bioremediation trials, though.

Uric acid could be used without prior treatment, but its synthesis is relatively expensive. However, uric acid is the main nitrogen excretion product of reptiles, birds and certain mammals. It is therefore readily available in poultry litter, in which it makes up to 55–63 % of total nitrogen and to 3 % (*w*/w) of the total weight [40]. Uric acid enters marine ecosystems in substantial amounts via faeces of seabirds. A recent study detected measurable effects of uric acid fertilisation in the vicinity of Great Cormorant (*Phalacrocorax carbo sinensis*) colonies in the Baltic Sea [12]. More than 50 % of the nitrogen taken up by algae at the observed sites originated from faecal uric acid deposition. While it is obvious that valuable nitrogen sources such as uric acid are quickly taken up by marine food webs, the mechanisms and microbial uric acid utilization and the microorganisms involved in this process remain largely unknown [5].

Trials in sediments and soil revealed that microbes related to *Acinetobacter baumannii* can use uric acid as a nitrogen source during hydrocarbon degradation [28]. When uric acid was applied to marine sediments in form of guano, microbes related to the genera *Alcanivorax*, *Halomonas* and *Alteromonas* could be enriched and isolated [27]. Uric acid is an intermediate of the purine metabolism and is oxidised by uricase enzymes. Members of the *Bacillus*, *Pseudomonas*, *Alcaligenes* and *Microbacterium* genera have been identified as being able to use uric acid as carbon and nitrogen source [28, 48]. It is therefore highly probable that marine oil degradation with uric acid as main nitrogen source requires a consortium of currently unknown uric acid-degrading microbes and highly adapted HCBs. This knowledge gap is very surprising as uric acid-based bioremediation approaches have been investigated in trials at different scales [28, 27, 42, 43].

This study aimed at the identification of marine microbial consortia members involved in the metabolism of uric acid in marine oil-degrading and uric acid-utilizing consortia.

Materials and Methods

Study Sites

The sampling sites were located along the northern and southern shores of the Mediterranean Sea and the Red Sea. In particular: (1) the site of El Max (31°9′31.20″N, 29°50′28.20″E) located west of the city of Alexandria, Egypt, the El Max seashore is the most contaminated in the Alexandria area exceeding the legal limits for heavy metals, PAHs and other crude oil-derived pollutants; (2) the Bizerte lagoon (37°16′ 7.72″N, 9°53′19.61″ E) in the north of Tunisia is polluted by petroleum components in the area adjacent to STIR refinery,

the Tunisian Company for Refining Industries; (3) the Jordanian coast in the Gulf of Aqaba (30°22′42″N, 25°24′57″E) in the north-west end of the Red Sea. The Gulf of Aqaba is the northernmost tropical marine ecosystem but hosts an oil terminal that yearly moves up to 30 million tons and is subjected to accidental oil spills at the oil terminal as well as spills (with high sulphur concentrations) during loading and bunkering operations at the industrial jetty; (4) the harbour of Ancona, Italy (43°37′N; 13°30′15″E), which is a major ferry terminal and industrial port on the Adriatic Sea and heavily contaminated with PAHs and heavy metals.

Microcosm Design and Set-up

Two different sizes of microcosms were set up for this trial (Table 1). For the analysis of microbial population dynamics, respiration and other parameters, a series of 16 microcosm flasks (two parallels each for a uric acid and an ammonium treatment for sediments from the Ancona, Aqaba, Bizerte and El Max sites, respectively) were set up in 500 mL Erlenmeyer flasks (microcosms 1–8). Seventy-five grams of sand, 5 mL of crude oil and 150 mL of the ONR7 medium mentioned above were used. Overall nutrient concentrations and C/N/P ratios were identical to the ones in the large microcosms mentioned above. All microcosms were incubated at 20 °C for 28 days in a shaking incubator at 120 rpm. The small microcosms were sampled on days 0, 2, 4, 6, 8, 10, 12, 15, 18, 21, 24 and 28. On these days, 1 mL of sediment was taken for DNA extraction, 1 mL of supernatant was taken for photometric measurements and 6 mL were taken for emulsification measurements. Fifty millilitres of each microcosm was taken on days 0, 4, 8, 12, 15, 18, 21, 24 and 28 to measure respiration activity.

The sample volume taken for each sampling day was replaced by an equivalent volume of modified ONR7a medium. For ammonium treatments, the equivalent amount of ammonium chloride and disodium hydrogen phosphate were added to compensate for loss of water-soluble nitrogen sources during sampling. As uric acid in the respective uric acid treatments is insoluble in water, sample volumes were replaced with ONR7a containing disodium hydrogen phosphate but no ammonium chloride.

Four control treatments with a total of eight control flasks were set up. A negative control contained only sterile sand and ONR7a. Two further controls contained sand, ONR7a, crude oil and either uric acid or ammonium chloride solution but no sediment sample. Finally, one control contained oil, sterile sand, ONR7a medium and a sediment sample from Ancona harbour, but no additional nitrogen source or phosphorus source was provided (microcosms 9–12).

To generate high DNA yields required for sequencing analysis, a series of up-scaled microcosms was set up (microcosms 13–20). One-litre Erlenmeyer flasks were filled with 150 g of sand (Sigma-Aldrich, St. Louis, USA), sterilized and spiked with 10 mL of sterile filtered Arabian light crude oil. One gram of sediment from each sampling site was mixed into the oil-spiked sand as the inoculum. For the Aqaba site, 2 g of sediment was used, as this sediment was very coarse. Three hundred millilitres of modified ONR7a medium [8] (omitting ammonium chloride and disodium hydrogen phosphate) was added. We added 5 mL of Arabian light crude oil, which based upon average literature values for density and molecular weight equals about 300 mM of C [49], 5 mM of NH_4Cl and 0.5 mM of Na_2HPO_4 resulting in a molar N/P ratio of approximately 10:1. For each uric acid treatment microcosm (UA), 0.21 g (1.25 mmol=5 mmol N) of uric acid was provided as nitrogen source while the ammonium treatment microcosms (NP) were each supplied with 2.5 mL of a 2 M ammonium chloride solution (5 mmol; pH 7.8). Both treatments also contained 2.5 mL of a 0.2 M disodium hydrogen phosphate solution (0.5 mmol; pH 7.8). Excess amounts of crude oil were added to compensate for the 35 % carbon losses due to evaporation of volatile hydrocarbons over the course of the experiment [49]. Including losses due to evaporation, the C/N/P ratio was approximately 400:10:1. One hundred and four millilitres of mesocosm water was replaced by an equal volume of modified ONR7 containing uric acid or ammonium as described above on days 0, 4, 8, 12, 15 and 18. The microcosms were destructively sampled on day 21.

Emulsification Measurements

Six millilitres of sample was pipetted into screw cap glass centrifuge tubes (15×150 mm). Six millilitres of *n*-hexane (Sigma-Aldrich, St. Louis, USA) was added and each tube was vortex-shaken at maximum rate for 60 s. The resulting emulsion was left to settle for 24 h at room temperature and the height of the interface which settled between hexane and the aqueous phase was measured with a calliper.

Respiration Measurements

Oxygen consumption was measured using a Micro-Oxymax Respirometer (Columbus Instruments, Columbus, OH, USA) to serve as a proxy for total aerobic metabolic activity. Fifty millilitre aliquots were transferred to 100 mL screw top glass bottles (VWR, Lutterworth, UK) and connected to the respirometer. Automatic volume determination was performed for each glass bottle prior to respiration measurement. Measurements were performed every 2 h for a total of 72 h. For each measurement, sensors and bottles were automatically purged with sterile air to avoid inhibitory effects of oxygen depletion.

Table 1 Composition of microcosms established in this study

Microcosm nr	Microcosm name	Flask size (mL)	Inoculum (location)	Sterile sand (g)	ONR7 medium (mL)	Uric Acid (mmol)	Crude oil (mL)	NH4Cl (mmol)	Na2HPO4 (mmol)
1	Ancona—ammonium	500	Ancona	75	150	0	5	5	0.5
		500	Ancona	75	150	0	5	5	0.5
2	Ancona—uric acid	500	Ancona	75	150	1.25	5	0	0.5
		500	Ancona	75	150	1.25	5	0	0.5
3	Aqaba—ammonium	500	Aqaba	75	150	0	5	5	0.5
		500	Aqaba	75	150	0	5	5	0.5
4	Aqaba—uric acid	500	Aqaba	75	150	1.25	5	0	0.5
		500	Aqaba	75	150	1.25	5	0	0.5
5	El Max—ammonium	500	El Max	75	150	0	5	5	0.5
		500	El Max	75	150	0	5	5	0.5
6	El Max—uric acid	500	El Max	75	150	1.25	5	0	0.5
		500	El Max	75	150	1.25	5	0	0.5
7	Bizerta—ammonium	500	Bizerta	75	150	0	5	5	0.5
		500	Bizerta	75	150	0	5	5	0.5
8	Bizerta—uric acid	500	Bizerta	75	150	1.25	5	0	0.5
		500	Bizerta	75	150	1.25	5	0	0.5
9	Control—sterile	500	none	75	150	0	0	0	0
		500	none	75	150	0	0	0	0
10	Control—ammonium	500	none	75	150	0	5	5	0.5
		500	none	75	150	0	5	5	0.5
11	Control—uric acid	500	none	75	150	1.25	5	0	0.5
		500	none	75	150	1.25	5	0	0.5
12	Control—non sterile	500	Ancona	75	150	0	5	0	0
		500	Ancona	75	150	0	5	0	0
13	Ancona—ammonium	1000	Ancona	150	300	2.5	10	10	1
14	Ancona—uric acid	1000	Ancona	150	300	2.5	10	10	1
15	Aqaba—ammonium	1000	Aqaba	150	300	2.5	10	10	1
16	Aqaba—uric acid	1000	Aqaba	150	300	2.5	10	10	1
17	El Max—ammonium	1000	El Max	150	300	2.5	10	10	1
18	El Max—uric acid	1000	El Max	150	300	2.5	10	10	1
19	Bizerta—ammonium	1000	Bizerta	150	300	2.5	10	10	1
20	Bizerta—uric acid	1000	Bizerta	150	300	2.5	10	10	1

Photometric Determination of Ammonium, Nitrate and Protein Concentration

Due to the presence of emulsified oil in most microcosms, all samples underwent a pre-treatment before photometric measurement. Briefly, each 1 mL sample was sonicated using a Soniprep 150 sonicator (MSE, London, UK) for 20 s in an ice bath. Subsequently, samples were centrifuged at 16,000×*g* in an Eppendorf centrifuge to separate biomass incorporating oil at the bottom of the centrifuge tube from free oil at the surface of the aqueous phase. Sub samples were taken from the centre of the aqueous phase, diluted and applied in photometric analysis. A nitroprusside-based assay was used [39] for the determination of ammonium concentrations and a vanadium chloride-based method [37] was used to measure nitrate concentration. Protein concentrations were determined as a proxy for microbial growth using the BioRad Protein assay (BioRad, Carlsbad, USA) according to the manufacturer's guidelines.

Isolation, 16S rRNA Gene Sequencing and Phylogenetic Analysis of Uric Acid-Utilising Microorganisms

Samples of 100 μL were taken from microcosms 13 to 20 on days 6 and 12 of the experiment. A serial dilution was performed using sterile modified ONR7a medium that contained neither nitrogen nor phosphorus source. One hundred microlitres of each dilution was plated on modified ONR7a agar plates containing 0.3 % (*w*/*v*) uric acid and 0.45 mM disodium hydrogen phosphate. Due to its low solubility in water, uric acid forms a precipitate, which makes the agar plates appear milky. The plates were incubated at 20 °C for up to 5 days. Isolates with capabilities to degrade uric acid were identified by clear "halos" around the individual colonies. Eight colonies of each variant were re-plated twice on modified ONR7a agar plates to obtain pure isolates. Each isolate was tested for the ability to use uric acid as the sole source of carbon and nitrogen in 15 mL polypropylene tubes containing 5 mL ONR7 liquid medium supplemented with uric acid and disodium hydrogen phosphate, as described above. Tubes were incubated at 20 °C for 5 to 7 days. Colony PCR of each isolate was performed using primers F530 and R1492 to amplify the 16S rRNA gene. Each 20 μL PCR reaction contained 2 μL of PCR Buffer B (Roboklon, Berlin, Germany), 2.5 mM $MgCl_2$, 200 μM of each dNTP (Promega, Madison, WI), 10 nM each of primer F530 (5′- GTG CCA GCM GCC GCG G-3′) and primer 1492r (5′- GGT TAC CTT GTT ACG ACT T-3′), 0.5 U of Taq DNA Polymerase (Roboklon, Berlin, Germany) and 4 μL of a PCR-enhancing mixture (3 M betaine and 1 % Tween 20). PCR products were visualised on 1 % agarose gels. Sequencing was performed at Macrogen (Amsterdam, Netherlands) with primers F530 and R1492. The processing and assembly of DNA sequences as well as testing for chimeric sequences was conducted using BioEdit as described before [2, 16]. Sequence alignment was performed against a database of validly published reference DNA sequences of typed strains using ClustalW [30]. The sequences were clustered by maximum parsimony according to the recommendation of the MODELTEST software [45] and phylogenetic tree was constructed using MEGA 4.0 as previously described [16]. DNA sequences of *Halomonas* isolates were submitted to the European Nucleotide Archive (ENA) under the accession numbers HG803097 to HG803140.

Nucleic Acid Extraction

As both Illumina sequencing and RISA performed in this study require different qualities and quantities of DNA, nucleic acids were isolated using two approaches. For Illumina sequencing (Microcosms 13–20), a modified CTAB-phenol-chloroform extraction was performed. Briefly, for the initial cell lysis, 20 g of sediment, 1 g of 2–3 mm glass beads (five to six glass beads) and 10 mg of lysozyme were placed in a 50-mL centrifuge tube. Fifteen millilitres of extraction buffer containing 10 % (*w*/*v*) sucrose, 20 % (*v*/*v*) modified CTAB solution (5 % CTAB; 0.35 M NaCl, 120 mM Na_2HPO_4 pH 8.0; to improve solubilisation of CTAB, this solution is a 1:1 mixture of 10 % CTAB/0.7 M NaCl and 240 mM Na_2HPO_4 solutions), 100 mM NaEDTA pH 8.0 and 100 mM Tris/HCl pH 8.0 was added to the sample, and all tubes were incubated on a shaker at 220 rpm and 30 °C for at least 30 min. Twenty milligrams of proteinase K was added to each tube, and all samples were incubated on a shaker at 220 rpm and 50 °C for at least 30 min. Two millilitres of a 20 % SDS (*w*/*v*) solution was added and all samples were incubated on a shaker at 100 rpm and 60 °C for 20 min. Finally, 0.5 g of activated charcoal powder was added to the mixtures, and the samples were incubated on a shaker at 100 rpm and 60 °C for 30 min. Resulting mixtures were centrifuged at 17,000×*g* for 10 min.

Resulting supernatants were transferred to another 50 mL centrifuge tube. The pellets were extracted again by adding 5 mL of extraction buffer to the pellet, mixing for 5 min and centrifugation as described above. The resulting supernatant was combined with the supernatant from the previous step. To remove organic contaminants, the combined supernatants were treated with 0.5 g of activated charcoal, which was subsequently removed by centrifugation at 20,000×*g* for 10 min. Supernatants were transferred to new 50 mL centrifuge tubes and 0.5 M NaEDTA solution was added to the supernatants for receive a final EDTA concentration of 2.5 mM. Deproteination and DNA extraction were performed by adding one supernatant volume of phenol/chloroform/isoamylalcohol (PCI) solution (25:24:1 (*v*/*v*); Sigma-Aldrich, St. Louis, USA). The mixtures of

PCI and supernatant were inverted manually for 2 min and subsequently centrifuged at 3,700×*g* for 10 min. The aqueous phase was transferred to a new centrifuge tube and extracted again with chloroform/isoamylalcohol (24:1 (*v*/*v*); Sigma-Aldrich, St. Louis, USA). The resulting supernatants were precipitated by adding 0.8 volumes of isopropanol and incubating at 4 °C overnight. Precipitates were collected by centrifugation at 18,000 rcf for 20 min at 4 °C. Pellets were washed once with 70 % ethanol and centrifuged at 18,000 rcf for 10 min. The supernatants were discarded, and remaining traces of ethanol were evaporated by air-drying. The pellets were dissolved in 100 μL of sterile deionised water. Nucleic acid extraction for RISA (microcosms 1–12) was performed with a similar but less time-consuming and less waste-producing protocol due to the large amount of samples. Briefly, a phenol-chloroform extraction [1] was used with an additional bead-beating step using one sterile 2 mm glass bead and bead beating at a setting of 4.0 for 20 s in a FP120 Cell Disruptor (Qbiogene, Carlsbad, USA) prior to the addition of SDS buffer.

PCR, Ribosomal Intergenic Spacer Analysis

PCR amplification of the intergenic spacers was performed using the primer set ITSF/ITSReub [6]. Each 20 μL reaction contained 2.5 mM $MgCl_2$, 200 μM of each dNTP (Promega, Madison, WI), 10 nM each of primer ITSF (5′- TCG TAA CAA GGT AGC CGT A-3′) and ITSReub (5′- GCC AAG GCA TCC ACC-3′) [6], 2 μL of PCR Buffer B (Roboklon, Berlin, Germany), 0.5 U of Taq DNA Polymerase (Roboklon, Berlin, Germany) and 4 μL of a PCR-enhancing mixture (3 M betaine and 1 % Tween 20). One nanogram of template DNA was used in each reaction. PCR was performed as described before [6] using a DNA Engine Tetrad 2 Thermal Cycler (BioRad, Hercules, USA). Gel electrophoresis was conducted on an Ingeny PhorU gel electrophoresis apparatus using 1× TAE 6 % acrylamide gels with 1× TAE buffer at 110 V for 16 h. The gels were stained with 40 mL 1× SYBR Gold (Life Technologies, Carlsbad, USA) staining solution and visualised on a ChemiDoc XRS gel documentation system (BioRad, Hercules, USA).

RISA Fingerprinting Analysis, Multivariate Statistical Analysis

Quantity One software (BioRad, Hercules, USA) was used for band identification and band matching, with a total of 112 band classes assigned. Following square root transformation, principal coordinate analysis was conducted with PAST using the Bray-Curtis dissimilarity [19]. Analysis of similarities (ANOSIM) was performed using PRIMER 6 [7]. One-way ANOSIMs of the whole data set were conducted for the parameters “Location (Inoculum)”, “Nitrogen source” and “Sampling time”. To investigate effects of different nitrogen sources on individual subsets of the data for each location, a two-way nested ANOSIM was conducted.

DNA Sequencing, Assembly, Gene Prediction and Annotation

Sequencing was performed by pair-end sequencing with an Illumina Hiseq 2000 sequencing system at BGI—Beijing Genomics Insititute (Hong Kong, People’s Republic of China). A total of 20,000,000 sequences with a mean read length of 170 nts were obtained per sample. For gene prediction, the software MetaGeneMark (version 2.10, default parameters; [44]) was used to predict the open reading frames (ORFs) based on the assembly results. The predicted amino acid sequences were then aligned using the KEGG database [23, 22, 24] through BLAST (version 2.2.23), and the relevant information was extracted and summarised with self-developed scripts. For Illumina Hiseq 2000 sequencing and data processing, the DNA samples were sequenced following standard pipelines of the Illumina platform. Data filtration was conducted with the following in-house scripts: (1) removal of reads with 3 N bases and removal of reads contaminated by adapters (15 bases overlapped by reads and adapter), (2) removal of reads with 20 bp low quality (20) bases and (3) removal of duplication contamination. The read removal process is simultaneously conducted for the read1 and read2 operation. The resulting data set can be used for subsequent analysis of quality data (Clean Data) [33]. SOAPdenovo (Version 1.0, http://soap.genomics.org.cn/soapdenovo.html) was used for the assembly of Illumina Hiseq 2000 sequences and to assemble filtered data. Assembly results with the best N_{50} contig length were optimized by in-house scripts [31].

Rarefaction curves of the observed species were established for each sample to analyse the species sampling coverage. Known bacteria, fungi and archaea sequences were extracted from the nucleotide database by an in-house script. Filtered reads were mapped to these sequences by SOAPaligner (version 2.21) [32]. Mapped reads were classified in different taxonomic levels (including domain, phylum, class, order, family, genus and species) and corresponding abundance was also calculated by in-house scripts. All rarefraction curves (data not shown) indicated closeness to saturation in each of the samples, which suggests that biases during the comparative analysis within the metagenomes herein reported

were not introduced due to differences in microbial coverage.

Accession Numbers

The projects have been registered as umbrella BioProjects at NCBI with the IDs PRJNA222667 [for MGS-AQ(UA)], PRJNA222664 [for MGS-ANC(UA)], PRJNA222665 [for MGS-BIZ(AMM)], PRJNA222666 [for MGS-ElMAX(UA)] and PRJNA222663 [for MGS-ANC(AMM)]. These Whole Genome Shotgun projects have been deposited at DDBJ/EMBL/GenBank under the accession numbers AZIG00000000 [for MGS-AQ(UA)], AZIH00000000 [for MGS-ANC(UA)], AZII00000000 [for MGS-BIZ(AMM)], AZIJ00000000 [for MGS-ElMAX(UA)] and AZIK00000000 [for MGS-ANC(AMM)]. The versions described in this paper are versions AZIG0100000 [for MGS-AQ(UA)], AZIH0100000 [for MGS-ANC(UA)], AZII0100000 [for MGS-BIZ(AMM)], AZIJ0100000 [for MGS-ElMAX(UA)] and AZIK0100000 [for MGS-ANC(AMM)]. Abbreviations used for database deposition are as follows: MGS, MetaGenome Sequence; AQ(UA), Aqaba uric acid (microcosm 16); ANC(UA), Ancona uric acid (microcosm 14); ElMAX(UA), El Max uric acid (microcosm 18); ANC(AMM), Ancona ammonium (microcosm 13); BIZ(AMM), Bizerte ammonium (microcosm 19).

Results

Microbial Metabolic Activity in Microcosms

All microcosms showed a strong increase in respiration rate and emulsification immediately after the start of the experiment corresponding to high aerobic microbial activity (Fig. 1). However, total rates of respiration for all uric acid treatments were eightfold higher at its peak compared to the initial values. These values were higher than the peak values for the ammonium treatments, which, in turn, were fivefold higher than the initial values. The peak values for respiration were reached on day 12 in the uric acid-containing microcosms (2, 4, 6, 8) and between days 8 and 15 in the ammonium-containing microcosms (1, 3, 5, 7). Following their respective peaks, respiration dropped to base levels after day 18 in uric acid treatments

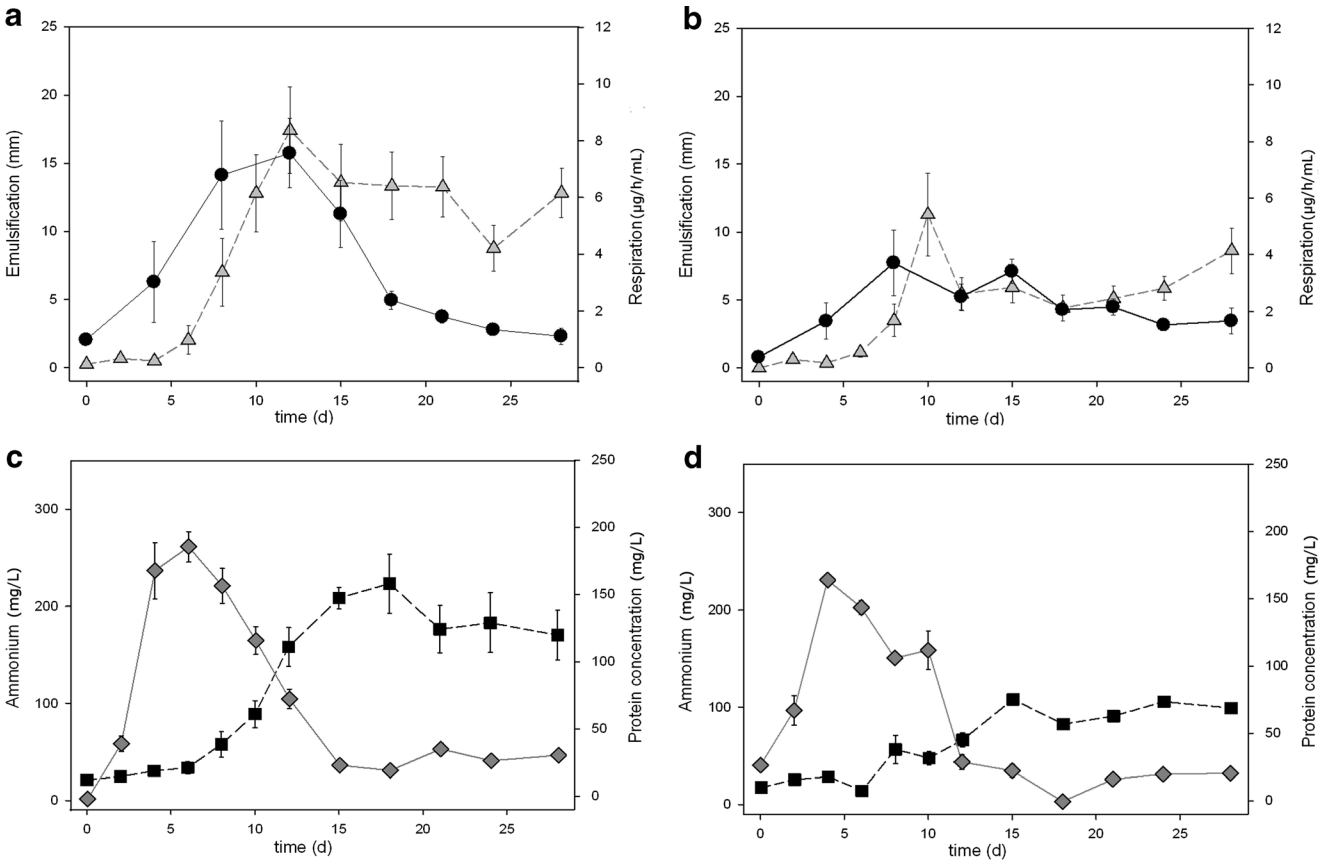

Fig. 1 **a**–**d** Observations of protein and ammonium concentrations, and microbial respiration in microcosms. Panels **a** and **c** show data collected from uric acid enrichments (microcosms 1, 3, 5, 7), and **b** and **d** from ammonium enrichments (microcosms 2, 4, 6, 8). *Filled circles* represent respiration rates; *open triangles* indicate emulsification rates. *Filled squares* indicate total protein concentrations, whereas *open diamonds* show ammonium concentrations. *All data points* represent the mean of triplicates from each sampling point. *Bars* represent standard error

but remained elevated in the ammonium treatments due to a continuous influx of ammonium during sampling procedures. The analysis of total respiration showed that uric acid treatments had, on average, a 1.5-fold higher total respiration (620 mg/L O_2) than ammonium treatments (376 mg/L O_2).

The emulsification assay served as a proxy for the activity of hydrocarbon degrading microbes. Emulsification occurred in both treatments after day 4 of the experiment and peaked at day 10 in both cases. Following the maximum, emulsification dropped to 50 % of the peak value but remained constant until the end of the experiment. The error bars for all curves are relatively high, which can be explained by temporal shifts in metabolic activity in individual microcosms by ±2 days.

The photometric quantitation of ammonium and protein concentrations shows an anticyclic trend in both treatments. Ammonium becomes readily available at high concentrations in both the uric acid and ammonium treatments. The ammonium concentration increased immediately after the start of the experiment (with ammonium values not detectable in uric acid treatments at day 0 of the trial) and peaked at day 4. Following the peak, ammonium concentrations rapidly decreased from days 6 to 18 in both microcosms and remained low in uric acid treatments in contrast to NP microcosm which were resupplied with ammonium during sampling procedures. Small residual amounts of ammonium could be detected in both treatments at the end of the experiment.

Conversely, protein concentrations, which served as a proxy of total biomass, increased in both treatments from day 6 of the experiment onward. However, the concentrations dropped after day 18 in all uric acid treatments but increased constantly in ammonium treatments.

Dynamic Changes in Microbial Community Composition

Microbial community changes and composition were analysed using Ribosomal Intergenic Spacer Analysis (RISA) and Pair-end sequencing. Figure 2 shows the results of the Principal Coordinate Analysis (PCoA). The individual fingerprints used for this analysis are presented in the Supplementary Fig. 1. The PCoA plot shows no distinctively separated clusters, indicating that the microbial communities in the microcosms are essentially similar over the course of the experiment. This similarity can be explained by the choice of samples, which come from sites with a legacy of hydrocarbon pollution as well as from the same body of water and climate zone. The data points for both the NP and UA treatments overlap for all sampling sites, indicating that the treatments ultimately produce identical microbial communities. This result is supported by the ANOSIM results presented in Supplementary Table 1a.

Statistically significant similarities could be detected when analysing the factor "nitrogen source". High similarities (*R* value −0.156) were detected when using two-way ANOSIM

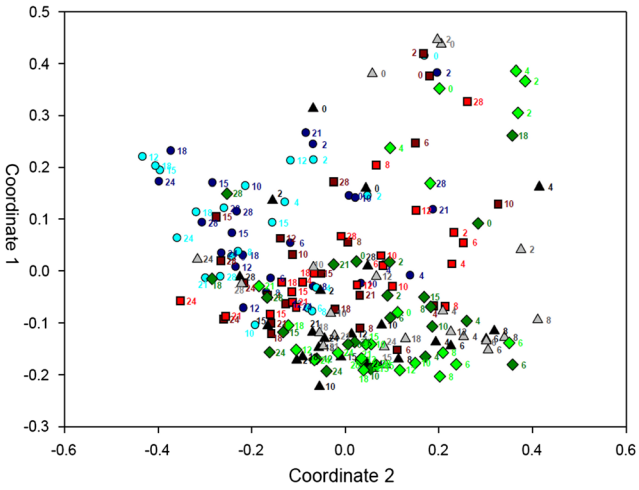

Fig. 2 Principal Coordinate Analysis of RISA fingerprints. *Light colours* indicate ammonium enrichments; *dark colours* indicate uric acid enrichments. *Blue circles* represent enrichments from Ancona, Italy (microcosms 1, 2); *red squares* show samples from Aqaba, Jordan (microcosms 3, 4). *Grey triangles* show samples from El Max, Alexandria, Egypt (microcosms 5, 6), whereas *green diamonds* represent enrichments from Bizerte Lagoon, Tunisia (microcosms 7, 8). *Numbers* correspond to the sampling day of each data point

to investigate the similarities between the UA and NP treatments for samples at each location. Data points from individual locations, on the other hand, show subtle differences separating the Ancona and Aqaba samples, although there is some degree of congruence for the Northern African samples; however, the ANOSIM analysis did not indicate significant similarities between the microbial communities from individual locations (Supplementary Table 1b). Most obvious is the separation of the early sampling points (days 0–10) in the upper right section of Fig. 2 from the bulk of the late sampling points (days 12–28). This trend coincides with the peaks of both emulsification (days 10–12 in both treatments) and protein production (days 12–20), which is strongly supported by the ANOSIM results presented in Supplementary Table 1c. Significant similarities could be detected in the RISA profiles for samples taken between days 4 and 8, as well as for samples taken between days 12 to 28.

Metagenome Analysis of Marine Oil-Degrading Consortia: Bacterial Diversity and Composition

DNA isolated from each microbial community sampled from microcosms 13–20 at the day 21 was sequenced using Illumina HiSeq 2000. The data and annotation features resulting from the assemblies of each sample are shown in Supplementary Table 2a, b and c. Three samples from uric acid enrichments and two samples from ammonium enrichments were chosen to ensure that all sampling sites were covered and to allow a direct comparison of at least one site. The samples for sequencing were selected based upon the results of RISA and whether the ANOSIM analysis showed high

similarities between the ammonium and uric acid treatments for a particular site, omitting redundant samples. However, to confirm these similarities, both treatments of the Ancona microcosms were analysed. The results of this analysis, presented in Fig. 3, show compositional similarities between the uric acid and ammonium treatments of the Ancona sample when the 16S rRNA partial gene sequences obtained in the non-assembled Illumina reads were surveyed. For this purpose, we used only sequences with a length of >100 nucleotides. Similarities could be observed between the uric acid treatments of the Ancona and El Max site (microcosms 14, 18), as well as between the ammonium treatments of the Ancona and Bizerte sites (microcosms 13, 19). The Aqaba uric acid treatment (microcosm 16) showed relatively little similarity to any other treatments and was characterised by a high percentage of *Pseudomonadaceae*. Table 2 indicates that *Pseudomonas* spp. were the most abundant microbes in every treatment. They were more abundant in the uric acid treatments, and their percentage increased along a North–south gradient for these treatments. Specialised hydrocarbon-degrading microbes belonging to the genera *Alcanivorax*, *Cycloclasticus*, *Oleiphilus*, *Oleispira* and *Thalassolituus* were detected in all treatments. Most prominent among these microbes were the *Alcanivorax* spp., which were more abundant after NP (from 4.99 to 16.51 % total reads) rather than uric acid treatments (from 0.44 to 3.94 % total reads). The analysis of the metagenomic data showed that most *Alcanivorax*-like DNA sequences belonged to *Alcanivorax borkumensis*.

In parallel to this result, the ammonium treatments contained a higher percentage (~9.0-fold increment) of *Alphaproteobacteria*, consisting mostly of *Roseovarius* and *Sulfitobacter* spp. Conversely, uric acid treatments were more likely to contain *Marinobacter* spp. (up to ~2.0-fold) and *Halomonas* spp. (up to ~3.8-fold). Direct comparison of both Ancona treatments showed a 1.5-fold higher percentage of *Halomonas* spp. and a twofold higher percentage of *Marinobacter* spp. but an eightfold lower abundance of *Alphaproteobacteria* in the uric acid treatments. Furthermore, the percentage of *Psychrobacter* spp. in the Ancona uric acid treatment was more than 30-fold elevated in comparison to the corresponding ammonium treatment. The percentage of *Pseudomonas* spp. and *Alcanivorax* spp., however, remained similarly high in both ammonium and uric acid treatments.

Genomic Signatures Associated with Uric Acid Metabolism

In the metagenomes, we identified 176,914 potential protein-coding genes (cut-off of ≥20 amino acid-long sequences), with El Max containing the highest number (61,277). Functional assignment of the predicted genes was made on the basis of BLASTP analysis against a reference dataset for Clusters of Orthologous Groups (COGs) and Kyoto Encyclopedia of Genes and Genomes (KEGG) assignments. Circa 63.1–67.9 % could be assigned to COG, and 54.0–63.7 % could be assigned to KEGG pathways (Supplementary Table 2a, b and c). On average, 6.6 to 12.8 genes belonged to COG and from 5.6 to 11.2 genes belonged to KEGG, depending on the sample.

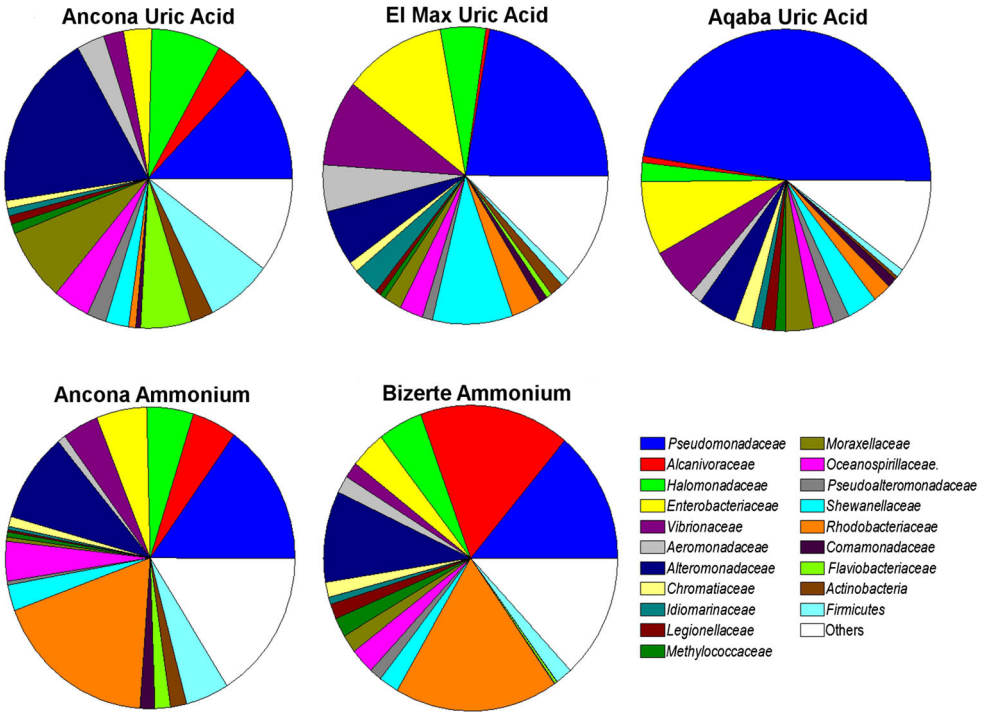

Fig. 3 Relative abundances of microbial families within annotated metagenomes based on the 16S small subunit rRNA data taken on day 21 from the following samples: Ancona uric acid (microcosm 14), Ancona ammonium (microcosm 13), Bizerte ammonium (microcosm 19), Aqaba uric acid (microcosm 16) and El Max uric acid (microcosm 18). Only lineages with abundance of reads >1 % (SSU rRNA tags) are shown. Members of families belonging to Actinobacteria and Firmicutes were combined

Table 2 Percentages of microbial genera within metagenomes of samples from day 21 from the following microcosms: Ancona uric acid, Anacona ammonium, Bizerte ammonium, Aqaba uric acid and El Max uric acid. The data are based on the frequency of the appearance of reads of SSU rRNA. Genera were combined into families, classes or phyla where necessary

		Bizerte NP	Ancona NP	Ancona UA	El Max UA	Aqaba UA
Alphaproteobacteria	*Jannaschia* spp.	0.41	0.49	0.01	0.08	0.05
	Loktanella spp.	0.71	0.84	0.04	0.13	0.10
	Oceanicola spp.	0.48	0.65	0.03	0.13	0.05
	Paracoccus spp.	0.80	0.62	0.01	0.28	0.12
	Rhodobacter spp.	0.80	0.67	0.01	0.21	0.10
	Roseobacter spp.	0.20	0.16	0.01	0.03	0.02
	Roseovarius spp.	1.44	1.39	0.08	0.28	0.13
	Ruegeria spp.	1.10	1.08	0.05	0.16	0.11
	Sulfitobacter spp.	2.01	1.45	0.08	0.19	0.28
	Thalassospira spp.	0.00	0.51	0.00	0.06	0.02
Betaproteobacteria	*Acidovorax* spp.	0.00	0.21	0.09	0.11	0.44
	Alcaligenes spp.	0.01	0.00	0.00	0.05	0.14
	Polaromonas spp.	0.00	0.08	0.04	0.05	0.12
Gammaproteobacteria	*Aeromonas* spp.	0.96	0.54	1.52	2.77	1.09
	Alcanivorax spp.	16.35	4.94	3.94	0.35	0.64
	Acinetobacter spp.	0.66	0.05	0.93	1.13	1.31
	Azotobacter spp.	0.34	0.50	0.45	0.48	0.95
	Citrobacter spp.	0.20	0.29	0.11	0.76	0.54
	Chromohalobacter spp.	0.75	0.48	0.59	0.13	0.12
	Colwellia spp.	0.19	0.23	0.11	0.44	0.28
	Cronobacter spp.	0.14	0.00	0.07	0.70	0.48
	Cycloclasticus spp.	0.52	0.01	0.04	0.01	0.00
	Enterobacter spp.	0.31	0.42	0.17	0.70	0.48
	Gallibacterium spp.	0.06	0.07	0.06	0.09	0.22
	Haemophilus spp.	0.10	0.11	0.08	0.16	0.25
	Hahella spp.	0.19	0.12	0.23	0.16	0.44
	Halomonas spp.	3.64	4.18	6.05	4.18	1.40
	Idiomarina spp.	0.68	0.26	0.76	2.67	0.97
	Legionella spp.	1.59	0.23	0.91	0.63	1.52
	Marichromatium spp.	0.18	0.15	0.14	0.16	0.31
	Marinobacter spp.	6.40	6.32	16.76	3.14	1.97
	Marinobaterium spp.	0.78	1.48	1.09	1.00	1.09
	Marinomonas spp.	0.48	0.94	0.47	0.96	0.60
	Methylophaga spp.	0.19	0.19	0.22	0.14	0.30
	Microbulbifer spp.	0.69	0.82	0.60	1.10	0.52
	Moraxella spp.	0.42	0.17	0.06	0.23	0.37
	Oceanimonas spp.	0.44	0.16	0.43	1.15	0.10
	Oceanospirillum spp.	0.12	0.29	0.16	0.23	0.18
	Oleiphilus spp.	0.05	0.03	0.15	0.04	0.08
	Oleispira spp.	0.05	0.14	0.13	0.11	0.05
	Pantoea spp.	0.30	0.52	0.36	1.33	0.63
	Photobacterium spp.	0.41	0.86	0.52	2.15	0.83
	Pseudoalteromonas spp.	1.27	0.37	1.92	0.85	1.63
	Pseudomonas spp.	12.93	14.08	12.07	21.14	45.57
	Psychromonas spp.	0.21	0.22	0.26	1.12	0.34
	Psychrobacter spp.	0.64	0.21	6.81	0.51	1.26
	Rheinheimeria spp.	0.42	0.13	0.10	0.27	0.45

Table 2 (continued)

		Bizerte NP	Ancona NP	Ancona UA	El Max UA	Aqaba UA
	Salmonella spp.	0.44	0.38	0.19	1.68	1.14
	Shewanella spp.	2.19	2.78	2.59	9.12	3.38
	Thalassolituus spp.	0.24	0.80	0.04	0.04	0.02
	Thalassomonas spp.	0.24	0.19	0.10	0.40	0.29
	Thiomicrospira spp.	0.26	0.40	0.63	0.66	0.40
	Thiorhodococcus spp.	0.17	0.13	0.11	0.11	0.23
	Vibrio spp.	0.96	2.38	1.14	5.08	3.85
	Xenorhabdus spp.	0.18	0.60	0.32	0.33	0.49
	Methylococcaceae	2.00	0.54	1.05	0.63	1.16
	Xanthomonadaceae	2.43	0.20	0.15	1.63	0.25
Deltaproteobacteria	*Deltaproteobacteria*	0.33	0.68	0.29	0.43	0.84
Flavobacteria	*Chryseobacterium* spp.	0.00	0.53	0.01	0.03	0.00
	Flavobacterium spp.	0.00	0.37	0.79	0.10	0.04
Actinobacteria	*Actinobacteria*	0.05	1.81	2.56	1.51	0.34
Firmicutes	*Firmicutes*	1.86	4.86	7.42	1.04	0.89
Spirochaeta	*Leptospira* spp.	0.00	0.03	0.03	0.06	0.17
	Others	28.02	35.68	23.87	24.43	17.90

All annotated data sets were examined for gene homologs involved in uric acid utilisation pathways. In both eukaryotes and prokaryotes, two urate hydroxylases (EC 1.7.3.3 and EC 1.14.13.113) have previously been shown to convert uric acid into 5-hydroxyisourate, which is ultimately broken down into urea and finally into ammonium. However, no genes with similarity to genes coding for either of these two enzymes could be detected in any of the datasets. In contrast, genes coding for enzymes that catalyse downstream reactions of uric acid utilisation, including allantoinase, allantoicase, allantoate amidohydrolase, ureidoglycolate hydrolase, 5-hydroxyisourate hydrolase and 2-oxo-4-hydroxy-4-carboxy-5-ureidoimidazoline (OHCU) decarboxylases, could be found (Supplementary Table 3a, b, c, d and e). The percentages of genes involved in uric acid metabolism were up to threefold higher in UA enrichments; they were particularly enriched (~0.11 % protein-coding genes) in Aqaba uric acid treatments while being particularly depleted in the Bizerte ammonium treatments (0.02 % total protein-coding genes). However, we note that the NP-treated microcosm from Ancona port also contained a significant amount of those genes (0.06 % total protein-coding genes). Binning analysis by BLASTP search further suggests that at least 15 (for Aqaba—uric acid), 11 (for Ancona—ammonium), 14 (for Ancona—uric acid), 2 (for Bizerte—ammonium) and 15 (for El Max—uric acid) distinct microorganisms may be potentially involved in the metabolism of uric acid and/or its degradation products. A direct comparison between the Ancona ammonium and uric acid treatments revealed that only 4 out of 25 of such microorganisms were shared, suggesting that most of the uric acid-utilization microbes are distinct to those using ammonium. The possibility that the microbes in the Ancona—ammonium enrichment possess genes encoding pathways for uric acid utilization could not be ruled out; however, the data presented in this study suggests that in the presence of uric acid such proteins do not support bacterial growth and thus under these conditions other microbes are enriched. Supplementary Tables 3a, b, c, d and e show genes for uric acid catabolism with similarity to the genes found in members of *Aeromonadaceae*, *Halomonadaceae*, *Pseudomonaceae* and *Rhodobactereaceae* within the three metagenomes from the uric acid enrichments, whereas the metagenomes from the ammonium enrichments predominantly contained uric acid catabolism genes from *Alteromonadaceae*, *Oceanospirillaceae* and *Rhodobacteraceae*. To further investigate which of these potential degrading organisms may play a role in uric acid metabolism, a cultivation-approach was used.

Isolation of Uric Acid-Degrading Bacteria

Uric acid-degrading bacteria were picked based upon the formation of a halo around the colony and purified to a single colony by triple repetitive plating on the same type of agar. As mentioned above, all isolates were successfully grown in ONR7a liquid media containing uric acid as sole source of nitrogen and carbon.

The 16S rRNA gene sequencing results (Supplementary Table 4) revealed that 44 of the 47 isolates belonged to the genus *Halomonas*. Two further isolates from the

Bizerte enrichment belonged to the genus *Marinobacter*, and one isolate from the El Max enrichment was identified as a member of the genus *Pelomonas*. Phylogenetic analysis (Fig. 4) showed that isolates were closely related to *Halomonas alkaliphila*, *Halomonas cupida*, *Halomonas salfondinae*, *Halomonas titanicae*, *Halomonas venusta* and *Halomonas ventosae*. With a few exceptions, the majority of the isolates showed location specificity. Most of the isolates from Ancona were closely related to *H. alkaliphila*; however, the isolates from Aqaba were predominately related to *H. venusta* and *Halomonas hydrothermalis*. The majority of isolates from the Bizerte enrichments clustered with *H. salfodinae* and *Halomonas pacifica*. Finally, all but two isolates from the El Max/Alexandria enrichments were distantly related to *H. cupida* and *Halomonas shangliensis*.

The analysis of the metagenomic data mentioned above showed that genes with a high similarity to genetic material from *Halomonas* spp. were present in all five metagenomes, albeit in low percentages, ranging from 1.4 to 6.1 % as revealed by abundance of SSU rRNA signatures. The percentage of *Halomonas*-like sequences was elevated in the uric acid enrichments.

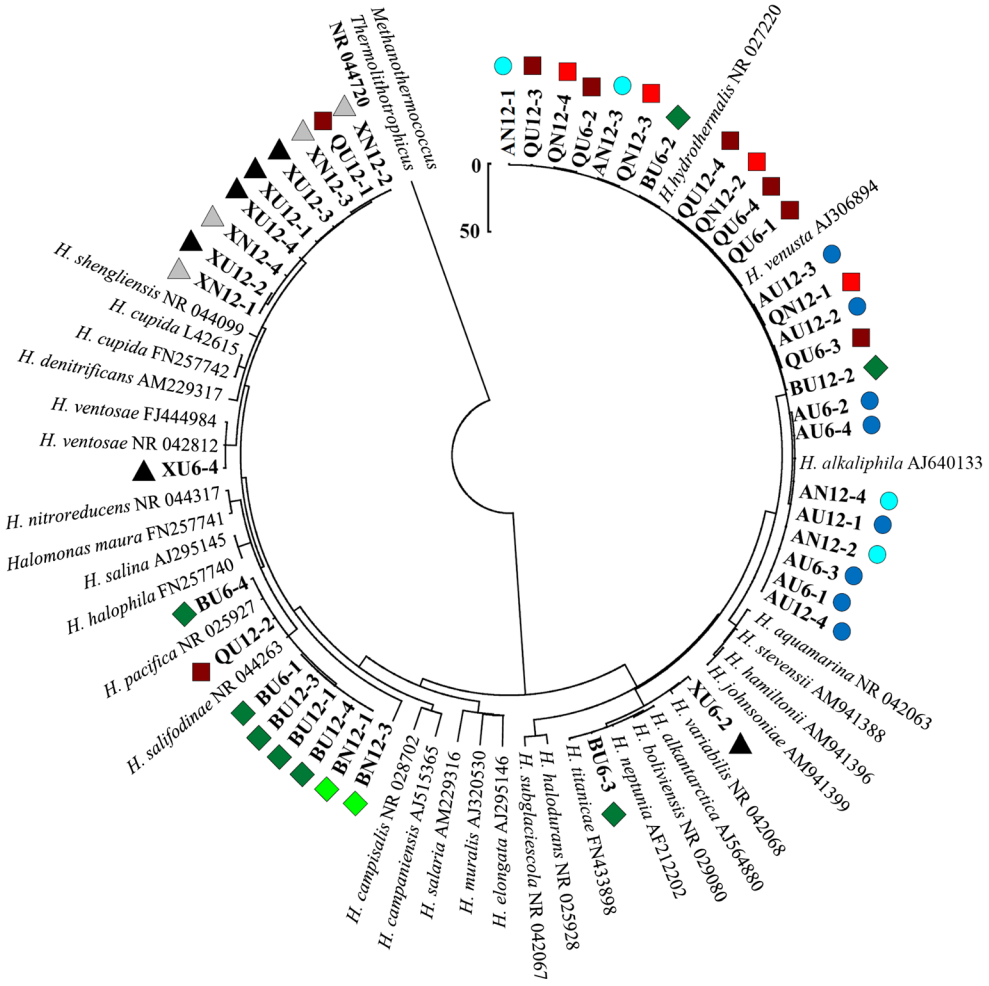

Fig. 4 Rooted phylogenetic tree of 16S rRNA gene sequences from *Halomonas* spp. isolates grown on ONR7 agar containing uric acid. The prefix codes B (*diamonds*), X (*triangles*) Q (*squares*) and A (*circles*) represent the experimental sites Bizerte, El Max, Aqaba and Ancona, respectively. The prefix codes U and N represent the experimental treatment: "UA" or "NP," respectively. The colour coding of symbols corresponds to the colours used in Fig. 2. Sequences were clustered by maximum parsimony according to the recommendation of the MODELTEST software [45]. The 16S rRNA gene sequences of the most closely related sequences from type strains of *Halomonas* species were acquired from the NCBI nucleotide database. The evolutionary history was inferred using the Maximum Parsimony method [9]. The bootstrap consensus tree inferred from 500 replicates is taken to represent the evolutionary history of the taxa analysed [11]. Branches corresponding to partitions reproduced in less than 50 % bootstrap replicates are collapsed. The MP tree was obtained using the Close-Neighbor-Interchange algorithm [41] with search level 3 [11, 41] in which the initial trees were obtained with the random addition of sequences (10 replicates). The tree is drawn to scale, with branch lengths calculated using the average pathway method [41]. *Scale bar* reflects the total nucleotide mismatch numbers in the whole sequence. All positions containing gaps and missing data were eliminated from the dataset (Complete Deletion option). There were a total of 952 positions in the final dataset, out of which 97 were parsimony informative. Phylogenetic analyses were conducted in MEGA4 [47]

Discussion

Comparison of Uric Acid and Ammonium as Nitrogen Source in Sediment Microcosms

Ammonium concentrations were measured as a proxy for nitrogen uptake in ammonium treatments and uric acid utilization in uric acid treatments, as it was the sole nitrogen source in the ammonium treatments but also an intermediate of uric acid conversion in the uric acid treatments. The ammonium treatments did show a relatively low ammonium concentration at the beginning of the experiment with a subsequent increase. This result indicates a general problem with ammonium and phosphate additions to seawater. As seawater is a saline solution, the addition of further ions may lead to precipitation. The addition of phosphate to artificial seawater leads to precipitation of calcium or magnesium ammonium phosphate or phosphates of trace elements that could affect microbial growth [3]. In this study, phosphate was added to artificial seawater that contained Fe and other trace elements that precipitate with both ammonium and phosphate (e.g. as a ferrous ammonium phosphate). The secondary increase of ammonium concentrations could be explained by consumption of both iron and phosphate for microbial growth and a subsequent release of ammonium into the medium.

The ammonium concentrations in the uric acid treatments increased rapidly to approximately 270 mg/L, which corresponds to 80 % of the total uric acid nitrogen introduced into the microcosms. As uric acid was the only nitrogen-containing substance in these microcosms, it stands to reason that it is quickly and almost entirely converted into ammonium. Photometric measurements of nitrate showed no significant increase in its concentrations (data not shown) in either treatment throughout the course of the experiment; it can therefore be assumed that uric acid was entirely transformed into ammonium.

Several recent studies have focused on the use of uric acid as a stand-alone nitrogen source or as a bioremediation strategy in combination with other substances. Koren et al. [28] described the use of pure uric acid in hydrocarbon-polluted sediments and succeeded in isolating a strain of *A. baumannii* that directly used uric acid for hydrocarbon degradation. In a further study, Knezevich et al. [27] described the application of guano as a complex source of uric acid and a soluble nitrogen source for bioremediation using both *A. borkumensis* and mixed oil-degrading microbial communities in an open system. While the uric acid-fed communities showed rapid growth, with cell numbers of up to 10^8 cells/mL and degradation of 70 % of total oil hydrocarbons, the cell numbers in the NPK-fertilised experiment remained 2 orders of magnitude lower and oil degradation was negligible. The data presented in our study is in concordance with a number of previous publications [27, 42, 43] which report enhanced microbial growth similar to what could be observed for the uric acid treatments. Microbial communities grew more rapidly and developed cell numbers 3 orders of magnitude higher than comparable treatments with soluble nitrogen sources [43]. Furthermore, aliphatic hydrocarbon degradation and PAH degradation were both significantly accelerated in presence of uric acid [42, 43]. Comparison of growth rates furthermore indicated that addition of molasses and rhamnolipids may speed up the microbial growth in the experiment, but is not stringently required for oil-degrading microbes to reach comparable cell numbers [42].

Microbial Population Dynamics of Microbial Communities Utilising Uric Acid

Two recent studies have investigated the use of fertilisers containing uric acid by oil-degrading microbial communities [27, 43]. The findings from both studies indicate the presence of *A. borkumensis* in enrichments or microcosms supplied with uric acid. In the study of Knezevich et al. [27], *Alcanivorax* spp., *Alteromonas* and *Halomonas* spp. were enriched and isolated. The results of our study also show abundance of *Alcanivorax* spp. in all samples. However, all uric acid enrichments showed a significantly lower abundance of these microbes in uric acid enrichments compared to ammonium enrichments. Despite the extensive research into the *Alcanivorax* genus, only one strain able to use uric acid as nitrogen source has been described to date [27]. The data from our study suggests that the degradation of uric acid could be performed by other members of the microbial consortium present in uric acid-amended hydrocarbon spiked enrichments. Uric acid enrichment also showed a high conversion rate into ammonium and elevated respiration rates in contrast to ammonium enrichment from days 0 to 9. However, the use of uric acid from days 4 to 6 did not lead to an increase in protein or biomass production. This result could be due to the extremely low C/N ratio of uric acid, which limits the total amount of biomass microbes can produce when grown on uric acid alone. Figure 1a, c shows that both emulsification and protein production begin to increase from day 6 onward. At this time, large quantities of uric acid have already been turned over into ammonium.

Therefore, microbial hydrocarbon degradation using uric acid as a nitrogen source could be described as a two-stage process involving the primary conversion of uric acid into ammonium and a secondary stage in which marine hydrocarbonoclastic microbes use ammonium as the primary nitrogen source.

This two-stage process can also be observed in Fig. 2, as most DNA fingerprints converged in a large cluster towards the end of the experiment. Similar trends have been observed in previous studies with similar experimental conditions [14–16]. Microbial climax communities with high similarity

formed within 14 days of the experiment, yet a subtle location specificity of the communities can be observed. While these differences can be observed within the DNA fingerprints from Aqaba, Ancona, Bizerte and El Max (Fig. S1), they are not statistically significant, as shown by multivariate analysis. The results of ANOSIM analysis indicated that the microbial communities showed significant similarities at two stages during the experiment, within days 4 to 8 and from day 12 to the end of the experiment, supporting the hypothesis of a two-stage process. The formation of a highly similar climax community within 14 to 21 days in different locations has been observed in a previous study involving the Irish Sea, the North Sea and the Mediterranean [16]. While obligate marine oil-degrading bacteria, most notably *Alcanivorax* species, form the backbone and most active hydrocarbon degraders of these consortia [14, 15], there is a certain degree of variability in the composition of other consortium members. In contrast to the intense clustering, the data points from days 0 to 6 of the experiment are located outside of this cluster, indicating a community change. The ANOSIM results (Supplementary Table 1c) indicate that within this period a highly similar community that differs from the oil-degrading climax community established after day 12 formed in all microcosms.

Metagenome sequencing was conducted for five samples from Aqaba, Ancona, Bizerte and El Max (microcosms 13, 14, 16, 18, 19), which were selected after the RISA fingerprinting. One sample from each Aqaba, Bizerte and El Max was chosen to cover location-specific characteristics of the sediment, while two samples from Ancona (one for the uric acid and one for the ammonium treatment) were selected to directly compare the effects of both treatments in one location. The sample material was based upon single biological replicate to preserve maximum coverage and sequencing depth as well as for other technical reasons. This procedure however does not take in account possible culture variability. A solution to this problem could be pooling of replicate samples, which reduce this bias; it would also reduce the overall coverage. Multiplexing of individual samples in a single sequencing run on the other hand bears the risk of adapter misidentification while true replication of samples (e.g. for a time series of microcosm samples) is still financially prohibitive. To ensure the validity of metagenome data in this study, rarefraction curves were established for each of the metagenome data sets and that were close to saturation and exhibited low standard deviation.

Metagenome sequencing confirmed the composition of the microbial consortia to be dominated by *Pseudomonas* spp. and to some extent by *Alcanivorax* spp. in all cases. *Pseudomonas* spp. were the most abundant species in all consortia, while the Ancona—uric acid, Ancona—ammonium and Bizerte—ammonium samples contained 4–16 % of *Alcanivorax* spp.-related 16S rRNA reads in the whole SSU rRNA dataset. The samples from El Max and Aqaba showed an overall similar species composition to the other samples, but a significantly higher percentage of *Pseudomonas* spp. This data is only apparently in contrast to previous studies conducted with similar microcosms that showed a significantly higher percentage of *Alcanivorax* spp. [14, 16] considering that the current study used the sediment rather than seawater as the inoculum. Furthermore, the genomes of *Pseudomonas* spp. are known to possess six or more rRNA operons, in contrast to the three rRNA operons present in the genome of *A. borkumensis*. This difference in the number of operons could result in an overestimation of the numbers of pseudomonads from 16S rRNA-related reads affiliated with *Pseudomonas* spp. in comparison to *Alcanivorax* spp. Most notably, the composition of uric acid and ammonium-based enrichments from Ancona proved to be similar, as both communities were enriched from identical inocula and effectively supplied with ammonium, in the latter case directly added to the medium while in the former case deriving from uric acid conversion. In addition to the clustering of uric acid and ammonium enrichment fingerprints in Fig. 2, these findings indicated that given identical experimental parameters, uric acid supplementation could effectively produce identical oil-degrading consortia due to the quick conversion of uric acid into ammonium. This suggestion is statistically supported by nested two-way ANOSIM analysis of the RISA location data sets.

Uric Acid Conversion and Uric Acid-Degrading Isolates

The analysis of the five metagenomes annotated within this study remained inconclusive regarding uric acid metabolism. Neither of the genomes showed any genes coding for uricase enzymes. However, urate oxidase activity has also been detected in other classes of enzymes, e.g. a laccase from a *Lysobacter* species [46]. It is therefore possible that the actual genes responsible for urate oxidation in the analysed samples could not be detected because they were annotated differently. Genes coding for ureidoglycolate hydrolase (EC 5.3.19), 5-hydroxisoureate hydrolase (EC 3.5.2.17), allantoicase (EC 3.5.3.4.), allantoinase (EC 3.5.2.5) and OHCU decarboxylase (EC 4.1.1.-), on the other hand, were identified within the genomes. These genes are involved in uric acid metabolism and appeared three times more frequently in the metagenomes of the uric acid-based enrichments in relation to the total number of sequences. Furthermore, uric acid catabolism genes in ammonium-based enrichments were mostly similar to the genes of *Oceanospirillaceae* and *Rhodobacteriaceae*, whereas the uric acid catabolism genes in the uric acid-based enrichments were predominantly similar to genes found in members of *Pseudomonadaceae* and *Halomonadaceae*. The analysis of 16S rRNA data in the metagenomes showed comparable percentages of *Halomonas* spp. and *Pseudomonas* spp. in the uric acid treatments compared to ammonium treatments (Fig. 3,

Table S3a, b, c, 3d and 3e). However, the direct comparison of the ammonium and uric acid treatments for the Ancona site revealed higher percentages of *Halomonas* spp. in the presence of uric acid and comparable percentages of *Pseudomonas* spp. in both treatments. The evidence from the metagenome analysis, therefore, indicates that the *Halomonas* spp. rather than the *Pseudomonas* spp. are the main utilisers of uric acid in this experiment.

In addition to the metagenome analysis, major degraders of uric acid were identified by cultivation and isolation at various points during the experiment. Ninety-three percent of the isolates belonged to the genus *Halomonas*, a ubiquitous, oligotrophic, highly salt-tolerant and metabolically versatile group of microbes [36]. *Halomonas* strains capable of biopolymer and bioemulsifier production have been previously cultured [17, 18]. Members of this genus with hydrocarbon-degradation capabilities have also been isolated [38] and detected in oil-degrading consortia using culture-independent techniques [26]. In contrast, the strains grown in this study were isolated in absence of hydrocarbons with uric acid as sole source of carbon, nitrogen and energy. While the results of this approach are subject to the limitations of our cultivation techniques, the presence of similar *Halomonas* species is confirmed by their detection within the metagenomic data of all five samples mentioned above. Sequences of *Halomonas* spp. made up between 1.4 and 6.1 % of the total amount of rRNA gene sequences.

The *Halomonas* isolates displayed a certain location specificity, with most isolates from each sampling site clustering together independently of experiment time and nitrogen source. This clustering could be because the genus *Halomonas* is understudied, and relatively few genomes and DNA sequences of few isolates are present in the databases. Another possibility is that the metabolic versatility of this genus [36] may have lead to the selection of specific *Halomonas* strains with uricase activity adapted to the unique abiotic parameters at the specific sampling site, suggesting a biogeographic distribution of this genus.

Prospects for Uric Acid Application in Bioremediation Techniques

This study investigates the population dynamics of oil-spiked marine sediment microcosms supplied with ammonium or uric acid in equal amounts and C/N/P ratios using identical crude oil batches. These procedures enable the direct comparison of microbial communities utilising either nitrogen source. The use of uric acid as a nitrogen source has been extensively discussed, experimented on and even patented, yet the mechanism of uric acid utilisation in an actual microbial community remains unknown. In our study, marine microbial communities dominated by *Pseudomonas* spp. and *Alcanivorax* spp., the most prominent, ubiquitous and competitive obligate hydrocarbon marine microbes, have been found. It was shown that uric acid could be quickly transformed into ammonium by members of the *Halomonas* genus. This observation was made for sediments originating from four independent sites located around the Mediterranean (Ancona, Bizerte, El Max) and the Red Sea (Aqaba), which implies that a similar pattern likely occurs on a more global scale.

As each uric acid molecule contains four nitrogen atoms, such a nitrogen source can be applied in lower molarities compared to ammonium. While problems with leaching can be successfully overcome by paraffin coating (urea) or the use of slow-release fertilisers (ammonium, nitrate) [14], these treatments require industrial processes that greatly reduce the cost-efficiency of bioremediation. Uric acid, on the other hand, can be found in concentrations of 3–6 % (*w*/*w*) in poultry faeces, making up 60 % of the total nitrogen. The global production of up to 50 billion chickens produces 50 million tons of faecal matter every year with an estimated content of 1.5 to 3 million tons of uric acid [40]. Poultry litter is currently used as an agricultural fertiliser after sterilisation through heat treatment and drying and are well established on the fertiliser market. This study has shown that uric acid can be quickly transformed into ammonium, which in turn is utilised by highly efficient oil-degrading microbes in marine sediments. This process was observed in sediment collected from various locations in different water bodies without the addition of allochtonous microbial communities, suggesting that cost-effective uric acid-based biostimulation techniques can be successfully achieved in a wide range of marine sediments.

Acknowledgments The authors would like to thank Anna Foster, Sarah Chesworth and Gordon Turner for their help with photometric and respiration measurements. With exception of XH and JC, all authors were supported by the FP7 Project ULIXES (FP7-KBBE-2010-266473). This work was further funded by grant BIO2011-25012 from the Spanish Ministry of the Economy and Competitiveness. FM was supported by Università degli Studi di Milano, European Social Fund (FSE) and Regione Lombardia (contract "Dote Ricerca"). DD acknowledges support of KAUST, King Abdullah University of Science and Technology. PG acknowledges the support of the European Commission through the project Kill-Spill (FP7, Contract Nr 312139). CG would like to thank Mr. Kyungsun Lee of Macrogen Inc. for his courtesy regarding sequencing services, J. Cans, B. Strid and C. Hudson for continued advice and inspiration as well as Delphine Lallias for her help with multivariate statistics and John Flannery for proofreading this manuscript.

References

1. Anderson DG, McKay LL (1983) Simple and rapid method for isolating large plasmid DNA from lactic streptococci. Appl Environ Microbiol 46:549–552
2. Ashelford KE, Chuzhanova NA, Fry JC, Jones AJ, Weightman AJ (2005) At least 1 in 20, 16S rRNA sequence records currently held in public repositories is estimated to contain substantial anomalies. Appl Environ Microbiol 71:7724–7736

3. Atlas EL (1975) Phosphate equilibria in seawater and interstitial waters. PhD thesis. Oregon State Univ., Corvallis, Oregon.
4. Atlas RM, Bartha R (1972) Degradation and mineralization of petroleum by two bacteria isolated from coastal waters. Biotechnol Bioeng 14:297–308
5. Capone DG, Bronk DA, Mulholland MR & Carpenter EJ (2008) Nitrogen in the marine environment. (Academic Press, 2008). at http://www.sciencedirect.com/science/book/9780123725226.
6. Cardinale M et al (2004) Comparison of different primer sets for use in automated ribosomal intergenic spacer analysis of complex bacterial communities. Appl Environ Microbiol 70:6147–6156
7. Clarke KR, Gorley RN (2006) PRIMER v6: user manual/tutorial. PRIMER-E, Plymouth
8. Dyksterhouse SE, Gray JP, Herwig RP, Lara JC, Staley JT (1995) *Cycloclasticus pugetii* gen. nov., sp. nov., an aromatic hydrocarbon-degrading bacterium from marine sediments. Int J Syst Bacteriol 45:116–123
9. Eck RV, Dayhoff MO (1966) Atlas of protein sequence and structure. National Biomedical Research Foundation, Silver Springs
10. Fava F, Berselli S, Conte P, Piccolo A, Marchetti L (2004) Effects of humic substances and soya lecithin on the aerobic bioremediation of a soil historically contaminated by polycyclic aromatic hydrocarbons (PAHs). Biotechnol Bioeng 88:214–223
11. Felsenstein J (1985) Confidence limits on phylogenies: an approach using the bootstrap. Evolution 39:783–791
12. Gagnon K, Rothäusler E, Syrjänen A, Yli-Renko M, Jormalainen V (2013) Seabird fertilizes Baltic Sea littoral food webs. PLoS ONE 8: e61284
13. Garcia HE, Locarnini RA, Boyer TP, Antonov JI, Zweng MM, Baranova OK & Johnson DR (2010) World Ocean Atlas 2009, Volume 4: Nutrients (phosphate, nitrate, silicate). S. Levitus, Ed. NOAA Atlas NESDIS 71, U.S. Government Printing Office, Washington, D.C.
14. Gertler C, Gerdts G, Timmis KN, Yakimov MM, Golyshin PN (2009) Populations of heavy fuel oil-degrading marine microbial community in presence of oil sorbent materials. J Appl Microbiol 107:590–605
15. Gertler C, Gerdts G, Timmis KN, Golyshin PN (2009) Microbial consortia in mesocosm bioremediation trial using oil sorbents, slow-release fertilizer and bioaugmentation. FEMS Microbiol Ecol 69:288–300
16. Gertler C, Näther DJ, Cappello S, Gerdts G, Quilliam RS, Yakimov MM, Golyshin PN (2012) Composition and dynamics of biostimulated indigenous oil-degrading microbial consortia from the Irish, North and Mediterranean Seas: a mesocosm study. FEMS Microbiol Ecol 81:520–536
17. Gutierrez T, Singleton DR, Berry D, Yang T, Aitken MD, Teske A (2013) Hydrocarbon-degrading bacteria enriched by the deepwater horizon oil spill identified by cultivation and DNA-SIP. ISME J 7: 2091–2104
18. Gutierrez T, Berry D, Yang T, Mishamandani S, McKay L, Teske A, Aitken MD (2013) Role of bacterial exopolysaccharides (EPS) in the fate of the oil released during the Deepwater Horizon Oil Spill. PLoS ONE 8:e67717
19. Hammer Ø, Harper DAT, Ryan PD (2001) PAST: palaeontological statistics software package for education and data analysis. Palaeontol Electron 4:9
20. Hazen TC, Dubinsky EA, DeSantis TZ, Andersen GL, Piceno YM, Singh N, Jansson JK et al (2010) Deep-sea oil plume enriches indigenous oil-degrading bacteria. Science 330:204–208
21. Head IM, Jones DM, Röling WFM (2006) Marine microorganisms make a meal of oil. Nat Rev Microbiol 4:173–182
22. Kanehisa M, Goto S, Kawashima S, Okuno Y, Hattori M (2004) The KEGG resource for deciphering the genome. Nucleic Acids Res 32:277–280
23. Kanehisa M (1997) A database for post-genome analysis. Trends Genet 13:375–376
24. Kanehisa M, Goto S, Hattori M, Aoki-Kinoshita KF, Itoh M, Kawashima S et al (2006) From genomics to chemical genomics: new developments in KEGG. Nucleic Acids Res 34:354–357
25. Kasai Y, Kishira H, Sasaki T, Syutsubo K, Watanabe K, Harayama S (2002) Predominant growth of Alcanivorax strains in oil-contaminated and nutrient-supplemented sea water. Environ Microbiol 4:141–147
26. Kleinsteuber S, Riis V, Fetzer I, Harms H, Müller S (2006) Population dynamics within a microbial consortium during growth on diesel fuel in saline environments. Appl Environ Microbiol 72: 3531–3542
27. Knezevich V, Koren O, Ron EZ, Rosenberg E (2006) Petroleum bioremediation in seawater using guano as the fertilizer. Bioremed J 10:83–91
28. Koren O, Knezevic V, Ron EZ, Rosenberg E (2003) Petroleum pollution bioremediation using water-insoluble uric acid as the nitrogen source. Appl Environ Microbiol 69:6337–6339
29. Kube M, Chernikova TN, Al-Ramahi Y, Beloqui A, Lopez-Cortez N, Guazzaroni ME, Heipieper HJ, Klages S, Kotsyurbenko OR, Langer I, Nechitaylo TY, Lünsdorf H, Fernández M, Juárez S, Ciordia S, Singer A, Kagan O, Egorova O, Petit PA, StogiosP KY, Tchigvintsev A, Flick R, Denaro R, Genovese M, Albar JP, Reva ON, Martínez-Gomariz M, Tran H, Ferrer M, Savchenko A, Yakunin AF, Yakimov MM, Golyshina OV, Reinhardt R, Golyshin PN (2013) Genome sequence and functional genomics analysis of the oil-degrading bacterium *Oleispira antarctica*. Nat Commun 4: 2156
30. Larkin MA, Blackshields G, Brown NP, Chenna R, McGettigan PA, McWilliam H, Valentin F, Wallace IM, Wilm A, Lopez R, Thompson JD, Gibson TJ, Higgins DG (2007) Clustal W and Clustal X version 2.0. Bioinformatics 21:2947–2948
31. Li R, Li Y, Kristiansen K, Wang J (2008) SOAP: short oligonucleotide alignment program. Bioinformatics 24:713–714
32. Li R, Yu C, Li Y, Lam TW, Yiu SM, Kristiansen K, Wang J (2009) SOAP2: an improved ultrafast tool for short read alignment. Bioinformatics 25:1966–1967
33. Li R, Zhu H, Ruan J, Qian W, Fang X, Shi Z, Li Y, Li S, Shan G, Kristiansen K, Li S, Yang H, Wang J, Wang J (2010) De novo assembly of human genomes with massively parallel short read sequencing. Genome Res 20:265–272
34. Lee K, Tremblay GH, Levy EM (1993) Bioremediation: application of slow-release fertilizers on low-energy shorelines. Int Oil Spill Conf Proc 1993:449–454
35. Lindstrom JE et al (1991) Microbial populations and hydrocarbon biodegradation potentials in fertilized shoreline sediments affected by the T/V Exxon Valdez oil spill. Appl Environ Microbiol 57: 2514–2522
36. Mata JA, Martínez-Cánovas J, Quesada E, Béjar VA (2002) Detailed phenotypic characterisation of the type strains of *Halomonas* species. Syst Appl Microbiol 25:360–375
37. Miranda KM, Espey MG, Wink DA (2001) A rapid, simple spectrophotometric method for simultaneous detection of nitrate and nitrite. Nitric Oxide 5:62–71
38. Mnif S, Chamkha M, Sayadi S (2009) Isolation and characterization of *Halomonas* sp. strain C2SS100, a hydrocarbon-degrading bacterium under hypersaline conditions. J Appl Microbiol 107: 785–794
39. Mulvaney, R. (1996) in Methods of soil analysis part 3: chemical methods. 1123–1184 Soil Science Society of America, Inc.
40. Nahm KH (2003) Evaluation of the nitrogen content in poultry manure. World's Poult Sci J 59:77–88
41. Nei M, Kumar S (2000) Molecular evolution and phylogenetics. Oxford University Press, New York

42. Nikolopoulou M, Kalogerakis N (2008) Enhanced bioremediation of crude oil utilizing lipophilic fertilizers combined with biosurfactants and molasses. Mar Pollut Bull 56:1855–1861
43. Nikolopoulou M, Pasadakis N, Kalogerakis N (2013) Evaluation of autochthonous bioaugmentation and biostimulation during microcosm-simulated oil spills. Mar Pollut Bull 72:165–173
44. Noguchi H, Park J et al (2006) MetaGene: prokaryotic gene finding from environmental genome shotgun sequences. Nucleic Acids Res 34:5623–5630
45. Posada D, Crandall KA (1998) MODELTEST: testing the model of DNA substitution. Bioinformatics 14:817–818
46. Tamaki H, Matsuoka T, Yasuda Y, Hanada S, Kamagata Y, Nakamura K, Sakasegawa S (2010) A novel laccase with urate oxidation activity from Lysobacter sp. T-15. J Biochem 148:481–489
47. Tamura K, Dudley J, Nei M, Kumar S (2007) MEGA4: molecular evolutionary genetics analysis (MEGA) software version 4.0. Mol Biol Evol 24:1596–1599
48. Vogels GD, Van der Drift C (1976) Degradation of purines and pyrimidines by microorganisms. Bacteriol Rev 40:403–468
49. Wang Z, Hollebone BP, Fingas M, Fieldhouse B, Sigouin L, Landriault M, SmithP, Noonan J & Thouin G (2003) Characteristics of spilled oils, fuels, and petroleum products: 1. Composition and properties of selected oils. United States Environmental Protection Agency, National Exposure Research Laboratory, EPA/600/R-03/072
50. Wrenn BA, Zheng H, Kohar ES, Lee K, Venosa AD (2001) Effect of pulsed additions of nutrients on oil biodegradation in continuous-flow beach microcosms. Int Oil Spill Conf Proc 2001:339–344
51. Yakimov MM, Gentile G, Bruni V, Cappello S, D'Auria G, Golyshin PN, Giuliano L (2004) Crude oil-induced structural shift of coastal bacterial communities of Rod Bay (Terra Nova Bay, Ross Sea, Antarctica) and characterization of cultured cold-adapted hydrocarbonoclastic bacteria. FEMS Microbiol Ecol 49:419–432
52. Yakimov MM, Timmis KN, Golyshin PN (2007) Obligate oil-degrading marine bacteria. Curr Opin Biotechnol 18:257–266

Capítulo 4: Reconstrucción de rutas de biodegradación en microcosmos enriquecidos con amonio y ácido úrico

Resumen

El nitrógeno es un nutriente clave para favorecer el crecimiento y los procesos de biodegradación. Sin embargo, en el medio marino se encuentra a muy baja concentración. Para degradar un gramo de petróleo necesitamos 0,04 gramos de nitrógeno, por lo que constituye un factor limitante para este proceso. Para combatir los vertidos de petróleo se pueden añadir diferentes fuentes de nitrógeno para promover el crecimiento de las bacterias que degradan de los hidrocarburos del petróleo. Esto convierte la elección del nutriente en un paso crucial en el proceso de bioestimulación para degradar los hidrocarburos acumulados en vertidos reales. Entre ellos encontramos el amonio (AMM), efectivo en pruebas de micro- y mesocosmos, pero que presenta problemas de precipitación en el medio natural. En el Capítulo anterior hemos demostrado el potencial del ácido úrico para favorecer la biodegradación de hidrocarburos. Queda por estudiar como su uso influye en las capacidades biodegradativas de las comunidades bioestimuladas en comparación con otros bioestimulantes modelo como el AMM. Por ello, en este estudio, empleando los métodos bioinformáticos generados en el Capítulo 2 y las secuencias metagenómicas generadas en el Capítulo 3, se han reconstruido las redes catabólicas de dos microcosmos formados a partir de sedimentos de la zona crónicamente contaminada del puerto de Ancona, utilizando AMM y AU como fertilizantes.

Las secuencias metagenómicas de los microcosmos (27.893 marcos de lectura abierta en UA y 32.180 en AMM), se analizaron en base a los siguientes pasos: a) anotación funcional de las enzimas relacionadas con la biodegradación de hidrocarburos; b) reconstrucción catabólica de las rutas de degradación de compuestos aromáticos; c) validación experimental mediante metabolómica dirigida de las capacidades biodegradativas inferidas de los datos *in silico*; y d) afiliación taxonómica de los genes catabólicos para identificar el papel de diferentes grupos bacterianos.

Se identificaron en los metagenomas de los microscosmos UA y AMM un total de 45 (para UA) y 65 (para AMM) genes que codifican enzimas catabólicas. La abundancia relativa de los mismos demostró que la bioestimulación con AMM y AU no tiene un efecto marcado en la abundancia de dichos genes. Se observó también que ambos microcosmos presentan un alto grado de similitud a nivel de composición bacteriana. El análisis de los genes catabólicos permitió la reconstrucción de las rutas de biodegradación preferentes en cada uno de los microcosmos. Así, se observó que la bioestimulación con diferentes fuentes de nitrógeno provoca cambios en las capacidades catabólicas y en la degradación preferencial de aromáticos. Estas diferencias fueron comprobadas experimentalmente en: i) la degradación de benzoato/2-clorobenzoato y naftaleno vía gentisato (potenciadas en AMM); ii) la degradación de 4-aminobenzene-sulfonato, p-cumato, dibenzofurano y ftalato (sólo observadas en AMM); iii) y la degradación de orcinol, fenilpropionato, homoprotocatecuato, benceno e ibuprofeno (detectadas únicamente en UA). La afiliación taxonómica demuestra la participación diferencial de bacterias de 10 géneros y de los filos *Firmicutes* y *Actinobacteria* en la degradación de 18 compuestos aromáticos diferentes. Los resultados de este estudio pueden ser de gran utilidad a la hora de planificar nuevas estrategias de biorremediación. Se sugiere la combinación de diferentes bioestimulantes para la degradación de un mayor número de compuestos aromáticos presentes en el crudo.

frontiers in Microbiology

ORIGINAL RESEARCH
published: 24 November 2015
doi: 10.3389/fmicb.2015.01270

Degradation Network Reconstruction in Uric Acid and Ammonium Amendments in Oil-Degrading Marine Microcosms Guided by Metagenomic Data

Rafael Bargiela[1], Christoph Gertler[2†], Mirko Magagnini[3], Francesca Mapelli[4], Jianwei Chen[5], Daniele Daffonchio[4,6], Peter N. Golyshin[2] and Manuel Ferrer[1]**

[1] Systems Biotechnology, Department of Biocatalysis, Institute of Catalysis, Consejo Superior de Investigaciones Científicas, Madrid, Spain, [2] School of Biological Sciences, Bangor University, Bangor, UK, [3] EcoTechSystems Ltd., Ancona, Italy, [4] Department of Food, Environmental and Nutritional Sciences, University of Milan, Milan, Italy, [5] Beijing Genomics Institute, Shenzhen, China, [6] Biological and Environmental Science and Engineering Division, King Abdullah University of Science and Technology, Thuwal, Saudi Arabia

Biostimulation with different nitrogen sources is often regarded as a strategy of choice in combating oil spills in marine environments. Such environments are typically depleted in nitrogen, therefore limiting the balanced microbial utilization of carbon-rich petroleum constituents. It is fundamental, yet only scarcely accounted for, to analyze the catabolic consequences of application of biostimulants. Here, we examined such alterations in enrichment microcosms using sediments from chronically crude oil-contaminated marine sediment at Ancona harbor (Italy) amended with natural fertilizer, uric acid (UA), or ammonium (AMM). We applied the web-based AromaDeg resource using as query Illumina HiSeq meta-sequences (UA: 27,893 open reading frames; AMM: 32,180) to identify potential catabolic differences. A total of 45 (for UA) and 65 (AMM) gene sequences encoding key catabolic enzymes matched AromaDeg, and their participation in aromatic degradation reactions could be unambiguously suggested. Genomic signatures for the degradation of aromatics such as 2-chlorobenzoate, indole-3-acetate, biphenyl, gentisate, quinoline and phenanthrene were common for both microcosms. However, those for the degradation of orcinol, ibuprofen, phenylpropionate, homoprotocatechuate and benzene (in UA) and 4-aminobenzene-sulfonate, *p*-cumate, dibenzofuran and phthalate (in AMM), were selectively enriched. Experimental validation was conducted and good agreement with predictions was observed. This suggests certain discrepancies in action of these biostimulants on the genomic content of the initial microbial community for the catabolism of petroleum constituents or aromatics pollutants. In both cases, the emerging microbial communities were phylogenetically highly similar and were composed by very same proteobacterial families. However, examination of taxonomic assignments further revealed different catabolic pathway organization at the organismal level, which should be considered for designing oil spill mitigation strategies in the sea.

Keywords: ammonium, biostimulation, crude oil degradation, enrichment, Mediterranean Sea, metagenomics, microcosm, uric acid

OPEN ACCESS

Edited by:
Eamonn P. Culligan, Cork Institute of Technology, Ireland

Reviewed by:
Romy Chakraborty, Lawrence Berkeley National Lab, USA
Efthymios Ladoukakis, National Technical University of Athens, Greece

****Correspondence:***
Manuel Ferrer
mferrer@icp.csic.es;
Peter N. Golyshin
p.golyshin@bangor.ac.uk

†Present address:
Christoph Gertler, Friedrich Loeffler Institute– Federal Research Institute for Animal Health, Institute for Novel and Emerging Infectious Diseases, 17493 Greifswald, Germany

Specialty section:
This article was submitted to Evolutionary and Genomic Microbiology, a section of the journal Frontiers in Microbiology

Received: *06 July 2015*
Accepted: *30 October 2015*
Published: *24 November 2015*

Citation:
Bargiela R, Gertler C, Magagnini M, Mapelli F, Chen J, Daffonchio D, Golyshin PN and Ferrer M (2015) Degradation Network Reconstruction in Uric Acid and Ammonium Amendments in Oil-Degrading Marine Microcosms Guided by Metagenomic Data. Front. Microbiol. 6:1270. doi: 10.3389/fmicb.2015.01270

INTRODUCTION

Oil pollution still is a global problem (Yakimov et al., 2007; Bargiela et al., 2015). At present, in many sea regions containment and recovery of oil using booms and skimmers is the method of choice for oil spill first responders (Walther, 2014). Especially in the open sea, the use of dispersants in combination with biostimulation and bioaugmentation agents based on non-toxic, natural low cost formulations, is encouraged, although the majority of tests have been performed at lab-scale (Das and Chandran, 2010; Nikolopoulou and Kalogerakis, 2010; Alvarez et al., 2011; Nikolopoulou et al., 2013). In marine systems, the low concentration of nitrogen, phosphorous, and oxygen, together with their low bioavailability are main factors limiting the degradation of carbon-rich hydrophobic compounds (Howarth and Marino, 2006; Venosa et al., 2010; Ly et al., 2014). Attempts have been made to use different nitrogen sources to promote the growth and selection of different microbial strains with greater catabolic capacity for combating oil spills compared to natural attenuation (Teramoto et al., 2009; Venosa et al., 2010). However, crude oil biodegradation requires about 0.04 g of nitrogen per gram of oil (Atlas, 1981) which makes the choice of nitrogen source pivotal for the whole treatment. Recent data highlighted the possible link between N cycling processes and hydrocarbon degradation in marine sediments (Scott et al., 2014). Therefore, it is essential to select appropriated N-containing biostimulants.

The sources of nitrogen for the degradation tests – mostly performed at lab-scale and in minor occasions at field-scale – included nitrate, ammonium (AMM), urea, uric acid (UA), amino acids and the hydrophobic substance lecithin (Garcia-Blanco et al., 2007; Li et al., 2007; Martínez-Pascual et al., 2010; Venosa et al., 2010; Nikolopoulou et al., 2013; Mohseni-Bandpi et al., 2014). Slow-release nitrogen (AMM-based) fertilizers have also been successfully used for growth stimulation in microbial oil remediation (Miyasaka et al., 2006; Teramoto et al., 2009; Reis et al., 2013). However, AMM has been proved ineffective in treatment of real oil spill due to co-precipitation with phosphates in seawater. In a recent study, we have shown that biodegradable natural fertilizers like UA can be used as cost-efficient biostimulant for enhancing bacterial growth in polluted sediments (Gertler et al., 2015). Each nitrogen source has its advantages and disadvantages, yet overall results have shown that the microbial populations were initially different from those found in the absence of biostimulants and that the degradation efficiency generally increased. It is therefore critical to establish how the whole microbial biodegradation network is affected and whether different pollutants are preferentially degraded as a consequence of amendments of biostimulants.

In an early work using the recently developed AromaDeg analysis (Duarte et al., 2014) and a meta-network graphical approach, we reconstructed the catabolic networks associated to microbial communities in a number of chronically polluted sites (Bargiela et al., 2015). The approach focuses on the usage of metagenomic data, which directly leads to a network that included catabolic reactions associated to genes encoding enzymes annotated in the genomes of the community organisms. We found key catabolic variations associated to changes in community structure and environmental constraints (Bargiela et al., 2015). In this work, this approach was applied to draft the catabolic networks of two different enrichment microcosms set up with sediments from chronically crude oil-contaminated marine sediments from Ancona harbor (Italy) and the natural fertilizer UA or AMM as nitrogen sources (Gertler et al., 2015). Ancona harbor is very close to the urban area and hosts a multi-purpose port receiving cruise liners, passenger ferries, commercial liners and fishing boats. A minor part of the related airborne pollutants is due to the vessels calling at the port while the main contribution comes from road traffic and other human activities. Furthermore, sediments in Ancona harbor are heavily contaminated due to its role as a major ferry terminal and industrial port on the Adriatic Sea. We hypothesize that the microbial community shifts previously observed after addition of UA and AMM (Gertler et al., 2015) may have an influence in the selection of certain catabolic pathways. Potential protein-coding genes ($\geq$20 amino acids long) obtained by direct Illumina HiSeq sequencing of DNA material of the corresponding microcosms (Gertler et al., 2015) constituted the input information in our study.

MATERIALS AND METHODS

Study Site, Microcosm Set-up and Sequence Accession Numbers

The starting point of this study were the meta-sequences previously obtained by direct sequencing from two microcosm sets created using sediment samples from the harbor of Ancona (Italy; 43°37′N, 13°30′15″E), as described previously (Gertler et al., 2015). Both microcosm setups were identical in size, composition, incubation, sampling regime and nutrient concentration with exception of the type of nitrogen source applied. Either AMM or UA were supplied in equimolar amounts of nitrogen. Briefly, one-liter Erlenmeyer flasks (duplicates) were filled with 150 g of sand (Sigma–Aldrich, St. Louis, MO, USA), sterilized and spiked with 10 mL of sterile filtered Arabian light crude oil. One gram of sediment from the sampling site was mixed into the oil-spiked sand as the inoculum. Three hundred milliliters of modified ONR7a medium (Dyksterhouse et al., 1995) (omitting AMM chloride and disodium hydrogen phosphate) was added. We added 5 mL of Arabian light crude oil, which based upon average literature values for density and molecular weight equals about 300 mM of C (Wang et al., 2003), 5 mM of NH_4Cl and 0.5 mM of Na_2HPO_4 resulting in a molar N/P ratio of approximately 10:1. For UA treatment microcosm, 0.21 g (1.25 mmol = 5 mmol N) of UA was provided as nitrogen source while the AMM treatment microcosms were each supplied with 2.5 mL of a 2 M AMM chloride solution (5 mmol; pH 7.8). Both treatments also contained 2.5 mL of a 0.2 M disodium hydrogen phosphate solution (0.5 mmol; pH 7.8). Excess amounts of crude oil were added to compensate for the 35% carbon losses due to evaporation of volatile hydrocarbons over the course of the experiment. Including losses due to evaporation, the C/N/P ratio was approximately 400:10:1. Control treatments

were set up: (i) a negative control contained only sterile sand and ONR7a; (ii) two further controls contained sand, ONR7a, crude oil and either UA or AMM chloride solution but no sediment sample; and (iii) one control contained oil, sterile sand, ONR7a medium and a sediment sample, but no additional nitrogen source or phosphorus source was provided. No significant growth was detected under tested control conditions. Under the given assay conditions, the utilization of UA as carbon source is minimal, as the amount of carbon introduced by UA into the microcosms was disproportionately low in contrast to the residual carbon in the sediment and the carbon introduced in form of oil. Briefly, we added 300 mmols of carbon in form of oil and only 6.25 mmols of carbon in form of UA. In addition, the molar ratio C/N in the system (between 10:1 and 40:1, depending UA or AMM was added) implies there was excess of carbon in the medium and thus the growth was limited by N.

The resulting microbial communities from microcosms were destructively sampled after 21 days of incubation at 20°C, the isolated DNA subjected to the paired-end sequencing (Illumina HiSeq 2000) at Beijing Genomics Institute (BGI; China), and gene calling performed as described (Gertler et al., 2015). Taxonomic affiliations of potential protein-coding genes were predicted as described previously (Guazzaroni et al., 2013; Bargiela et al., 2015).

The meta-sequences are available at the National Center for Biotechnology Information (NCBI) with the IDs PRJNA222664 [for MGS-ANC(UA)] and PRJNA222663 [for MGS-ANC(AMM)]. The Whole Genome Shotgun projects are also available at DDBJ/EMBL/GenBank under the accession numbers AZIH00000000 [for MGS-ANC(UA)] and AZIK00000000 [for MGS-ANC(AMM)]. All original non-chimeric 16S small subunit rRNA hypervariable tag 454 sequences were archived at the EBI European Read Archive under accession number PRJEB5322. Note that the samples were named based on the code 'MGS', which refers to MetaGenome Source, followed by a short name indicating the origin of the sample and the nitrogen source, as follows: MGS-ANC(AMM) (the harbor of Ancona and AMM as nitrogen source); MGS-ANC(UA) (the harbor of Ancona and UA as nitrogen source).

Biodegradation Network Reconstruction: Scripts and Commands for Graphics

The web-based AromaDeg resource (Duarte et al., 2014) was used for catabolic network reconstruction. AromaDeg is a web-based resource with an up-to-date and manually curated database that includes an associated query system which exploits phylogenomic analysis of the degradation of aromatic compounds. This database addresses systematic errors produced by standard methods of protein function prediction by improving the accuracy of functional classification of key genes, particularly those encoding proteins of aromatic compounds' degradation. In brief, each query sequence from a genome or metagenome [MGS-ANC(AMM) and MGS-ANC(UA), in this study] that matches a given protein family of AromaDeg is associated with an experimentally validated catabolic enzyme performing an aromatic compound degradation reaction. Individual reactions, and thus the corresponding substrate pollutants and intermediate degradation products, can be linked to reconstruct catabolic networks. We have recently designed an in-house script allowing the automatic reconstruction of such networks in a graphical format, which was used in present work. The script allows visualization and comparison of the abundance levels of genes encoding catabolic enzymes assigned to distinct degradation reactions as well as substrates or intermediates possibly degraded by distinct microbial communities. The complete workflow, including the scripts and commands used for catabolic network reconstruction has recently been reported (Bargiela et al., 2015).

Note that the sequence material used in the present investigation for biodegradation network reconstruction was based upon single biological microcosm replicate to preserve maximum coverage and sequencing depth as well as for other technical reasons, as described previously (Gertler et al., 2015). For each of the metagenome datasets the rarefaction curves of the observed species were estimated to analyze the species sampling coverage, and found that the rarefaction curves indicate closeness to saturation in each of the samples (Gertler et al., 2015). Therefore, with a single run of paired-end Illumina sequencing we determined populations that really represent the actual state of the microbial community in the microcosms and that biases were not introduced due to differences in microbial coverage. Whether or not more replicates may introduce some differences in the present study was not examined. However, because of the low standard deviation in the cultures (also checked for the representativeness of the microcosm by 16S small subunit rRNA hypervariable tag 454 sequences fingerprinting; Gertler et al., 2015) and the fact that sampled 16S rRNA diversity indicated closeness to saturation, we considered that the presented data are valid. Note that experimental validations (see Experimental Validations of Predicted Biodegradation Capacities) were performed in triplicates (with appropriated standard deviations), on the basis of which metagenome-based predictions were confirmed. Therefore, we considered that the differences at the taxonomic, gene content levels and catabolic capacities herein presented are most likely due to actual biological variability and are not random.

Experimental Validations of Predicted Biodegradation Capacities

The ability of each of the microcosms to grow on pollutants expected to be degraded, was confirmed as follows. First, UA and AMM microcosms (in triplicates) were obtained as described above but omitting Arabian light crude oil; instead, a mix of pollutants containing naphthalene, 2,3-dihydroxybiphenyl, benzene, *p*-cumate, orcinol, 2-chlorobenzoate, phthalate and phenylpropionate, all from Fluka-Aldrich-Sigma Chemical Co. (St. Louis, MO, USA), was added at a final concentration of 2 ppm each. These pollutants were selected on the basis of existing analytical methods to quantify their concentrations (Bargiela et al., 2015). Control cultures without the addition of sediments but with chemicals and cultures plus sediments but without the addition of chemicals were set up.

The extent of degradation in test and control samples was quantified as follows. Briefly, bacterial cells (from 300 ml culture)

were separated by centrifugation at 13,000 *g* at room temperature for 10 min. After supernatant separation, bacterial pellet was used for methanol extraction by adding 1.2 mL of cold (−80°C) high-performance liquid chromatography (HPLC)-grade methanol. The samples were then vortex-mixed (for 10 s) and sonicated for 30 s (in a Sonicator® 3000; Misonix) at 15 W in an ice cooler (−20°C). This protocol was repeated twice more with a 5-min storage at −20°C between each cycle, and the final pellet was removed following centrifugation at 12,000 *g* for 10 min at 4°C. Methanol solution was stored at −80°C in 20-mL penicillin vials until they were analyzed by mass spectrometry and different and complementary separation techniques, namely liquid chromatography electrospray ionization quadrupole time-of-flight mass spectrometry (LC-ESI-QTOF-MS) in positive and negative mode, and gas chromatography-mass spectrometry (GC-MS), as described previously (Bargiela et al., 2015). The abundance levels of mass signatures of tested pollutants and key degradation intermediates, namely, salicylate, gentisate, catechol, benzoate and protocatechuate, were used as indicator of the presence of the corresponding enzymes encoded by catabolic genes.

RESULTS AND DISCUSSION

Bacterial Community Structures in Microcosms

A graphical approach recently described (Bargiela et al., 2015) was applied to draft the catabolic networks of two different oil-degrading marine microcosms. They were obtained from Ancona harbor sediments which were applied in a series of two enrichment microcosms, where AMM or UA were supplied to introduce equivalent amounts of nitrogen. Using partial 16S rRNA gene sequences obtained in the non-assembled Illumina reads through a metagenomic approach, it was firstly found a relatively high degree of similarity in the emerging communities (Gertler et al., 2015). Proteobacteria were the most abundant (AMM: 74.5%; UA: 74.2%, total sequences), in agreement with the fact that this bacterial group is the most abundant in other chronically crude oil-contaminated marine sediments within the Mediterranean Sea (Bargiela et al., 2015). Noticeably, all proteobacterial families were found in both microcosms (for details see **Table 1**). However, differences in the abundance of some community members could be observed on the basis of corresponding read frequency. As an example, the percentage of members of the *Rhodobacteraceae* and *Enterobacteriaceae* was elevated in microcosms supplied with AMM (18.2% AMM vs. 0.8% in UA and 5.6% in AMM vs. 3.2% in UA, correspondingly). Conversely, lower percentages of members of the *Alteromonadaceae* (9.6%/19.2%), *Halomonadaceae* (5.6%/7.8%), *Moraxellaceae* (0.5%/7.9%) and *Flavobacteriaceae* (1.8%/5.7%) could be detected in the AMM-supplemented microcosm in comparison to UA-based microcosms. At a genus level, 55 out of 57 identified proteobacterial taxa were common in both communities. However, enrichments containing AMM were characterized by higher percentages (referred to total reads) of Alphaproteobacteria, such as *Roseovarius* sp. (1.4% in AMM vs. 0.1% in UA), *Ruegeria* spp. (1.1%/0.1%) and *Sulfitobacter* sp. (1.5%/0.1%), and some Gammaproteobacteria such as *Vibrio* sp. (2.4%/1.1%). In stark contrast to this, the UA-based enrichments showed significantly elevated percentages of members of the Firmicutes (7.4% in UA enrichments/4.9% in AMM enrichments) and Gammaproteobacteria, such as *Aeromonas* spp. (1.5%/0.5%) and *Pseudoalteromonas* sp. (1.9%/0.4%). Highly elevated percentages in UA enrichments were observed for the genera *Acinetobacter* (0.9% in UA enrichments/0.1% in AMM enrichments), *Halomonas* (6.1%/4.2%), *Marinobacter* (16.8%/6.3%) and *Psychrobacter* (6.8%/0.2%). A direct comparison of percentages of potentially oil degrading microbial genera in both microcosms showed a higher percentage of *Acinetobacter* sp. (0.9%/0.1%), *Idiomarina* sp. (0.8%/0.3%), *Oleiphilus* sp. (0.2%/0.03%) and *Marinobacter* sp. (16.8%/6.3%) but lower percentages of *Alcanivorax* sp. (3.9%/4.9%) and *Thalassolituus* sp. (0.04/0.8%) in the UA treatments (Gertler et al., 2015).

TABLE 1 | Relative abundance of microbial families within the AMM and UA microcosms.

Family or phylum[1]	Relative abundance (%) based on 16S small subunit rRNA data[1]	
	MGS-ANC(AMM)	MGS-ANC(UA)
Pseudomonadaceae	15,24	12,98
Alcanivoraceae	4,99	3,94
Halomonadaceae	5,20	7,80
Enterobacteriaceae	5,62	3,15
Vibrionaceae	4,01	2,26
Aeromonadaceae	0,90	3,11
Alteromonadaceae	9,57	19,18
Chromatiaceae	1,06	0,85
Idiomarinaceae	0,36	0,81
Legionellaceae	0,23	0,91
Methylococcaceae	0,54	1,05
Moraxellaceae	0,45	7,89
Oceanospirillaceae	4,26	4,15
Pseudoalteromonadaceae	0,40	2,18
Shewanellaceae	2,78	2,59
Rhodobacteraceae	18,20	0,81
Comamonadaceae	1,64	0,54
Flavobacteriaceae	1,75	5,69
Actinobacteria	1,81	2,56
Firmicutes	4,86	7,42
Others	16,12	10,29

Results are based on the analysis of the partial 16S ribosomal RNA (rRNA) gene sequences extracted from non-assembled DNA sequences obtained by paired-end Illumina HiSeq 2000 sequencing.

[1]*Only lineages with abundance of reads >1% are shown. Data from Gertler et al. (2015).*

Biodegradation Networks

As we were interested in obtaining networks that emphasized the catabolic differences within both microcosms, we selected a metagenomic approach to query the presumptive degradation capacities associated to both microcosms. The identification

depends heavily on gene abundance and, despite the fact that a substantial faction of less abundant DNA in metagenomes remains undiscovered, the identified catabolic genes are assumed to represent the dominant presumptive pathways in each system. A rarefaction curve of the observed species for both samples to analyze species sampling coverage indicated closeness to saturation in each of the two microcosms (Gertler et al., 2015). In combination with the fact that both samples were sequenced to a similar extent (24,752,834 bp for AMM and 19,364,101 bp for UA; Gertler et al., 2015), this suggests that biases during the comparative analysis within the metagenomes were not introduced due to differences in microbial and sequence coverage.

Using as a query the 27,893 (for UA) and 32,180 (for AMM) potential protein-coding genes (for ≥20 amino acids-long polypeptides) (Gertler et al., 2015), we identified respectively a total of 45 (or 0.16% relative abundance in UA referred to the total number of protein-coding genes) and 65 (or 0.20% relative abundance in AMM) genes encoding catabolic enzymes with matches in AromaDeg (Duarte et al., 2014). This suggests that the biostimulants did not have much influence on the relative abundance of catabolic genes. However, significant differences can be observed when examining the diversity of genes encoding catabolic enzymes assigned to different families (**Figure 1**). The amount of genes encoding Rieske non-heme iron oxygenases and extradiol dioxygenases (EXDO) of the cupin superfamily increased 2- and 4-fold, respectively, and proved more abundant in the AMM microcosm in comparison to those in the UA microcosm (**Figure 1**).

The differences in family shifts may have an influence on degradation capacities provided by microorganisms in AMM and UA microcosms. To assess this, the presumptive aromatic degradation reactions and the substrate pollutants or intermediates possibly degraded by each of the two communities were predicted, and the corresponding degradation networks constructed (**Figure 2**). For that we used the AromaDeg web system that allows identifying catabolic genes and appropriated scripts and commands for graphics (for details see Biodegradation Network Reconstruction: Scripts and Commands for Graphics). Unambiguous reaction specificities could be detected for 35 (in UA) and 48 (in AMM) catabolic genes and were considered in the degradation network (**Figure 2**). However, no clear specificities could be assigned to 4 (in UA) and 11 (in AMM) Rieske oxygenases and 12 (six in UA and six in AMM) EXDO, which subsequently were not considered in the network. As shown in **Figure 2**, on the basis of the presence of genes encoding catabolic genes involved in particular transformations, the potential degradation of nine intermediates involved in the degradation of six key pollutants (2-chlorobenzoate, indole-3-acetate, biphenyl, gentisate, quinoline

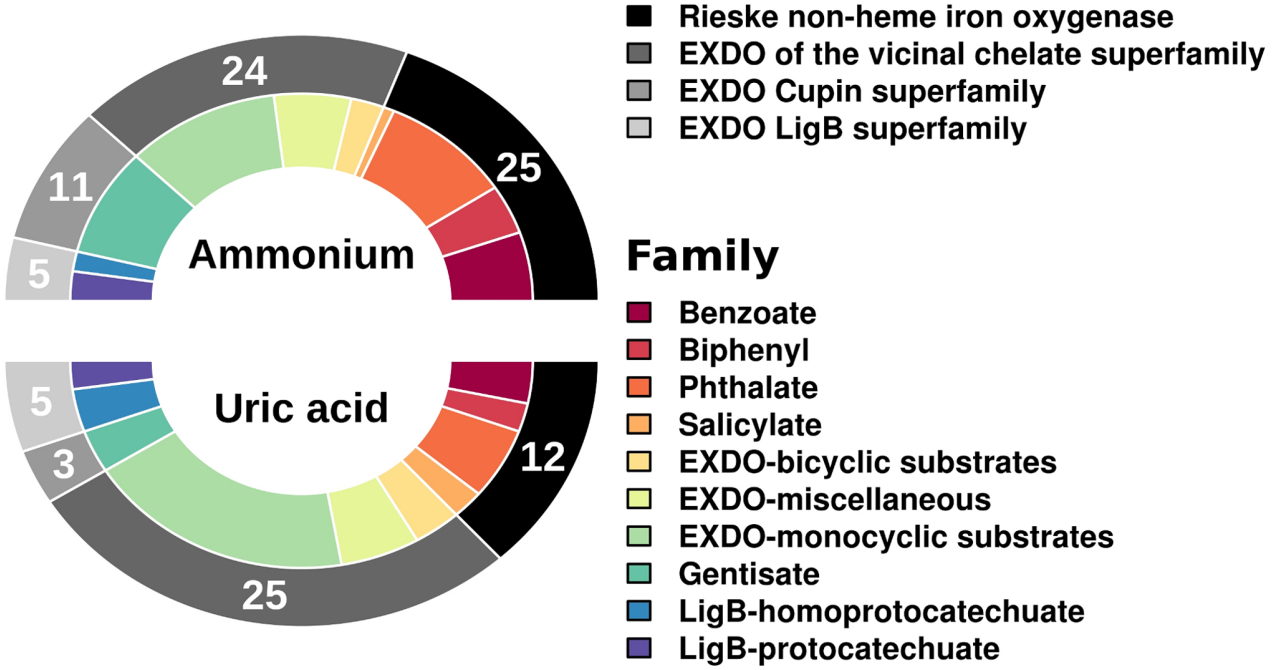

FIGURE 1 | Number and diversity of sequences of gene families encoding key catabolic enzymes involved in the degradation of aromatic pollutants. Catabolic genes were identified as follows. Briefly, predicted open reading frames (ORFs) in the metagenomic DNA sequences were filtered by sequence homology (>50%) and minimum alignment length (> 50 amino acids) according to their similarity to the AromaDeg sequences of key aromatic catabolic gene families (and sub-families) involved in the degradation of aromatic pollutants (Duarte et al., 2014). After a manual check, a final list of gene sequences encoding enzymes potentially involved in degradation was prepared.

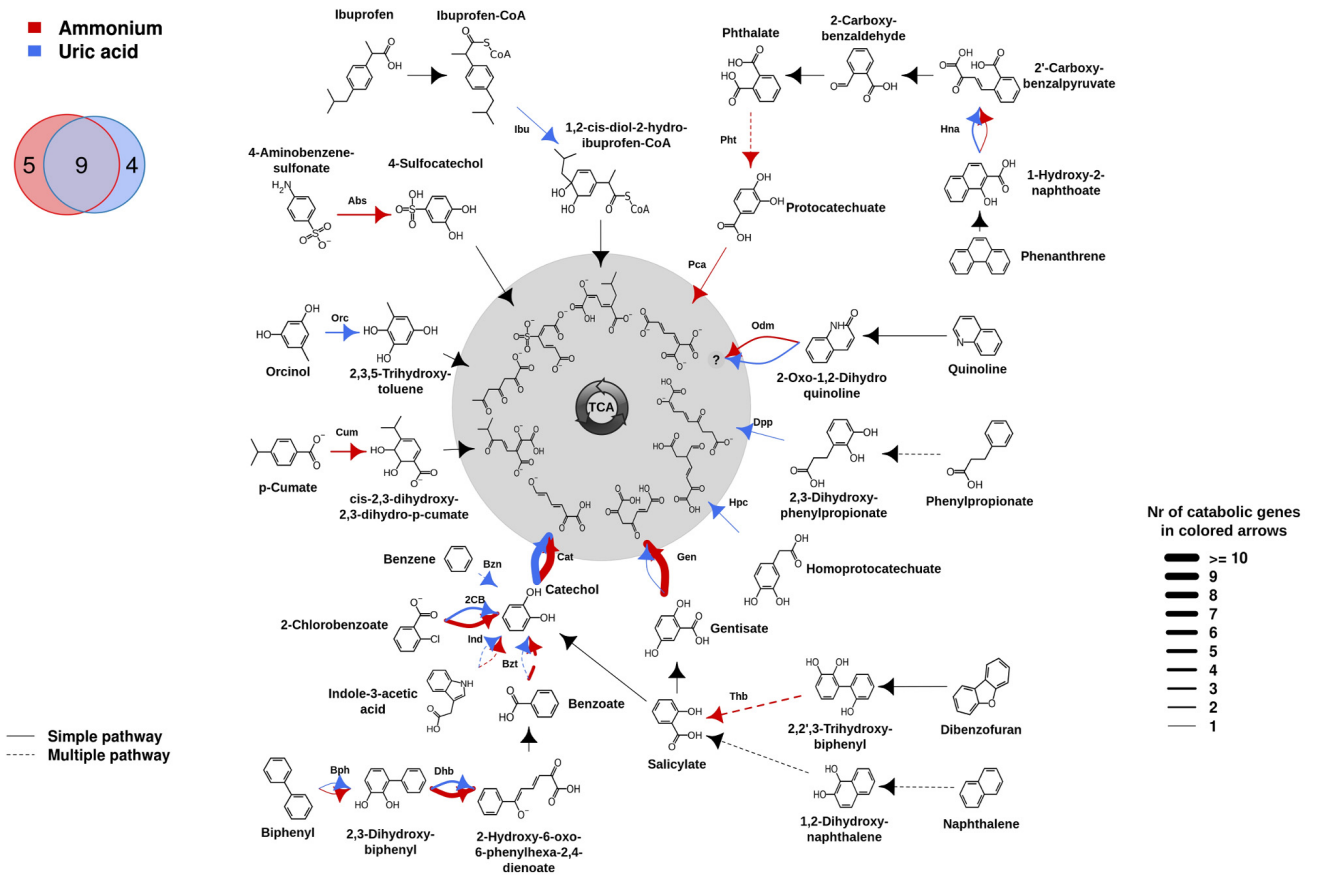

FIGURE 2 | Potential aromatic catabolic networks in the AMM and UA microcosms (see color code). The biodegradation network reconstruction was performed as described in "Materials and Methods." Briefly, catabolic genes were identified as described in the **Figure 1** legend. For network reconstruction, each sequence subsequently was assigned to a metabolic substrate as well as a product (as defined by Duarte et al., 2014) with an assigned code. The putative substrates and products processed in the sample were connected, creating a metabolic network using appropriate scripts and commands (for details, see Bargiela et al., 2015). The number of each catabolic gene assigned to degradation reactions, is represented by the thickness of the lines in the figure and the complete list of substrates possibly degraded by the communities are summarized. Common and microcosm-specific initial pollutants or intermediates for which presumptive degradation signatures were identified are specifically indicated in the Venn diagram. Solid lines represent single step reactions while dotted lines represent degradation steps where multiple reactions are involved (for details see Bargiela et al., 2015). Codes for proteins encoded by genes as follows: Abs, 4-aminobenzenesulfonate 3,4-dioxygenase; Bph, biphenyl dioxygenase; Bzn, benzene dioxygenase; Bzt, benzoate dioxygenase; Cat, catechol 2,3-dioxygenase; 2CB, 2-chlorobenzoate dioxygenase; Cum, *p*-cumate dioxygenase; Dhb, 2,3-Dihydroxybiphenyl dioxygenase; Dpp, 2,3-dihydroxyphenylpropionate dioxygenase; Gen, gentisate dioxygenase; Hna, 1-hydroxy-2-naphthoate dioxygenase; Hpc, homoprotocatechuate 2,3-dioxygenase; Ibu, ibuprofen-CoA dioxygenase; Ind, Rieske oxygenase involved in indole acetic acid degradation; Odm, 2-oxo-1,2-dihydroxyquinoline monooxygenase; Orc, orcinol hydroxylase; Pca, protocatechuate 3,4-dioxygenase; Pht, phthalate 4,5-dioxygenase; Thb, 2,2′,3-trihydroxybiphenyl dioxygenase.

and phenanthrene) was found to be common for both microcosms. They include the transformation of biphenyl by Bph, 2,3-dihydroxybiphenyl by Dhb, benzoate by Bzt, indole-3-acetate by Ind, catechol by Cat, gentisate by Gen, 2-oxo-1,2-dihydroquinoline by Odm, 1-hydroxy-2-naphthoate by Hna, and 2-chlorobenzoate by 2-chlorobenzoate dioxygenase (2CB). Within them, genes encoding Cat were most abundant in both communities (UA: 17; AMM: 14), in agreement with the fact that catechol is the central intermediate for most cyclic aerobic hydrocarbons degradation (Pérez-Pantoja et al., 2009; Vilchez-Vargas et al., 2013). Gentisate and benzoate/2-chlorobenzoate may be most likely preferentially degraded by microorganisms in the AMM microcosm (10 Gen and 4 Bzt/2CB) in comparison to the UA microcosm (1 Gen and 1 Bzt/2CB). Genomic signatures for the degradation of orcinol (or 3,5-dihydroxytoluene) by Orc, phenylpropionate by Dpp, homoprotocatechuate by Hpc, and benzene by Bzn, were only found in the UA microcosm. The potential degradation of ibuprofen by Ibu, although not being a constituent of the crude oil but possibly originated from bilge water from the cruise lines or urban run-off, was also identified in UA microcosm. In stark contrast, the degradation of 4-aminobenzene-sulfonate by Abs, *p*-cumate by Cum, dibenzofuran by Thb, phthalate by Pht and protocatechuate by Pca, was characteristic for the AMM microcosm.

Note that within all pollutants predicted as being potentially degraded by bacteria inhibiting Ancona port (**Figure 2**), independently whether they are enriched with AMM or UA, only the potential degradation of

ibuprofen and 4-aminobenzene-sulfonate was not found associated to bacteria from other chronically crude oil-contaminated sites in oil-polluted sites along the coastlines of the Mediterranean Sea (Bargiela et al., 2015). This suggests that the pollution type and pollutant diversity in Ancona port, which receives chemicals such as alkyl benzene sulfonate detergents and drugs coming from human activities (Martínez-Pascual et al., 2010; Paíga et al., 2013), may have supported the presence of ibuprofen- and sulfonate benzene-growing bacteria. Such bacteria may be further stimulated by either the addition of UA or AMM, respectively.

Experimental Analysis of Catabolic Capacities in AMM and UA Microcosms

Experimental validation assays were conducted to prove the extent of agreement with metagenomic-based predictions. For that, AMM and UA enrichment cultures were set up in triplicates as described in Section "Experimental Validations of Predicted Biodegradation Capacities," in which instead of Arabian light crude oil as the carbon source (used for the initial microcosms), naphthalene, 2,3-dihydroxybiphenyl, benzene, *p*-cumate, orcinol, 2-chlorobenzoate, phthalate and phenylpropionate (2 ppm each) were used. The capacity to degrade other pollutants predicted as potential substrates such as ibuprofen, phenanthrene, dibenzofuran, indole-3-acetic acid, 4-aminobenzene-sulfonate and quinoline, could not be experimentally proved because no analytical procedures could be designed for their analysis in the pollutant mix.

Samples were taken at 21 days of incubation at 20°C. Fingerprinting by LC-ESI-QTOF-MS and GC-MS was used to confirm the degradation of the initial substrates as well as the existence of degradation intermediates in both cultures. A careful inspection of the mass signatures confirmed the lowering in the abundance level of naphthalene, 2,3-dihydroxybiphenyl, and 2-chlorobenzoate, and the presence of catechol, salicylate, gentisate, and benzoate in both microcosms (**Figure 3**). This demonstrates that the naphthalene-to-salicylate-to-gentisate, 2,3-dihydroxybiphenyl-to-benzoate-to-catechol, and 2-chlorobenzoate-to-catechol degradation pathways occurred or were active in both microcosms. Note that the lower abundance level of gentisate in AMM microcosm may correlate with the 10-fold overabundance of genes encoding Gen enzymes in AMM as compared to UA; this may decrease the pool of gentisate in the microcosm when growing in naphthalene. We further found a decreased level of *p*-cumate only associated to the AMM enrichment. Phthalate degradation mostly associated to the AMM microcosm, as confirmed by the higher extend of phthalate degradation by meaning of its residual percentage at the end of the assay (21 ± 1.8% in AMM vs. 92.2 ± 2.3% in UA) and the 22.2-fold higher abundance of protocatechuate in AMM compared to UA assays. In addition, decreased level of orcinol, benzene and phenylpropionate associated only to UA enrichments (**Figure 3**). Accordingly, the benzene-to-catechol, orcinol-, and phenylpropionate-degradation pathways occurred or were active in the UA microcosm, while *p*-cumate degradation mostly occurred in the AMM enrichments.

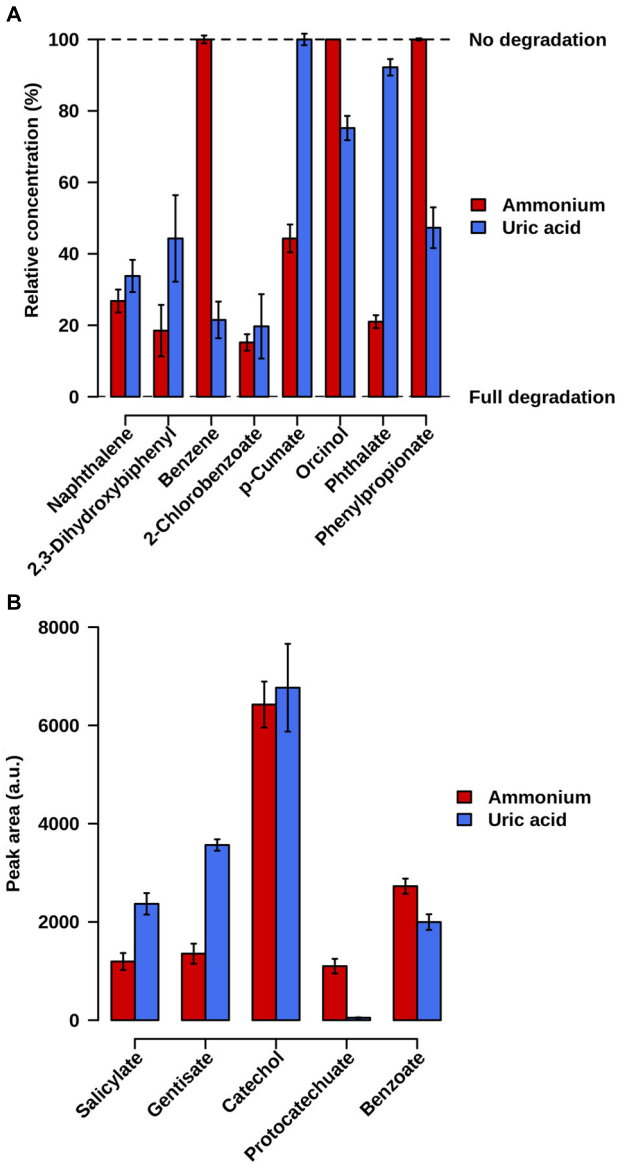

FIGURE 3 | Relative abundance level of initial substrate pollutants (A) and key chemical intermediates (B), in AMM and UA microcosms containing naphthalene, 2,3-dihydroxybiphenyl, benzene, *p*-cumate, orcinol, 2-chlorobenzoate, phthalate and phenylpropionate (2 ppm each) as carbon source. (A) The remaining relative concentration of the initial pollutants used to set up enrichment cultures is shown; 100%, no degradation of initial substrate pollutant; 0%, total degradation (absence of pollutant). **(B)** Values represent the peak area of degradation intermediates in arbitrary units (a.u.). The values were calculated, in triplicate microcosms, by comparing the presence and abundance level after 21-days of the microcosm at 20°C experiment compared to the initial point and after considering the controls assays. Standard deviations (SD) are shown.

The identification of degrading capacities on microcosms depends heavily on enrichment conditions (including cultivation time frame) and bacteria and protein abundance. While these

drawbacks are known, the experimental data presented above (**Figure 3**) fully confirmed our sequence-based predictions (**Figure 2**) for the degradation of all eight pollutants tested in each of the two amendments. This suggests that the differences herein predicted in UA and AMM microcosms (**Figure 2**) are due to real biological differences and not random. Uncertainty remains only for phthalate degradation in UA microcosm: experimental analysis demonstrated the slight degradation of this chemical (**Figure 3**), which was not predicted by sequence analysis (**Figure 2**).

Phylogenetic Identities of Catabolic Genes

We further attempted to analyze the contributions of particular sets of microbes to the entire reconstructed catabolic network, where multiple proteins from multiple organisms may contribute to organic pollutants' decomposition.

As the community structure of the two enrichment cultures was well-characterized (Gertler et al., 2015), the taxonomic affiliations of the catabolic genes identified could be unambiguously established at the family and phylum level. For that, we used tools recently published that provide a high level of confidence (Guazzaroni et al., 2013; Bargiela et al., 2015). **Figure 4** shows the contribution of members assigned to the different bacterial families and phyla in both microcosms to pollutant degradation. They included populations closely related to members of *Aeromonadaceae, Alcanivoracaceae, Alteromonadaceae, Halomonadaceae, Oceanospirillaceae, Piscirickettsiaceae, Pseudomonadaceae, Rhodobacteraceae, Vibrionaceae,* and *Xhantomonadaceae*, as well as to a lesser extent for the phyla Actinobacteria and Firmicutes. These comprise bacterial groups well known for their oil biodegrading capabilities (Yakimov et al., 2007; Jin et al., 2012; Guazzaroni et al., 2013). A further careful examination of the data presented

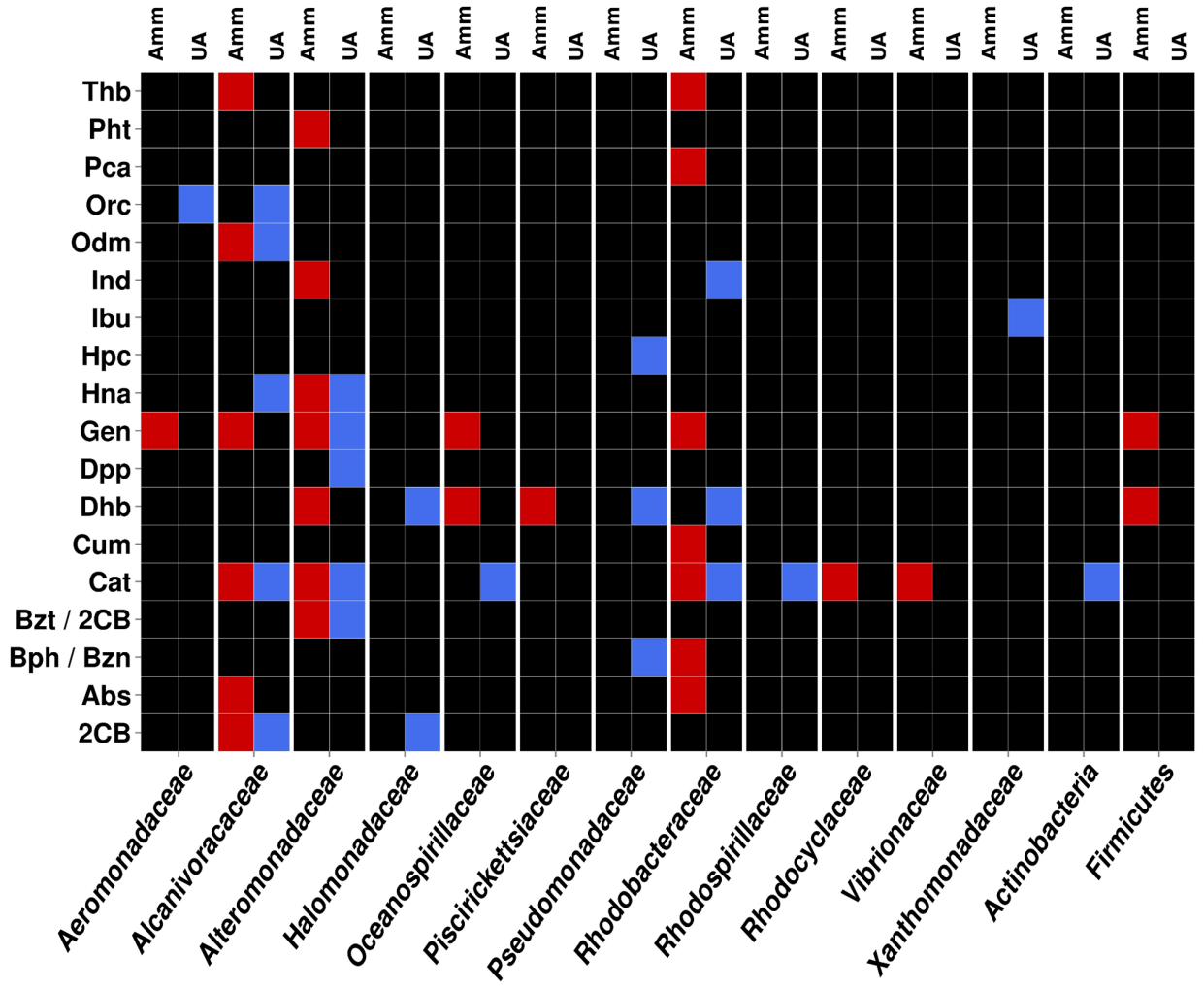

FIGURE 4 | Heat map showing the contribution of the most relevant bacterial members of AMM and UA microcosm to the degradation network in Figure 2. Contributions of each of the distinct members with unambiguous taxonomic assignation per each of the catabolic gene classes found to constitute the AMM and UA communities are differentiated by a color code. The color indicates the presence of a catabolic gene independently of the abundance level. Gene names/codes are identical to those presented in **Figure 2**.

in **Figure 4** clearly leads to the occurrence of a different pathway organization at organism level for the catabolism of 18 different pollutants predicted to be degraded.

As can be seen in **Figure 4**, members of *Alcanivoracaceae, Alteromonadaceae,* and *Rhodobacteraceae* were the major contributors to the networks. They contribute, in combination, to the degradation of 16 out of 18 pollutants predicted in the catabolic network, including dibenzofuran, phenanthrene, indolacetic acid, biphenyl, *p*-cumate, 2-chlorobenzoate, phenylpropionate, aminobenzenesulfonate and gentisate. This is in agreement with the fact that they were among the most abundant members in the established microcosms based on 16S rRNA (**Table 1** and **Figure 5**). Interestingly, *Pseudomonadaceae* which was the second most abundant microbial clade at the level of 16S rRNA in both microcosms (**Table 1** and **Figure 5**), did not contribute to the degradation network in AMM but it does in the UA microcosm (**Figure 4**), where it supports the biphenyl-to-benzoate and homoprotocatechuate degradation.

As shown in **Figure 4**, among the common degradation capacities, a number of observations can be made. First, the degradation of indole acetate by Ind was supported by members of *Alteromonadaceae* in AMM and *Rhodobacteraceae* in UA, which suggests a catabolic replacement. This was also observed for the degradation of biphenyl and benzene (by Bph/Bzn), most likely supported by members of the *Pseudomonadaceae* in UA but *Rhodobacteraceae* in AMM. We identified members of five proteobacterial families (*Aeromonadaceae, Alcanivoracaceae, Alteromonadaceae, Oceanospirillaceae*, and *Rhodobacteraceae*) and of the Firmicutes phylum as key groups for the degradation of gentisate (by Gen) in AMM. By contrast, only members of *Alteromonadaceae* were predicted to support gentisate catabolism in UA. In agreement with this it has been found that AMM promotes the growth of such multiple marine bacteria with the ability to utilize naphthalene (the precursor of gentisate) as a sole carbon in enrichment cultures (Hedlund et al., 1999). Also, the increased abundance of bacteria of the Firmicutes phylum has been demonstrated during bio-stimulation with ammonia (Guazzaroni et al., 2013). The naphthalene-to-gentisate catabolism by bacteria of the family *Alteromonadaceae* has also been found during microcosm assays using seawater and sediment samples obtained after an oil spill along the Korean shoreline without AMM addition (Jin et al., 2012); this agrees with the enrichment of gentisate catabolism by bacteria of this family in UA microcosm.

Multiple bacteria also contributed to the degradation of catechol (by Cat), with members of *Alcanivoracaceae, Alteromonadaceae,* and *Rhodobacteraceae* being common in both treatments. These bacterial groups are known for their capacity to degrade aromatics and haloaromatics to catechol, which can be further catabolised (Brusa et al., 2001; Antunes et al., 2011). Members of the Actinobacteria phyum and *Oceanospirillaceae* family contributed to catechol catabolism exclusively in the UA microcosm, whereas those of *Vibrionaceae* family did so in the AMM treatment. Note that, in accordance with the fact that *cat* genes are the most abundantly present (**Figure 2**) in both microcosms, the number of bacterial groups

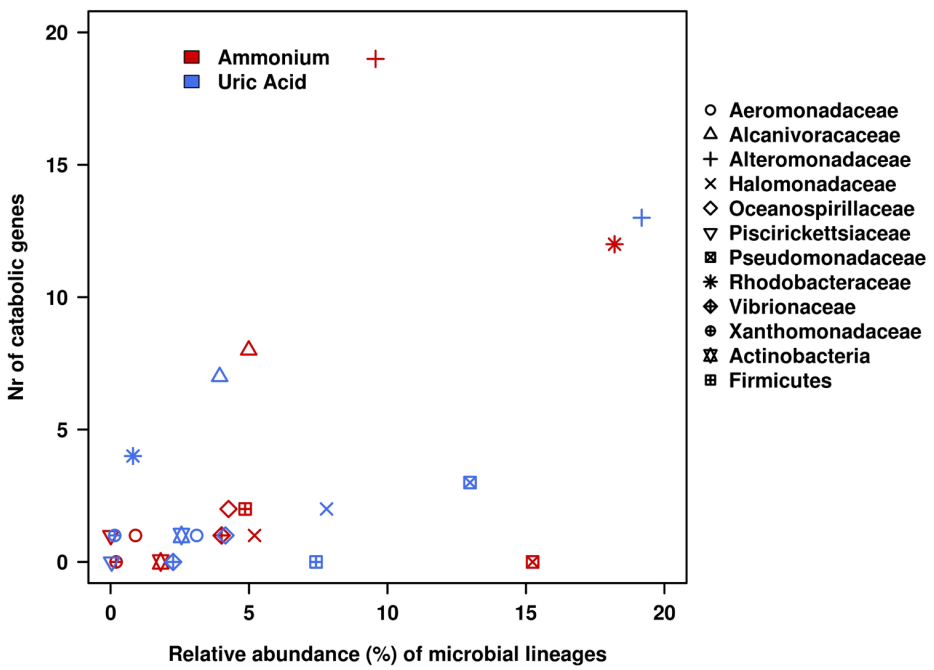

FIGURE 5 | Relative contributions of bacterial lineages in terms of catabolic genes and 16S rRNA gene within the AMM and UA microcosms. Catabolic genes were identified by using the web-based AromaDeg resource (Duarte et al., 2014) and their taxonomic assignation at the level of the family or higher was performed as reported (Guazzaroni et al., 2013; Bargiela et al., 2015). The relative abundance of microbial lineages was based on the analysis of 16S small subunit rRNA partial sequences obtained in the non-assembled Illumina reads (Gertler et al., 2015).

involved in its catabolism was also the highest (8 in total; **Figure 4**). Therefore, a number of bacterial groups within the microcosms exhibit also partial catabolism redundancy.

Interestingly, we noticed that bacteria from the *Halomonadaceae* family contributed also to degradation of aromatics, particularly, 2-chlorobenzoate (through 2CB) and biphenyl (through Dhb) in the UA microcosm (**Figure 4**). This suggests that halomonads not only participate in the conversion of UA to AMM, which further stimulated growth of hydrocarbonoclastic bacteria (Gertler et al., 2015), but also play specific roles in degradation as herein suggested. This agrees with the fact that bacteria from the genus *Halomonas* are capable of degrading chlorobenzoates (de la Haba et al., 2011) and aromatics compounds such as benzoate and catechol (Piubeli et al., 2012), that are intermediate products of biphenyl and 2-chlorobenzoate degradation.

CONCLUSION

Here, we report that different biostimulants applied in chronically polluted sediments have caused significant alteration in degradation capacities, while having no major effect on the taxonomic composition of microbial communities at the level of the family or higher. Experimental validation was conducted for at least eight of the predicted catabolic capacities, and good agreement with metagenomics-based predictions was observed. On the other hand, the metagenomics-guided metabolic reconstruction allowed us to refine the assignment of roles of community members in the utilization of multiple substrates and found different pathway organization at organism level. For example, while biphenyl degradation by Bph, DhB, and Bzt enzymes seems to be carried out by bacteria of *Pseudomonadaceae*, *Halomonadaceae,* and *Rhodobacteraceae* in UA, those of *Alteromonadaceae, Oceanospirillaceae, Picirickettsiaecae,* and Firmicutes may be involved in an alternative pathway in AMM. This demonstrates that different microbial members within microcosms obtained with different nitrogen sources may exhibit partial functional redundancy, and thus, may have a high level of common catabolic capacities. The present investigation provides an estimation of such common and distinct degrading capacities. Indeed, herein we found that 50% of the predicted degradation capacities were common for microorganisms in AMM and UA microcosms (**Figure 2**). However, according to the microbial biodegradation networks herein reconstructed, we also found that the two different biostimulants investigated, UA and AMM, have also changed substrate utilization capacities and preferences, which must be considered for the design of petroleum bioremediation techniques. This was demonstrated by showing that UA enriched for bacteria with the capability of degrading pollutants otherwise not degraded, or possibly degraded at low level, by those stimulated by the addition of AMM, and vice versa.

Therefore, the results of this study show that smart formulations based on the application of multiple nitrogen sources, rather than commonly used single sources (mostly AMM), for example, may increase the efficiency of the biological removal of the widest diversity of aromatic pollutants and could be essential to support effective biodegradation strategies in response to an oil spill incident or in response to chronical pollution. Thus, as herein demonstrated, the utilization of both AMM and UA in conjunction will have a double aim. In one side, AMM may most likely enhance the bio-stimulation of bacterial populations capable of degrading heavy oil components such as naphthalene, phenathrene and dibenzofuran, as well as sulfonated-benzenes and substituted benzoate derivatives such as p-cumate (**Figure 2**). In other side, UA will promote the growth of bacteria most active against benzene, orcinol-, ibuprofen- and phenyl-propionate (**Figure 2**). This will provoke a significant increase in multiple aromatics consumption in polluted areas. Having said that, this work seems to introduce a promising way for future oil-based contamination handling techniques. In this context, it would be very interesting to test the overall cleaning capacity (if any) on a real oil-contaminated marine sample. For that, also another point will be to use the combination of the UA and AMM, which was herein not presented in microcosm assays. It would be interesting to see their combinatory effect in the overall degradation capacity and taxonomic distribution of the microbial niche depending also on their ratio, so to find optimal nitrogen-containing formulations in real scenarios.

We would like to stress the attention to the fact that similarities regarding microbial community composition in the AMM microcosm from Ancona port with those reported in enrichments from surface water bodies at other Mediterranean sites, were found (Gertler et al., 2012). However, a similar comparison with the results from UA microcosm cannot be established because the limited information available. In fact, to the best of our knowledge, there have been only three studies that thoroughly investigated the use of UA in bioremediation trials (Koren et al., 2003; Knezevich et al., 2006; Nikolopoulou et al., 2013). Those studies, however, did not use UA in comparison to other nitrogen sources such as AMM, both in respect to their effect in microcosm population structures and catabolic preferences. Accordingly, herein we reported first evidences linking UA to catabolic preferences at the bacterial level, in comparison to the commonly use nitrogen source AMM.

ACKNOWLEDGMENTS

This research was supported by the European Community Projects MAGICPAH (FP7-KBBE-2009-245226), ULIXES (FP7-KBBE-2010-266473) and KILL-SPILL (FP7-KBBE-2012-312139). We thank EU Horizon 2020 Program for the support of the Project INMARE H2020-BG-2014-2634486. This work was further funded by grants BIO2011-25012, PCIN-2014-107 and BIO2014-54494-R from the Spanish Ministry of Economy and Competitiveness. The authors gratefully acknowledge the financial support provided by the European Regional Development Fund (ERDF). The present investigation was also funded by the Spanish Ministry of Economy and Competitiveness within the ERA NET IB2, grant number ERA-IB-14-030. FM was supported by Università degli Studi di Milano, European Social Fund (FSE) and Regione Lombardia (contract "Dote Ricerca").

REFERENCES

Alvarez, V. M., Marques, J. M., Korenblum, E., and Seldin, L. (2011). Comparative bioremediation of crude oil-amended tropical soil microcosms by natural attenuation, bioaugmentation, or bioenrichment. *Appl. Environ. Soil Sci.* 2011, 156320. doi: 10.1155/2011/156320

Antunes, A., Ngugi, D. K., and Stingl, U. (2011). Microbiology of the Red Sea (and other) deep-sea anoxic brine lakes. *Environ. Microbiol. Rep.* 3, 416–433. doi: 10.1111/j.1758-2229.2011.00264.x

Atlas, R. M. (1981). Microbial degradation of petroleum hydrocarbons: an environmental perspective. *Microbiol. Rev.* 45, 180–209.

Bargiela, R., Mapelli, F., Rojo, D., Chouaia, B., Tornés, J., Borin, S., et al. (2015). Bacterial population and biodegradation potential in chronically crude oil-contaminated marine sediments are strongly linked to temperature. *Sci. Rep.* 5, 11651. doi: 10.1038/srep11651

Brusa, T., Borin, S., Ferrari, F., Sorlini, C., Corselli, C., and Daffonchio, D. (2001). Aromatic hydrocarbon degradation patterns and catechol 2,3-dioxygenase genes in microbial cultures from deep anoxic hypersaline lakes in the eastern Mediterranean sea. *Microbiol. Res.* 156, 49–58. doi: 10.1078/0944-5013-00075

Das, N., and Chandran, P. (2010). Microbial degradation of petroleum hydrocarbon contaminants: an overview. *Biotechnol. Res. Int.* 2011, 941810. doi: 10.4061/2011/941810

de la Haba, R. R., Sánchez-Porro, C., and Ventosa, A. (2011). "Taxonomy, phylogeny, and biotechnological interest of the family Halomonadaceae," in *Halophiles and Hypersaline Environments: Current Research and Future Trends*, eds A. Ventosa, A. Oren, and Y. Ma (Heidelberg: Springer), 27–64.

Duarte, M., Jauregui, R., Vilchez-Vargas, R., Junca, H., and Pieper, D. H. (2014). AromaDeg, a novel database for phylogenomics of aerobic bacterial degradation of aromatics. *Database (Oxford)* 2014:bau118. doi: 10.1093/database/bau118

Dyksterhouse, S. E., Gray, J. P., Herwig, R. P., Lara, J. C., and Staley, J. T. (1995). *Cycloclasticus pugetii* gen. nov., sp. nov., an aromatic hydrocarbon-degrading bacterium from marine sediments. *Int. J. Syst. Bacteriol.* 45, 116–123. doi: 10.1099/00207713-45-1-116

Garcia-Blanco, S., Venosa, A. D., Suidan, M. T., Lee, K., Cobanli, S., and Haines, J. R. (2007). Biostimulation for the treatment of an oil-contaminated coastal salt marsh. *Biodegradation* 18, 1–15. doi: 10.1007/s10532-005-9029-3

Gertler, C., Bargiela, R., Mapelli, F., Han, X., Chen, J., Hai, T., et al. (2015). Conversion of uric acid into ammonium in oil-degrading marine microbial communities: a possible role of Halomonads. *Microb. Ecol.* 70, 724–740. doi: 10.1007/s00248-015-0606-7

Gertler, C., Näther, D. J., Cappello, S., Gerdts, G., Quilliam, R. S., Yakimov, M. M., et al. (2012). Composition and dynamics of biostimulated indigenous oil-degrading microbial consortia from the Irish, North and Mediterranean Seas: a mesocosm study. *FEMS Microbiol. Ecol.* 81, 520–536. doi: 10.1111/j.1574-6941.2012.01377.x

Guazzaroni, M. E., Herbst, F. A., Lores, I., Tamames, J., Peláez, A. I., López-Cortés, N., et al. (2013). Metaproteogenomic insights beyond bacterial response to naphthalene exposure and bio-stimulation. *ISME J.* 7, 122–136. doi: 10.1038/ismej.2012.82

Hedlund, B. P., Geiselbrecht, A. D., Bair, T. J., and Staley, J. T. (1999). Polycyclic aromatic hydrocarbon degradation by a new marine bacterium, *Neptunomonas naphthovorans* gen. nov., sp. nov. *Appl. Environ. Microbiol.* 65, 251–259.

Howarth, R. W., and Marino, R. (2006). Nitrogen as the limiting nutrient for eutrophication in coastal marine ecosystems: evolving views over three decades. *Limnol. Oceanogr.* 51, 364–376. doi: 10.4319/lo.2006.51.1_part_2.0364

Jin, H. M., Kim, J. M., Lee, H. J., Madsen, E. L., and Jeon, C. O. (2012). Alteromonas as a key agent of polycyclic aromatic hydrocarbon biodegradation in crude oil-contaminated coastal sediment. *Environ. Sci. Technol.* 46, 7731–7740. doi: 10.1021/es3018545

Knezevich, V., Koren, O., Ron, E. Z., and Rosenberg, E. (2006). Petroleum bioremediation in seawater using guano as the fertilizer. *Bioremediat. J.* 10, 83–91. doi: 10.1080/10889860600939492

Koren, O., Knezevic, V., Ron, E. Z., and Rosenberg, E. (2003). Petroleum pollution bioremediation using water-insoluble uric acid as the nitrogen source. *Appl. Environ. Microbiol.* 69, 6337–6339. doi: 10.1128/AEM.69.10.6337-6339.2003

Li, H., Zhao, Q., Boufadel, M. C., and Venosa, A. D. (2007). A universal nutrient application strategy for the bioremediation of oil-polluted beaches. *Mar. Pollut. Bull.* 54, 1146–1161. doi: 10.1016/j.marpolbul.2007.04.015

Ly, J., Philippart, C. J. M., and Kromkamp, J. C. (2014). Phosphorus limitation during a phytoplankton spring bloom in the western Dutch Wadden Sea. *J. Sea Res.* 88, 109–120.

Martínez-Pascual, E., Jiménez, N., Vidal-Gavilan, G., Viñas, M., and Solanas, A. M. (2010). Chemical and microbial community analysis during aerobic biostimulation assays of non-sulfonated alkyl-benzene-contaminated groundwater. *Appl. Microbiol. Biotechnol.* 88, 985–995. doi: 10.1007/s00253-010-2816-8

Miyasaka, T., Asami, H., and Watanabe, K. (2006). Impacts of bioremediation schemes on bacterial population in naphthalene-contaminated marine sediments. *Biodegradation* 17, 227–235. doi: 10.1007/s10532-005-5018-9

Mohseni-Bandpi, A., Esrafili, A., Nasseri, S., Ashmagh, F. R., Jorfi, S., and Ja'fari, M. (2014). Effectiveness of biostimulation through nutrient content on the bioremediation of phenanthrene contaminated soil. *J. Environ. Health Sci. Eng.* 12, 143. doi: 10.1186/s40201-014-0143-1

Nikolopoulou, M., and Kalogerakis, N. (2010). "Biostimulation strategies for enhanced bioremediation of marine oil spills including chronic pollution," in *Handbook of Hydrocarbon and Lipid Microbiology*, ed. K. N. Timmis (Berlin: Springer-Verlag), 2521–2529.

Nikolopoulou, M., Pasadakis, N., and Kalogerakis, N. (2013). Evaluation of autochthonous bioaugmentation and biostimulation during microcosm-simulated oil spills. *Mar. Pollut. Bull.* 72, 165–173. doi: 10.1016/j.marpolbul.2013.04.007

Paíga, P., Santos, L. H., Amorim, C. G., Araújo, A. N., Montenegro, M. C., Pena, A., et al. (2013). Pilot monitoring study of ibuprofen in surface waters of north of Portugal. *Environ. Sci. Pollut. Res. Int.* 20, 2410–2420. doi: 10.1007/s11356-012-1128-1

Pérez-Pantoja, D., Donoso, R., Junca, H., Gonzalez, B., and Pieper, D. H. (2009). "Phylogenomics of aerobic bacterial degradation of aromatics," in *Handbook of Hydrocarbon and Lipid Microbiology*, ed. K. N. Timmis (Berlin: Springer-Verlag), 1356–1397.

Piubeli, F., Grossman, M. J., Fantinatti-Garboggini, F., and Durrant, L. R. (2012). Identification and characterization of aromatic degrading halomonasin hypersaline produced water and cod reduction by bioremediation by the indigenous microbial population using nutrient addition. *Chem. Eng. Trans.* 27, 385–390.

Reis, E. A., Rocha-Leão, M. H., and Leite, S. G. (2013). Slow-release nutrient capsules for microorganism stimulation in oil remediation. *Appl. Biochem. Biotechnol.* 169, 1241–1249. doi: 10.1007/s12010-012-0022-0

Scott, N. M., Hess, M., Bouskill, N. J., Mason, O. U., Jansson, J. K., and Gilbert, J. A. (2014). The microbial nitrogen cycling potential is impacted by polyaromatic hydrocarbon pollution of marine sediments. *Front. Microbiol.* 5:108. doi: 10.3389/fmicb.2014.00108

Teramoto, M., Suzuki, M., Okazaki, F., Hatmanti, A., and Harayama, S. (2009). Oceanobacter-related bacteria are important for the degradation of petroleum aliphatic hydrocarbons in the tropical marine environment. *Microbiology* 155, 3362–3370. doi: 10.1099/mic.0.030411-0

Venosa, A. D., Campo, P., and Suidan, M. T. (2010). Biodegradability of lingering crude oil 19 years after the Exxon Valdez oil spill. *Environ. Sci. Technol.* 44, 7613–7621. doi: 10.1021/es101042h

Vilchez-Vargas, R., Geffers, R., Suárez-Diez, M., Conte, I., Waliczek, A., Kaser, V. S., et al. (2013). Analysis of the microbial gene landscape and transcriptome for aromatic pollutants and alkane degradation using a novel internally calibrated microarray system. *Environ. Microbiol.* 15, 1016–1039. doi: 10.1111/j.1462-2920.2012.02752.x

Walther, H. R. III. (2014). *Clean Up Techniques used for Coastal Oil Spills: An Analysis of Spills Occurring in Santa Barbara, California, Prince William sound, Alaska, the Sea of Japan and the Gulf Coast*. Ph.D. thesis, Environmental Management, University of San Francisco, San Francisco, CA.

Wang, Z., Hollebone, B. P., Fingas, M., Fieldhouse, B., Sigouin, L., Landriault, M., et al. (2003). *Characteristics of Spilled Oils, Fuels, and Petroleum Products: 1. Composition and Properties of Selected Oils*. Research Triangle Park, NC: United States Environmental Protection Agency, National Exposure Research Laboratory, EPA/600/R-03/072.

Yakimov, M. M., Timmis, K. N., and Golyshin, P. N. (2007). Obligate oil-degrading marine bacteria. *Curr. Opin. Biotechnol.* 18, 257–266. doi: 10.1016/j.copbio.2007.04.006

Conflict of Interest Statement: The authors declare that the research was conducted in the absence of any commercial or financial relationships that could be construed as a potential conflict of interest.

Capítulo 5: Importancia de los procesos degradativos en zonas crónicamente contaminadas por petróleo medida por metaproteómica y metabolómica

Resumen

En los Capítulos anteriores se ha demostrado como los factores geoquímicos y ambientales y la bioestimulación con diferentes fuentes de nitrógeno pueden modular y afectar la composición y las capacidades catabólicas de comunidades microbianas en ambientes marinos crónicamente contaminados. Además, se ha demostrado que los continuos vertidos de petróleo en la cuenca del Mar Mediterráneo han promovido el desarrollo de comunidades microbianas versátiles, capaces de degradar un amplio número de contaminantes, que son moduladas en función de factores clave como la temperatura y la adición de bioestimulantes. En este estudio se pretende esclarecer cual es la importancia de los procesos de biodegradación en el marco del metabolismo global de una comunidad microbiana. ¿Son los procesos catabólicos una parte importante en ambientes crónicamente contaminados? ¿O no? Estas son preguntas a las que se pretende contestar en este estudio. El análisis del ARN 16S y la secuenciación del metagenoma no son suficientes para conocer completamente las fracciones activas de una comunidad microbiana. Por el contrario, la metaproteómica y la metabolómica permiten conocer la identidad y/o la abundancia relativa de las proteínas expresadas y de los metabolitos producidos en el ambiente, reflejando los componentes metabólicos de la comunidad microbiana. Es por ello, que el presente trabajo busca combinar técnicas de metaproteómica y metabolómica para analizar la parte activa del metabolismo en tres zonas diferentes del Mar Mediterráneo contaminados de forma crónica por petróleo: la zona del hundimiento del carguero Haven (HAV), y los puertos de Messina (Sicilia, MES) y Priolo Gargallo (Siracusa, PRI), todos ellos en zonas costeras de Italia.

El análisis se compone de los siguientes pasos: a) medida de los parámetros ambientales y geoquímicos de las diferentes muestras; b) extracción e identificación de las proteínas expresadas en cada una de las tres muestras por espectrometría de masas; c) afiliación taxonómica de las proteínas expresadas para identificar el papel de diferentes grupos microbianos; y d) extracción e identificación de metabolitos por cromatografía líquida acoplada a espectrometría de masas.

Se identificaron un total de 651 proteínas y 4776 metabolitos en las tres muestras. De ellas solo 106 proteínas eran comunes a las tres comunidades, lo que sugiere amplias diferencias a nivel metabólico. Solo 50 de las 651 proteínas estaban relacionadas con el metabolismo de compuestos C_1, ninguna de las cuales se relacionaba directamente con la biodegradación de hidrocarburos, ni fueron asignadas a algún grupo bacteriano especialista en estos procesos. Esto junto con el hecho de que solo 24 de los 4776 metabolitos identificados se atribuyen a contaminantes o intermediarios de su degradación demuestra que los procesos de biodegradación en los ambientes contaminados de forma crónica estudiados representan un parte menor del metabolismo microbiano y que la tasa de biodegradación es posiblemente baja. Dicho esto, el estudio refleja otros procesos metabólicos relevantes como el metabolismo de compuestos C_1 (incluido el metabolismo de CH_4 y CH_3OH), y azufre que demuestran un alto grado de cooperación y sinergia entre los distintos grupos microbianos presentes en cada una de las muestras.

RESEARCH ARTICLE

Metaproteomics and metabolomics analyses of chronically petroleum-polluted sites reveal the importance of general anaerobic processes uncoupled with degradation

Rafael Bargiela[1], Florian-Alexander Herbst[2,3*], Mónica Martínez-Martínez[1], Jana Seifert[2,4], David Rojo[5], Simone Cappello[6], María Genovese[6], Francesca Crisafi[6], Renata Denaro[6], Tatyana N. Chernikova[7], Coral Barbas[5], Martin von Bergen[2,8], Michail M. Yakimov[6], Manuel Ferrer[1] and Peter N. Golyshin[7**]*

[1] Consejo Superior de Investigaciones Científicas (CSIC), Institute of Catalysis, Madrid, Spain
[2] Department of Proteomics, UFZ – Helmholtz Centre for Environmental Research, Leipzig, Germany
[3] Center for Microbial Communities, Department of Chemistry and Bioscience, Aalborg University, Aalborg, Denmark
[4] Institute of Animal Science, Universität Hohenheim, Stuttgart, Germany
[5] Centro de Metabolómica y Bioanálisis (CEMBIO), Facultad de Farmacia, Universidad CEU San Pablo, Madrid, Spain
[6] Institute for Coastal Marine Environment, CNR, Messina, Italy
[7] School of Biological Sciences, Bangor University, Gwynedd, UK
[8] Department of Metabolomics, UFZ – Helmholtz Centre for Environmental Research, Leipzig, Germany

Received: December 21, 2014
Revised: May 21, 2015
Accepted: July 20, 2015

Crude oil is one of the most important natural assets for humankind, yet it is a major environmental pollutant, notably in marine environments. One of the largest crude oil polluted areas in the word is the semi-enclosed Mediterranean Sea, in which the metabolic potential of indigenous microbial populations towards the large-scale chronic pollution is yet to be defined, particularly in anaerobic and micro-aerophilic sites. Here, we provide an insight into the microbial metabolism in sediments from three chronically polluted marine sites along the coastline of Italy: the Priolo oil terminal/refinery site (near Siracuse, Sicily), harbour of Messina (Sicily) and shipwreck of MT Haven (near Genoa). Using shotgun metaproteomics and community metabolomics approaches, the presence of 651 microbial proteins and 4776 metabolite mass features have been detected in these three environments, revealing a high metabolic heterogeneity between the investigated sites. The proteomes displayed the prevalence of anaerobic metabolisms that were not directly related with petroleum biodegradation, indicating that in the absence of oxygen, biodegradation is significantly suppressed. This suppression was also suggested by examining the metabolome patterns. The proteome analysis further highlighted the metabolic coupling between methylotrophs and sulphate reducers in oxygen-depleted petroleum-polluted sediments.

Keywords:
Anaerobic / Crude oil / Hydrocarbonoclastic / Mediterranean Sea / Metabolomics / Microbiology

Additional supporting information may be found in the online version of this article at the publisher's web-site

Correspondence: Dr. Manuel Ferrer, CSIC - Institute of Catalysis, Marie Curie 2, 28049, Madrid, Spain
E-mail: mferrer@icp.csic.es

*These authors contributed equally to this work.
**Additional corresponding author: Professor Peter N. Golyshin, E-mail: p.golyshin@bangor.ac.uk
Colour Online: See the article online to view Figs. 2–4 in colour.

1 Introduction

Anthropogenic crude oil discharge into seawater, together with the chemical diversity of crude oil components and environmental constraints such as depth, temperature, O_2 concentration and nutrient input, have been commonly reported to distinctly influence the large-scale distribution of microbial populations and the geochemical and biodegradation processes the populations mediate [1–4]. The relative abundance of bacteria specialised in the degradation of alkanes and polycyclic aromatic hydrocarbons (PAH) and the global gene expression are modulated by variations in the crude oil inputs in the sea [5–9]. These effects have been reported for bacteria of the genera *Alcanivorax*, *Marinobacter*, *Oleispira*, *Thalassolituus*, *Oleiphilus*, *Cycloclasticus* and *Neptunomonas* [5,9,10] and for selected catabolic genes, e.g., those encoding alkane monooxygenases, catechol 1,2-dioxygenases, catechol 2,3-dioxygenases, naphthalene dioxygenase components, and genes relevant to carbon, nitrogen, phosphorous, sulphur and iron cycling [1–3,12]. Recent studies of the Deepwater Horizon oil spill have further revealed that such shifts occurred within 1 month of the spill [13].

Compared to sites in which accidental crude oil spills occurred, such as the Gulf of Mexico [13] or the *Prestige* Tanker accident off the NW coast of Spain [14], the Mediterranean Sea has been generally neglected by the international research community regarding studies on marine oil pollution. However, this area hosts large numbers of pipeline terminals, oil refineries and offshore platforms and 20% of global crude oil traffic [15, 16] with numerous reported tanker accidents [17, 18]. The scale of the pollution in the Mediterranean is severe, despite Mediterranean Sea only represents approximately 1% of the total sea surface of the planet. Several studies and reports have also demonstrated that selected areas in the Mediterranean Sea are polluted with toxic compounds other than crude oil components [19], leading to a synergistic increase in the overall toxicity [20]. Additionally, compared to open oceanic areas, the Mediterranean Sea is a semi-enclosed basin, and the chemical species are trapped and tend to accumulate rapidly because the theoretical flushing time of Mediterranean water takes as long as approximately 70–90 years.

Although enhanced crude oil inputs in the Mediterranean Sea basin may sustain versatile microbial populations, the distribution and metabolic potential of these populations (in the context of physico–chemical conditions such as the water temperature, O_2 and nutrient concentrations and crude-oil input) are poorly understood. Typically, the analysis of microbial communities includes an initial assessment of the structure of the population using conventional 16S rRNA gene clone libraries and metagenome sequencing [21]. Further, the reconstruction of metabolic capacities of microbial communities is performed, but this analysis (using e.g. metatranscriptomics data) is challenging [22]. This, in turn, promotes the application of metaproteomics, by which at least the identity and/or the relative number and abundance of expressed proteins can be detected in the environment [23]. Simultaneously, a number of approaches have been specifically designed to integrate gene and protein expression data [24,25] with metabolic fluxes [26,27], to characterise presumptive active metabolic pathways under different conditions.

Sediment samples were selected for the study for following reasons. The release of thousands of tons of petroleum hydrocarbons (PHs) from anthropogenic activities affects the marine environment and causes severe ecological and economical damage. Once released at the sea surface, PHs are undergoing both weathering processes (evaporation of volatile fraction, photo-oxidation) and emulsification [12–15]. As a result, significant amount of PHs become heavier, form tar and settle on the sediments [14]. Marine sediments are often fine-grained and the abundance of clay minerals coupled with high organic loads encourages sorption of the most hydrophobic hydrocarbons. Sedimentary accretion can result in burial of hydrocarbons in zones of low redox potential. As a consequence, hydrocarbons have been found in fine-grained coastal sediments many decades after a spill due to slow anaerobic biodegradation.

In the present paper, we analysed major metabolic patterns in the three distinct oil-polluted sites of the Mediterranean Sea using an integrated metaproteomics and metabolomics approach. Moreover, based on the proteins being identified, we suggested active metabolic pathways at the organismal level, which is relevant to disentangle the role of each member in the community. Syntrophy between different microbial members in carbon and sulphur cycling has been suggested. A low contribution of microbial members to pollutant catabolism was also established.

2 Materials and methods

2.1 Study sites

The sampling sites were located along the Northern and Southern Italian coast [16]. The investigated sites, in order of latitude, included the following. The first site was the Gulf of Genoa in the northernmost part of the Ligurian Sea in the proximity of the Arenzano Harbour (Genoa, Italy; 44°22′25.75″N, 8°41′59.58″E) where the Tanker *Haven* (*HAV*) sunk in 1991 [28]. M/T *Haven*, formerly *Amoco Milford Haven*, was a large crude carrier leased to Troodos Shipping. On April 11, 1991, the tanker carrying a cargo load of 144.000 tons of crude oil exploded during a routine operation and spilled about 50.000 tons of petroleum into the Mediterranean. Italian authorities attempted to tow the MT *Haven* closer to shore to reduce the coastal area affected by the oil spill and to

Abbreviations: **EPA**, Environmental Protection Agency; **FID**, flame ionisation detector; **HAV**, Haven tanker; **LTQ**, linear trap quadrupole; **MES**, Messina; **MPS**, metaproteome source; **PAH**, polyaromatic hydrocarbon; **Pet Hyd**, total petroleum hydrocarbon; **PRI**, Priolo; **TERCH**, total extracted and resolved hydrocarbons; **UPLC**, ultra performance liquid chromatography

improve access to the wreck, but the ship broke into two pieces and sank after burning for three days. After 17 years (in 2008), the Italian Government commissioned the recovery of this area, but the ship and the remaining tar continue to pollute the Mediterranean coasts of Italy and France [28]. The second site was the harbour of Messina (*MES*) (Sicily, Italy 38°11'42.27"N, 15°34'25.01"E), a marine harbour that generally suffers chronic petroleum pollution because of intensive maritime traffic and its limited hydrodynamic regimen and restricted area [29,30]. The third site was the harbour of Priolo (*PRI*) Gargallo (Siracusa, Italy; 37°10'27.46"N, 15°12'7.51"E), which is characterised by heavy industrialisation and intensive tanker traffic transporting both crude and refined oil [31]. The samples were named based on the code 'MPS', which refers to the MetaProteome Source, followed by a short name indicating the origin of the sample as follows: MPS-HAV (*Haven* Tanker at the Gulf of Genoa); MPS-MES (the harbour of Messina); and MPS-PRI (the harbour of Priolo Gargallo).

2.2 Environmental measurements and sample collection

Sediment samples (5.0 kg) were collected at a water depth of 1.0 to 78.0 m (June 2011) by scuba. The temperature, salinity, pH, redox potentials and dissolved oxygen were measured by a portable multiparametric probe analyser (WP 600 Series Meters Eutech Instruments Pte Ltd, Singapore). The oxygen concentration was determined using the Winkler method with an automatic endpoint detection burette 716 DNS Titrino (Metrohm AG, Herisau, Switzerland). Samples for measurements of NO_3^-, NO_2^- and PO_4^{3-} were stored at −20°C, and nutrient concentrations were determined later in triplicate in the laboratory using a "SEAL AutoAnalyser QuAAtro" following classical methods [32] with slight modifications adapted for sediments. A conductivity calibration was performed with a KCl 0.01 mol/L control solution. Reference solutions with pH values of 7.0 and 9.0 were employed for the pH metre. The concentrations of microelements were determined through Inductively Coupled Plasma-Mass Spectrometry (ICP/MS). Ammonium was determined using the indophenol blue technique (IOC, 1983). The dissolved organic carbon content was determined by the dichromate wet oxidation method; the total organic matter content was calculated by multiplying the values of the organic carbon by 1.8. The amount of total extracted and resolved hydrocarbons (TERHC) was determined as follows. Briefly, TERCH were extracted from sediments following the 3550C EPA (Environmental Protection Agency) procedure. In total, a 500 mL mixture of CH_2Cl_2:CH_3COCH_3 (1:1 v/v) was added to 1000 g of dry sediments and sonicated for 2 min in an ultrasound bath (Branson 1200 Ultrasonic Cleaner, Branson, USA). Samples were further shaken at 150 rpm for 30 min, centrifuged for 10 min at 5000 *g* and the supernatant was passed through a ceramic column filled with anhydrous Na_2SO_4 (Sigma-Aldrich, Milan, Italy). The identical treatment of sediments was repeated with 500 mL of CH_2Cl_2, and the obtained solvents were combined and volatilised until dryness. The residues were re-suspended in CH_2Cl_2 prior to the gas chromatography (GC) analysis. All measurements were performed using a Master GC DANI Instruments (Development Analytical Instruments) equipped with a SSL injector and flame ionisation detector (FID). The sample (1 μL) was injected in the splitless mode at 330°C. The analytical column was a Restek Rxi-5 Sil MS with Integra-Guard, 30 m x 0.25 mm (ID x 0.25 μm film thickness). The helium carrier gas was maintained at a constant flow of 1.5 mL/min. TERCH were calculated using the mean response factors of *n*-alkanes, i.e., individual *n*-alkane concentrations from *n*-C_{15} to *n*-C_{40}; additionally, pristane and phytane concentrations were calculated for each sample. The amount of TERCH was expressed as ppm (part per million) or mg/kg.

2.3 Protein extraction

Sediment samples were subjected to protein isolation using a two-step protocol. First, before protein extraction, the sediment samples underwent differential centrifugation to eliminate the majority of the crude oil attached to the sediment material (oil interferes with the protein extraction). Therefore, 10.0 g of the sediment samples were mixed with 30.0 mL of sterilised saline solution (5 mM sodium pyrophosphate and 150 mM NaCl) containing Tween 80 (a final concentration of 15 mg/L; Fluka-Aldrich-Sigma Chemical Co. (Saint Louis, MO, USA)) in an ice water bath. After re-suspension, the samples were kept in a water bath ultra-sonicator (Bandelin SONOREX, Berlin, Germany), maintained at 4°C on ice, and sonicated (60 W output) for 5 min at 4°C. The samples were then centrifuged at 100 *g* at 4°C for 2 min to remove the sediment material. The resulting supernatant was then centrifuged at 13,000 *g* for 15 min at 4°C to pellet the sediment samples containing microbial cells. The whole-cell protein extraction was then performed as previously described [33] by heating one volume of mixture of disruption buffer with one volume of the sediment material (obtained as above) at 80°C for 1 h; during this treatment, the samples were sonicated for 2 min in an ultrasound bath every 10 min. The disruption buffer contained 150 mM NaCl, 2% w/v sodium dodecyl sulphate (SDS), 100 mM ethylenediaminetetraacetic acid (EDTA), 1 M Tris HCl, 100 mM 1,4-dithio-D-threitol (DTT) and a quarter tablet of Complete Protease Inhibitors (Roche Applied Science, Germany) for each 1 mL of buffer. The above procedure was followed by 7 cycles of 5 s sonication in a probe sonicator (Sonicator® 3000; Misonix, Berlin, Germany) and 5 min of centrifugation at 15 000 *g*; the supernatant was spin filtered at 15°C for 7 h using Vivaspin filters (Sartorius, Germany) with a molecular weight (MW) cut off of 10,000 Da (after 100-fold SDS dilution using 20 mM triethylammonium bicarbonate buffer (TEAB)). Urea was added prior to spin filtering (a final concentration of 4 M) for a better recovery of proteins [33]. Finally, the quantitation of the

extracted protein was performed using the Bradford Protein Assay (Bio-Rad) [34]. An average total amount of 150 ± 12 μg total proteins were obtained per each 10 grams of sediment samples, as calculated by Bradford Protein Assay [34].

The heating step at 80°C was critical for the efficiency of the protein recovery in the sediment samples compared with standard freeze/thaw cycles; this step was also beneficial when extracting proteins from biofilm material [33]. No adverse side-effects (i.e. protein modifications) due to this heating step have previously been reported [33]. To avoid oxidation, buffers were degassed before heating steps, and the headspaces of buffers and solutions were flushed with argon. Some deamidation could be observed during quality control, which might be influenced by the extraction protocol and the heating. This was accepted as a tradeoff to ensure lysis/extraction and to prevent enzymatic degradation, but should be monitored in future quantitative studies.

2.4 Mass spectrometry and data analysis

Protein solutions were dried using a Concentrator 5301 (Eppendorf, Hamburg, Germany). Further, the protein pellets were solubilised in Laemmli-buffer prior to 1D SDS-PAGE for removal of interfering substances and pre-fractionation. The lanes of a short gel (Supporting Information Figure 1) of approximately 5 cm were cut into ten slices, reduced, carbamidomethylated and subjected to in-gel tryptic digestion as previously described [35]. The purification and de-salting was performed by ZipTipC18 columns (Merck Millipore, Billerica, MA, USA), resulting in ten fractions per sample. Peptides were reconstituted in 0.1% v/v formic acid, and mass spectrometric measurement was performed using a nanoAcquity ultra performance liquid chromatography (UPLC) (Waters, Milford, MA, USA) coupled linear trap quadrupole (LTQ)-Orbitrap Velos (Thermo Fisher Scientific, Waltham, MA, USA). Samples were injected with the autosampler and concentrated on a trapping column (nanoAcquity UPLC column, C18, 180 μm × 2 cm, 5 μm, Waters) with water containing 0.1% v/v formic acid at flow rates of 15 μL/min. After 6 min, the peptides were eluted into a separation column (nanoAcquity UPLC column, C18, 75 μm × 15 cm, 1.75 μm, Waters). Chromatography was performed with 0.1% formic acid in solvent A (100% water) and B (100% acetonitrile). The gradient was 2 to 15% B (0-10 min), 15 to 40% B (10–77 min), 85% B (77–87 min), followed by re-equilibration at 2% B for 13 min. For an unbiased analysis, a continuous scan of the eluted peptide ions was performed between 300 and 2000 m/z (automatically switching to MS/MS CID mode on ions exceeding an intensity of 2000) with ten MS/MS events per survey scan. For MS/MS CID measurements, a dynamic precursor exclusion of 120 s was enabled.

To increase the rates of protein identification and to decrease the false negatives rate, the MetaGenomic Sequences (BioProject IDs PRJNA222659 (for MGS-HAV), PRJNA222657 (for MGS-MES) and PRJNA222658 (for MGS-PRI) at NCBI; AZIB00000000 (for MGS-HAV), AZIC00000000 (for MGS-MES) and AZIF00000000 (for MGS-PRI) at DDBJ/EMBL/GenBank) containing a total number of 54,323 unique/non-redundant sequence entries were complemented by a two-step database approach [36] as described elsewhere [37]. In brief, mass spectra were first searched against prokaryotic entries of the National Center for Biotechnology Information non-redundant database (NCBInr) using Thermos Proteome Discoverer and Mascot. The unfiltered results (4404 entries) were exported to serve as a complementing database in the main search [37]. The final database, a combination of the metagenome and NCBInr sequences, was used for protein identification in MaxQuant (v. 1.5.1.0) [38]. Although the use of metagenomic sequences is not necessarily beneficial as previously discussed [23], it was also not possible to know beforehand if a metagenome might be needed or not. For that reason, we combined public databases and metagenomic sequences obtained for the samples herein investigated. Roughly 20% of the proteins were exclusively matched with the metagenomic data derived from these three Mediterranean sites.

The oxidation of methionine was defined as a variable modification, and the carbamidomethylation of cysteine was defined as a fixed modification. The three different sample sets were divided into different parameter groups and matching was disabled. All remaining standard settings were maintained. These included a peptide and protein false discovery rate (FDR) below 1%, at least one peptide, a precursor mass tolerance of 4.5 ppm after mass recalibration and a fragment ion mass tolerance of 0.5 Da. The threshold of only one identified peptide per protein identification was used because FDR controlled experiments counter intuitively suffer from the two-peptide rule [39]. Protein grouping was automatically performed by MaxQuant based on the law of parsimony. The mass spectrometry proteomics data have been deposited to the ProteomeXchange Consortium (http://www.proteomexchange.org) via the PRIDE partner repository [40] with the dataset identifier PXD001490.

Predicted protein sequences were aligned against NCBInr using a BLASTP search. Taxonomic binning of the sequences was performed by summarising the top significant BLASTP hits with e-values ≤ 0.00001. Additionally, composition-based binning of contigs containing the genes encoding the identified proteins was performed using the GOHTAM Web-server [41] to ensure taxonomic affiliations.

2.5 Metabolomic fingerprint analysis of sediment samples

The metabolites were extracted from sediment samples as follows. In 100 mL Erlenmeyer flasks, 5 g of sediments were mixed with 10 mL of cold (–80°C) high-performance liquid chromatography (HPLC)-grade methanol (MeOH). The samples were sonicated in a probe sonicator (Sonicator® 3000; Misonix, Berlin, Germany) for 120 sec (at 15 W) in an ice

water bath. This procedure was repeated 4 times, and the samples were kept on ice for at least 2 min between each step. After sonication, the supernatant was removed by centrifugation at 10 000 *g* for 30 min at 4°C, and the supernatant was stored in 20 mL serum vials at –80°C. The MeOH extracts were filtered using 0.2 μm nylon syringe filters (Thermo Scientific, Rockwood, USA) and analysed by liquid chromatography quadrupole time-of-flight mass spectrometry (LC-Q-TOF-MS). The analytical run began with the analysis of Quality Controls (QCs) followed by sampling in a random order; a QC sample was injected in between blocks of four samples until the end of the run. All vials were maintained at 4°C throughout the run. Each metabolic fingerprint was achieved using a liquid chromatography system consisting of a degasser, binary pump, and autosampler (1290 infinity, Agilent; Santa Clara, CA, USA). A total of 0.5 μL was applied to a reverse-phase column (Zorbax Extend C_{18} 50 × 2.1 mm, 3 μm; Agilent), which was maintained at 60°C during the analysis. The system operated in the positive and negative ion mode at a flow rate of 0.6 mL/min of solvent A (water with 0.1% formic acid) and solvent B (acetonitrile with 0.1% formic acid). The gradient was 5% B (0–1 min), 5 to 80% B (1–7 min), 80 to 100% B (7–11.5 min) and 100 to 5% B (11.5–12 min) followed by re-equilibration at 5% B for 3 min (15 min of total analysis time). Data were collected in the positive and negative electrospray ionisation (ESI) mode in separate runs on a Q-TOF (Agilent 6550 iFunnel). Both ion modes operated in the full scan mode (m/z 50 to 1000 in positive and m/z 50 to 1100 in negative ion mode). For each mode, the capillary voltage was 3000 V, the scan rate was 1.0 spectra/s, the gas temperature was 250°C, the drying gas flow was 12 L/min, and the nebuliser was 52 psi. The MS-TOF parameters for the positive ion mode were as follows: fragmentor 175 V, skimmer 65 V and octopole radio frequency voltage (OCT RF Vpp) 750 V. The identical MS-TOF parameters were used in the negative ion mode, except the fragmentor was set to 250 V. Two reference masses were used for each mode: m/z 121.0509 ($[C_5H_4N_4+H]^+$) and m/z 922.0098 ($[C_{18}H_{18}O_6N_3P_3F_{24}+H]^+$) during the positive analysis and m/z 112.9855 ($[C_2O_2F_3\text{-}H]^-$) and m/z 1033.9881 ($[C_{18}H_{18}O_6N_3P_3F_{24}+\text{TFA-H}]^-$) during the negative analysis. The reference masses were continuously infused into the system to permit constant mass correction. The chromatograms deconvolution and peak integration were performed using Mass Hunter Qualitative Analysis (B.05.00, Agilent).

3 Results and discussion

3.1 Study sites: physical–chemical characteristics

The rationale behind the sampling strategy was to target sites with aged and chronic contaminations and in diverse environmental locations in the Mediterranean basin. So, the samples herein investigated were inevitably rather heterogeneous (e.g., distinct, conductivity, and NH_4^+, PO_4^{3-}, dissolved organic carbon, microelements and O_2 concentrations and different hydrocarbon loads). However, they are representative for some of the most prevalent types of chronically polluted sites that are distributed within the Mediterranean [16]. Moreover, they constitute the basis of a proof-of-concept for an integrated approach (metaproteome and metabolome-based study) to unravel core environmental parameters regulating active microbial populations and activities. As shown in Table 1, at the sampling time the three studied sites exhibited the following most distinct characteristics: (i) a temperature ranging from 15°C (for HAV) to 23°C (for MES); (ii) a pH from 6.85 (for PRI) to 8.05 (for HAV); (iii) an oxygen concentration ranging from anoxic (for PRI) to 6.0–6.50 mg/L (for HAV); (iv) a conductivity ranging from 49.0 (for HAV and PRI) to 70.0 (for MES) mS/cm; (v) a total concentration of alkane (C_{10}–C_{40}) of 500 (for MES) to 260 000 (for HAV) mg/kg sediment; (vi) a total concentration of polyaromatic hydrocarbons (PAH) of <1 (for PRI) to 182 (for HAV) mg/kg sediment; (vii) an ammonium concentration ranging from 0.6 (for HAV) to 2.3 (for PRI) μmol/L; (viii) a PO_4^{3-} concentration ranging from 0.1 (for HAV) to 0.45 (for PRI) μmol/L; and (ix) a NO_3^-concentration ranging from 6 (for HAV) to 29 (for PRI) μmol/L. Values for other parameters are given in Table 1.

The total concentration of hydrocarbons in the sediments (Table 1) exceeded that in clean seawater (15 ppm) by more than 70-fold. This excess likely occurs because the investigated sites are subjected to chronic petroleum pollution [16].

3.2 Metaproteomic analysis: general comments

We selected a shotgun metaproteomic approach to query the active populations within the chronically contaminated sites. The identification depends heavily on protein abundance, and although we are aware that a substantial fraction of the present proteome stays hidden, the identified proteins are assumed to represent the dominant pathways in each system. In total, 651 non-redundant proteins were unambiguously identified (with a total numbers of proteins of 310 in MPS-HAV, 333 in MPS-MES and 388 in MPS-PRI) (Supporting Information Table 1). Because the proteome analysis could be correlated with the corresponding reference metagenome datasets, the metaproteome sizes were found within a common range observed for other communities and, as it is often the case, a few times smaller than those observed for cultured organisms [42–45]. Although distinct environmental sites were investigated, 106 of 651 proteins (or 16.2%) comprised the subset that was common in all three samples. A total of 90, 143 and 144 sampling site-specific proteins were identified for HAV, MES and PRI, respectively. This indicated that the HAV, MES and PRI communities displayed overlaps but also considerable heterogeneity at the proteome level and regarding functional categories of identified proteins. The metaproteomic approach applied here, based on the relative

Table 1. Overall physical–chemical characteristics of the investigated sediment samples

Parameters[a)]	HAV	MES	PRI
GPS coordinates	44°22′25.75″N 8°41′59.58"E	38°11′42.267"N 15°34′25.014"E	37°10′27.462"N 15°12′7.505"E
Depth (m)	78.0	1.0	6.0
C_{10}-C_{40} (ppm)[b)]	260 000	500	3922
PAH (ppm)[b)]	182	100	<1
Temperature (°C)	15.0	23.0	19.0
Dissolved O_2 (mg/L)[c)]	6.0–6.5	1.0-2.2	0
pH	8.05	7.37	6.85
Conductivity (mS/cm)	49.0	70.0	49.0
Ammonium (mkmol/L)	0.6–0.7	7	420
Calcium (mg/L)	420	420	420
PO_4^{3-} (mkmol/L)	0.1	0.3	0.45
NO_3^-(mkmol/L)	6	8	29
NO_2^- (mkmol/L)	3	2	4
Diss_org_carb (mg/L)[d)]	5.00	50.00	125.00
Part_org _carb (μM)[d)]	1.40	1.44	1.89
[Microelements] (nM)[e)]	392.0	408.0	883.0
Open reading frames (ORF)[f)]	8388	40 077	5858
Non-redundant proteins[g)]	310	333	388

a) Triplicate measurements were performed with standard deviations lower than 5%.
b) Total extracted and resolved petroleum hydrocarbons (TERHC) were extracted and alkanes and polyaromatic hydrocarbons (PAH) determined.
c) PRI is an anoxic site; MES is a micro-aerophilic environment.
d) Abbreviations are as follows: Diss_org_carb, dissolved organic carbon; Part_org _carb, particulate organic carbon.
e) Microelements include Sc, Cr, Mn, Fe, Ni, Co, As, Se, Mo, Ag, Sn, Sb, Ba, La, Ce, Sm, Eu, Tb, Hf, Au, Hg and heavy metals such as Zn, Cd, Pb and Cu.
f) Gene prediction results from sequencing data obtained by Illumina HiSeq and Roche 454 sequencing of metagenomic DNA from the microbial communities in the three polluted sediments collected in the Mediterranean Sea. For accession numbers, see the Materials and Methods section.
g) Number of non-redundant proteins unambiguously identified in the metaproteomes.

number of identified proteins, allowed us to compare the taxonomic annotations and to evaluate the differences between the contributions of particular groups of organisms in the overall communities and to predict the importance of particular sets of proteins for the overall functioning of the community.

3.3 Identities of expressed proteins

Taxonomic classifications revealed that the proteins assigned to Bacteria were predominant to a similar extent in all three samples (HAV: 94% (or 291 proteins); MES: 91.6% (or 305); PRI: 90.3% (or 350) of the total proteins). The percentage of proteins binned to Archaea negatively correlated with O_2 concentration in situ; the highest percentage was obtained at the site with the lowest O_2 concentration ($r^2 = 0.98$; p-value $= 0.067$) (Fig. 1). By contrast, the relative percentage of archaeal proteins did not correlate with in situ temperature (Fig. 1, inset) as well as crude oil input (or petroleum hydrocarbon concentration [ppm]) or other environmental parameter whose values are given in Table 1. Evidently, the decrease in O_2 concentrations may stimulate the growth of strictly anaerobic archaea, such as methanogens, thus resulting in the enhanced expression of their proteins. Among all identified archaeal proteins, those associated with the methanogenic *Methanosarcinales* were most numerous in all three sites (HAV: 4.8% (or 14); MES: 6.2% (or 21); PRI: 5.4% (or 21), of the total proteins), as revealed by their higher relative number compared with proteins from other archaeal members (Fig. 2A). In addition to proteins assigned to *Methanosarcinales*, the diversity of archaeal proteins likely originated from *Archaeoglobales*, *Aciduliprofundum*, *Halobacteriales*, *Thermococcales* and *Thermoplasmatales*. All these organisms were observed in PRI but were missing in HAV and MES (Fig. 2A).

Within the bacterial sub-proteomes, proteins assigned to the phylum *Proteobacteria* were predominant in all samples (HAV: 66% (or 205); MES: 57% (or 189); PRI: 81% (or 314), referring to total protein numbers). The distribution at the level of classes of *Proteobacteria* (Fig. 2B) revealed only significant differences in the number of proteins assigned to *Deltaproteobacteria*, displaying significantly lower protein expression levels in MES when compared to HAV (8.4-fold, in terms of numbers identified) and PRI (9.5-fold). The proteins assigned to *Epsilonproteobacteria* were more numerous in PRI than in HAV (7.2-fold) and MES (11.6-fold) (Fig. 2B). Because PRI is an anaerobic environment (Table 1), the higher numbers of proteins from *Epsilonproteobacteria* most likely reflect their association with anoxic sites; notably, members of this class have also been found to be abundant in

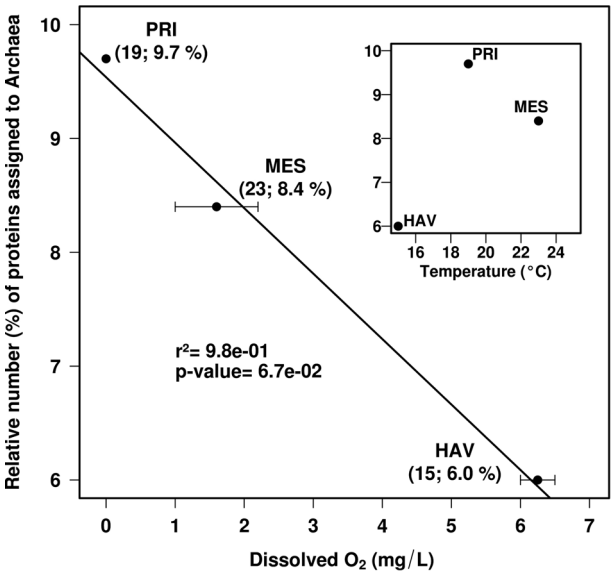

Figure 1. Oxygen concentration as an environmental factor driving the occurrence of proteins assigned to Archaea at the three studied sites. A significant negative correlation ($r^2 = 0.98$; $P = 6.7 \times 10^{-2}$; *t*-test) was noted between the relative percentage of proteins assigned to Archaea referred to the total number of proteins (to avoid artefacts because of different sample sizes) and the site oxygen concentration. No such correlation was found with other environmental parameters such as site temperature (inset) or other parameters whose values are given in Table 1. The absolute numbers and relative percentage of proteins assigned to Archaea are given in brackets.

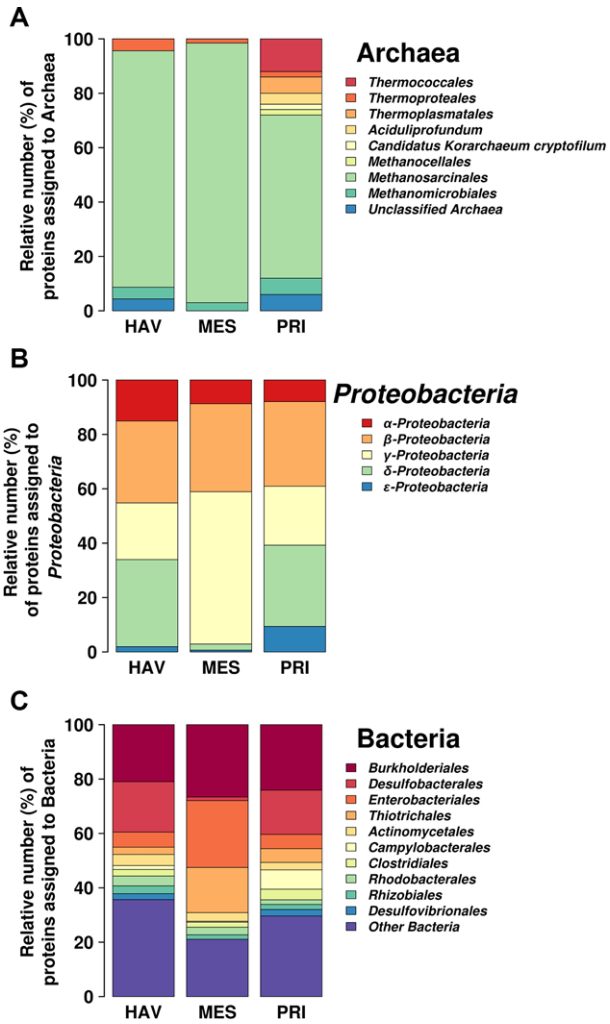

Figure 2. Relative number and distribution of archaeal (A) and bacterial (B, C) proteins in the metaproteomes of marine sediment samples, based on taxonomic bins for proteome-derived proteins with taxonomic annotation. Distributions in (A) and (C) are at the level of the order, whereas (B) indicates the classes within the phylum *Proteobacteria*.

pollutant-degrading microbial consortia operating under aerobic conditions [43, 46]. However, the proteins assigned to *Gammaproteobacteria* were detected at higher number in MES than in HAV (2.8-fold) and PRI (2.6-fold) (Fig. 2B). In addition to proteins from the phylum *Proteobacteria*, the proteins likely derived from *Firmicutes* (HAV: 7.8% (or 24); MES: 6.2% (or 21); PRI: 8.1% (or 27), of the total proteins) and *Acidobacteria* (HAV: 5.8% (or 18); MES: 4.4% (or 15); PRI: 4.8% (or 19), of the total proteins) formed the second and third predominant groups. Additional groups of Bacteria that expressed proteins at identifiable quantities in our assay are summarised in Fig. 2C. These findings were verified by a phylogenetic analysis of NCBInr derived peptides using the web-based Unipept tool [47]. Note, that no identified proteins in our dataset were affiliated with the genus of typical specialised hydrocarbonoclastic (HCB) bacteria [5, 9, 10], other than *Cycloclasticus* in HAV. This may correlate with the fact that they were not found in the sediment samples (except those assigned to *Cycloclasticus* in HAV), as revealed by SSU rRNA hypervariable tag analysis; see original non-chimeric SSU rRNA hypervariable tag 454 sequences that are archived at the EBI European Read Archive under accession number PRJEB5322, for details.

Among all proteins, the ten functional groups associated to the most numerous identified proteins were the following (Supporting Information Table 1): (i) ABC transporters or outer membrane proteins (116, or 18% of the total), (ii) hypothetical proteins (109, or 17%); (iii) ribosomal proteins (32, or 5%); (iv) AprAB adenosine-5-phosphosulfate reductases (22, or 3.4%); (v) DsrAB sulfite reductases (18, or 2.8%); (vi) TonB-dependent receptors (14, or 2.2%); (vii) chaperones (14 or 2.2%); (viii) glutamate decarboxylases/dehydrogenases/synthases (13, or 2%); (ix) ATP synthases (9, or 1.4%); and (x) proteins for the C_1-compounds uptake and methanogenesis [9 methyl-coenzyme M reductases, 7 methanol dehydrogenases and 7 methanol-5-hydroxybenzimidazolylcobamide methyltransferases; or 3.5%]). These functional groups suggest that apart from the transport and energy production systems, the metabolism of sulphur, C_1-compounds and glutamate are among the most

active functions within all communities, albeit at different levels. These metabolisms have been commonly found to be markedly stimulated under anaerobic conditions [48, 49]. Proteins involved in glutamate conversion were only found in HAV and PRI (11 and eight non-redundant proteins, respectively), but not in MES; the fact that glutamate metabolism is generally activated in response to low temperature stress [50] and that both HAV and PRI were characterised by a much lower sea-water temperature compared to MES (Table 1), suggests that low temperature in combination with anaerobic stress might be responsible for the noted differences. As mentioned, a high number of proteins (109, or 17% of the total) were identified with a hypothetical role, suggesting that their function could be associated with anaerobic conditions. However, insights into their physiological roles remain limited, and further experimental evidence is needed.

3.4 Differences at the metabolic and organismal levels as revealed through metaproteomics

Recent studies have utilised the proteomics approach to determine active metabolic pathways operating in microbial communities [23]. Here, on the basis of their probable functions, we were able to capture overall functional differences of the three chronically polluted sites at the level of metabolic pathways (specifically, in relation to sulphur and C_1 metabolism) and hypothesised different pathway organisations at the organism level. These differences are detailed below.

C_1 metabolism: A total of 31 proteins (or 5.1% of the total proteome) potentially involved in the CH_4, CH_3OH and CO metabolism (HAV: 11; MES: 20; PRI: 19) were detected (Supporting Information Table 1; Fig. 3). This corresponds to 23% of the theoretical number of proteins (*in silico* proteome) presumptively involved in C_1 metabolism, as determined after examining the potential protein-coding genes ($\geq$ 20 amino acids long) from the meta-sequences (see accession number in Section 2.4). Protein signatures for the initial step of CH_4 conversion to CH_3OH were only found in HAV; this conversion can be performed by methane monooxygenase from bacterial members of the order *Methylococcales* (the top hit BAH22843, beta-subunit, PmoB). A possible explanation for the presence of methane monooxygenase for methanotrophy in HAV but not in PRI and MES may be due to the presence of a higher accumulation of petroleum hydrocarbons in HAV (Table 1) and thus the presence of difficult-to-degrade alkanes and aromatics [12].

Enzymatic pathways for C_1-compounds uptake and (methylotrophic) methanogenesis were detected in all three communities, although to different extents (Supporting Information Table 1; Fig. 3). The evidence for this pathway were the presence of: (i) methanol corrinoid proteins, methanol-5-hydroxybenzimidazolylcobamide methyltransferases and-methylcobalamin:coenzyme M methyltransferases converting CH_3OH to methyl-CoM; and (ii) methyl-coenzyme M reductases. In addition, trimethylamine:corrinoid methyltransferases that convert trimethylamine to methyl-CoM and dimethylamine, were also found in the proteomes. Notably, all these enzymes were unambiguously attributed to *Methanosarcinales*.

Signatures for methanol-utilising bacterial methylotrophs were also identified in the proteomes. Proteins for the subsequent conversion of CH_3OH to formaldehyde by methanol dehydrogenase were only detected in MES and PRI (Fig. 3). *Proteobacteria*, notably those associated to members of the orders *Thiotrichales* (in MES and PRI), *Vibrionales* (in MES) and *Rhizobiales* (in MES), were presumably capable of the utilisation of CH_3OH (Fig. 4). Methanol conversion to formaldehyde was not evident in HAV proteome data. Enzymes for the subsequent metabolism of formaldehyde were found in MES and PRI, namely formaldehyde-activating enzymes that transform formaldehyde to tetrahydromethanopterin (THMPT). Notably, the occurrence of the latter conversion was supported by proteins assigned to *Methanosarcinales* (in MES and PRI) and *Thiotrichales* (in PRI). No signatures for the conversion of formaldehyde to formate were observed, although a formate dehydrogenase (binned to *Rhodospirillales*) converting formate to CO_2 was found in MES and PRI. A carbon monoxide dehydrogenase (CODH catalytic subunit; top hit WP_031450384.1) (binned to *Desulfobacterales*) for the carbonyl branch of the Wood-Ljungdahl pathway was found in PRI (Fig. 3). Finally, a carbon dioxide concentrating mechanism/carboxysome shell protein (top hit WP_015107688.1), a structural protein (with no catalytic function and no Enzyme Nomenclature [EC] number) involved in the storage of enzymes participating in CO_2 metabolism, such as carbonic anhydrase and RubisCO [51], was found in both MES and PRI.

Taken together, the presence of two active processes is suggested: methylotrophic methanogenesis mediated by Archaea (*Methanosarcinales*) and methanol/formaldehyde detoxification by a set of bacteria. In addition, all studied communities possess highly developed trophic networks based on assimilatory and dissimilatory metabolism of C_1-compounds.

The taxonomy-guided pathway reconstruction emphasised differences at the organism level in relation to the CH_4 and CH_3OH metabolism. Thus, Fig. 3 shows the contribution of major organisms in all three sites, in which a clear pathway partitioning and metabolic coupling between community members are discernible. The metabolism and activation of CH_4 seems to be supported by a bacterial member of the *Methylococcales* order. Finally, the further methylotrophic conversion of CH_3OH was dominated by bacterial proteins (from members of the orders *Thiotrichales*, *Vibrionales*, *Rhizobiales*, *Rhodospirillales* and *Desulfobacterales*) and, to some extent, by archaeal proteins from methylotrophic methanogens of *Methanosarcinales*.

Sulphur metabolism, energy conservation and detoxification: A total of 54 proteins (or 8.3% of the total) that were potentially involved in the metabolism of sulphur compounds were detected (Supporting Information Table 1; Fig. 4). While these proteins were numerous in HAV (28) and PRI (45), they were

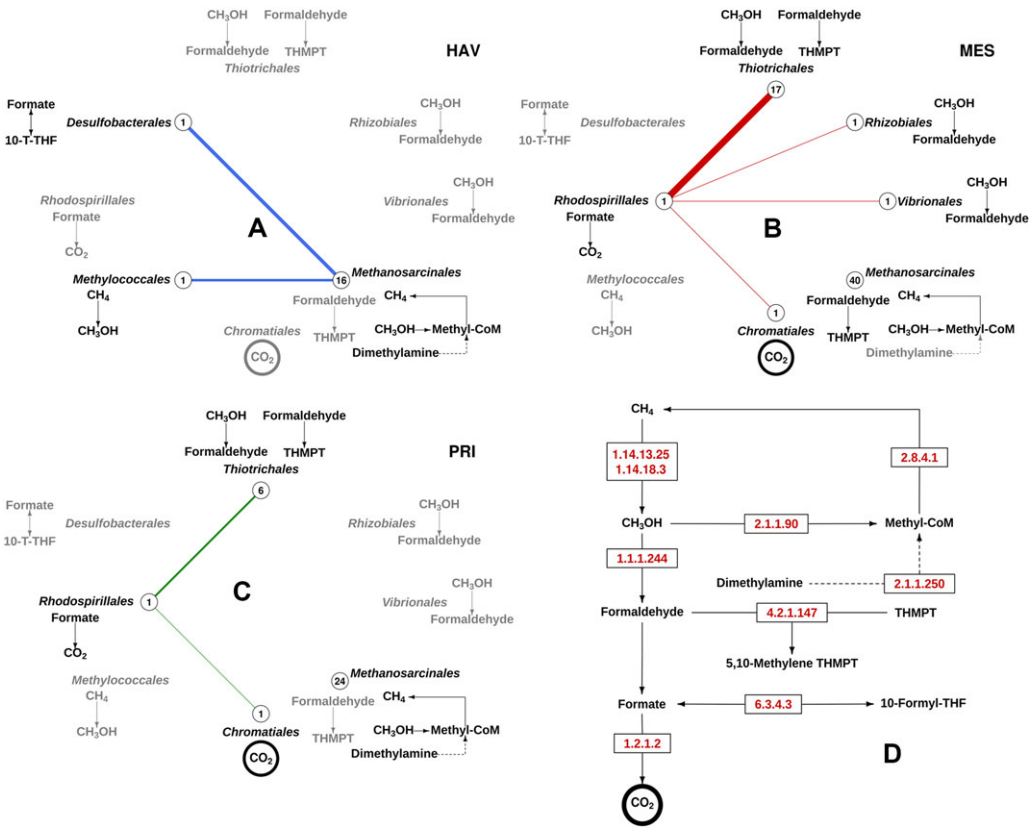

Figure 3. Reconstruction of the C_1 metabolism at the organismal level in the microbial communities inhabiting petroleum-polluted marine sediments based on the proteome analysis. Panels A, B and C, represent the active pathways in HAV, MES and PRI, respectively. The complete C_1 metabolism that included the metabolic coupling of CH_4 and CH_3OH metabolism and the Wood-Ljungdahl pathway is shown in Panel (D). As shown, only a small portion of the reactions within the entire C_1 metabolism (D) was identified as being active in HAV, MES and PRI (A–C). The presence of enzymes for each transformation and the taxonomic affiliation of polypeptides are shown. Circles in A–C represent the relative number of proteins (referred to the total number proteins assigned to these pathways) in a sample assigned to each taxonomic group (the total number of proteins of each is indicated in the circles). Solid lines (HAV, blue; MES, red; PRI, green) in A–C display the syntrophy between different members as they participate in contiguous reactions, as described in panel (D). The relative number of proteins assigned to these syntrophic reactions is presented by the line thickness. In panels (A–C), the grey colour indicates transformations for which no proteins in the proteome were identified, whereas the black colour represents transformations for which proteins were found (putatively active reactions). Transformations in the CH_4 and CH_3OH metabolism for which no proteome evidence were found (e.g., the glutathione (GSH) pathway connecting methanol with CO_2) are not indicated. Note: the representation of CO_2 in a circle (bottom of each panel) represents the presence of a carbon dioxide concentrating carboxysome shell protein, a structural protein involved in CO_2 accumulation within the cells, but with no catalytic function.

absent in MES (Fig. 4). This is particularly noticeable given that the metagenome sequence data set of sample MES was 4.8 and 6.9-fold bigger compared with those of samples HAV and PRI, respectively (Table 1). The absence of these proteins as revealed in the MPS-MES proteome reflects their low biological significance in MES. In fact, 27 potential protein-coding genes (≥ 20 amino acids long) presumptively involved in sulphur metabolism were found in the metagenomic sequences of MES (see the accession number in Section 2.4), all of which had the protein expression levels below our detection limit (Supporting Information Table 1; Fig. 4).

We detected AprAB (adenosine-5-phosphosulfate reductases) and DsrAB (sulfite reductases converting sulphite (SO_3^{2-}) to adenylyl sulphate (or facilitating the reverse reaction) and sulphide (H_2S)) both in HAV (23 proteins in total) and PRI (36 proteins in total) (Fig. 4). Such genes have also been detected in the Deepwater Horizon deep-sea plume at numbers higher than in non-plume samples, as sulphite reduction has been likely coupled with hydrocarbon degradation [12]. A total of 15 AprAB proteins conformed to the common set in the two sites. The proteins in HAV were assigned to *Desulfobacterales* (15), *Desulfovibrionales* (2), *Nitrospirales* (1), *Sedimenticola* (1) and *Syntrophobacterales* (2). Proteins in PRI were assigned to *Desulfobacterales* (21), *Chromatiales* (5), *Syntrophobacterales* (3), *Clostridiales* (2), *Desulfovibrionales* (2), *Hydrogenophilales* (2) and *Sedimenticola* (1). The presence of protein signatures for active sulphite reduction in HAV and PRI, agrees also with the identification of

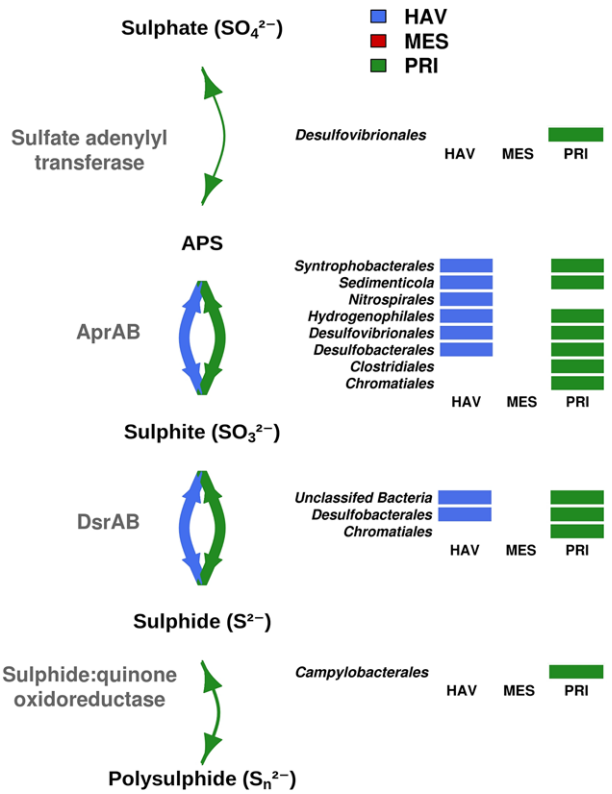

Figure 4. Reconstruction of the sulphur metabolism patterns in microbial communities inhabiting petroleum-polluted marine sediments based on the proteome analysis. The presence of enzymes for each transformation (linked by solid lines) and the taxonomic affiliation of polypeptides are shown. The thickness of the solid lines represents the relative number of enzymes (referred to the total number proteins assigned to these pathways) associated to each of the transformations in the pathway. Transformations in the sulphur metabolism for which no proteome evidence were found (e.g., sulphur assimilation metabolism via ATP sulfurilase) are not indicated.

ten heterodisulfide reductases in both sediments (five each) but not in MES; they were assigned to *Desulfobacterales* (Supporting Information Table 1). Such proteins could provide electrons for sulphite reduction, although, in analogy with methanogenic archaea, it was also speculated that they can also support the generation of a proton motive force [52].

One sulfate adenylyltransferase converting sulphate (SO_4^{2-}) to adenylyl sulphate (binned to *Desulfovibrionales*), two sulfide:quinone oxidoreductases converting *n* sulphide (*n* HS^-) to polysulphide, a defensive HS-oxidation pathway implying the dump of excess electrons from the cytoplasm/membrane (binned to *Campylobacterales*), and a rhodanese involved in the detoxification of cyanide (CN^-) (binned to *Methanosarcinales*), were only found in PRI. Taken together, the PRI microbial community contained high number of proteins involved in various metabolic pathways of both oxidised and reduced sulphur intermediates. Note that, in contrast to sulphite reduction (see above), gene transcripts for the oxidation and detoxification of sulphur compounds were neither found in the Deepwater Horizon deep-sea plume [12], nor in HAV and MES, suggesting the environmental settings in PRI could particularly enrich for those processes.

3.5 Community metabolic activity associated with biodegradation

Only one relevant protein, a carboxymuconolactone decarboxylase (EC: 4.1.1.4) involved in the protocatechuate catabolism, was identified in the metaproteomes (Supporting Information Table 1). The protein, identical to EGD01850 from *Burkholderiales* (100% sequence identity), was only found in HAV and PRI. This suggests that the examined metaproteomes contained minimal signatures for active biodegradation pathways, possibly because of the low rates of biodegradation processes in chronically petroleum-polluted sediments that are limited by low oxygen (or the presence of other forms of organic matter). This environment encouraged the prevalence of proteins involved in the metabolism of C_1–compounds, suggesting the latter segment of the carbon cycle is more active under the given conditions.

Metabolome profiling might be more sensitive in the detection of presumptive chemical signatures indicating biodegradation capabilities of petroleum constituents. Our protocol comprised of the isolation of metabolites obtained from sediment material followed by a metabolome-wide scan via a combination of mass spectrometry (MS) with liquid chromatography (LC) separation. A total of 1485 (LC-MS negative mode) and 3390 (LC-MS positive mode) mass features were found in each analysis after deconvolution (Supporting Information Table 2). Empirical formulas were assigned to accurate masses with a maximum error of 5 ppm using a CEU Mass Mediator (http://biolab.uspceu.com/mediator), and putative chemical species were identified.

Only 24 out of 4776 metabolite mass features (or 0.5% of the total) were tentatively attributed as pollutants or chemical intermediates, thus suggesting that the accumulation of those compounds occurred at a low level, reflecting low degradation rates. It is therefore important to evaluate whether such subtle contribution can be considered to fall within a common range. It is notable, however, that no report to date has described the metabolomic profiling of microbial communities in other contaminated marine sediments; therefore, little is known about whether the observed results are within a common range. The fact that HCB are the specialists for the degradation of alkanes and polycyclic aromatic hydrocarbons (PAH) [5], and that those were absent in our datasets (see Fig. 2), together with the lower rates of degradation under anoxic conditions, may agree with the lack of detection of such chemical signatures in the three investigated sites at a higher level. In addition to that, it is noteworthy that protein signatures for phosphorous uptake and metal reduction, often stimulated by oil contamination [12], were not found in our datasets. This suggests that petroleum oil biodegradation

in the chosen experimental sites occurs at a lower level than in the recently reported studies on Deepwater Horizon or other contaminated sites.

Having said that, we are fully aware about the limitations of MS which may introduce a bias certain due to the secondary reactions in the ion source and collision reactions in the MS and that the identification was tentative. Additionally, to ensure the metabolite identity, pure reference compounds for MS/MS analysis are needed in further experiments to unambiguously identify the substrates/pollutants and the degradation intermediates.

4 Concluding remarks

In conclusion, by examining the metaproteomes and metabolomes of three chronically polluted sites, we found that the examined sites contained only minimal signatures of active biodegradation pathways, possibly because of the low rates of biodegradation processes in chronically petroleum-polluted sediments that are limited by the presence of low oxygen (or presence of other forms of bioavailable organic matter). This environment encouraged the prevalence of proteins involved in the metabolism of C_1–compounds, suggesting the latter segment of the carbon cycle is more active under the given conditions. Our study highlights the presence of methanotrophic bacteria that can oxidise methane through sequential reactions catalysed by a series of enzymes including methane monooxygenase, methanol dehydrogenase, formaldehyde dehydrogenase and formate dehydrogenase. This full conversion was suggested to be active only in the HAV sampling site, which corresponds to the highest concentration of oxygen. MES and PRI did not show evidence for active methane oxidizers, but rather displayed a high diversity of methanol-consuming bacteria, which was also observed in HAV. Methanol, which may be produced as an intermediate of organic matter (and hydrocarbon) biodegradation, can thus be used by prokaryotic communities inhabiting all three sites as another source of carbon and energy [53]. Our results have revealed the presence of microorganisms presumably active in methane oxidation to be uniquely present in HAV. The first step in the aerobic methane oxidation was only found in HAV, agreeing with the higher O_2 concentration in this site compared with MES and PRI. Additionally, all three sediments contained microorganisms that utilise C_1 compounds such as methanol. Accordingly, the ability to utilise methanol and select other single carbon compounds (but not methane) was found in MES and PRI, whereas PRI and HAV were populated by trimethylamine-utilising microbes. Our results (Fig. 3 showing the simplified metaproteomics-based reconstruction of methane and methanol metabolism) displayed the contributions of different archaeal and bacterial groups and their link to active methane and methanol cycling (three groups in HAV and six in MES and four in PRI). Among the eight groups involved in those metabolisms, only one group (*Methanosarcinales*) was found in all three samples. Figures 3 and 4 depict possible microbial metabolic networks and also point at syntrophic interactions. Seemingly, individual members of the network could operate only a small part of the particular pathway. We hypothesise that the identified proteins do represent enzymes for predominant reactions and that corresponding transformations may be complementary to those supported by other community members making, therefore, the entire pathway complete. Furthermore, the results of this study draw attention to the yet untapped diversity of proteins from archaea and bacteria operating in the Mediterranean Sea sediments under conditions of limited oxygen concentrations.

This research was supported by the European Community Projects KILL-SPILL *(*FP7-KBBE-2012-312139*)*,MAGICPAH *(*FP7-KBBE-2009-245226*),* MicroB3 *(*OCEAN2011.2-287589*) and* ULIXES *(*FP7-KBBE-2010-266473*). We thank EU Horizon 2020 Program for the support of the Project INMARE H2020-BG-2014-2634486. This work was further funded by grants BIO2011-25012, PCIN-2014-107 and BIO2014-54494-R from the Spanish Ministry of Economy and Competitiveness. The present investigation was also funded by the Spanish Ministry of Economy and Competitiveness within the ERA NET IB2, grant number ERA-IB-14-030. CB and DR would like to acknowledge funding from the* Spanish Ministry of the Economy and Competitiveness *(*CTQ2014-55279-R*). We would like to thank the PRIDE team for providing data deposition support.*

The authors have declared no conflict of interest.

5 References

[1] Liang, Y., VanNostrand, J. D., Deng, Y., He, Z. et al., Functional gene diversity of soil microbial communities from five oil-contaminated fields in China. *ISME J.* 2011, *5*, 403–413.

[2] Mason, O. U., Hazen, T. C., Borglin, S., Chain, P. S. et al., Metagenome, metatranscriptome and single-cell sequencing reveal microbial response to Deepwater Horizon oil spill. *ISME J.* 2012, *6*, 1715–1727.

[3] Gutierrez, T., Singleton, D. R., Berry, D., Yang, T. et al., Hydrocarbon-degrading bacteria enriched by the Deepwater Horizon oil spill identified by cultivation and DNA-SIP. *ISME J.* 2013, *7*, 2091–2104.

[4] Kimes, N. E., Callaghan, A. V., Aktas, D. F., Smith, W.L. et al., Metagenomic analysis and metabolite profiling of deep-sea sediments from the Gulf of Mexico following the Deepwater Horizon oil spill. *Front. Microbiol.* 2013, *4*, 50.

[5] Head, I. M., Jones, D. M., Röling, W. F., Marine microorganisms make a meal of oil. *Nat. Rev. Microbiol.* 2006, *4*,173–182.

[6] Kostka, J. E., Prakash, O., Overholt, W. A., Green, S. J. et al., Hydrocarbon-degrading bacteria and the bacterial community response in gulf of Mexico beach sands impacted by the deepwater horizon oil spill. *Appl. Environ. Microbiol.* 2011, *77*, 7962–7974.

[7] Beazley, M. J., Martinez, R. J., Rajan, S., Powell, J. et al., Microbial community analysis of a coastal salt marsh affected by the Deepwater Horizon oil spill. *PLoS One* 2012, *7*, e41305.

[8] Ortmann, A. C., Anders, J., Shelton, N., Gong, L. et al., Dispersed oil disrupts microbial pathways in pelagic food webs. *PLoS One* 2012, *7*, e42548.

[9] Rivers, A. R., Sharma, S., Tringe, S. G., Martin, J. et al., Transcriptional response of bathypelagic marine bacterioplankton to the Deepwater Horizon oil spill. *ISME J.* 2013, *7*, 2315–2329.

[10] Golyshin, P. N., Werner, J., Chernikova, T. N., Tran, H. et al., Genome sequence of *Thalassolituus oleivorans* MIL-1 (DSM 14913T). *Genome Announc.* 2013, *1*, e0014113.

[11] Kube, M., Chernikova, T. N., Al-Ramahi, Y, Beloqui, A. et al., Genome sequence and functional genomic analysis of the oil-degrading bacterium *Oleispira antarctica*. *Nat. Commun.* 2013, *4*, 2156.

[12] Lu, Z., Deng, Y., VanNostrand, J. D., He, Z. et al., Microbial gene functions enriched in the Deepwater Horizon deep-sea oil plume. *ISME J.* 2012, *6*, 451–460.

[13] Hazen, T. C., Dubinsky, E. A., DeSantis, T. Z., Andersen, G. L. et al., Deep-sea oil plume enriches indigenous oil-degrading bacteria. *Science* 2010, *330*, 204–208.

[14] Acosta-González, A., Rosselló-Móra, R., Marqués, S., Characterisation of the anaerobic microbial community in oil-polluted subtidal sediments: aromatic biodegradation potential after the Prestige oil spill. *Environ. Microbiol.* 2013, *15*, 77–92.

[15] Kluser, S., Richard, J. P., Giuliani, G., DeBono, A. et al., Illegal oil discharge in European Seas. Coll. Environment Alert Bulletin, UNEP/DEWA-Europe/GRID-Geneva, 2006, pp. 19–22.

[16] Daffonchio, D., Ferrer, M., Mapelli, F., Cherif, A. et al., Bioremediation of southern Mediterranean oil polluted sites comes of age. *Nat. Biotechnol.* 2013, *30*, 743–748.

[17] Pavlakis, P., Tarchi, D., Sieber, A. J., On the monitoring of illicit wessel discharges: a reconnaissance study in the Mediterranean Sea. European Commission, EUR 19906 EN. 2001, pp. 3–13.

[18] Ferraro, G., Bernardini, A., David, M., Meyer-Roux, S. et al., Towards an operational use of space imagery for oil pollution monitoring in the Mediterranean basin: a demonstration in the Adriatic Sea. *Mar. Pollut. Bull.* 2007, *54*, 403–422.

[19] Fava, F., Bertin, L., Fedi, S., Zannoni, D., Methyl-beta-cyclodextrin-enhanced solubilisation and aerobic biodegradation of polychlorinated biphenyls in two aged-contaminated soils. *Biotechnol. Bioeng.* 2003, *81*, 381–390.

[20] Head, I. M., Bioremediation: towards a credible technology. *Microbiology* 1998, *144*, 599–608.

[21] Röling, W. F., Ferrer, M., Golyshin, P. N., Systems approaches to microbial communities and their functioning. *Curr. Opin. Biotechnol.* 2010, *21*, 532–538.

[22] Moran, M. A., Satinsky, B., Gifford, S. M., Luo, H. et al., Sizing up metatranscriptomics. *ISME J.* 2013, *7*, 237–243.

[23] Seifert, J., Herbst, F. A., Halkjaer Nielsen, P., Planes, F. J. et al., Progress and applications in metaproteogenomics for bridging the gap between genomic sequences and metabolic functions in microbial communities. *Proteomics* 2013, *13*, 2786–2804.

[24] Jerby, L., Shlomi, T., Ruppin, E., Computational reconstruction of tissue-specific metabolic models: application to human liver metabolism. *Mol. Syst. Biol.* 2010, *6*, 401.

[25] Rezola, A., Pey, J., deFigueiredo, L. F., Podhorski, A. et al., Selection of human tissue-specific elementary flux modes using gene expression data. *Bioinformatics* 2013, *29*, 2009–2016.

[26] Pey, J., Tobalina, L., deCisneros, J. P., Planes, F. J., A network-based approach for predicting key enzymes explaining metabolite abundance alterations in a disease phenotype. *BMC Syst. Biol.* 2013, *7*, 62.

[27] Zamboni, N., Kümmel, A., Heinemann, M., AnNET: a tool for network-embedded thermodynamic analysis of quantitative metabolome data. *BMC Bioinformatics* 2008, *9*, 199.

[28] Attias, L., Bucchi, A. R., Maranghi, F., Holt, S. et al., Crude oil spill in sea water: an assessment of the risk for bathers correlated to benzo(a)pyrene exposure. *Cent. Eur. J. Public Health* 1995, *3*, 142–145.

[29] Genovese, M., Crisafi, F., Denaro, R., Cappello, S. et al., Effective bioremediation strategy for rapid in situ cleanup of anoxic marine sediments in mesocosm oil spill simulation. *Front. Microbiol.* 2014, *5*, 162.

[30] Denaro, R., D'Aria, G., Di Marco, G., Genovese, M. et al., Assessing terminal restriction fragment length polymorphism suitability for the description of bacterial community structure and dynamics in hydrocarbon-polluted marine environments. *Environ. Microbiol.* 2005, *7*, 78–87.

[31] Cappello, S., Santini, S., Hassanshahian, M., Yakimov, M. M., Characterisation of oil-degrading bacteria isolated from Bilge water. *Water Air Soil Pollut.* 2012, *223*, 3219–3226.

[32] Grasshoff, K., Kremling, K., Ehrhardt, M., In: *Methods of Seawater Analysis*, 3rd ed. WILEY-VCH, Weinheim 1999, pp. 263–271.

[33] Méndez-García, C., Mesa, V., Sprenger, R. R., Richter, M. et al., Microbial stratification in low pH oxic and suboxic macroscopic growths along an acid mine drainage. *ISME J.* 2014, *8*, 1259–1274.

[34] Bradford, M. M., Rapid and sensitive method for the quantitation of microgram quantities of protein utilising the principle of protein-dye binding. *Anal. Biochem.* 1976, *72*, 248–254.

[35] Shevchenko, A., Tomas, H., Halvis, J, Olsen, J. V., Mann, M., In situ digestion for mass spectrometric characterisation of proteins and proteomes. *Nat. Protol.* 2006, *1*, 2856–2860.

[36] Jagtap, P., Goslinga, J., Kooren, J. A., McGowan, T. et al., A two-step database search method improves sensitivity in peptide sequence matches for metaproteomics and proteogenomics studies. *Proteomics* 2013, *13*, 1352–1357.

[37] Hansen, S. H., Stensballe, A., Nielsen, P. H., Herbst, F. A., Metaproteomics: evaluation of protein extraction from activated sludge. *Proteomics* 2014, *14*, 2535–2539.

[38] Cox, J., Mann, M., MaxQuant enables high peptide identification rates, individualised p.p.b.-range mass accuracies and proteome-wide protein quantification. *Nat. Biotechnol.* 2008, *26*, 1367–1372.

[39] Gupta, N., Pevzner, P. A., False discovery rates of protein identifications: a strike against the two-peptide rule. *J. Proteome Res.* 2009, *8*, 4173–4181.

[40] Vizcaíno, J. A., Côté, R. G., Csordas, A., Dianes, J.A. et al., The PRoteomics IDEntifications (PRIDE) database and associated tools: status in 2013. *Nucleic Acids Res.* 2013, *41*, D1063–D1069.

[41] Ménigaud, S., Mallet, L., Picord, G., Churlaud, C. et al., GOHTAM: a website for genomic origin of horizontal transfers, alignment and metagenomics. *Bioinformatics* 2012, *28*, 1270–1271

[42] Morris, B. E. L., Herbst, F. A., Bastida, F., Seifert, J. et al., Microbial interactions during residual oil and n-fatty acid metabolism by a methanogenic consortium. *Environ. Microbiol. Rep.* 2012, *4*, 297–306.

[43] Taubert, M., Vogt, C., Wubet, T., Kleinsteuber, S. et al., Protein-SIP enables time-resolved analysis of the carbon flux in a sulfate-reducing, benzene-degrading microbial consortium. *ISME J.* 2012, *6*, 2291–2301.

[44] Herbst, F. A., Bahr, A., Duarte, M., Pieper, D. H. et al., Elucidation of in situ polycyclic aromatic hydrocarbon degradation by functional metaproteomics (protein-SIP). *Proteomics* 2013, *13*, 2910–2920.

[45] Kleindienst, S., Herbst, F. A., Stagars, M., vonNetzer, F. et al., Diverse sulfate-reducing bacteria of the *Desulfosarcina/Desulfococcus* clade are the key alkane degraders at marine seeps. *ISME J.* 2014, *8*, 2029–2044.

[46] Bozinovski, D., Taubert, M., Kleinsteuber, S., Richnow, H. H. et al., Metaproteogenomic analysis of a sulfate-reducing enrichment culture reveals genomic organisation of key enzymes in the m-xylene degradation pathway and metabolic activity of proteobacteria. *Syst. Appl. Microbiol.* 2014, *37*, 488–501.

[47] Mesuere, B., Devreese, B., Debyser, G., Aerts, M. et al., Unipept: tryptic peptide-based biodiversity analysis of metaproteome samples. *J. Proteome Res.* 2012, *11*, 5773–5780.

[48] Jones, D. M., Head, I. M., Grey, N. D., Adams, J. J. et al., Crude-oil biodegradation via methanogenesis in subsurface petroleum reservoirs. *Nature* 2008, *451*, 176–180.

[49] Costa, K. C., Leigh, J. A., Metabolic versatility in methanogens. *Curr. Opin. Biotechnol.* 2014, *29*, 70–55.

[50] Fonseca, P, Moreno, R., Rojo, F., Growth of *Pseudomonas putida* at low temperature: global transcriptomic and proteomic analyses. *Environ. Microbiol. Rep.* 2011, *3*, 329–339.

[51] Moroney, J. V., Ynalvez, R. A., Proposed carbon dioxide concentrating mechanism in *Chlamydomonas reinhardtii*. *Eukaryot. Cell* 2007, *6*, 1251–1259.

[52] Strittmatter, A. W., Liesegang, H., Rabus, R., Decker, I., Amann, J. et al., Genome sequence of *Desulfobacterium autotrophicum* HRM2, a marine sulfate reducer oxidizing organic carbon completely to carbon dioxide. *Environ. Microbiol.* 2009, *11*, 1038–1055.

[53] Siddique, T., Penner, T., Semple, K., Foght, J. M., Anaerobic biodegradation of longer-chain n-alkanes coupled to methane production in oil sands tailings. *Environ. Sci. Technol.* 2011, *45*, 5892–5899.

Capítulo 6: Discusión y consideraciones finales de la tesis doctoral

Contenido del capítulo

Capítulo 6: Discusión, consideraciones finales y conclusión de la Tesis Doctoral

Discusión

La intención de este capítulo es recoger los aspectos comunes más importantes de los 4 trabajos expuestos anteriormente (**capítulo segundo, tercero, cuarto y quinto**) para poder discutirlos de forma conjunta. Como quedará reflejado, los cuatro trabajos publicados que constituyen esta memoria han seguido una línea de investigación común de cuyos resultados podemos extraer una serie de conclusiones generales que se describen a continuación.

1. Características generales de las zonas contaminadas analizadas

En la presente Tesis Doctoral se han analizado 9 zonas marinas contaminadas por la presencia crónica de petróleo o derivados de éste. Ocho de ellas se encuentran localizadas en diferentes puntos (**Figura 16**) repartidos por la cuenca del Mar Mediterráneo, mientras que la restante se encuentra en el Mar Rojo. Esta última zona se seleccionó por su alta temperatura media y porque debido al calentamiento global, representa el posible futuro del Mar Mediterráneo si sus aguas siguen aumentando de temperatura. Concretamente, las zonas a estudiar, ordenadas de mayor a menor latitud, fueron:

- La zona del Mar de Linguria (golfo de Génova, Italia; 44º 22' 25,75" N, 8º 4º' 59,58" E) donde se hundió el carguero Haven (**HAV**) el 11 de septiembre de 1991, vertiendo 50.000 toneladas de petróleo en el Mar Mediterráneo (Viarengo et al., 2007).

- El puerto de Ancona (**ANC**, Italia; 43º 37' N, 13º 30' 15" E) el cual es un importante puerto industrial, además de terminal de ferrys, en el Mar Adriático, fuertemente contaminado con hidrocarburos poliaromáticos y metales pesados (Dell'Anno et al., 2009).

- El puerto de Messina (**MES**, Sicilia, Italia; 38º 11' 42,27" N, 15º 34' 25,01" E), que sufre la entrada continua de petróleo debido al intenso tráfico marí-

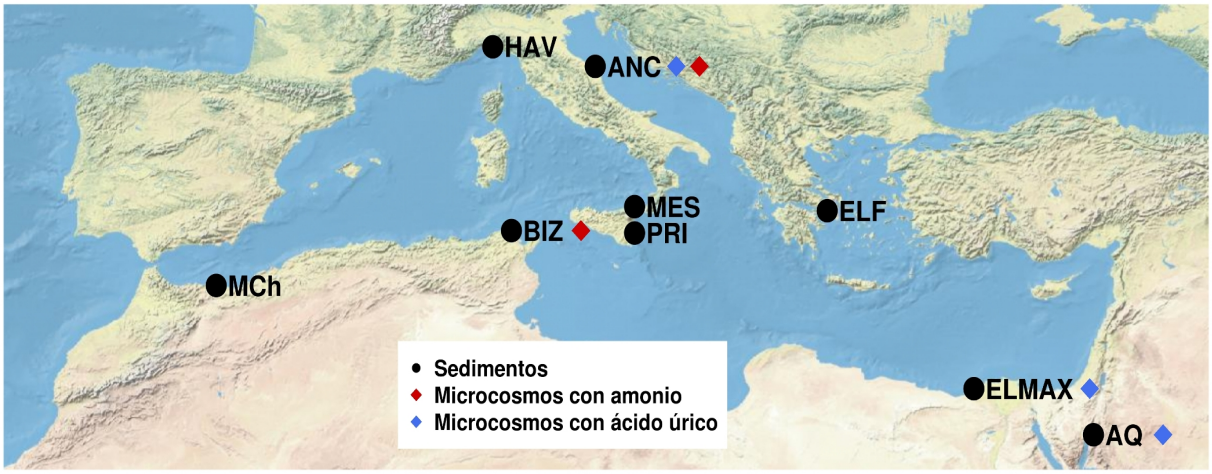

Figura 16: Localización de las zonas muestreadas. Mar Chica (Marruecos), MCh; La zona de hundimiento del carguero Haven (costa de Génova, Italia), HAV; puerto de Ancona (Italia), ANC; puerto de Priolo Gargallo (Siracusa, Italia), PRI; Puerto de Messina (Sicilia, Italia), MES; lago Bizerta (Túnez), BIZ; El Max (Egipto), ELMAX; bahia de Elefsina (Grecia), ELF. Los rombos rojos indican aquellas muestras en donde se realizaron experimentos de microcosmos enriquecidos con amonio, y los azules microcosmos enriquecidos con ácido úrico.

timo y al limitado régimen hidrodinámico debido a su área limitada (Cappello et al., 2007b).

- La costa adyacente a una refinería de petróleo localizada en la bahía de Elefsina (**ELF**, 38º 2' 16,28'' N, 23º 30' 45,85'' E), al Noroeste de Atenas (Grecia), contaminada por los escapes de petróleo producidos desde la refinería (Nikolopoulou et al., 2013).

- El lago de Bizerta (**BIZ**, 37º 16' 7,72'' N, 9º 53' 19,61'' E), localizado en la zona Norte de Túnez, fuertemente industrializada y sometida a continuos vertidos de contaminantes industriales, agrícolas y aguas residuales (Barhoumi et al., 2014).

- El puerto de Priolo (**PRI**) Gargallo (Siracusa, Italia; 37º 10' 27,46'' N, 15º 12' 7,51'' E), caracterizado por la fuerte industrialización y el tráfico intensivo de cargueros que transportan tanto crudo como petróleo refinado (Di Leonardo et al., 2014).

- El lago de Mar Chica (**MCh**, 35° 8' 52'' N, 2° 50' 53'' O), en la zona Noroeste de la costa Mediterránea de Marruecos, que a pesar de su interés biológico como ecosistema, recibe una entrada continua de contaminación procedente de actividades industriales y agrícolas (Piazza et al., 2009).

- La zona de El Max (**ELMAX**, 31º 9' 31,20'' N, 29º 50' 28,20'' E), localizada al Oeste de la ciudad de Alejandría (Egipto), considerada la zona costera más contaminada del área de Alejandría debido a sus índices de metales pesados, hidrocarburos poliaromáticos y otros derivados del petróleo (Ranya, 2014).

- La zona del Golfo de Acaba (**AQ**, 30º 22' 42'' N, 25º 24' 57'' E), en las costas de Jordania en la zona Norte del Mar Rojo, el cual es el mar del hemisferio Norte más tropical y contiene una gran cantidad de terminales petrolíferas desde donde se mueven entre 20-30 millones de toneladas al año, produciendo vertidos accidentales tanto desde las terminales como desde los barcos usados para su transporte (Al-Najjar et al., 2011).

El conjunto de las zonas de muestreo abarca diferentes zonas clave del Mar Mediterráneo, con parámetros geográficos, ambientales y geoquímicos (**Tabla 2**) diferentes: se abarca una enorme área geográfica, con amplios rangos de latitud (de 44º a 30º N) y longitud (de 2º a 25º E); la temperatura oscila desde los 13,0 ºC (PRI) hasta los 26,5ºC (AQ); la concentración de O_2 indica que encontramos tanto muestras óxicas como anóxicas (PRI) o semi-anóxicas (MES); y la concentración de hidrocarburos oscila entre 116 y 260.000 ppm.

Se tomó la decisión de trabajar con muestras de sedimentos en lugar de agua marina, ya que numerosos estudios han demostrado que en zonas sometidas a contaminación crónica, los contaminantes tienden a depositarse de forma más acusada en los sedimentos (Mandalakis et al., 2004; Mandalakis et al., 2014). Por lo tanto, el estudio de los mismos es determinante para

Localización	Mar Mediterráneo							Mar Rojo
Código de la muestra	ELF	HAV	PRI	BIZ	ELMAX	Mch	MES	AQ
Profundidad (m)	15,7	78,0	6,0	1,0	9,2	32,0	1,0	18,0
[Hidrocarburos del petróleo] (ppm)	500	260000	4000	116	1822	5100	1000	2400
Temperatura (ºC)	13,0	15,0	19,0	13,3	20,0	21,3	23,0	26,0
O2 Disuelto (mg/L)	6,0	6,0-6,5	0,0	3,0	18,0	22,0	1,0-2,2	20,0
pH	7,5	8,05	6,85	7,76	7,59	8,62	7,37	8,3
Conductividad (Ms/cm)	57,0	49,0	49,0	13,1	77,0	53,6	70,0	89,0
Amonio (mkmol/L)	20,2	0,6-0,7	420,0	8,4	8,8	60,0	7,0	8,5
Calcio (mg/L)	50,94	420	408	35,8	71,3	87,37	430	125,78
Carbono orgánico disuelto (mg/L)	143,00	5,00	125,00	1,00	59,53	130,00	50,00	26,00
Carbono orgánico particulado (µM)	1,20	1,40	1,89	2,80	1,37	2,01	1,44	2,29
[Microelementos] [nM]	150,30	392,00	883,00	238,03	411,00	67,30	408,00	238,03
Células por gramo de sedimento	~$2,30^{e+08}$ ($1,40^{e+08}$)	~$1,90^{e+09}$ ($1,15^{e+09}$)	~404^{+e08} ($3,67^{e+08}$)	~$2,63^{e+08}$ ($1,44^{e+08}$)	~$3,03^{e+08}$ ($1,98^{e+08}$)	~$2,63^{e+08}$ ($2,29^{e+08}$)	~$2,22^{e+08}$ ($1,41^{e+08}$)	~$3,43^{e+08}$ ($1,93^{e+08}$)

Tabla 2: Características fisico-químicas de las muestras seleccionadas

estudiar el efecto de la contaminación crónica en las comunidades microbianas.

2. Tipos de estudios y objetivo general

En la presente Tesis Doctoral se pretende dar un paso más allá de un simple análisis de biodiversidad de las zonas seleccionadas del Mar Mediterráneo y Mar Rojo. Para ello, se ha combinado el uso de diferentes técnicas "-ómicas":

1) La extracción directa y secuenciación masiva de ácidos nucleicos para fenotipado y estudio de diversidad mediante análisis de ARN 16S.
2) Análisis del contenido genómico de las comunidades microbianas mediante secuenciación masiva (metagenómica) y su posterior análisis para la predicción de las rutas de biodegradación de hidrocarburos.
3) Estudio, a nivel de sistema, del perfil de los metabolitos hallados en cada una de las comunidades microbianas, a través del uso de metabolómica no dirigida.
4) Validación experimental, mediante el uso de metabolómica dirigida sobre enriquecimientos selectivos, de las capacidades catabólicas predichas mediante el análisis de secuencias.
5) Estudio de la expresión de proteínas de las comunidades microbianas por metaproteómica.

Estos análisis se realizaron sobre las muestras de ELF, HAV, PRI, MES, BIZ, ELMAX, MCh y AQ, donde los puntos 1-4) han sido la base para los estudios realizados en el **capítulo 2**, mientras que el 5) es la base para los estudios del **capítulo 5**. El objetivo es determinar cómo la contaminación crónica que caracteriza a estos sedimentos afecta a la distribución, expresión de proteínas y capacidad catabólica de las comunidades microbianas que los habitan, atendiendo a la influencia de los diferentes factores ambientales y geoquímicos de cada zona.

Por otra parte, se construyeron microcosmos a partir de los sedimentos de las muestras anteriores junto a una muestra de ANC, añadiendo crudo ligero como fuente de carbono y diferentes fuentes de nitrógeno (NH_4 y ácido úrico) como agentes bioestimulantes. Esto tiene por objetivo enriquecer y seleccionar bacterias marinas de gran potencial para degradar petróleo, utilizando diferentes bioestimulantes. Sobre ellos se llevaron a cabo los siguientes procedimientos:

1) Análisis de parámetros relacionados con la actividad metabólica.
2) Análisis de diversidad y contenido genómico a partir de la secuenciación directa de ácidos nucleicos.
3) Aislamiento de bacterias relevantes en el proceso de degradación.
4) Predicción de las rutas de biodegradación de hidrocarburos a partir de los datos de secuenciación masiva.

Los pasos 2-4) sólo se realizaron en los microcosmos de 4 de las muestras (ANC, BIZ, ELMAX y AQ), ya que fueron los únicos para los que se obtuvieron enriquecimientos (tanto con NH4 como con ácido úrico) estables y estadísticamente significativos. Los puntos 1-3) sientan las bases del **capítulo 3,** mientras que el 4) constituye el núcleo central del **capítulo 4**. Este último tiene por objetivo analizar el efecto que los diferentes bioestimulantes ejercen sobre las diferentes rutas de biodegradación.

El hilo conductor que une los estudios expuestos del capítulo 2 al 5 se resume en la **Figura 17**. A continuación procederemos a discutir los resultados que se pueden obtener a partir de los cuatro estudios realizados.

3. Efecto de los factores geoquímicos y la bioestimulación sobre las comunidades microbianas

Para analizar el efecto de los diferentes factores y la bioestimulación sobre la microbiota nos centraremos primero en su influencia sobre la estructura y diversidad de las comunidades microbianas, y posteriormente discutiremos su efecto sobre la diversidad catabólica observada en las zonas estudiadas.

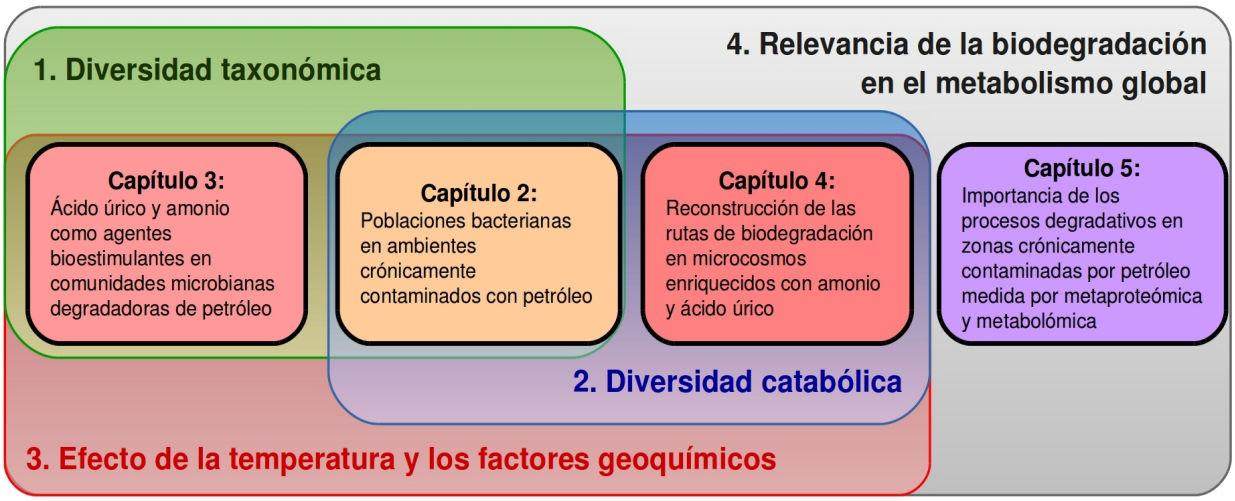

Figura 17: Estructuración de la discusión de la Tesis Doctoral. Los capítulos segundo y tercero nos permiten discutir la diversidad taxonómica de las zonas analizadas. Los capítulos segundo y cuarto permiten profundizar acerca de la diversidad catabólica de las zonas analizadas. Los capítulos segundo, tercero y cuarto permiten observar la influencia de diferentes fuentes de nitrógeno sobre las comunidades microbianas. Por último, el quinto capítulo establece la contribución al metabolismo global de los procesos de biodegradación.

3.1. Diversidad bacteriana en las zonas estudiadas y correlación con factores geoquímicos y bioestimulación

Una visión general de la distribución taxonómica de las bacterias que componen las comunidades microbianas de los sedimentos y los correspondientes microcosmos analizados (**Figura 18**) muestra que el filo *Proteobacteria* es el más abundante con mucha diferencia, seguido del filo *Bacteroidetes* (en la mayoría de los casos, excepto en AQ y ANC). La fuerte presencia del filo *Proteobacteria*, sobre todo de la clase *y-Proteobacteria,* es habitual en este tipo de muestras debido a la abundancia de taxones con miembros capaces de degradar hidrocarburos (Harayama et al., 2004; Head et al., 2006). El filo *Bacteroidetes* está ampliamente distribuido en ambientes marinos y suele encontrarse en hábitats ricos en nutrientes ya que muchos de sus miembros son capaces de degradar partículas de materia orgánica de alto peso molecular y biopolímeros como proteínas y polisacáridos (Bauer et al., 2006; Kabisch et al., 2014). Por lo tanto, la presencia mayoritaria de estos dos filos coincide con la capacidad biodegradativa de muchos de sus miembros. Además, la presencia de estos filos ha sido detectada en otras zonas donde se han producidos vertidos accidentales (**Figura 18**), como el ocurrido en la cosa del golfo de México (mayoría de *Proteobacteria*) o el incidente del *Prestige* en Galicia (mayoría de *Proteobacteria* y *Bacteroidetes*).

Sin embargo, en comparación con las zonas del golfo de México y el vertido del Prestige, es llamativa la ausencia de miembros del género *Alcanivorax*, *Oleispira*, *Thalassolituus y Oleiphilus,* o la reducida presencia de *Cycloclasticus*, ampliamente conocido por su ubicuidad y su capacidad para degradar hidrocarburos alifáticos y/o aromáticos (Yakimov et al., 1998; Dyksterhouse et al., 1995; ver sección 3.1 del **capítulo 1**). No obstante, a pesar de su ausencia en las muestras de sedimentos, los resultados de los experimentos con microcosmos sí muestran un aumento de la abundancia de estos grupos (**Figura 19**) tras un enriquecimientos con crudo ligero y distintas fuentes de nitrógeno. Así, las familias *Alcanivoraceae* y *Oceanospirillaceae* no son detectadas en los sedimentos o sólo se detectan en algunas muestras en un número muy bajo (< 0,5%), pero alcanzan una abundancia relativa de entre 3,0 y 19,0% de las secuencias de ARN 16S en los microcosmos. Estos resultados son indicativo de que, aunque las bacterias hidrocarbonoclásticas no hayan sido detectadas en las secuencias de ARN 16S de los sedimentos, su ausencia no es total, sino que permanecen en muy baja concentración con respecto a los otros grupos bacterianos, sin ser detectados en la amplificación de los genes

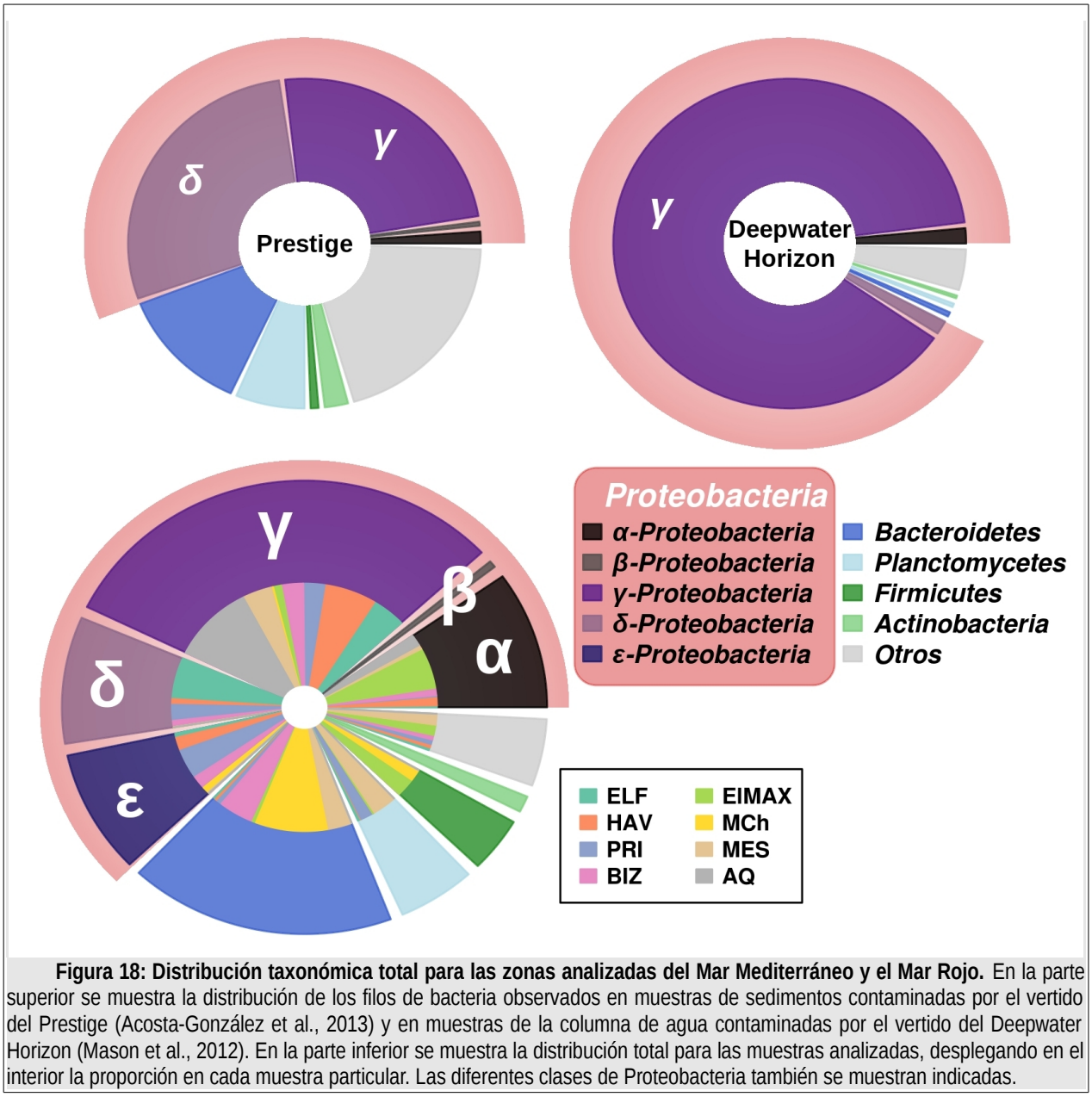

Figura 18: Distribución taxonómica total para las zonas analizadas del Mar Mediterráneo y el Mar Rojo. En la parte superior se muestra la distribución de los filos de bacteria observados en muestras de sedimentos contaminadas por el vertido del Prestige (Acosta-González et al., 2013) y en muestras de la columna de agua contaminadas por el vertido del Deepwater Horizon (Mason et al., 2012). En la parte inferior se muestra la distribución total para las muestras analizadas, desplegando en el interior la proporción en cada muestra particular. Las diferentes clases de Proteobacteria también se muestran indicadas.

de ARN 16S. Otros grupos bacterianos muestran la misma tendencia, como ocurre, por ejemplo, con las familias *Pseudomonadaceae* y *Alteromonadaceae,* que representan entre un 13,8 y un 49,2% de las secuencias de ARN 16S de los microcosmos. Algunos miembros de estos grupos, como los pertenecientes a los géneros *Pseudomonas* o *Marinobacter*, presentan la capacidad para degradar diferentes tipos de hidrocarburos (Fathepure, 2014; Harayama et al., 2004). Ambos géneros sólo han sido detectados en algunas de las muestras de sedimentos; siempre en un porcentaje bajo de las secuencias de ARN de 16S (< 1,39% de *Pseudomonas* y < 2,86% para *Marinobacter*).

Pese a la presencia común de los grupos mayoritarios, se aprecia una notable diferencia en la distribución taxonómica entre unas zonas y otras, tanto en su diversidad como en la abundancia de los diferentes grupos bacterianos. Esto sugiere la posible influencia de los factores geoquímicos sobre la estructura final de las comunidades microbianas. El análisis de las diferentes

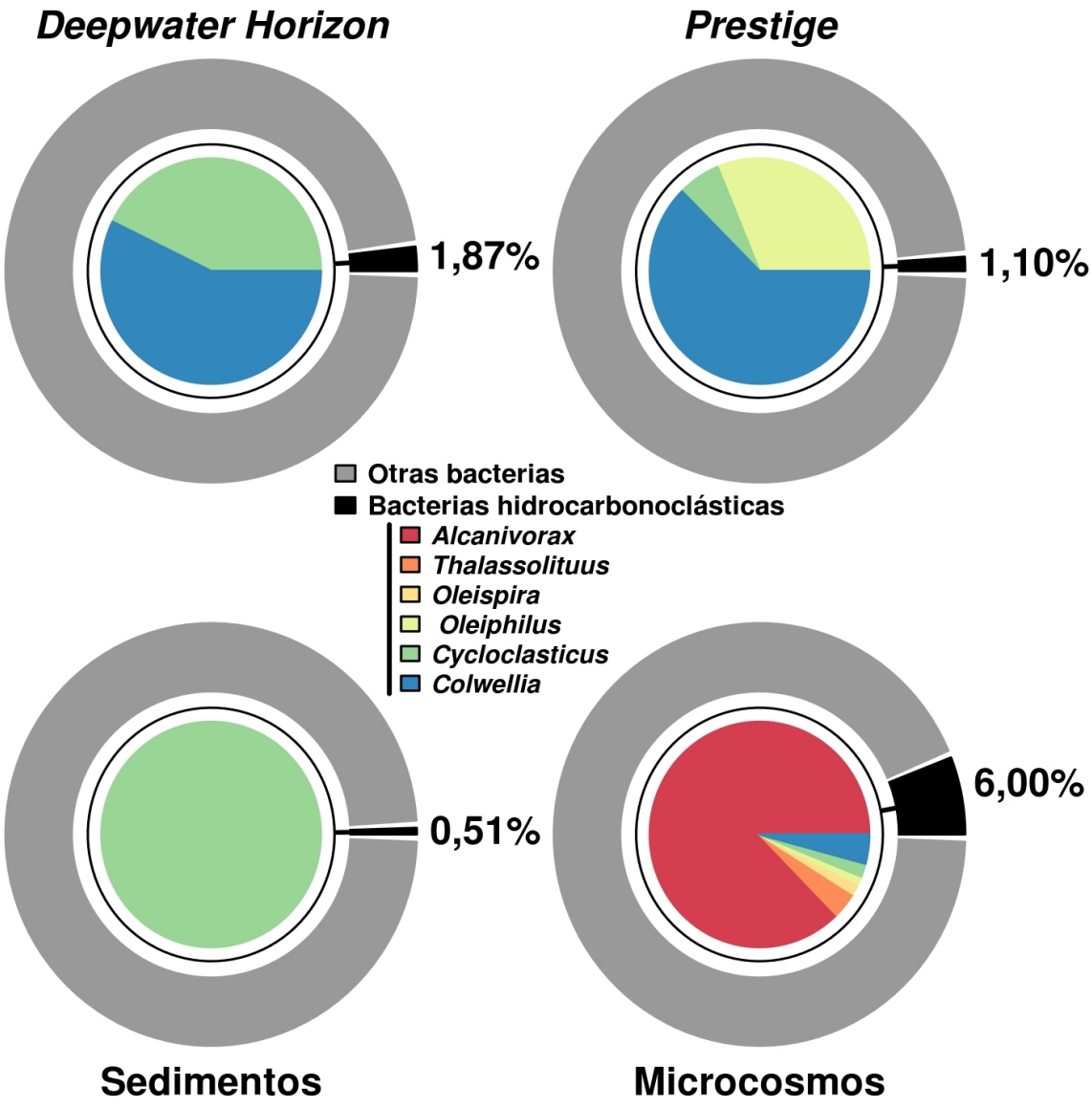

Figura 19: Distribución de las principales bacterias hidrocarbonoclásticas. La parte de arriba muestra la abundancia relativa para este tipo de bacterias en los vertidos del Golfo de México y el *Prestige*, mientras que abajo se muestra la encontrada en las muestras analizadas, para los sedimentos y los microcosmos. Se puede apreciar como, a pesar de que la mayoría de las especies no se detectan en los sedimentos, al analizar los enriquecimientos en los microcosmos estas especies afloran, probando su presencia.

variables sobre el índice de diversidad revela que éste está directamente relacionado con la temperatura y la composición química de los sedimentos, independientemente de otros factores como la concentración de O_2 e hidrocarburos.

Por una parte, se ha demostrado que el índice de diversidad desciende según aumenta la temperatura de los sedimentos (**Figura 20**). Esto se ve bien reflejado en la muestra de AQ, la cual presenta la mayor temperatura de todas, y una comunidad microbiana muy poco diversa (**Figura 21**). Aunque no es la primera vez que se detecta el efecto de la temperatura sobre la biodiversidad microbiana (Bagi et al., 2013; Everroad et al., 2012), es la primera vez que se demuestra en zonas geográfica-

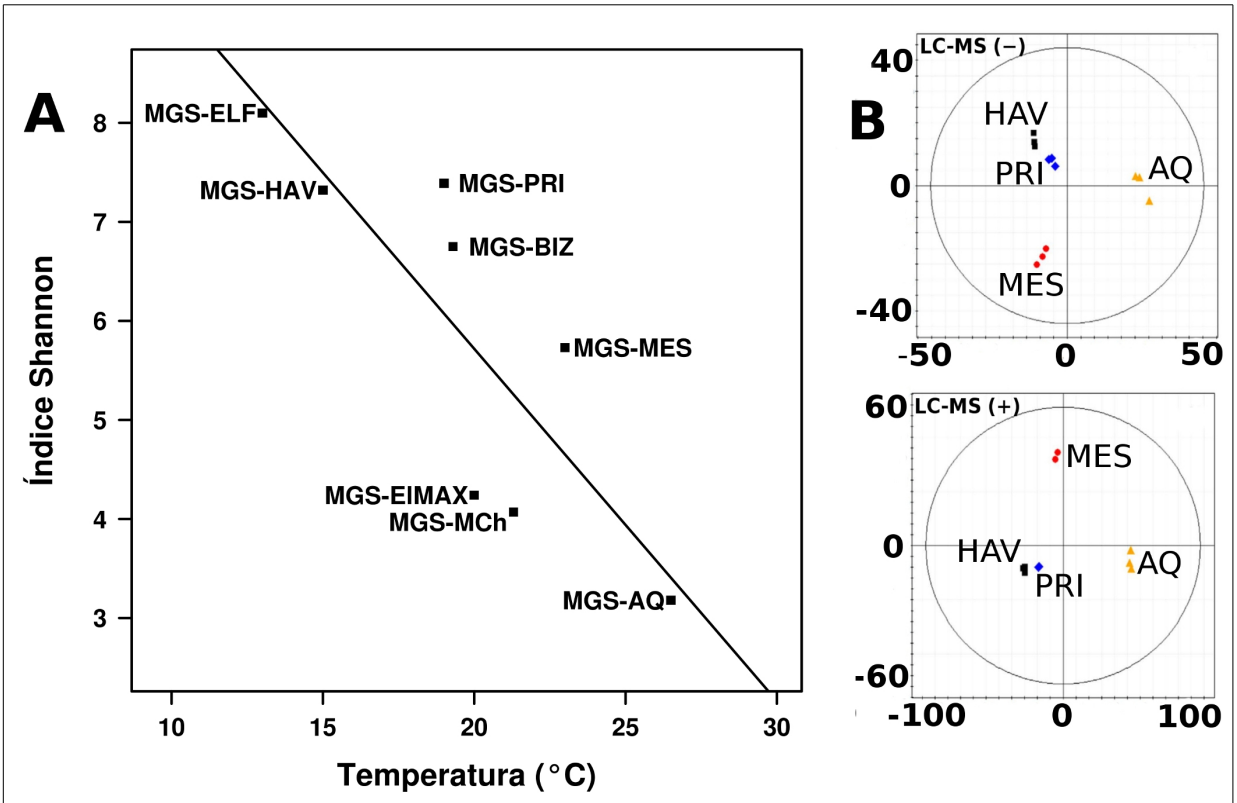

Figura 20: Efecto de la temperatura sobre la diversidad. A) El gráfico muestra la regresión lineal (p-valor=0,0105) del índice Shannon sobre la temperatura de las muestras. B) PCA para las dos técnicas de metabolómica utilizadas sobre 4 de las muestras de sedimentos (Bargiela et al., 2015c)

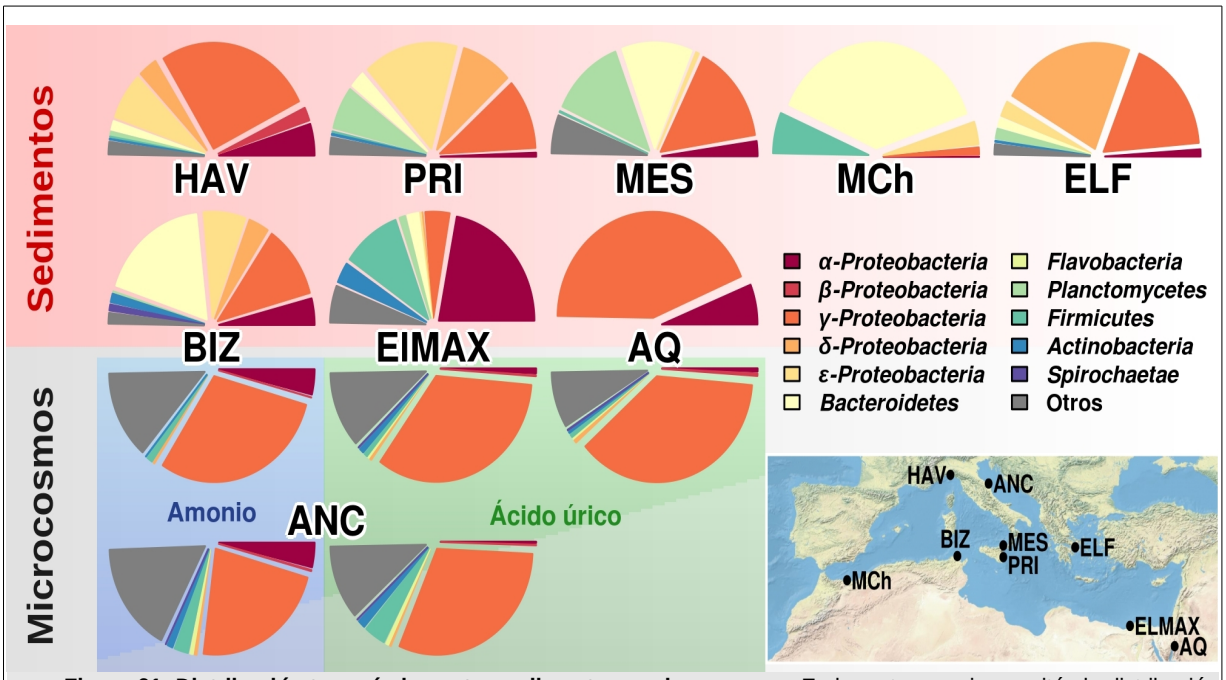

Figura 21: Distribución taxonómica entre sedimentos y microcosmos. En la parte superior se sitúa la distribución taxonómica para las muestras en las que sólo se analizaron los sedimentos (ELF, HAV, PRI, MCh y MES). En la zona intermedia se sitúan aquellas para las que se analizaron muestras de sedimentos y de microcosmos (BIZ, ELMAX y AQ), diferenciando aquellas con microcosmos enriquecido en amonio o en ácido úrico. En la parte inferior se sitúan las dos muestras de microcosmos analizadas de la zona de ANC (Amonio y Ácido úrico).

mente distantes y muy heterogéneas. La temperatura puede afectar a la capacidad de los microorganismos para captar y metabolizar los nutrientes, incluídos los contaminantes (Mendoza, 2014).

Por otra parte, el análisis por componentes principales de la composición química de los sedimentos (**capítulo 2**) ha demostrado que aquellas muestras con una composición de moléculas similar presentan una estructura microbiana semejante. La composición química de los sedimentos viene definida por un lado por los contaminantes (tanto por su composición como por su diversidad) introducidos antropogénicamente en el medio medio marino, y por otro por aquellos metabolitos derivados de la actividad metabólica de las bacterias que lo habitan. Esto es importante ya que estos metabolitos derivados de la acción bacteriana pueden influir a su vez en el crecimiento, expresión génica y actividad metabólica de otros miembros de la comunidad microbiana.

CONCLUSIÓN: La temperatura es el factor geoquímico clave en la biodiversidad microbiana de los sedimentos marinos del Mar Mediterráneo y Mar Rojo crónicamente contaminados. Su aumento en pocos grados se asocia a un descenso de biodiversidad.

Esta correlación puede estar ligada al efecto adicional de otros factores, ya que no se ha demostrado este efecto de la temperatura en otro conjunto de ambientes geográficamente distantes.

Este factor adicional, a raíz de los resultados de esta Tesis Doctoral, puede constituirlo la composición química de los sedimentos: aquellos con composición química similar presentan una composición microbiana parecida.

Si atendemos a los datos mostrados en el **capítulo 4**, el efecto producido por la diferencia en una única especie química, en este caso la fuente de nitrógeno (usando NH_4 o ácido úrico), no da lugar a cambios significativamente diferentes en la composición global de la comunidad microbiana. Así, independientemente del bioestimulante utilizado y los sedimentos analizados, la composición final de la microbiota es bastante similar entre todos los microcosmos (**Figura 21**). Esto apoya la hipótesis de que es el conjunto global de los metabolitos presentes en los sedimentos marinos lo que puede inducir modificaciones relevantes en la comunidad microbiana y no una única molécula individual, como se demuestra en el **capítulo 2**. Pero, por otra parte, en el **capítulo 5** hemos comprobado que los contaminantes representan una mínima parte del perfil metabolómico de los sedimentos. Esto se debe a que son finalmente los metabolitos derivados de la actividad microbiana los que más contribuyen al metaboloma de los sedimentos.

3.2.Diversidad catabólica en las zonas estudiadas y correlación con factores geoquímicos y bioestimulación

Una vez hemos visto cómo la temperatura y la composición química modulan la estructura de la comunidad microbiana, queda preguntarnos si estos factores influyen además en su actividad catabólica ¿Afectan estos factores a la capacidad de los microorganismos para degradar los diferentes compuestos del crudo u otros contaminantes vertidos al medio marino?

Uno de los aspectos más importantes abordados en esta Tesis Doctoral ha sido estudiar la capacidad de degradación de las comunidades microbianas de estas zonas crónicamente contaminadas por hidrocarburos. Para ello se ha analizado la abundancia relativa de genes relacionados con biodegradación de cada muestra y realizado una reconstrucción catabólica que ha permitido predecir la habilidad putativa de cada comunidad microbiana para llevar a cabo el catabolismo de diferentes contaminantes. Para realizar este tipo de reconstrucciones se precisa de una anotación refinada que permita una identificación fiable de las posibles secuencias relacionadas con los procesos de biodegradación. Sin embargo, la mayoría de las secuencias de proteínas en las bases de datos públicas no han sido caracterizadas experimentalmente. Esto, unido al uso rutinario de métodos de asignación de función basados en homología, provoca que se produzcan anotaciones y predicciones de función erróneas (Duarte et al., 2014). Estas carencias hacen que nazca la necesidad de de-

sarrollar un nuevo método de identificación y visualización de estas rutas catabólicas. En el curso de esta Tesis Doctoral se ha elaborado un método computacional de reconstrucción catabólica que permite aliviar estos problemas, resumido a continuación.

3.2.1. Desarrollo del método de reconstrucción catabólica

En un primer paso creamos una base de datos interna de secuencias relacionadas con procesos de degradación de alcanos e hidrocarburos aromáticos, que se encuentran depositadas en las bases de datos. El conjunto de estas secuencias, que contiene secuencias de enzimas caracterizadas experimentalmente, fue publicado en un primer estudio (Guazzaroni et al., 2013) donde se analizaron las rutas de biodegradación presentes en la comunidad microbiana de un suelo contiguo a una planta química. Posteriormente, esta base de datos fue actualizada y optimizada por el grupo del Dr. D. Pieper (Duarte et al., 2014) en la denominada base de datos AromaDeg.

El siguiente paso consiste en la comparación de los diferentes ORF del genoma o metagenoma contra las secuencias de AromaDeg, para lo que se pueden seguirse diferentes criterios. Se comenzó utilizando la herramienta rpsBlast, filtrando los resultados de acuerdo a su *score* (>45) y el *p-value* (<10e^{-3}). Las secuencias seleccionadas fueron finalmente comprobadas manualmente contra la base de datos no redundante (nr) del NCBI (Bargiela et al., 2015c). Posteriormente, se añadió al método un análisis filogenético (Pérez-Pantoja et al., 2010; Sjolander, 2004), por el cual primero las secuencias son filtradas mediante Blast según el porcentaje de identidad (>50%) y la longitud de alineamiento (>50 amino ácidos) con las secuencias de AromaDeg, asignándolas a una familia enzimática. Esto permite la generación de árboles filogenéticos (**Figura 22**) que muestran la proximidad entre las secuencias del metagenóma y las pertenecientes a la familia asignada. El análisis manual de estos árboles permite asignar una función a cada secuencia según su vecino más próximo, ofreciendo un método más fiable de anotación (Bargiela et al., 2015b).

El último paso consiste en el proceso de reconstrucción catabólica, que fue automatizado mediante el uso del lenguaje de programación R y el paquete igraph (Csardi and Nepusz, 2006). Para ello, se diseñó un código enzimático interno que clasifica las enzimas relacionadas con biodegradación según su reacción (Bargiela et al., 2015c). Estas reacciones son ordenadas según su sustrato y producto, comunicándose entre sí a través de un sistema de nodos (especies químicas) y enlaces (las propias reacciones). Esta relación se dispone en una tabla sobre la que se añaden las frecuencias de los diferentes tipos de secuencias enzimáticas, que se utiliza posteriormente para la generación gráfica de la reconstrucción. Este proceso permite generar una red de biodegradación, a partir de datos secuenciación masiva, en la que se pueden incorporar datos de la abundancia de genes que codifican enzimas para cada

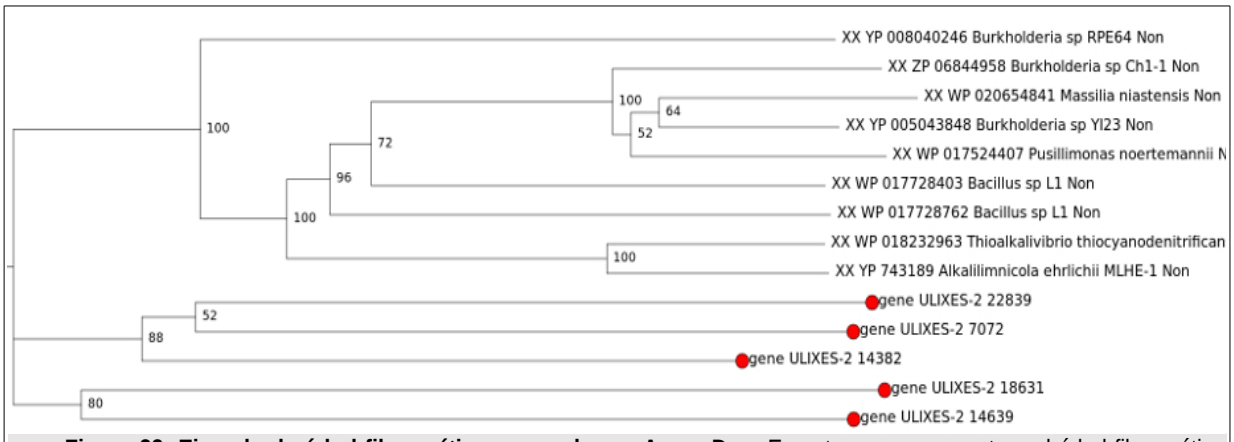

Figura 22: Ejemplo de árbol filogenético generado por AromaDeg. En este caso se muestran el árbol filogenético para la familia de las ftalato dioxigenasas. Las secuencias problema se indican con un punto rojo.

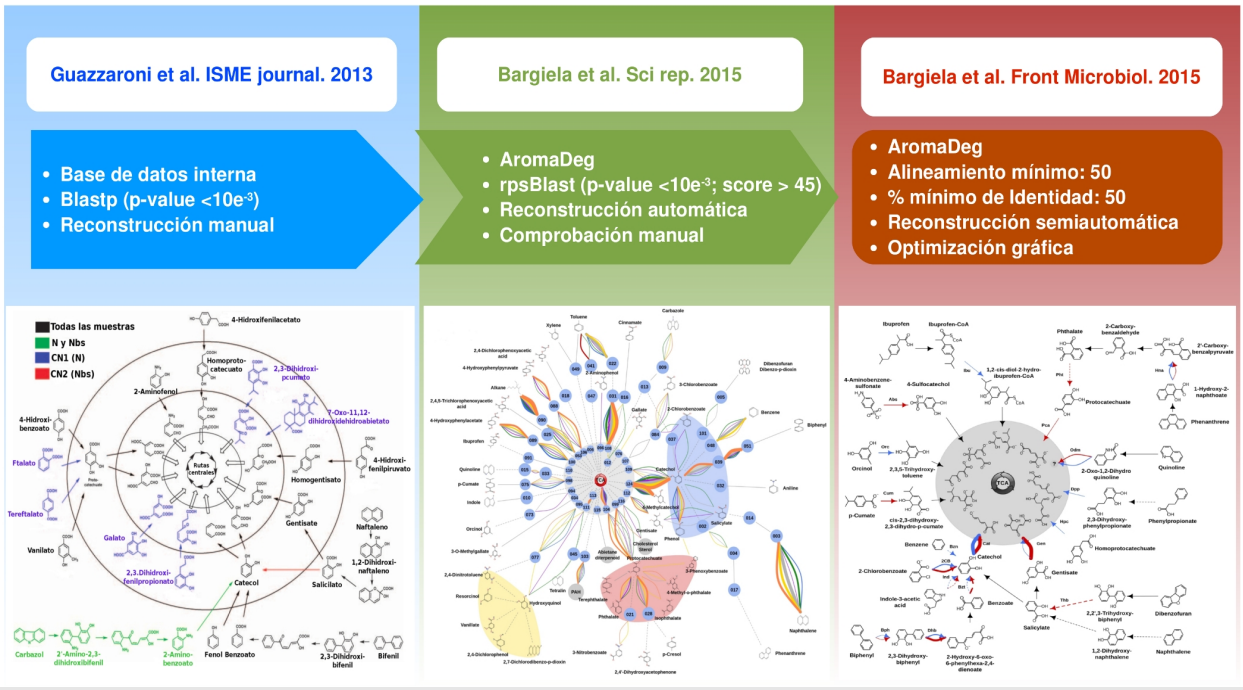

Figura 23: Evolución del método de reconstrucción metabólica desarrollado durante la Tesis Doctoral.

una de las reacciones. Esto último es importante, ya que es de ayuda cuando se realizan estudios comparativos.

Con el fin de mejorar la visualización gráfica, el método fue optimizado posteriormente (Bargiela et al., 2015a). Aunque se continúa con el sistema de nodos y enlaces, la nomenclatura interna para enzimas y sustratos fue eliminada, pasando a utilizar directamente la empleada en AromaDeg. Utilizando el código CID de pubchem (Bolton et al., 2008) para cada compuesto extraemos automáticamente, mediante herramienta desarrolladas en lenguaje Perl (Wall & Loukides, 2000), las fórmulas químicas en formato SMILE. Estas fórmulas son procesadas utilizando el paquete OASA (http://bkchem.zirael.org/oasa_en), para el lenguaje de programación Python (Rossum and Drake, 2001), derivado del programa para dibujo químico Bkchem (http://bkchem.zirael.org). Con ello, se genera la imagen de cada producto y sustrato, que son utilizadas a través del entorno de programación R (R Development Core Team, 2008) para mejorar notablemente la visualización gráfica de la reconstrucción metabólica. La **Figura 23** muestra un resumen de la evolución del método de reconstrucción.

Adicionalmente, para comprobar la calidad de la reconstrucción se realiza una validación experimental mediante metabolómica dirigida en microcosmos en los que se realizan enriquecimientos selectivos para cada compuesto para el que se ha predicho su degradación computacionalmente. Después de 3 semanas mantenidos a una temperatura similar a la correspondiente en cada muestra, se evalúa la degradación de cada compuesto por espectrometría de masas.

Durante esta Tesis Doctoral se emplearon dos tipos de datos para la generación de las reconstrucciones catabólicas. Por un lado, datos de secuenciación masiva obtenidos por secuenciación directa de ADN de las comunidades microbianas aisladas directamente de las muestras ambientales o de los enriquecimientos. Por otro lado, se utilizaron los genomas depositados en las bases de datos, de aquellas bacterias más similares a las identificadas por secuenciación del gen de ARNr 16S de las comunidades microbianas que fueron objeto de estudio. Gracias a la metabolómica dirigida en enriquecimientos selectivos se pudo demostrar que la utilización de este tipo de secuencias mejora las redes catabólicas obtenidas inicialmente usando los datos meta-

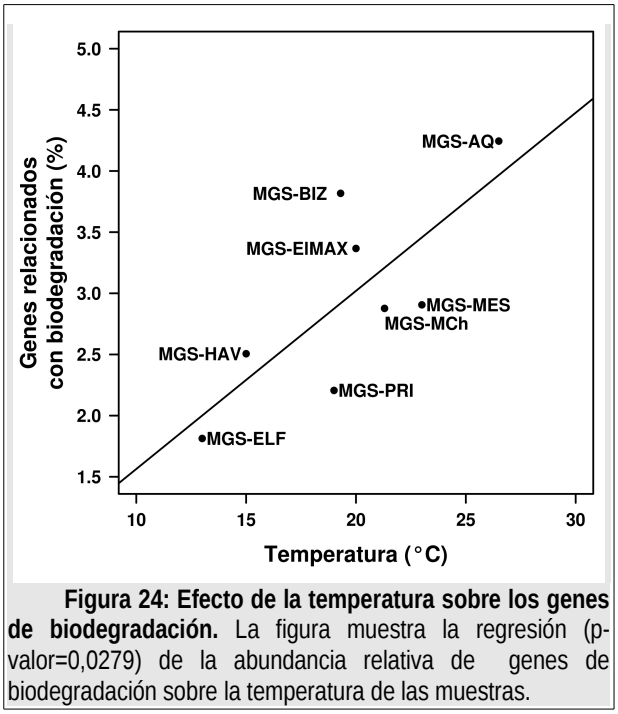

Figura 24: Efecto de la temperatura sobre los genes de biodegradación. La figura muestra la regresión (p-valor=0,0279) de la abundancia relativa de genes de biodegradación sobre la temperatura de las muestras.

genómicos, sin introducir errores significativos en la predicción (Bargiela et al., 2015c).

3.2.2. Análisis de la influencia de los factores geoquímicos y temperatura en el catabolismo de contaminantes

Siguiendo el procedimiento mencionado en el apartado anterior, se ha predicho la capacidad de degradación para al menos 53 compuestos diferentes, de los cuales 25 se pudieron comprobar experimentalmente (**Figura 25**), en comunidades microbianas de sedimentos marinos crónicamente contaminados procedentes del Mar Mediterráneo y Mar Rojo. Del análisis comparativo de las muestras entre sí y su comparación con otros ambientes contaminados (Prestige y Golfo de México), se han obtenido diferentes conclusiones.

En primer lugar, se demostró como la temperatura en ambientes crónicamente contaminados tiene un efecto directo sobre la abundancia relativa de genes relacionados con biodegradación, independientemente de otros factores como la concentración de O_2 o la de hidrocarburos. Así, el porcentaje de estos genes aumenta conforme asciende la temperatura de la zona (**Figura 24**). Lim y colaboradores (Lim et al., 2001), observaron que la tasa de biodegradación en un bioreactor aeróbico de fase sólida aumentaba a medida que ascendía la temperatura cuando esta se encontraba en un rango de 20 a 50ºC. Este aumento va acompañado de un incremento en la tasa de respiración, lo que podría estar relacionado con el aumento en la tasa de biodegradación. You y colaboradores (You et al., 2013), estudiaron la tasa de biodegradación de BTEX (benceno, tolueno, etilbenceno y xileno) en cultivos mixtos de *Pseudomonas putida* YNS1, analizando la influencia de diferentes factores, como la temperatura, sobre la tasa de degradación de estos compuestos. En sus resultados observaron que las mayores tasas de degradación de BTEX se obtenían en el rango de 20 a 35ºC (en el que entrarían las muestras de mayor temperatura analizadas en la presente Tesis Doctoral: BIZ, ELMAX, MCh, MES y AQ). La baja tasa de degradación a bajas temperaturas la achacaron a una reducción en la tasa de crecimiento bacteriano, inactivación de las enzimas, reducción de la biodisponibilidad de los sustratos y la desprotonización de la superficie bacteriana.

Lo expuesto anteriormente sugiere que temperaturas moderadamente altas incrementan la abundancia relativa de genes implicados en degradación. Eso, a su vez, puede favorecer ciertas rutas frente a otras. Así ocurre, por ejemplo, con la degradación del catecol, la degradación del bifenilo, la degradación del naftaleno vía gentisato o la degradación del ftalato (Bargiela et al., 2015c). Estas capacidades están presentes en todas las comunidades analizadas, aunque más favorecidas en ambientes más cálidos. Pese a esto, los datos presentados en el **capítulo 5** basados en proteómica indican que la mayoría de estos genes no se expresan a niveles altos en comparación con otras enzimas del metabolismo central. Por lo tanto, todavía queda por definir el efecto real de las diferentes a nivel de abundancia de genes.

En comparación con aquellas zonas “limpias” sobre las que ocurre un vertido accidental, como la costa gallega (*Prestige*) o el Golfo de México (*Deepwater Horizon*), esperaríamos que las zonas crónicamente conta-

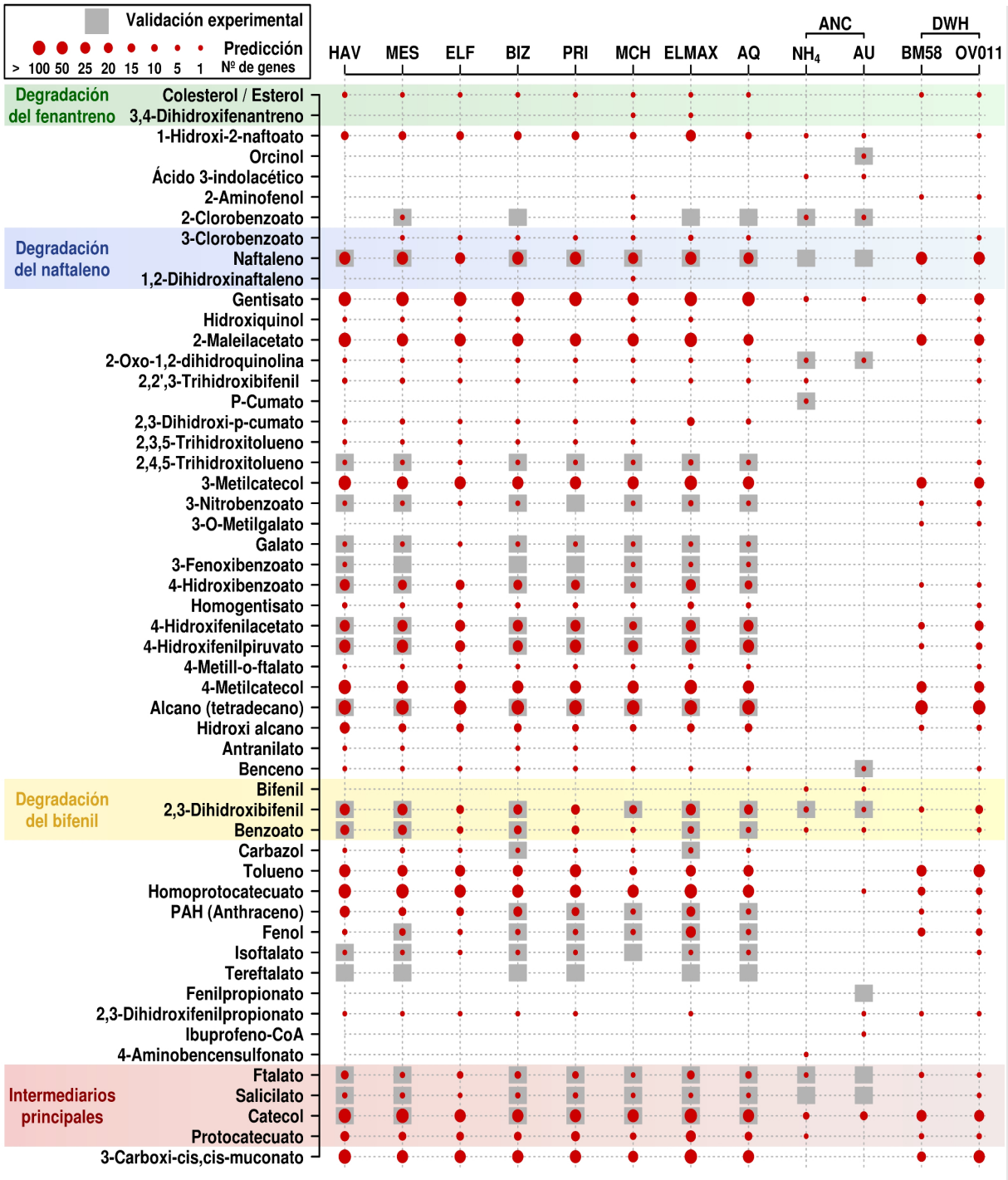

Figura 25: Listado de compuestos para los que se ha predicho su degradación en las reconstrucciones metabólicas. Las predicciones para cada compuesto en cada muestra se señalan con un círculo rojo, cuyo tamaño es proporcional al número de genes putativos encontrados que codifican enzimas relacionadas con la degradación del compuesto. En caso de estar confirmada experimentalmente por metabolómica dirigida se señala con un rectángulo gris. En la tabla se muestran tanto las muestras de sedimentos (ordenadas por latitud de mayor a menor), como los microcosmos basados en las muestras de ANC y 2 muestras procedentes del accidente del Golfo de México (DWH, *Deepwater Horizon*), recogidas a ~1100m de profundidad: OV011 corresponde a la zona del accidente, muestras que BM58 fue recogida a 10 km de la zona donde ocurrió el vertido.

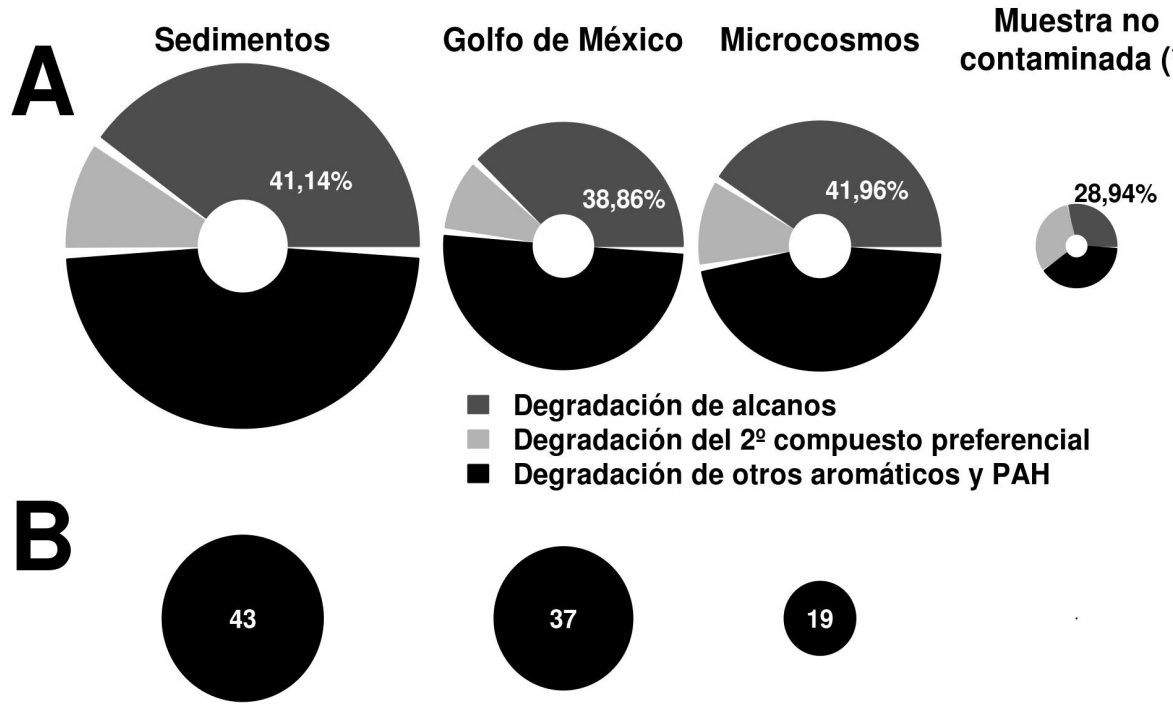

Figura 26: Proporción de genes relacionados con la degradación de alcanos respecto al resto de genes involucrados en biodegradación. A) muestra la proporción observada en las muestras de sedimentos, el accidente del Deepwater Horizon (DWH), las muestras de microcosmos de ANC, y una muestra sin contaminar procedente de la zona profunda del Golfo de México, fuera de la nube de contaminación (Rivers et al. 2013). El tamaño de cada círculo es directamente proporcional a la abundancia relativa de genes de biodegradación con respecto al resto de genes en el metagenoma. B) Muestra el número total de compuestos diferentes para los que se ha detectado capacidad de degradación en los diferentes tipos de muestras. ***** A pesar de que la muestra no contaminada fue tomada a 8 km de la zona del accidente del Golfo de México y fuera de la nube de contaminación, no constituye una muestra de agua completamente limpia. Además, la estimación de los genes de biodegradación está basada en datos de homología con KEGG, al contrario que el resto de muestras.

minadas estuvieran mejor adaptadas a la presencia de contaminantes, mostrando redes catabólicas con mayor potencial de degradación que las otras zonas. Esto ha quedado demostrado en la presente Tesis Doctoral, como explicaremos a continuación.

Por una parte, hemos observado que en las zonas más próximas al origen de un vertido (Golfo de México) las comunidades microbianas presentan la capacidad para degradar un mayor número de contaminantes. Así, la muestra OV011 procedente del Golfo de México y más próxima a la zona del accidente presenta capacidad para la degradación de 37 contaminantes diferentes, frente a los 24 observados en la muestra BM58, a 10 km de distancia (**Figura 25**).

Por otra parte, los sedimentos de las zonas crónicamente contaminadas estudiadas en la presente Tesis Doctoral presentan una capacidad para degradar una mayor diversidad de contaminantes (un total de 43 compuestos diferentes) que los observados en las muestras del Golfo de México (**Figura 26**). De esta forma, observamos que la degradación de compuestos como el galato, el 3-fenoxibenzoato, el 2,3,5-trihidroxitolueno, el 3,4-dihidroxifenantreno o el antraceno sólo se detecta en las muestras de sedimentos.

Además, los diferentes tipos de contaminación qe caracterizan a cada zona del Mar Mediterráneo pueden afectar a su vez a la presencia de diferentes tipos de bacterias, que podrían mostrar diferentes capacidades de degradación. De esta forma podemos observar

como, por ejemplo, la degradación del 1,2-dihidroxinaftaleno sólo es detectada en MCh, o que la degradación del antranilato sólo se observa en 4 de los sedimentos (HAV, PRI, MES y BIZ).

Las rutas mayoritarias observadas en todas las muestras estudiadas corresponden a la hidroxilación de alcanos y la degradación de compuestos que constituyen intermediarios principales de otras rutas de degradación, como el catecol y el gentisato. Concretamente, el número de genes observado para la hidroxilación de alcanos es muy superior al observado para el resto de rutas, tanto en los sedimentos (41,14% de los genes de biodegradación), como en las muestras procedentes del Golfo de México (38,89%), superando varias veces al segundo compuesto con mayor número de genes (**Figura 26**). Este aspecto no fue analizado sobre las comunidades de los microcosmos de ANC, ya que la base de datos AromaDeg sólo incluye genes para la degradación de aromáticos. Sin embargo, si analizamos los metagenomas de ANC con la misma base de datos que los sedimentos y las muestras del Golfo de México (Bargiela et al., 2015c; Guazzaroni et al., 2013), observamos una proporción similar (41,96%). Esto indica que la hidroxilación de alcanos es una ruta preferencial en este tipo de

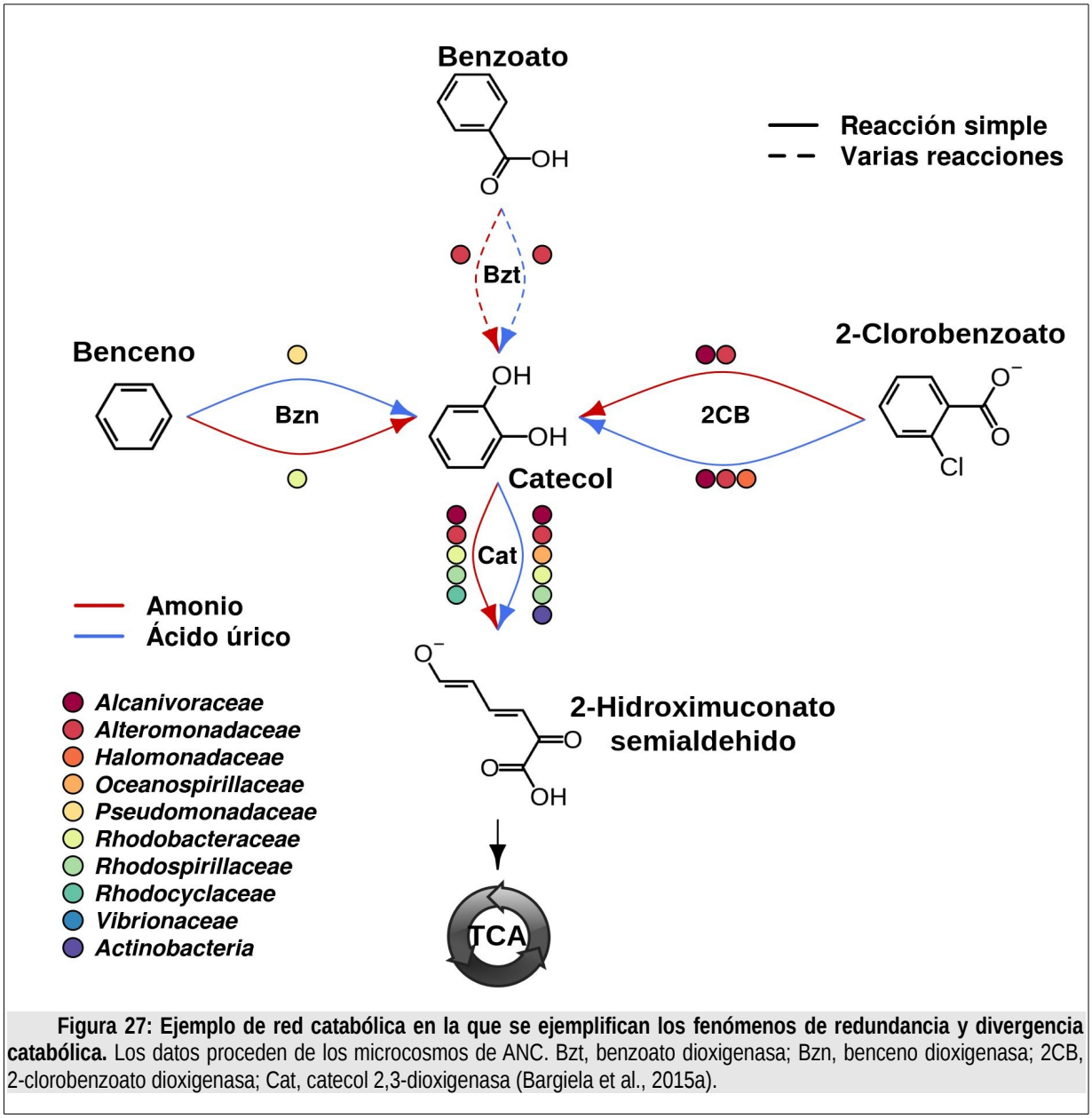

Figura 27: Ejemplo de red catabólica en la que se ejemplifican los fenómenos de redundancia y divergencia catabólica. Los datos proceden de los microcosmos de ANC. Bzt, benzoato dioxigenasa; Bzn, benceno dioxigenasa; 2CB, 2-clorobenzoato dioxigenasa; Cat, catecol 2,3-dioxigenasa (Bargiela et al., 2015a).

comunidades microbianas, independientemente de la localización geográfica o el tipo de entrada de hidrocarburos recibida, en comparación con las comunidades que habitan zonas de agua "limpia" **Figura 26**, donde estos genes son menos abundantes (Mason et al., 2012; Rivers et al., 2013).

Teniendo en cuenta los puntos anteriores, ha quedado demostrado que los ambientes crónicamente contaminados presentan un mayor número de genes implicados en degradación, así como una mayor diversidad de moléculas que pueden degradar. Por lo tanto, podemos decir que no sólo la temperatura afecta al tamaño de las redes catabólicas en los sedimentos marinos, sino que también la diversidad de los contaminantes o moléculas introducidas en ellos antropogénicamente.

3.3.Relación entre la distribución taxonómica y la abundancia de los diferentes genes catabólicos

En la presente Tesis Doctoral hemos visto como la distribución taxonómica de las diferentes comunidades microbianas observadas en los sedimentos de las zonas analizadas son muy diferentes entre si. Sin embargo, al observar sus redes catabólicas (Bargiela et al., 2015) se aprecia que comparten la capacidad para degradar un gran número de compuestos diferentes (30 de los compuestos analizados en las redes, **Figura 25**). Esto nos indica que la capacidad para degradar determinados compuestos puede ser asumida por grupos microbianos diferentes. Por lo tanto, estas observaciones hacen referencia al concepto de redundancia funcional, por el cual dos comunidades microbianas diferentes pueden presentar un metabolismo similar.

Por otra parte, observando las comunidades microbianas que componen los dos microcosmos diferentes de ANC (enriquecidos con NH_4 y AU, respectivamente) podemos apreciar que, a pesar de su gran similitud, difieren funcionalmente en su capacidad catabólica, degradando un conjunto de contaminantes diferente (Bargiela et al., 2015a). Es por esto que, además de la redundancia catabólica observada en los sedimentos, entre las comunidades formadas en los microcosmos observamos un fenómenos de divergencia funcional (**Figura 27**), por el cual dos comunidades microbianas similares pueden mostrar metabolismos diferente.

Así, en el **capítulo 4** vemos como la presencia de una sola fuente de nitrógeno puede variar en un 50% la capacidad de una comunidad microbiana de degradar contaminantes. De esta forma, aunque las redes catabólicas para ambos microcosmos comparten la capacidad para la degradación de 8 compuestos diferentes, cada una de ellas presenta la huella para la degradación de 5 compuestos específicos (**Figura 25**).

Por último, queda por mencionar la capacidad de los diferentes microorganismos de una misma comunidad para completar la degradación de los compuestos. Así, las diferentes reacciones que completan una ruta de degradación pueden ser realizadas por varios tipos de organismos diferentes que colaboran entre sí para catabolizar completamente un contaminante. Este concepto ya ha sido demostrado en el **capítulo 5**, en donde se observa cómo diferentes tipos de microorganis-

CONCLUSIÓN: La temperatura es el factor geoquímico clave que afecta a la diversidad catabólica de los sedimentos marinos del Mar Mediterráneo y Mar Rojo crónicamente contaminados. Su aumento en pocos grados se asocia a un aumento dela diversidad catabólica.

Las comunidades microbianas de sedimentos de zonas crónicamente contaminadas presentan la capacidad de degradar un mayor número de componentes que aquellas procedentes de zonas contaminadas por un vertido accidental.

El uso de diferentes fuentes de nitrógeno favorece diferentes rutas catabólicas para comunidades microbianas similares.

La hidroxilación e alcanos es la ruta de degradación preferencial, independientemente del ambiente analizado.

Las comunidades de los sedimentos muestran redundancia funcional, ya que diferentes grupos taxonómicos pueden desempeñar una misma función.

También se ha observado que las comunidades de los microcosmos muestran divergencia funcional, ya que comunidades similares pueden mostrar metabolismos diferentes.

mos colaboran entre sí para completar la ruta metabólica de los compuestos C_1 o el metabolismo del azufre (Bargiela et al., 2015c).

4. Consideraciones finales sobre las comunidades microbianas analizadas

Los estudios realizados en la presente Tesis Doctoral han permitido obtener, por primera vez, información sobre la estructura y capacidades catabólicas de comunidades microbianas del Mar Mediterráneo y Mar Rojo. Ambas zonas están afectadas por una contaminación de origen antropogénico, debido a la entrada continua hidrocarburos y otros tipos de moléculas, que tienden a acumularse. En la presente Tesis Doctoral se ha demostrado que tanto la diversidad como el catabolismo bacteriano están fuertemente relacionados con la temperatura y el tipo de contaminación que caracterizan los ambientes crónicamente contaminados. Dicho esto, esta correlación se ha encontrado analizando sólo 9 sedimentos repartidos por el Mar Mediterráneo y el Mar Rojo, usando tres técnicas distintas (análisis de genes 16S rRNA, secuenciación de DNA y metabolómica), que dan relevancia estadística a los resultados. Pese a ello, el siguiente paso es completar el mismo tipo de análisis en un mayor número de sedimentos distribuidos por ambos mares con el fin de establecer relaciones de forma global.

Respecto a los resultados obtenidos durante el análisis de enriquecimientos en microcosmos, ha quedado demostrado que el uso combinado de distintos bioestimulantes (por ejemplo, fuentes de nitrógeno) puede contribuir a la mejora de los procesos de biorremediación. Dado que este hecho solo se ha demostrado en microcosmos, el siguiente paso es realizar investigaciones de campo en las que se pueda estudiar el empleo de mezclas de distintos nutrientes en zonas en las que haya ocurrido un vertido real. En este sentido, recientemente se ha producido un vertido de crudo en una zona de las costas de Sicilia (Playa de Gela) en la que actualmente estamos realizando investigaciones de este tipo, entre otras. Así, estamos evaluando como se modifican las comunidades bacterianas, las capacidades catabólicas y los niveles de degradación natural cuando se adicionan diferentes tipos de bioestimulantes. Conocer qué rutas de biodegradación son potenciadas en mayor medida con cada nutriente o mezcla de nutrientes y sus efectos sobre la microbiota podría permitir desarrollar en un futuro tratamientos a la carta según las características del ambiente y la composición de los contaminantes. Además, se podría analizar la utilización de varios nutrientes al mismo tiempo para observar si se fomenta la expresión de un mayor número de rutas.

Teniendo estas consideraciones presentes, los resultados obtenidos en esta Tesis Doctoral pueden ser de interés para el planteamiento de futuras investigaciones en el campo de la biorremediación en ambientes marinos afectados por la contaminación crónica por hidrocarburos o por vertidos reales. Así, por ejemplo, una posible vía de investigación podría concentrarse en determinar cuáles son las rutas de degradación que estimulan los diferentes bioestimulantes, de forma que, con el fin de mejorar los procesos de limpieza, diseñar tratamientos de bioestimulación a la carta adecuados a los parámetros geoquímicos y tipo de contaminación de la zona a descontaminar.

Capítulo 7: Conclusiones

- Los sedimentos marinos del Mar Mediterráneo y el Mar Rojo están habitados por una población muy heterogénea de bacterias, que pese a ello son redundantes en su capacidad para degradar los contaminantes que forman el crudo.

- El aumento en la temperatura de las aguas provoca una disminución en la diversidad taxonómica de dichas bacterias, un aumento en el contenido de genes que codifican enzimas implicadas en la degradación de alcanos y aromáticos y favorece rutas de degradación preferenciales, como la degradación del naftaleno vía gentisato.

- Los sedimentos marinos de ambientes crónicamente contaminados contienen bacterias con una capacidad catabólica X veces superior al de aquellas de ambientes donde ocurren vertidos accidentales y X veces superior al de las aguas no contaminadas.

- Se ha demostrado por primera vez el potencial del ácido úrico como agente bioestimulante económico para estimular la biodegradación de hidrocarburos. Pese a ello se recomienda la combinación de diferentes bioestimulantes para la degradación completa de todos los componentes del petróleo en caso de vertidos accidentales.

- Se ha demostrado que, pese a la contaminación crónica que caracteriza el Mar Mediterráneo, los procesos de biodegradación de sustancias contaminantes son minoritarios frente a otras capacidades metabólicas.

- Se han generado herramientas bioinformáticas que permiten reconstruir y predecir rutas de biodegradación en cualquier tipo de comunidad microbiana, empleando datos “-ómicos” con los que realizar estudios comparativos. El método, permite generar predicciones con una confianza de al menos 90%, puede ayudar a planificar nuevas estrategias de biorremediación.

Referencias

Acosta-González, A., Rosselló-Móra, R., & Marqués, S. (2013). Characterization of the anaerobic microbial community in oil-polluted subtidal sediments: aromatic biodegradation potential after the Prestige oil spill. *Environmental Microbiology*, *15*(1), 77–92. http://doi.org/10.1111/j.1462-2920.2012.02782.x

Al-Awadhi, H., Dashti, N., Kansour, M., Sorkhoh, N., & Radwan, S. (2012). Hydrocarbon-utilizing bacteria associated with biofouling materials from offshore waters of the Arabian Gulf. *International Biodeterioration & Biodegradation*, *69*, 10–16. http://doi.org/10.1016/j.ibiod.2011.12.008

Alcaide, M., Tornés, J., Stogios, P. J., Xu, X., Gertler, C., Leo, R. D., … Ferrer, M. (2013). Single residues dictate the co-evolution of dual esterases: MCP hydrolases from the α/β hydrolase family. *Biochemical Journal*, *454*(1), 157–166. http://doi.org/10.1042/BJ20130552

Almeda, R., Wambaugh, Z., Chai, C., Wang, Z., Liu, Z., & Buskey, E. J. (2013). Effects of Crude Oil Exposure on Bioaccumulation of Polycyclic Aromatic Hydrocarbons and Survival of Adult and Larval Stages of Gelatinous Zooplankton. *PLoS ONE*, *8*(10). http://doi.org/10.1371/journal.pone.0074476

Al-Najjar, T., Rasheed, M., Ababneh, Z., Ababneh, A., & Al-Omarey, H. (2011). Heavy metals pollution in sediment cores from the Gulf of Aqaba, Red Sea. *Natural Science*, *03*(09), 775–782. http://doi.org/10.4236/ns.2011.39102

Altschul, S. F., Gish, W., Miller, W., Myers, E. W., & Lipman, D. J. (1990). Basic local alignment search tool. *Journal of Molecular Biology*, *215*(3), 403–410. http://doi.org/10.1016/S0022-2836(05)80360-2

Armstrong, R. N. (2000). Mechanistic Diversity in a Metalloenzyme Superfamily†. *Biochemistry*, *39*(45), 13625–13632. http://doi.org/10.1021/bi001814v

Arora, P. K., & Bae, H. (2014). Integration of bioinformatics to biodegradation. *Biological Procedures Online*, *16*, 8. http://doi.org/10.1186/1480-9222-16-8

Arora, P. K., Kumar, M., Chauhan, A., Raghava, G. P., & Jain, R. K. (2009). OxDBase: a database of oxygenases involved in biodegradation. *BMC Research Notes*, *2*, 67. http://doi.org/10.1186/1756-0500-2-67

Atlas, R. M. (1981). Microbial degradation of petroleum hydrocarbons: an environmental perspective. *Microbiological Reviews*, *45*(1), 180–209.

Austin, R. N., & Groves, J. T. (2011). Alkane-oxidizing metalloenzymes in the carbon cycle. *Metallomics*, *3*(8), 775. http://doi.org/10.1039/c1mt00048a

Awal, M. R. (2009). Environmentally Conscious Petroleum Engineering. In M. Kutz & A. Elkamel (Eds.), *Environmentally Conscious Fossil Energy Production* (pp. 1–86). John Wiley & Sons, Inc. Retrieved from http://onlinelibrary.wiley.com/doi/10.1002/9780470432747.ch1/summary

Bælum, J., Borglin, S., Chakraborty, R., Fortney, J. L., Lamendella, R., Mason, O. U., … Jansson, J. K. (2012). Deep-sea bacteria enriched by oil and dispersant from the Deepwater Horizon spill. *Environmental Microbiology*, *14*(9), 2405–2416. http://doi.org/10.1111/j.1462-2920.2012.02780.x

Bagi, A., Pampanin, D. M., Lanzén, A., Bilstad, T., & Kommedal, R. (2013). Naphthalene biodegradation in temperate and arctic marine microcosms. *Biodegradation*, *25*(1), 111–125. http://doi.org/10.1007/s10532-013-9644-3

Ball, A., & Truskewycz, A. (2013). Polyaromatic hydrocarbon exposure: an ecological impact ambiguity. *Environmental Science and Pollution Research*, *20*(7), 4311–4326. http://doi.org/10.1007/s11356-013-1620-2

Bargiela, R., Gertler, C., Magagnini, M., Mapelli, F., Chen, J., Daffonchio, D., … Ferrer, M. (2015)a. Degradation network reconstruction in uric acid and ammonium amendments in oil-degrading marine microcosms guided by metagenomic data. *Frontiers in Microbiology*, *6*, 1270.

Bargiela, R., Herbst, F.-A., Martínez-Martínez, M., Seifert, J., Rojo, D., Cappello, S., … Golyshin, P. N. (2015)b. Metaproteomics and metabolomics analyses of chronically petroleum-polluted sites reveal the importance of general anaerobic processes uncoupled with degradation. *PROTEOMICS*, *15*(20), 3508–3520. http://doi.org/10.1002/pmic.201400614

Bargiela, R., Mapelli, F., Rojo, D., Chouaia, B., Tornés, J., Borin, S., … Ferrer, M. (2015)c. Bacterial population and biodegradation potential in chronically crude oil-contaminated marine sediments are strongly linked to temperature. *Scientific Reports*, *5*. http://doi.org/10.1038/srep11651

Barhoumi, B., Clérandeau, C., Gourves, P.-Y., Le Menach, K., Megdiche, Y. El, Peluhet, L., … Cachot, J. (2014). Pollution biomonitoring in the Bizerte lagoon (Tunisia), using combined chemical and biomarker analyses in grass goby, Zosterisessor ophiocephalus (Teleostei, Gobiidae). *Marine Environmental Research*, *101*, 184–195. http://doi.org/10.1016/j.marenvres.2014.07.002

Barry, K. P., & Taylor, E. A. (2013). Characterizing the Promiscuity of LigAB, a Lignin Catabolite Degrading Extradiol Dioxygenase from Sphingomonas paucimobilis SYK-6. *Biochemistry*, *52*(38), 6724–6736. http://doi.org/10.1021/bi400665t

Bauer, M., Kube, M., Teeling, H., Richter, M., Lombardot, T., Allers, E., … Glöckner, F. O. (2006). Whole genome analysis of the marine Bacteroidetes“Gramella forsetii” reveals adaptations to degradation of polymeric organic matter. *Environmental Microbiology*, *8*(12), 2201–2213. http://doi.org/10.1111/j.1462-2920.2006.01152.x

Boll, M., Fuchs, G., & Heider, J. (2002). Anaerobic oxidation of aromatic compounds and hydrocarbons. *Current Opinion in Chemical Biology*, *6*(5), 604–611. http://doi.org/10.1016/S1367-5931(02)00375-7

Boll, M., Löffler, C., Morris, B. E. L., & Kung, J. W. (2014). Anaerobic degradation of homocyclic aromatic compounds via arylcarboxyl-coenzyme A esters: organisms, strategies and key enzymes. *Environmental Microbiology*, *16*(3), 612–627. http://doi.org/10.1111/1462-2920.12328

Bolognesi, C., Perrone, E., Roggieri, P., & Sciutto, A. (2006). Bioindicators in monitoring long term genotoxic impact of oil spill: Haven case study. *Marine Environmental Research*, *62*, *Supplement 1*, S287–S291. http://doi.org/10.1016/j.marenvres.2006.04.047

Boonmak, C., Takahashi, Y., & Morikawa, M. (2014). Cloning and expression of three ladA-type alkane monooxygenase genes from an extremely thermophilic alkane-degrading bacterium Geobacillus thermoleovorans B23. *Extremophiles*, *18*(3), 515–523. http://doi.org/10.1007/s00792-014-0636-y

Bowman, J. S., & Deming, J. W. (2014). Alkane hydroxylase genes in psychrophile genomes and the potential for cold active catalysis. *BMC Genomics*, *15*(1). http://doi.org/10.1186/1471-2164-15-1120

Brandt, A. R., Millard-Ball, A., Ganser, M., & Gorelick, S. M. (2013). Peak Oil Demand: The Role of Fuel Efficiency and Alternative Fuels in a Global Oil Production Decline. *Environmental Science & Technology*, *47*(14), 8031–8041. http://doi.org/10.1021/es401419t

Brown, C. K., Vetting, M. W., Earhart, C. A., & Ohlendorf, D. H. (2004). Biophysical Analyses of Designed and Selected Mutants of Protocatechuate 3,4-Dioxygenase. *Annual Review of Microbiology*, *58*(1), 555–585.

http://doi.org/10.1146/annurev.micro.57.030502.090927

Cappello, S., Caruso, G., Zampino, D., Monticelli, L. s., Maimone, G., Denaro, R., … Giuliano, L. (2007a). Microbial community dynamics during assays of harbour oil spill bioremediation: a microscale simulation study. *Journal of Applied Microbiology*, *102*(1), 184–194. http://doi.org/10.1111/j.1365-2672.2006.03071.x

Cappello, S., Caruso, G., Zampino, D., Monticelli, L. s., Maimone, G., Denaro, R., … Giuliano, L. (2007b). Microbial community dynamics during assays of harbour oil spill bioremediation: a microscale simulation study. *Journal of Applied Microbiology*, *102*(1), 184–194. http://doi.org/10.1111/j.1365-2672.2006.03071.x

Carbajosa, G., Trigo, A., Valencia, A., & Cases, I. (2009). Bionemo: molecular information on biodegradation metabolism. *Nucleic Acids Research*, *37*(Database issue), D598–D602. http://doi.org/10.1093/nar/gkn864

Caspi, R., Altman, T., Billington, R., Dreher, K., Foerster, H., Fulcher, C. A., … Karp, P. D. (2014). The MetaCyc database of metabolic pathways and enzymes and the BioCyc collection of Pathway/Genome Databases. *Nucleic Acids Research*, *42*(D1), D459–D471. http://doi.org/10.1093/nar/gkt1103

Chakraborty, J., Ghosal, D., Dutta, A., & Dutta, T. K. (2012). An insight into the origin and functional evolution of bacterial aromatic ring-hydroxylating oxygenases. *Journal of Biomolecular Structure and Dynamics*, *30*(4), 419–436. http://doi.org/10.1080/07391102.2012.682208

Chakraborty, R., Wu, C. H., & Hazen, T. C. (2012). Systems biology approach to bioremediation. *Current Opinion in Biotechnology*, *23*(3), 483–490. http://doi.org/10.1016/j.copbio.2012.01.015

Chang, H.-K., & Zylstra, G. J. (1998). Novel Organization of the Genes for Phthalate Degradation from Burkholderia cepacia DBO1. *Journal of Bacteriology*, *180*(24), 6529–6537.

Chen, Q., Bao, M., Fan, X., Liang, S., & Sun, P. (2013). Rhamnolipids enhance marine oil spill bioremediation in laboratory system. *Marine Pollution Bulletin*, *71*(1–2), 269–275. http://doi.org/10.1016/j.marpolbul.2013.01.037

Coll, M., Piroddi, C., Steenbeek, J., Kaschner, K., Ben Rais Lasram, F., Aguzzi, J., … Voultsiadou, E. (2010). The Biodiversity of the Mediterranean Sea: Estimates, Patterns, and Threats. *PLoS ONE*, *5*(8). http://doi.org/10.1371/journal.pone.0011842

Contzen, M., & Stolz, A. (2000). Characterization of the Genes for Two Protocatechuate 3,4-Dioxygenases from the 4-Sulfocatechol-Degrading Bacterium Agrobacterium radiobacter Strain S2. *Journal of Bacteriology*, *182*(21), 6123–6129.

Cooley, R. B., Dubbels, B. L., Sayavedra-Soto, L. A., Bottomley, P. J., & Arp, D. J. (2009). Kinetic characterization of the soluble butane monooxygenase from Thauera butanivorans, formerly “Pseudomonas butanovora.” *Microbiology*, *155*(Pt 6), 2086–2096. http://doi.org/10.1099/mic.0.028175-0

Culpepper, M. A., & Rosenzweig, A. C. (2012). Architecture and active site of particulate methane monooxygenase. *Critical Reviews in Biochemistry and Molecular Biology*, *47*(6), 483–492. http://doi.org/10.3109/10409238.2012.697865

Daffonchio, D., Ferrer, M., Mapelli, F., Cherif, A., Lafraya, Á., Malkawi, H. I., … Fava, F. (2013). Bioremediation of Southern Mediterranean oil polluted sites comes of age. *New Biotechnology*, *30*(6), 743–748. http://doi.org/10.1016/j.nbt.2013.05.006

Daling, P. S., Leirvik, F., Almås, I. K., Brandvik, P. J., Hansen, B. H., Lewis, A., & Reed, M. (2014). Surface weathering and dispersibility of MC252

crude oil. *Marine Pollution Bulletin*. http://doi.org/10.1016/j.marpolbul.2014.07.005

Danovaro, R. (2003). Pollution threats in the Mediterranean Sea: An overview. *Chemistry and Ecology*, *19*(1), 15–32. http://doi.org/10.1080/0275754031000081467

Danovaro, R., Company, J. B., Corinaldesi, C., D'Onghia, G., Galil, B., Gambi, C., … Tselepides, A. (2010). Deep-Sea Biodiversity in the Mediterranean Sea: The Known, the Unknown, and the Unknowable. *PLoS ONE*, *5*(8). http://doi.org/10.1371/journal.pone.0011832

Dash, H. R., Mangwani, N., Chakraborty, J., Kumari, S., & Das, S. (2013). Marine bacteria: potential candidates for enhanced bioremediation. *Applied Microbiology and Biotechnology*, *97*(2), 561–571. http://doi.org/10.1007/s00253-012-4584-0

Das, N., & Chandran, P. (2010). Microbial Degradation of Petroleum Hydrocarbon Contaminants: An Overview. *Biotechnology Research International*, *2011*, e941810. http://doi.org/10.4061/2011/941810

Desai, C., Pathak, H., & Madamwar, D. (2010). Advances in molecular and "-omics" technologies to gauge microbial communities and bioremediation at xenobiotic/anthropogen contaminated sites. *Bioresource Technology*, *101*(6), 1558–1569. http://doi.org/10.1016/j.biortech.2009.10.080

Descorps-Declère, S., Lemoine, F., Sculo, Q., Lespinet, O., & Labedan, B. (2008). The multiple facets of homology and their use in comparative genomics to study the evolution of genes, genomes, and species. *Biochimie*, *90*(4), 595–608. http://doi.org/10.1016/j.biochi.2007.09.010

de Soysa, T. Y., Ulrich, A., Friedrich, T., Pite, D., Compton, S. L., Ok, D., … Barresi, M. J. (2012). Macondo crude oil from the Deepwater Horizon oil spill disrupts specific developmental processes during zebrafish embryogenesis. *BMC Biology*, *10*, 40. http://doi.org/10.1186/1741-7007-10-40

Díaz, E., Jiménez, J. I., & Nogales, J. (2013). Aerobic degradation of aromatic compounds. *Current Opinion in Biotechnology*, *24*(3), 431–442. http://doi.org/10.1016/j.copbio.2012.10.010

Di Leonardo, R., Mazzola, A., Tramati, C. D., Vaccaro, A., & Vizzini, S. (2014). Highly contaminated areas as sources of pollution for adjoining ecosystems: The case of Augusta Bay (Central Mediterranean). *Marine Pollution Bulletin*, *89*(1–2), 417–426. http://doi.org/10.1016/j.marpolbul.2014.10.023

Dobslaw, D., & Engesser, K.-H. (2015). Degradation of toluene by ortho cleavage enzymes in Burkholderia fungorum FLU100. *Microbial Biotechnology*, *8*(1), 143–154. http://doi.org/10.1111/1751-7915.12147

Duarte, M., Jauregui, R., Vilchez-Vargas, R., Junca, H., & Pieper, D. H. (2014). AromaDeg, a novel database for phylogenomics of aerobic bacterial degradation of aromatics. *Database: The Journal of Biological Databases and Curation*, *2014*. http://doi.org/10.1093/database/bau118

Dyksterhouse, S. E., Gray, J. P., Herwig, R. P., Lara, J. C., & Staley, J. T. (1995). Cycloclasticus pugetii gen. nov., sp. nov., an Aromatic Hydrocarbon-Degrading Bacterium from Marine Sediments. *International Journal of Systematic Bacteriology*, *45*(1), 116–123. http://doi.org/10.1099/00207713-45-1-116

Everroad, R. C., Otaki, H., Matsuura, K., & Haruta, S. (2012). Diversification of Bacterial Community Composition along a Temperature Gradient at a Thermal Spring. *Microbes and Environments*, *27*(4), 374–381. http://doi.org/10.1264/jsme2.ME11350

Fantroussi, S. El, & Agathos, S. N. (2005). Is bioaugmentation a feasible strategy for pollutant removal and site remediation? *Current Opinion in Microbiology*, *8*(3), 268–275.

http://doi.org/10.1016/j.mib.2005.04.011

Fathepure, B. Z. (2014). Recent studies in microbial degradation of petroleum hydrocarbons in hypersaline environments. *Frontiers in Microbiology*, *5*. http://doi.org/10.3389/fmicb.2014.00173

Ferraro, D. J., Gakhar, L., & Ramaswamy, S. (2005). Rieske business: Structure–function of Rieske non-heme oxygenases. *Biochemical and Biophysical Research Communications*, *338*(1), 175–190. http://doi.org/10.1016/j.bbrc.2005.08.222

Fetzner, S. (2012). Ring-Cleaving Dioxygenases with a Cupin Fold. *Applied and Environmental Microbiology*, *78*(8), 2505–2514. http://doi.org/10.1128/AEM.07651-11

Fodelianakis, S., Antoniou, E., Mapelli, F., Magagnini, M., Nikolopoulou, M., Marasco, R., … Kalogerakis, N. (2015). Allochthonous bioaugmentation in ex situ treatment of crude oil-polluted sediments in the presence of an effective degrading indigenous microbiome. *Journal of Hazardous Materials*, *287*, 78–86. http://doi.org/10.1016/j.jhazmat.2015.01.038

Fuchs, G. (2008). Anaerobic Metabolism of Aromatic Compounds. *Annals of the New York Academy of Sciences*, *1125*(1), 82–99. http://doi.org/10.1196/annals.1419.010

Fuchs, G., Boll, M., & Heider, J. (2011). Microbial degradation of aromatic compounds — from one strategy to four. *Nature Reviews Microbiology*, *9*(11), 803–816. http://doi.org/10.1038/nrmicro2652

Gabor Csardi and Tamas Nepusz. (2006). The igraph software package for complex network research. *InterJournal*, *Complex Systems*, 1695.

Gakhar, L., Malik, Z. A., Allen, C. C. R., Lipscomb, D. A., Larkin, M. J., & Ramaswamy, S. (2005). Structure and Increased Thermostability of Rhodococcus sp. Naphthalene 1,2-Dioxygenase. *Journal of Bacteriology*, *187*(21), 7222–7231. http://doi.org/10.1128/JB.187.21.7222-7231.2005

Gallego, S., Vila, J., Tauler, M., Nieto, J. M., Breugelmans, P., Springael, D., & Grifoll, M. (2014). Community structure and PAH ring-hydroxylating dioxygenase genes of a marine pyrene-degrading microbial consortium. *Biodegradation*, *25*(4), 543–556. http://doi.org/10.1007/s10532-013-9680-z

Gao, J., Ellis, L. B. M., & Wackett, L. P. (2010). The University of Minnesota Biocatalysis/Biodegradation Database: improving public access. *Nucleic Acids Research*, *38*(suppl 1), D488–D491. http://doi.org/10.1093/nar/gkp771

Genovese, M., Crisafi, F., Denaro, R., Cappello, S., Russo, D., Calogero, R., … Yakimov, M. M. (2014). Effective bioremediation strategy for rapid in situ cleanup of anoxic marine sediments in mesocosm oil spill simulation. *Frontiers in Microbiology*, *5*. http://doi.org/10.3389/fmicb.2014.00162

Gerasch, A., Faber, D., Küntzer, J., Niermann, P., Kohlbacher, O., Lenhof, H.-P., & Kaufmann, M. (2014). BiNA: A Visual Analytics Tool for Biological Network Data. *PLoS ONE*, *9*(2). http://doi.org/10.1371/journal.pone.0087397

Gertler, C., Bargiela, R., Mapelli, F., Han, X., Chen, J., Hai, T., … Golyshin, P. N. (2015). Conversion of Uric Acid into Ammonium in Oil-Degrading Marine Microbial Communities: a Possible Role of Halomonads. *Microbial Ecology*, *70*(3), 724–740. http://doi.org/10.1007/s00248-015-0606-7

Gertler, C., Gerdts, G., Timmis, K. n., Yakimov, M. m., & Golyshin, P. n. (2009). Populations of heavy fuel oil-degrading marine microbial community in presence of oil sorbent materials. *Journal of Applied Microbiology*, *107*(2), 590–605. http://doi.org/10.1111/j.1365-2672.2009.04245.x

Geys, R., Soetaert, W., & Van Bogaert, I. (2014). Biotechnological opportunities in biosurfactant

production. *Current Opinion in Biotechnology*, *30*, 66–72. http://doi.org/10.1016/j.copbio.2014.06.002

Gillespie, I. M. M., & Philp, J. C. (2013). Bioremediation, an environmental remediation technology for the bioeconomy. *Trends in Biotechnology*, *31*(6), 329–332. http://doi.org/10.1016/j.tibtech.2013.01.015

Golyshin, P. N., Chernikova, T. N., Abraham, W.-R., Lünsdorf, H., Timmis, K. N., & Yakimov, M. M. (2002). Oleiphilaceae fam. nov., to include Oleiphilus messinensis gen. nov., sp. nov., a novel marine bacterium that obligately utilizes hydrocarbons. *International Journal of Systematic and Evolutionary Microbiology*, *52*(3), 901–911. http://doi.org/10.1099/ijs.0.01890-0

Golyshin, P. N., Martins Dos Santos, V. A. P., Kaiser, O., Ferrer, M., Sabirova, Y. S., Lünsdorf, H., … Timmis, K. N. (2003). Genome sequence completed of Alcanivorax borkumensis, a hydrocarbon-degrading bacterium that plays a global role in oil removal from marine systems. *Journal of Biotechnology*, *106*(2–3), 215–220. http://doi.org/10.1016/j.jbiotec.2003.07.013

Gong, Y., Zhao, X., Cai, Z., O'Reilly, S. E., Hao, X., & Zhao, D. (2014). A review of oil, dispersed oil and sediment interactions in the aquatic environment: Influence on the fate, transport and remediation of oil spills. *Marine Pollution Bulletin*, *79*(1–2), 16–33. http://doi.org/10.1016/j.marpolbul.2013.12.024

Gray, J. S. (2002). Biomagnification in marine systems: the perspective of an ecologist. *Marine Pollution Bulletin*, *45*(1–12), 46–52. http://doi.org/10.1016/S0025-326X(01)00323-X

Guazzaroni, M.-E., Herbst, F.-A., Lores, I., Tamames, J., Peláez, A. I., López-Cortés, N., … Ferrer, M. (2013). Metaproteogenomic insights beyond bacterial response to naphthalene exposure and bio-stimulation. *The ISME Journal*, *7*(1), 122–136. http://doi.org/10.1038/ismej.2012.82

Guitart, C., Frickers, P., Horrillo-Caraballo, J., Law, R. J., & Readman, J. W. (2008). Characterization of Sea Surface Chemical Contamination after Shipping Accidents. *Environmental Science & Technology*, *42*(7), 2275–2282. http://doi.org/10.1021/es703125e

Gutierrez, T., Singleton, D. R., Berry, D., Yang, T., Aitken, M. D., & Teske, A. (2013). Hydrocarbon-degrading bacteria enriched by the Deepwater Horizon oil spill identified by cultivation and DNA-SIP. *The ISME Journal*, *7*(11), 2091–2104. http://doi.org/10.1038/ismej.2013.98

Harayama, S., Kasai, Y., & Hara, A. (2004). Microbial communities in oil-contaminated seawater. *Current Opinion in Biotechnology*, *15*(3), 205–214. http://doi.org/10.1016/j.copbio.2004.04.002

Hassanshahian, M., Emtiazi, G., Caruso, G., & Cappello, S. (2014). Bioremediation (bioaugmentation/biostimulation) trials of oil polluted seawater: A mesocosm simulation study. *Marine Environmental Research*, *95*, 28–38. http://doi.org/10.1016/j.marenvres.2013.12.010

Hawley, E. R., Piao, H., Scott, N. M., Malfatti, S., Pagani, I., Huntemann, M., … Hess, M. (2014). Metagenomic analysis of microbial consortium from natural crude oil that seeps into the marine ecosystem offshore Southern California. *Standards in Genomic Sciences*, *9*(3), 1259–1274. http://doi.org/10.4056/sigs.5029016

Head, I. M. (1998). Bioremediation: towards a credible technology. *Microbiology*, *144*(3), 599–608.

Head, I. M., Jones, D. M., & Röling, W. F. M. (2006). Marine microorganisms make a meal of oil. *Nature Reviews. Microbiology*, *4*(3), 173–182. http://doi.org/10.1038/nrmicro1348

Head, I. M., & Swannell, R. P. (1999). Bioremediation of petroleum hydrocarbon contaminants in marine habitats. *Current Opinion in Biotechnology*, *10*(3), 234–239. http://doi.org/10.1016/S0958-1669(99)80041-X

Hedlund, B. P., Geiselbrecht, A. D., Bair, T. J., & Staley, J. T. (1999). Polycyclic Aromatic Hydrocarbon Degradation by a New Marine Bacterium, Neptunomonas naphthovorans gen. nov., sp. nov. *Applied and Environmental Microbiology*, *65*(1), 251–259.

Heider, J. (2007). Adding handles to unhandy substrates: anaerobic hydrocarbon activation mechanisms. *Current Opinion in Chemical Biology*, *11*(2), 188–194. http://doi.org/10.1016/j.cbpa.2007.02.027

Heinemann, M., & Sauer, U. (2010). Systems biology of microbial metabolism. *Current Opinion in Microbiology*, *13*(3), 337–343. http://doi.org/10.1016/j.mib.2010.02.005

Herbst, F.-A., Bahr, A., Duarte, M., Pieper, D. H., Richnow, H.-H., von Bergen, M., … Bombach, P. (2013). Elucidation of in situ polycyclic aromatic hydrocarbon degradation by functional metaproteomics (protein-SIP). *PROTEOMICS*, *13*(18-19), 2910–2920. http://doi.org/10.1002/pmic.201200569

He, Z., Gentry, T. J., Schadt, C. W., Wu, L., Liebich, J., Chong, S. C., … Zhou, J. (2007). GeoChip: a comprehensive microarray for investigating biogeochemical, ecological and environmental processes. *The ISME Journal*, *1*(1), 67–77. http://doi.org/10.1038/ismej.2007.2

Huijbers, M. M. E., Montersino, S., Westphal, A. H., Tischler, D., & van Berkel, W. J. H. (2014). Flavin dependent monooxygenases. *Archives of Biochemistry and Biophysics*, *544*, 2–17. http://doi.org/10.1016/j.abb.2013.12.005

Jackson, P. M., & Smith, L. K. (2014). Exploring the undulating plateau: the future of global oil supply. *Philosophical Transactions of the Royal Society of London A: Mathematical, Physical and Engineering Sciences*, *372*(2006), 20120491. http://doi.org/10.1098/rsta.2012.0491

Jiménez, N., Viñas, M., Guiu-Aragonés, C., Bayona, J. M., Albaigés, J., & Solanas, A. M. (2011). Polyphasic approach for assessing changes in an autochthonous marine bacterial community in the presence of Prestige fuel oil and its biodegradation potential. *Applied Microbiology and Biotechnology*, *91*(3), 823–834. http://doi.org/10.1007/s00253-011-3321-4

Jouanneau, Y., Micoud, J., & Meyer, C. (2007). Purification and Characterization of a Three-Component Salicylate 1-Hydroxylase from Sphingomonas sp. Strain CHY-1. *Applied and Environmental Microbiology*, *73*(23), 7515–7521. http://doi.org/10.1128/AEM.01519-07

Jurelevicius, D., Couto, C. R. de A., Alvarez, V. M., Vollú, R. E., Dias, F. de A., & Seldin, L. (2014). Response of the Archaeal Community to Simulated Petroleum Hydrocarbon Contamination in Marine and Hypersaline Ecosystems. *Water, Air, & Soil Pollution*, *225*(2), 1–12. http://doi.org/10.1007/s11270-014-1871-7

Kabisch, A., Otto, A., König, S., Becher, D., Albrecht, D., Schüler, M., … Schweder, T. (2014). Functional characterization of polysaccharide utilization loci in the marine Bacteroidetes “Gramella forsetii” KT0803. *The ISME Journal*, *8*(7), 1492–1502. http://doi.org/10.1038/ismej.2014.4

Karydis, M., & Kitsiou, D. (2011). Eutrophication and environmental policy in the Mediterranean Sea: a review. *Environmental Monitoring and Assessment*, *184*(8), 4931–4984. http://doi.org/10.1007/s10661-011-2313-2

Khara, P., Roy, M., Chakraborty, J., Ghosal, D., & Dutta, T. K. (2014). Functional characterization of diverse ring-hydroxylating oxygenases and induction of complex aromatic catabolic gene clusters in Sphingobium sp. PNB. *FEBS Open Bio*, *4*, 290–300. http://doi.org/10.1016/j.fob.2014.03.001

Khelifi, N., Amin Ali, O., Roche, P., Grossi, V., Brochier-Armanet, C., Valette, O., … Hirschler-

Réa, A. (2014). Anaerobic oxidation of long-chain n-alkanes by the hyperthermophilic sulfate-reducing archaeon, Archaeoglobus fulgidus. *The ISME Journal*, *8*(11), 2153–2166. http://doi.org/10.1038/ismej.2014.58

Kimes, N. E., Callaghan, A. V., Aktas, D. F., Smith, W. L., Sunner, J., Golding, B., … Morris, P. J. (2013). Metagenomic analysis and metabolite profiling of deep-sea sediments from the Gulf of Mexico following the Deepwater Horizon oil spill. *Frontiers in Microbiology*, *4*. http://doi.org/10.3389/fmicb.2013.00050

Kimes, N. E., Callaghan, A. V., Suflita, J. M., & Morris, P. J. (2014). Microbial transformation of the Deepwater Horizon oil spill—past, present, and future perspectives. *Frontiers in Microbiology*, *5*, 603. http://doi.org/10.3389/fmicb.2014.00603

King, G. M., Kostka, J. E., Hazen, T. C., & Sobecky, P. A. (2015). Microbial Responses to the Deepwater Horizon Oil Spill: From Coastal Wetlands to the Deep Sea. *Annual Review of Marine Science*, *7*(1), 377–401. http://doi.org/10.1146/annurev-marine-010814-015543

Kluser, S., Richard, J.-P., Giuliani, G., De Bono, A., & Peduzzi, P. (2006). Illegal oil discharge in European seas. Retrieved from http://archive-ouverte.unige.ch/unige:23134

Kniemeyer, O., Musat, F., Sievert, S. M., Knittel, K., Wilkes, H., Blumenberg, M., … Widdel, F. (2007). Anaerobic oxidation of short-chain hydrocarbons by marine sulphate-reducing bacteria. *Nature*, *449*(7164), 898–901. http://doi.org/10.1038/nature06200

Koren, O., Knezevic, V., Ron, E. Z., & Rosenberg, E. (2003). Petroleum Pollution Bioremediation Using Water-Insoluble Uric Acid as the Nitrogen Source. *Applied and Environmental Microbiology*, *69*(10), 6337–6339. http://doi.org/10.1128/AEM.69.10.6337-6339.2003

Kostka, J. E., Prakash, O., Overholt, W. A., Green, S. J., Freyer, G., Canion, A., … Huettel, M. (2011). Hydrocarbon-Degrading Bacteria and the Bacterial Community Response in Gulf of Mexico Beach Sands Impacted by the Deepwater Horizon Oil Spill▿. *Applied and Environmental Microbiology*, *77*(22), 7962–7974. http://doi.org/10.1128/AEM.05402-11

Kouzuma, A., & Watanabe, K. (2014). Microbial Ecology Pushes Frontiers in Biotechnology. *Microbes and Environments*, *29*(1), 1–3. http://doi.org/10.1264/jsme2.ME2901rh

Lanfranconi, M. P., Bosch, R., & Nogales, B. (2010). Short-term changes in the composition of active marine bacterial assemblages in response to diesel oil pollution. *Microbial Biotechnology*, *3*(5), 607–621. http://doi.org/10.1111/j.1751-7915.2010.00192.x

Li, H., Liu, Y. H., Luo, N., Zhang, X. Y., Luan, T. G., Hu, J. M., … Lu, J. Q. (2006). Biodegradation of benzene and its derivatives by a psychrotolerant and moderately haloalkaliphilic Planococcus sp. strain ZD22. *Research in Microbiology*, *157*(7), 629–636. http://doi.org/10.1016/j.resmic.2006.01.002

Li, L., Liu, X., Yang, W., Xu, F., Wang, W., Feng, L., … Rao, Z. (2008). Crystal Structure of Long-Chain Alkane Monooxygenase (LadA) in Complex with Coenzyme FMN: Unveiling the Long-Chain Alkane Hydroxylase. *Journal of Molecular Biology*, *376*(2), 453–465. http://doi.org/10.1016/j.jmb.2007.11.069

Lim, B. R., Huang, X., Hu, H. Y., Goto, N., & Fujie, K. (2001). Effects of temperature on biodegradation characteristics of organic pollutants and microbial community in a solid phase aerobic bioreactor treating high strength organic wastewater. *Water Science and Technology*, *43*(1), 131–138.

Liu, Z., & Liu, J. (2013). Evaluating bacterial community structures in oil collected from the sea surface and sediment in the northern Gulf of

Mexico after the Deepwater Horizon oil spill. *MicrobiologyOpen*, *2*(3), 492–504. http://doi.org/10.1002/mbo3.89

Luo, F., Gitiafroz, R., Devine, C. E., Gong, Y., Hug, L. A., Raskin, L., & Edwards, E. A. (2014). Metatranscriptome of an Anaerobic Benzene-Degrading, Nitrate-Reducing Enrichment Culture Reveals Involvement of Carboxylation in Benzene Ring Activation. *Applied and Environmental Microbiology*, *80*(14), 4095–4107. http://doi.org/10.1128/AEM.00717-14

Luo, Y.-R., Tian, Y., Huang, X., Kwon, K., Yang, S.-H., Seo, H.-S., … Zheng, T.-L. (2012). Sphingomonas polyaromaticivorans sp. nov., a polycyclic aromatic hydrocarbon-degrading bacterium from an oil port water sample. *INTERNATIONAL JOURNAL OF SYSTEMATIC AND EVOLUTIONARY MICROBIOLOGY*, *62*(Pt 6), 1223–1227. http://doi.org/10.1099/ijs.0.033530-0

Lu, Z., Deng, Y., Van Nostrand, J. D., He, Z., Voordeckers, J., Zhou, A., … others. (2011). Microbial gene functions enriched in the Deepwater Horizon deep-sea oil plume. *The ISME Journal*, *6*(2), 451–460.

Mandalakis, M., Gustafsson, Ö., Reddy, C. M., & Xu, L. (2004). Radiocarbon Apportionment of Fossil versus Biofuel Combustion Sources of Polycyclic Aromatic Hydrocarbons in the Stockholm Metropolitan Area. *Environmental Science & Technology*, *38*(20), 5344–5349. http://doi.org/10.1021/es049088x

Mandalakis, M., Polymenakou, P. N., Tselepides, A., & Lampadariou, N. (2014). Distribution of aliphatic hydrocarbons, polycyclic aromatic hydrocarbons and organochlorinated pollutants in deep-sea sediments of the southern Cretan margin, eastern Mediterranean Sea: A baseline assessment. *Chemosphere*, *106*, 28–35. http://doi.org/10.1016/j.chemosphere.2013.12.081

Martin, J. D., Adams, J., Hollebone, B., King, T., Brown, R. S., & Hodson, P. V. (2014). Chronic toxicity of heavy fuel oils to fish embryos using multiple exposure scenarios. *Environmental Toxicology and Chemistry*, *33*(3), 677–687. http://doi.org/10.1002/etc.2486

Mason, O. U., Hazen, T. C., Borglin, S., Chain, P. S. G., Dubinsky, E. A., Fortney, J. L., … Jansson, J. K. (2012). Metagenome, metatranscriptome and single-cell sequencing reveal microbial response to Deepwater Horizon oil spill. *The ISME Journal*, *6*(9), 1715–1727. http://doi.org/10.1038/ismej.2012.59

Mason, O. U., Scott, N. M., Gonzalez, A., Robbins-Pianka, A., Baelum, J., Kimbrel, J., … Jansson, J. K. (2014). Metagenomics reveals sediment microbial community response to Deepwater Horizon oil spill. *The ISME Journal*, *8*(7), 1464–1475. http://doi.org/10.1038/ismej.2013.254

Mayer, B. (Ed.). (2011). *Bioinformatics for Omics Data* (Vol. 719). Totowa, NJ: Humana Press. Retrieved from http://link.springer.com/10.1007/978-1-61779-027-0

McGenity, T. J., Folwell, B. D., McKew, B. A., & Sanni, G. O. (2012). Marine crude-oil biodegradation: a central role for interspecies interactions. *Aquatic Biosystems*, *8*, 10. http://doi.org/10.1186/2046-9063-8-10

McKew, B. A., Coulon, F., Yakimov, M. M., Denaro, R., Genovese, M., Smith, C. J., … McGenity, T. J. (2007). Efficacy of intervention strategies for bioremediation of crude oil in marine systems and effects on indigenous hydrocarbonoclastic bacteria. *Environmental Microbiology*, *9*(6), 1562–1571. http://doi.org/10.1111/j.1462-2920.2007.01277.x

Meckenstock, R. U., & Mouttaki, H. (2011). Anaerobic degradation of non-substituted aromatic hydrocarbons. *Current Opinion in Biotechnology*, *22*(3), 406–414.

http://doi.org/10.1016/j.copbio.2011.02.009

Megharaj, M., Ramakrishnan, B., Venkateswarlu, K., Sethunathan, N., & Naidu, R. (2011). Bioremediation approaches for organic pollutants: A critical perspective. *Environment International*, *37*(8), 1362–1375. http://doi.org/10.1016/j.envint.2011.06.003

Mendoza, D. de. (2014). Temperature Sensing by Membranes. *Annual Review of Microbiology*, *68*(1), 101–116. http://doi.org/10.1146/annurev-micro-091313-103612

Messina, E., Denaro, R., Crisafi, F., Smedile, F., Cappello, S., Genovese, M., … Yakimov, M. M. (n.d.). Genome sequence of obligate marine polycyclic aromatic hydrocarbons-degrading bacterium Cycloclasticus sp. 78-ME, isolated from petroleum deposits of the sunken tanker Amoco Milford Haven, Mediterranean Sea. *Marine Genomics*. http://doi.org/10.1016/j.margen.2015.10.006

Moreno, R., Jover, L., Diez, C., Sarda, F., & Sanpera, C. (2013). Ten Years after the Prestige Oil Spill: Seabird Trophic Ecology as Indicator of Long-Term Effects on the Coastal Marine Ecosystem. *PLoS ONE*, *8*(10). http://doi.org/10.1371/journal.pone.0077360

Müller, M. M., Kügler, J. H., Henkel, M., Gerlitzki, M., Hörmann, B., Pöhnlein, M., … Hausmann, R. (2012). Rhamnolipids—Next generation surfactants? *Journal of Biotechnology*, *162*(4), 366–380. http://doi.org/10.1016/j.jbiotec.2012.05.022

Muth, T., Benndorf, D., Reichl, U., Martens, L., & Rapp, E. (2013). Searching for a needle in a stack of needles: challenges in metaproteomics data analysis. *Mol. BioSyst.*, *9*(4), 578–585. http://doi.org/10.1039/C2MB25415H

Nepusz, C. G. C. and T. (2006). The igraph software package for complex network research. *InterJournal*, *Complex Systems*. Retrieved from http://igraph.org

Nikolopoulou, M., Eickenbusch, P., Pasadakis, N., Venieri, D., & Kalogerakis, N. (2013). Microcosm evaluation of autochthonous bioaugmentation to combat marine oil spills. *New Biotechnology*, *30*(6), 734–742. http://doi.org/10.1016/j.nbt.2013.06.005

Nikolopoulou, M., & Kalogerakis, N. (2008). Enhanced bioremediation of crude oil utilizing lipophilic fertilizers combined with biosurfactants and molasses. *Marine Pollution Bulletin*, *56*(11), 1855–1861. http://doi.org/10.1016/j.marpolbul.2008.07.021

Nikolopoulou, M., Pasadakis, N., & Kalogerakis, N. (2013). Evaluation of autochthonous bioaugmentation and biostimulation during microcosm-simulated oil spills. *Marine Pollution Bulletin*, *72*(1), 165–173. http://doi.org/10.1016/j.marpolbul.2013.04.007

Oil in the Sea III: Inputs, Fates, and Effects. (2003). Retrieved from http://www.nap.edu/catalog.php?record_id=10388

Omokoko, B., Jäntges, U. K., Zimmermann, M., Reiss, M., & Hartmeier, W. (2008). Isolation of the phe-operon from G. stearothermophilus comprising the phenol degradative meta-pathway genes and a novel transcriptional regulator. *BMC Microbiology*, *8*, 197. http://doi.org/10.1186/1471-2180-8-197

Païssé, S., Goñi-Urriza, M., Coulon, F., & Duran, R. (2010). How a Bacterial Community Originating from a Contaminated Coastal Sediment Responds to an Oil Input. *Microbial Ecology*, *60*(2), 394–405. http://doi.org/10.1007/s00248-010-9721-7

Peng, R.-H., Xiong, A.-S., Xue, Y., Fu, X.-Y., Gao, F., Zhao, W., … Yao, Q.-H. (2008). Microbial biodegradation of polyaromatic hydrocarbons. *FEMS Microbiology Reviews*, *32*(6), 927–955. http://doi.org/10.1111/j.1574-6976.2008.00127.x

Peng, R.-H., Xiong, A.-S., Xue, Y., Fu, X.-Y., Gao, F., Zhao, W., … Yao, Q.-H. (2010). A Profile of Ring-hydroxylating Oxygenases that Degrade Aromatic Pollutants. In D. M. Whitacre (Ed.),

Reviews of Environmental Contamination and Toxicology Volume 206 (pp. 65–94). Springer New York. Retrieved from http://link.springer.com/chapter/10.1007/978-1-4419-6260-7_4

Pérez-Cadahía, B., Laffon, B., Pásaro, E., & Méndez, J. (2004). Evaluation of PAH bioaccumulation and DNA damage in mussels (Mytilus galloprovincialis) exposed to spilled Prestige crude oil. *Comparative Biochemistry and Physiology Part C: Toxicology & Pharmacology*, *138*(4), 453–460. http://doi.org/10.1016/j.cca.2004.08.001

Pérez-Pantoja, D., Donoso, R., Junca, H., González, B., & Pieper, D. H. (2010). Phylogenomics of Aerobic Bacterial Degradation of Aromatics. In K. N. Timmis (Ed.), *Handbook of Hydrocarbon and Lipid Microbiology* (pp. 1355–1397). Springer Berlin Heidelberg. Retrieved from http://link.springer.com/referenceworkentry/10.1007/978-3-540-77587-4_95

Philipp, B., & Schink, B. (2012). Different strategies in anaerobic biodegradation of aromatic compounds: nitrate reducers versus strict anaerobes. *Environmental Microbiology Reports*, *4*(5), 469–478. http://doi.org/10.1111/j.1758-2229.2011.00304.x

Piazza, R., Moumni, B. E., Bellucci, L. G., Frignani, M., Vecchiato, M., Giuliani, S., … Gambaro, A. (2009). Polychlorinated biphenyls in sediments of selected coastal environments in northern Morocco. *Marine Pollution Bulletin*, *58*(3), 431–438. http://doi.org/10.1016/j.marpolbul.2008.11.020

Ranya A Amer, Y. R. A. F. (2014). Hydrocarbonoclastic marine bacteria in Mediterranean Sea, El-Max, Egypt: isolation, identification and site characterization. *Jokull*, *64*(4), 223–249.

Rebar, A. H., Lipscomb, T. P., Harris, R. K., & Ballachey, B. E. (1995). Clinical and Clinical Laboratory Correlates in Sea Otters Dying Unexpectedly in Rehabilitation Centers Following the Exxon Valdez Oil Spill. *Veterinary Pathology Online*, *32*(4), 346–350. http://doi.org/10.1177/030098589503200402

Redmond, M. C., & Valentine, D. L. (2012). Natural gas and temperature structured a microbial community response to the Deepwater Horizon oil spill. *Proceedings of the National Academy of Sciences*, *109*(50), 20292–20297. http://doi.org/10.1073/pnas.1108756108

Reis, I., Almeida, C. M. R., Magalhães, C. M., Cochofel, J., Guedes, P., Basto, M. C. P., … Mucha, A. P. (2013). Bioremediation potential of microorganisms from a sandy beach affected by a major oil spill. *Environmental Science and Pollution Research*, *21*(5), 3634–3645. http://doi.org/10.1007/s11356-013-2365-7

Rivers, A. R., Sharma, S., Tringe, S. G., Martin, J., Joye, S. B., & Moran, M. A. (2013). Transcriptional response of bathypelagic marine bacterioplankton to the Deepwater Horizon oil spill. *The ISME Journal*, *7*(12), 2315–2329. http://doi.org/10.1038/ismej.2013.129

Rodriguez-R, L. M., Overholt, W. A., Hagan, C., Huettel, M., Kostka, J. E., & Konstantinidis, K. T. (2015). Microbial community successional patterns in beach sands impacted by the Deepwater Horizon oil spill. *The ISME Journal*. http://doi.org/10.1038/ismej.2015.5

Rogowska, J., & Namieśnik, J. (2010a). Environmental Implications of Oil Spills from Shipping Accidents. In D. M. Whitacre (Ed.), *Reviews of Environmental Contamination and Toxicology Volume 206* (pp. 95–114). Springer New York. Retrieved from http://link.springer.com/chapter/10.1007/978-1-4419-6260-7_5

Rogowska, J., & Namieśnik, J. (2010b). Environmental implications of oil spills from shipping accidents. *Reviews of Environmental*

Contamination and Toxicology, *206*, 95–114. http://doi.org/10.1007/978-1-4419-6260-7_5

Rojo, F. (2009). Degradation of alkanes by bacteria. *Environmental Microbiology*, *11*(10), 2477–2490. http://doi.org/10.1111/j.1462-2920.2009.01948.x

Romero, I. C., Schwing, P. T., Brooks, G. R., Larson, R. A., Hastings, D. W., Ellis, G., … Hollander, D. J. (2015). Hydrocarbons in Deep-Sea Sediments following the 2010 Deepwater Horizon Blowout in the Northeast Gulf of Mexico. *PLoS ONE*, *10*(5). http://doi.org/10.1371/journal.pone.0128371

Ron, E. Z., & Rosenberg, E. (2014). Enhanced bioremediation of oil spills in the sea. *Current Opinion in Biotechnology*, *27*, 191–194. http://doi.org/10.1016/j.copbio.2014.02.004

Saa, L., Jaureguibeitia, A., Largo, E., Llama, M. J., & Serra, J. L. (2009). Cloning, purification and characterization of two components of phenol hydroxylase from Rhodococcus erythropolis UPV-1. *Applied Microbiology and Biotechnology*, *86*(1), 201–211. http://doi.org/10.1007/s00253-009-2251-x

Saha, R., Chowdhury, A., & Maranas, C. D. (2014). Recent advances in the reconstruction of metabolic models and integration of omics data. *Current Opinion in Biotechnology*, *29*, 39–45. http://doi.org/10.1016/j.copbio.2014.02.011

Sammarco, P. W., Kolian, S. R., Warby, R. A. F., Bouldin, J. L., Subra, W. A., & Porter, S. A. (2013). Distribution and concentrations of petroleum hydrocarbons associated with the BP/Deepwater Horizon Oil Spill, Gulf of Mexico. *Marine Pollution Bulletin*, *73*(1), 129–143. http://doi.org/10.1016/j.marpolbul.2013.05.029

Sauret, C., Christaki, U., Moutsaki, P., Hatzianestis, I., Gogou, A., & Ghiglione, J.-F. (2012). Influence of pollution history on the response of coastal bacterial and nanoeukaryote communities to crude oil and biostimulation assays. *Marine Environmental Research*, *79*, 70–78. http://doi.org/10.1016/j.marenvres.2012.05.006

Sauret, C., Séverin, T., Vétion, G., Guigue, C., Goutx, M., Pujo-Pay, M., … Ghiglione, J.-F. (2014). “Rare biosphere” bacteria as key phenanthrene degraders in coastal seawaters. *Environmental Pollution*, *194*, 246–253. http://doi.org/10.1016/j.envpol.2014.07.024

Seifert, J., Herbst, F.-A., Halkjær Nielsen, P., Planes, F. J., Jehmlich, N., Ferrer, M., & von Bergen, M. (2013). Bioinformatic progress and applications in metaproteogenomics for bridging the gap between genomic sequences and metabolic functions in microbial communities. *PROTEOMICS*, *13*(18-19), 2786–2804. http://doi.org/10.1002/pmic.201200566

Sheppard, P. J., Simons, K. L., Adetutu, E. M., Kadali, K. K., Juhasz, A. L., Manefield, M., … Ball, A. S. (2014). The application of a carrier-based bioremediation strategy for marine oil spills. *Marine Pollution Bulletin*, *84*(1–2), 339–346. http://doi.org/10.1016/j.marpolbul.2014.03.044

Sikkema, J., de Bont, J. A., & Poolman, B. (1995). Mechanisms of membrane toxicity of hydrocarbons. *Microbiological Reviews*, *59*(2), 201–222.

Simons, K. L., Sheppard, P. J., Adetutu, E. M., Kadali, K., Juhasz, A. L., Manefield, M., … Ball, A. S. (2013). Carrier mounted bacterial consortium facilitates oil remediation in the marine environment. *Bioresource Technology*, *134*, 107–116. http://doi.org/10.1016/j.biortech.2013.01.152

Sjolander, K. (2004). Phylogenomic inference of protein molecular function: advances and challenges. *Bioinformatics*, *20*(2), 170–179. http://doi.org/10.1093/bioinformatics/bth021

Smith, C. B., Tolar, B. B., Hollibaugh, J. T., & King, G. M. (2013). Alkane hydroxylase gene (alkB) phylotype composition and diversity in northern Gulf of Mexico bacterioplankton. *Frontiers in Microbiology*, *4*.

http://doi.org/10.3389/fmicb.2013.00370

Somboon, T., Gleeson, M. P., & Hannongbua, S. (2011). Insight into the reaction mechanism of cis,cis-muconate lactonizing enzymes: a DFT QM/MM study. *Journal of Molecular Modeling*, *18*(2), 525–531. http://doi.org/10.1007/s00894-011-1088-2

Stobbe, M. D., Jansen, G. A., Moerland, P. D., & van Kampen, A. H. C. (2012). Knowledge representation in metabolic pathway databases. *Briefings in Bioinformatics*, bbs060. http://doi.org/10.1093/bib/bbs060

Szaleniec, M., Dudzik, A., Kozik, B., Borowski, T., Heider, J., & Witko, M. (2014). Mechanistic basis for the enantioselectivity of the anaerobic hydroxylation of alkylaromatic compounds by ethylbenzene dehydrogenase. *Journal of Inorganic Biochemistry*, *139*, 9–20. http://doi.org/10.1016/j.jinorgbio.2014.05.006

Tamis, J. E., Jongbloed, R. H., Karman, C. C., Koops, W., & Murk, A. J. (2012). Rational application of chemicals in response to oil spills may reduce environmental damage. *Integrated Environmental Assessment and Management*, *8*(2), 231–241. http://doi.org/10.1002/ieam.273

Tapilatu, Y., Acquaviva, M., Guigue, C., Miralles, G., Bertrand, J.-C., & Cuny, P. (2010). Isolation of alkane-degrading bacteria from deep-sea Mediterranean sediments. *Letters in Applied Microbiology*, *50*(2), 234–236. http://doi.org/10.1111/j.1472-765X.2009.02766.x

Tobalina, L., Bargiela, R., Pey, J., Herbst, F.-A., Lores, I., Rojo, D., … Planes, F. J. (2015). Context-specific metabolic network reconstruction of a naphthalene-degrading bacterial community guided by metaproteomic data. *Bioinformatics*, *31*(11), 1771–1779. http://doi.org/10.1093/bioinformatics/btv036

Torres Pazmiño, D. E., Winkler, M., Glieder, A., & Fraaije, M. W. (2010). Monooxygenases as biocatalysts: Classification, mechanistic aspects and biotechnological applications. *Journal of Biotechnology*, *146*(1–2), 9–24. http://doi.org/10.1016/j.jbiotec.2010.01.021

Trigo, A., Valencia, A., & Cases, I. (2009). Systemic approaches to biodegradation. *FEMS Microbiology Reviews*, *33*(1), 98–108. http://doi.org/10.1111/j.1574-6976.2008.00143.x

Tyagi, M., da Fonseca, M. M. R., & Carvalho, C. C. C. R. de. (2011). Bioaugmentation and biostimulation strategies to improve the effectiveness of bioremediation processes. *Biodegradation*, *22*(2), 231–241. http://doi.org/10.1007/s10532-010-9394-4

UNEP/MAP. (2012). *State of the Mediterranean Marine and Coastal Environment*. Athens.

Vaillancourt, F. H., Bolin, J. T., & Eltis, L. D. (2006). The Ins and Outs of Ring-Cleaving Dioxygenases. *Critical Reviews in Biochemistry and Molecular Biology*, *41*(4), 241–267. http://doi.org/10.1080/10409230600817422

van Beilen, J. B., & Funhoff, E. G. (2007). Alkane hydroxylases involved in microbial alkane degradation. *Applied Microbiology and Biotechnology*, *74*(1), 13–21. http://doi.org/10.1007/s00253-006-0748-0

van Berkel, W. J. H., Kamerbeek, N. M., & Fraaije, M. W. (2006). Flavoprotein monooxygenases, a diverse class of oxidative biocatalysts. *Journal of Biotechnology*, *124*(4), 670–689. http://doi.org/10.1016/j.jbiotec.2006.03.044

Viarengo, A., Dondero, F., Pampanin, D. M., Fabbri, R., Poggi, E., Malizia, M., … Cossa, G. P. (2007). A Biomonitoring Study Assessing the Residual Biological Effects of Pollution Caused by the HAVEN Wreck on Marine Organisms in the Ligurian Sea (Italy). *Archives of Environmental Contamination and Toxicology*, *53*(4), 607–616. http://doi.org/10.1007/s00244-005-0209-2

Vila, J., Nieto, J. M., Mertens, J., Springael, D., & Grifoll, M. (2010). Microbial community structure of a heavy fuel oil-degrading marine consortium: linking microbial dynamics with polycyclic aromatic hydrocarbon utilization. *FEMS Microbiology Ecology*, *73*(2), 349–362. http://doi.org/10.1111/j.1574-6941.2010.00902.x

Vila, J., Tauler, M., & Grifoll, M. (2015). Bacterial PAH degradation in marine and terrestrial habitats. *Current Opinion in Biotechnology*, *33*, 95–102. http://doi.org/10.1016/j.copbio.2015.01.006

Vilchez-Vargas, R., Geffers, R., Suárez-Diez, M., Conte, I., Waliczek, A., Kaser, V. S., … Pieper, D. H. (2013). Analysis of the microbial gene landscape and transcriptome for aromatic pollutants and alkane degradation using a novel internally calibrated microarray system. *Environmental Microbiology*, *15*(4), 1016–1039. http://doi.org/10.1111/j.1462-2920.2012.02752.x

Vilchez-Vargas, R., Junca, H., & Pieper, D. H. (2010). Metabolic networks, microbial ecology and "omics" technologies: towards understanding in situ biodegradation processes. *Environmental Microbiology*, *12*(12), 3089–3104. http://doi.org/10.1111/j.1462-2920.2010.02340.x

Wang, C., Chen, B., Zhang, B., Guo, P., & Zhao, M. (2014). Study of weathering effects on the distribution of aromatic steroid hydrocarbons in crude oils and oil residues. *Environmental Science: Processes & Impacts*, *16*(10), 2408–2414. http://doi.org/10.1039/C4EM00266K

Wang, D.-Z., Xie, Z.-X., & Zhang, S.-F. (2014). Marine metaproteomics: Current status and future directions. *Journal of Proteomics*, *97*, 27–35. http://doi.org/10.1016/j.jprot.2013.08.024

Wang, W., & Shao, Z. (2012). Diversity of flavin-binding monooxygenase genes (almA) in marine bacteria capable of degradation long-chain alkanes. *FEMS Microbiology Ecology*, *80*(3), 523–533. http://doi.org/10.1111/j.1574-6941.2012.01322.x

Wang, W., & Shao, Z. (2013). Enzymes and genes involved in aerobic alkane degradation. *Frontiers in Microbiology*, *4*. http://doi.org/10.3389/fmicb.2013.00116

Wang, W., Zhong, R., Shan, D., & Shao, Z. (2014). Indigenous oil-degrading bacteria in crude oil-contaminated seawater of the Yellow sea, China. *Applied Microbiology and Biotechnology*, *98*(16), 7253–7269. http://doi.org/10.1007/s00253-014-5817-1

Xue, W., & Warshawsky, D. (2005). Metabolic activation of polycyclic and heterocyclic aromatic hydrocarbons and DNA damage: A review. *Toxicology and Applied Pharmacology*, *206*(1), 73–93. http://doi.org/10.1016/j.taap.2004.11.006

Yakimov, M. M., Denaro, R., Genovese, M., Cappello, S., D'Auria, G., Chernikova, T. N., … Giluliano, L. (2005). Natural microbial diversity in superficial sediments of Milazzo Harbor (Sicily) and community successions during microcosm enrichment with various hydrocarbons. *Environmental Microbiology*, *7*(9), 1426–1441. http://doi.org/10.1111/j.1462-5822.2005.00829.x

Yakimov, M. M., Giuliano, L., Denaro, R., Crisafi, E., Chernikova, T. N., Abraham, W.-R., … Golyshin, P. N. (2004). Thalassolituus oleivorans gen. nov., sp. nov., a novel marine bacterium that obligately utilizes hydrocarbons. *International Journal of Systematic and Evolutionary Microbiology*, *54*(1), 141–148. http://doi.org/10.1099/ijs.0.02424-0

Yakimov, M. M., Giuliano, L., Gentile, G., Crisafi, E., Chernikova, T. N., Abraham, W.-R., … Golyshin, P. N. (2003). Oleispira antarctica gen. nov., sp. nov., a novel hydrocarbonoclastic marine bacterium isolated from Antarctic coastal sea water. *International Journal of Systematic and Evolutionary Microbiology*, *53*(3), 779–785. http://doi.org/10.1099/ijs.0.02366-0

Yakimov, M. M., Golyshin, P. N., Lang, S.,

Moore, E. R. B., Abraham, W.-R., Lünsdorf, H., & Timmis, K. N. (1998). Alcanivorax borkumensis gen. nov., sp. nov., a new, hydrocarbon-degrading and surfactant-producing marine bacterium. *International Journal of Systematic Bacteriology*, *48*(2), 339–348. http://doi.org/10.1099/00207713-48-2-339

Yakimov, M. M., Timmis, K. N., & Golyshin, P. N. (2007). Obligate oil-degrading marine bacteria. *Current Opinion in Biotechnology*, *18*(3), 257–266. http://doi.org/10.1016/j.copbio.2007.04.006

Yang, H.-Y., Jia, R.-B., Chen, B., & Li, L. (2014). Degradation of recalcitrant aliphatic and aromatic hydrocarbons by a dioxin-degrader Rhodococcus sp. strain p52. *Environmental Science and Pollution Research*, *21*(18), 11086–11093. http://doi.org/10.1007/s11356-014-3027-0

You, Y., Shim, J., Cho, C.-H., Ryu, M.-H., Shea, P. J., Kamala-Kannan, S., … Oh, B.-T. (2013). Biodegradation of BTEX mixture by Pseudomonas putidaYNS1 isolated from oil-contaminated soil. *Journal of Basic Microbiology*, *53*(5), 469–475. http://doi.org/10.1002/jobm.201200067

Zhou, T. (2013). Computational Reconstruction of Metabolic Networks from KEGG. In B. Reisfeld & A. N. Mayeno (Eds.), *Computational Toxicology* (Vol. 930, pp. 235–249). Totowa, NJ: Humana Press. Retrieved from http://link.springer.com/10.1007/978-1-62703-059-5_10